UNIVERSITÀ
DEGLI STUDI
FIRENZE

DOTTORATO DI RICERCA IN
SCIENZE CHIMICHE

CICLO XXVI

COORDINATORE Prof. Goti Andrea

"Group-IV Organometallics for the Catalytic Polymerization and Hydroamination of Unactivated Olefins"

Settore Scientifico Disciplinare CHIM/06

Dottorando
Dott. Luconi Lapo

_____
(firma)

Tutore
Dott. Giambastiani Giuliano

_____
(firma)

Coordinatore
Prof. Goti Andrea

_____
(firma)

Anni 2011/2013

To my parents

Index

Preface

Millions of tons of polyolefin-based materials are produced yearly, in most cases under relatively mild conditions mediated by transition-metal catalysts. Through a simple insertion reaction, inexpensive and abundant olefins (such as ethylene and propene) are transformed into polymeric materials for a wide range of applications, including plastics, fibers, and elastomers. The discovery of the Ziegler–Natta catalysts and the seminal works at Phillips Petroleum in the 1950s not only revolutionized polyolefin production, but paved also the way to the development of modern organometallic chemistry. Despite its long history, the polyolefin industry keeps growing steadily and remains technologically driven by the continuous discovery of new catalysts, processes, and applications.

Since Ziegler-Natta's time, important milestones in the field of homogeneous oligomerization/polymerization catalysis were set-up one after the other; from nickel complexes with phosphine donors (SHOP-type catalysts) for the highly selective and efficient production of α-olefins to Group IV metallocene polymerization catalysts and their subsequent industrial exploitation (in the early 1980s) due to the discovery of partially hydrolyzed organoaluminum compounds (MAOs) as co-catalysts/activators. All these scientific successes have shown how discrete "single-site" molecular catalysts could offer unmatched opportunities, compared with heterogeneous systems, towards the tailored synthesis of new polymeric architectures as well as the in-depth understanding of complex reaction mechanisms.

An almost infinite variety of nitrogen-containing ligands in combination with either *d*- and *f*-block metals have been explored as efficient and selective oligomerization and polymerization catalysts. The major advantages of this ligand class are represented by the facile control of their stereoelectronic properties, their simple preparation from available and cheap building blocks and their easy handling and storage. All these considerations, together with the capability of most of their metal derivatives to impart high activity and selectivity in olefin upgrading processes, have contributed to make nitrogen-containing catalysts highly desirable for industry and academy.

The thesis work aims at providing new insights and perspectives in the field of oligomerization/polymerization catalysis mediated by early metal complexes stabilized by ligands containing nitrogen donor groups. To make an additional step forward, widening the catalyst application range, most of the developed catalytic systems have been scrutinized with respect to their ability to promote different catalytic cycles related to the production of various materials and commodities. Accordingly, neutral and/or cationic catalysts capable to engage in highly efficient α-olefin polymerization have also been successfully employed in the intramolecular hydroamination reaction of model primary and/or secondary aminoalkenes for the obtainment of pyrrolidine and/or piperidine heterocycles. Each contribution reported in this thesis work provides the readership with a complete account on a specific topic: from the synthesis of ligands and related complexes to mechanistic details (whenever applicable) up to the investigation of the catalyst performance and its future perspectives. To facilitate the comprehension of the work done, all data have been systematically reported according to a "publication format" just after a brief and general introduction on the two main catalytic processes investigated.

1

Introduction

1.1 Polymerization of α-olefins

Olefin polymerization has remarkably progressed over the last two decade, mainly thanks to the contribution of organometallic chemistry to the design of innovative ligand systems and metal complexes. The irreversible decrease of fossil-resources requires continuous efforts to improve the selectivity and productivity of the industrial processes as well as to reduce the environmental impact, especially in terms of energy and waste. Due to the wealth of possible ligand structures and metal combinations, organometallic-based catalysis can indeed address many of the issues of sustainable production of polymeric and composite materials.

Millions of tons of polyolefin-based materials are produced yearly, in most cases under relatively mild conditions mediated by transition metal catalysts. The discovery and commercialization of new oligomerization/polymerization technologies based on single-site catalysts still represent one of the most dynamic areas of organometallic chemistry, homogeneous catalysis and polymer science. Through a simple insertion reaction, inexpensive and abundant olefins are transformed into polymeric materials for a wide range of applications, including plastics, fibers and elastomers[1]. The extremely large number of tailored transition metal complexes (catalyst precursors) and main-group organometallic compounds (co-catalyst or activators)[2] have paved the way

towards the development of new polymerization processes and properly tailored polymer architectures.

The intense industrial activity in the field of polyolefins production and single-site catalysts commercialization (multibillion dollars per year), have deeply stimulated fundamental academic research, in turn strengthened by new and fruitful collaborations between research groups coming from both industry and academia. Although heterogeneous polymerization systems traditionally represent the workhorse of polymer industry, offering many important advantages over their homogeneous counterparts in commercial production, they suffer from a number of significant drawbacks. In particular, the control of either the polymer molecular weight distribution, co-monomer incorporation, or the relative/absolute polymer stereochemistry is inevitably linked to the precise identity of the catalyst active species. In contrast to heterogeneous systems, the readily tunable metal center coordination environment of homogeneous catalysts facilitates the control over all these polymerization features. Homogeneous catalysts can be commercially employed in solution-phase polymerization or heterogenized on solid supports for gas-phase or slurry polymerization processes.

Even though the polymerization of ethylene was discovered 1933, the first generation of effective transition metal polymerization catalysts was developed 20 years later by Ziegler[3] and Natta.[4] The Ziegler-Natta heterogeneous catalysts are based on early transition metals such as titanium, zirconium and hafnium, and polymerize ethylene at relatively low pressures and temperatures.[5] Although the heterogeneous catalysts are the basis of polymer industry, they present significant drawbacks. One important drawback is the presence of multiple active sites, which can exhibit their own rate constants for monomer enchainment, co-monomer incorporation and chain transfer.

After the initial discover of Ziegler-Natta catalysts, efforts were made to develop homogeneous models of the heterogeneous catalysts in order to prove both more amenable systems for mechanistic studies and particularly more efficient and selective catalysts.

In 1957, Natta and Breslow independently reported that $TiCl_2(Cp)_2$ after treatment with $AlEt_3$ or Et_2AlCl generated an active system for the olefin polymerization. Anyway, the activities observed with the homogeneous catalysts were lower compared to the heterogeneous systems and polymerization of α-olefins (i.e. propylene) were never achieved.[6,7]

The discovery of the Ziegler-Natta catalysts and the seminal works at Phillip Petroleum in the 1950s not only revolutionized polyolefin production, but also paved the way to the development of modern organometallic chemistry. Despite its long history, the polyolefin industry keeps growing steadily and remains technologically driven by the continuous discovery of new catalysts, processes and applications.

The polyolefin scenario changed dramatically in the early 1980s when Sinn and Kaminsky reported that partially hydrolyzed $AlMe_3$ was able to activate bis-cyclopentadienyl derivatives (metallocenes) of Group IV metals for the polymerization of both ethylene and α-olefins.[8] The partially-hydrolyzed $AlMe_3$ product is known with the name of methylaluminoxane (MAO) and its discovery was a real breakthrough as it allowed a much better control of the properties of polyethylene (PE) and polypropylene (PP) while maintaining or even improving the catalytic productivity.

Following the development of MAOs, Group IV metallocenes and half-sandwich amide complexes (constrained geometry catalysts) (**Scheme 1.1**) have provided the

most impressive results. It is now clear that the advent of the single-site catalysts as well as the discovery of MAO have initiated a revolution in the polymer synthesis so that their use for production of polyethylene and polypropylene is nowadays an industry reality.[9,10]

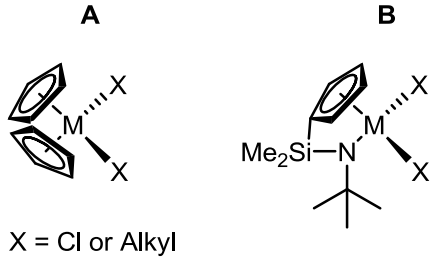

Scheme 1.1. Group IV metallocenes (**A**) and constrained geometry catalysts (half-sandwich) (**B**).

Besides the availability of suitable organometallic co-catalysts, the development of stereoselective, practical metallocene-based catalysts required the development of chiral, stereorigid metallocenes and of many new organic and organometallic reactions. Between 1984 and 1986, two key discoveries were made: the effect that different alkyl-substituted cyclopentadienyl ligands can induce on metallocene performances in olefin polymerization (the ligand effect) and the discovery that stereorigid, chiral metallocene catalysts can induce enantioselectivity in α-olefin insertion.[11] Since then, thanks to the combined efforts of industrial and academic research groups worldwide, an impressive leap forward toward the knowledge and control over the mechanicistic details of olefin insertion, chain growth, and chain release processes at the molecular level has been achieved.

During the first half of the 1990s, interest grew in developing new generation "non-metallocene" catalysts, partly to avoid the growing patent minefield in Group IV cyclopentadienyl systems, but also to harness the potential of other metals to polymerize ethylene on its own and with other olefinic monomers. It was a discovery in the mid-

1990s that had a galvanizing effect on researchers in the polyolefin catalysis field. Although some earlier work on nickel catalyst systems of the type employed in the Shell Higher Olefin Process (SHOP) had revealed the potential for late transition metals to polymerize ethylene,[12] it was the discovery of highly active (α-diimine)nickel catalysts capable of polymerizing ethylene to either linear or highly branched polyethylene, depending on the ligand backbone and reaction conditions, that dramatically demonstrated the possibilities for expanding the commercially useful metals beyond the first half of the transition series.[13]

In 1995 in fact, Brookhart and co-workers synthesized a new class of Ni^{II} and Pd^{II} polymerization catalysts stabilized by bulky α-diimine ligands (Shiff bases).[13,14] Depending on both the ligand backbone and the reaction conditions, the Ni^{II} catalysts of this type were capable of polymerizing ethylene to give a variety of materials, ranging from highly viscous liquids to rubbery elastomeric materials to rigid linear (**Scheme 1.2**). Moreover, these α-diimine catalysts were found to be highly tolerant to the presence of functional groups (e. g. polymerization of ketons).

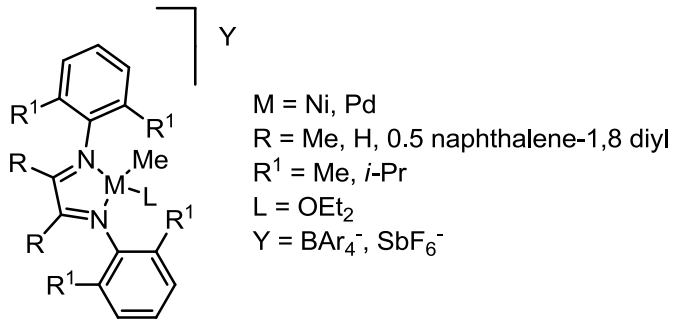

Scheme 1.2. α-diimine Ni^{II} and Pd^{II} catalyst precursors.

Since then, an almost infinite variety of imine-based ligands or, more generally, nitrogen-containing ligands in combination with either *d*- and *f*- block metals have been explored as efficient and selective oligomerization and polymerization catalysts. The

major advantages of this ligand class are represented by the facile control of their stereoelectronic properties, their simple preparation from available and cheap building blocks and their easy handling and storage. All these considerations, together with the capability of most of their metal derivatives to impart high activity and selectivity in olefin upgrading processes, have contributed to make nitrogen-containing catalysts highly desirable for industry and academy.

Another significant development over the past 10 years or so has been the introduction of systems capable of catalyzing the living polymerization of olefin monomers.[15] The absence of chain-transfer or chain-termination processes allows access to polyolefinic materials with very narrow molecular weight distributions (typically <1.1), block co-polymers, and polymers with novel topologies.

Recently an important class of C_1-symmetric dialkyl pyridylamidohafnium-based olefin polymerization catalysts was discovered by means of high throughput screening technologies by researchers at Dow and Symix (**Scheme 1.3**).[16,17,18] Performance of these catalysts is unique and truly remarkable. In particular, highly isotactic high molecular weight propene homopolymers and copolymers can be produced at very high reaction temperatures, enabling their production in solution process technologies.[19] Last but not least, under proper conditions, the active species are amenable to fast and reversible trans-alkylation with main group metal-alkyls (such as $ZnEt_2$); this can be used advantageously in the preparation of olefin block copolymers *via* "chain shuttling".[20]

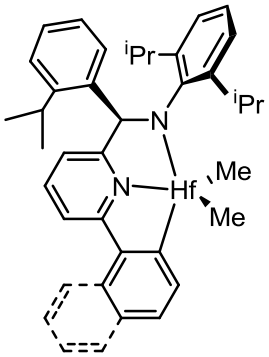

Scheme 1.3. Hafnium Pyridyl-Amido Dimethyl Complexes.

From a structural point of view, pre-catalysts shown in **Scheme 1.3** are unconventional and peculiar in several respects. A most notable feature is the ortho-metalation of the aryl substituent on the pyridine ring, resulting in tridentate ligation of the pyridyl-amido moiety and a slightly distorted trigonal bypyramidal Hf coordination.[18] A second important structural element is a stereogenic carbon linking the pyridyl and the amido fragments; albeit remote from the active site, this chiral center appears to influence the enantioselectivity in the insertion of prochiral α-alkenes.[18] A third feature is the high Lewis acidity of 5-coordinated $12e^-$ Hf(IV) center, which is further enhanced upon activation with co-catalysts.

Early- and late- transition metals complexes based on nitrogen-containing ligands occupy an important position in the field of modern homogeneous catalysis applied to highly efficient and selective oligomerization/polymerization processes.[1c,21,22] In particular, *N*,*N*-bidentate systems have represented a real breakthrough in the field of olefin polymerization catalysis, as witnessed by impressive number of papers and patents appearing in the last few years. The key feature of these organometallics is the facile tuning of their polymerization/oligomerization activity and selectivity by means of simple modifications of their ligand architecture. All these systems have to be

considered *pre*-catalysts, which require a preliminary activation with a co-catalyst, typically an organoaluminum or organoboron compound.

1.2 Catalyst's activators

In order to form active species for polymerization, the catalyst precursors must to be transformed into active catalysts by treatment with an appropriate activating species. The co-catalyst (generally called *activator*) presents specific features in order to preserve the catalysts' kinetic/thermodynamic characteristics all over the reaction. The co-catalysts become anionic after the activating process, constituting an essential part of a catalytically active cation-anion pair. The active metal catalyst is cationic and the anion derived from the activator is supposed to behave as a weakly coordinating ligand, which bulkiness being appropriate for delocalization of the negative charge. Therefore activators may significantly influence the polymerization characteristics and the polymer properties (**Scheme 1.4**).[2]

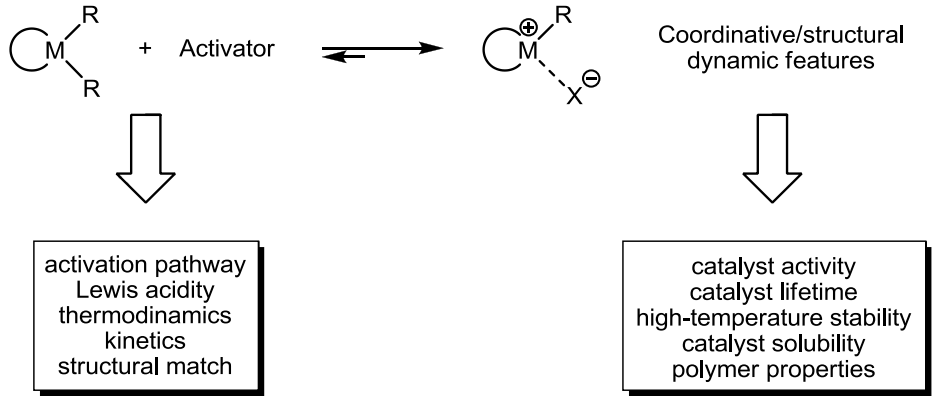

Scheme 1.4. Relationships between catalyst and co-catalyst in metal catalyzed olefin polymerization.

Common used activators vary according to the precursor nature. Heterogeneous Ziegler-Natta catalysts are used together with aluminum alkyls (AlR_3) or alkyl aluminum chloride (AlR_2Cl, $AlRCl_2$). Single-site Ziegler-Natta precursors are effectively activated by alkylaluminum compounds, while the less effect is achieved for

metallocene-based precursors. This fact collocated metallocenes out of the industrial interests, until Sinn and Kaminky discovered accidentally that addition of water to the non-active halogen-free polymerization $Cp_2ZrMe_2/AlMe_3$ system resulted in highly active ethylene polymerization catalyst.[23] The *in situ* formed activator was found to be methylaluminoxane (MAO), an oligomeric compound produced by partial hydrolysis of $AlMe_3$.

For the sake of simplicity, MAO is commonly referred to as linear chain or cyclic rings $[-Al(Me)-O-]_n$ containing three-coordinate aluminum centers, even if the true structure of MAO is still a matter of debate.[24] It may be a dynamic mixture of linear-, ring- and cage-complexes, all formed from methyl aluminoxane subunits during the controlled hydrolysis of trimethyl aluminum.[25,26,27] Some proposed structures for MAO include one-dimensional linear chains and cyclic rings containing three-coordinate Al centers, two dimensional structures, and three-dimensional clusters (**Scheme 1.5**).[2] A three-dimensional structure has been recently suggested by Sinn on the basis of structural similarities with *tert*-butylaluminoxanes[28] which form isolate cage structure.[29]

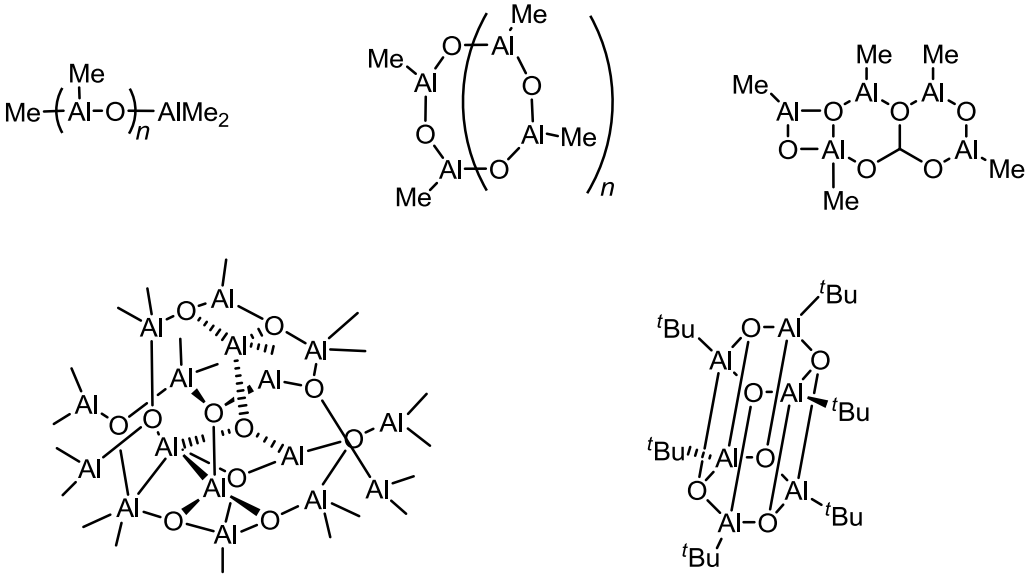

Scheme 1.5. Principal structures proposed for aluminoxanes.

Transition metal catalysts are usually achieved by reaction with MAO, modified methylaluminoxanes (MMAO) and alkyl aluminum (halides).

The presence of "free" trimethylaluminum (TMA) in equilibrium with the oligomeric part can have a non-innocent influence both in the catalyst activity and in the polymer molecular weight. Moreover small amount of aluminum trialkyls, added to the reaction system, also act as scavengers for background impurities, such as traces of moisture that could poison part of the catalyst. The fact that MAO has to be used in large excess relative to the transition metal complexes makes necessary a procedure to eliminate the "free" TMA. The most used strategy to eliminate "free" TMA from MAO solutions is to evaporate it to dryness even though it does not serve to eliminate the associated TMA. As recently demonstrated by Busico and co-workers, a procedure to eliminate the excess of TMA present in the commercially available MAO solution, can consist in the addition of a proper amount of a sterically hindered phenol, which forms alkyl-Al-phenoxides by reacting with TMA.[30]

The general mechanism by which MAO activates metal dihalide complexes for alkene insertion is shown in **Scheme 1.6**. The main function of MAO is to replace an halide ligand with a methyl group (ligand exchange) and subsequent halide abstraction, creating an ion pair made of a coordinative unsaturated complex cation and $[MAO]^-$ anions.[2,30]

Main drawbacks of using MAO as co-catalyst are: a) its relatively high cost, due to the high cost of the $AlMe_3$ parent compound, b) the large amount needed (typically Al/M = 10^3-10^4 M are used, although in supported systems Al/M ratios as low as 100 M has proven to be sufficient), c) the high residual content of catalyst residues (alumina) in the final product, especially for systems with no very high activity, as often in the case

of propene polymerization, and the intrinsic danger connected to the use of extremely pyrophoric $AlMe_3$. To solve the above problems, MAO surrogates have been investigated. Reports in the patent literature include the use of MAO/Al(^{i}Bu$_3$) mixtures[31] or the hydrolysis products of Al(^{i}Bu$_3$) and other branched aluminum alkyls.[32,33,34]

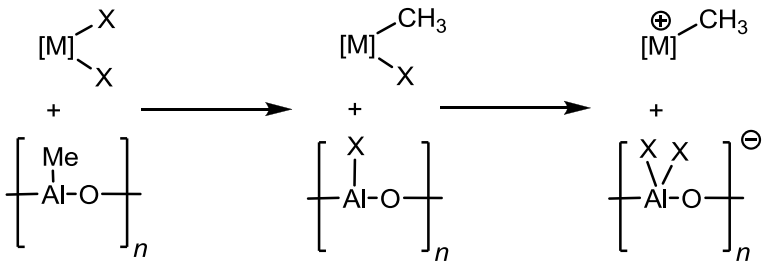

Scheme 1.6. Proposed mechanism for the formation of active species by reacting metal dihalide complexes with MAO.

A different strategy toward simpler and cheaper metal dialkyl complexes, usually the metal dimethyls L_nMMe_2 (for example M = Ti, Zr, Hf), has been the use of boron compounds such as (a) suitable Lewis acids as $B(C_6F_5)_3$ and its congeners,[35] (b) triphenylmethyl ("trityl") salts of noncoordinating anions, or (c) Brønsted acid capable of generating weakly coordinating counteranions. Among the last class of activators, anilinium salts such as $[HNR_2Ph]^+[B(C_6F_5)_4]^-$ (R = Me, Et) have been widely used.

The general activation pathways with boron compounds are shown in **Scheme 1.7**. The trityl cation Ph_3C^+ is a powerful alkide and hydride-abstracting (and oxidizing) reagent, and ammonium cations with formula $HNRR'_2{}^+$ can readily cleave M-R bonds via facile protonolysis.[2] In combination with $M(C_6F_5)_4^-$ (M = B, Al) non-coordinating/weakly coordinating anions, borate and aluminate activators, $[Ph_3C]^+[B(C_6F_5)_4]^-$,[36,37] $[HNRR'_2]^+[B(C_6F_5)_4]^-$,[38] and $[Ph_3C]^+[Al(C_6F_5)_4]^-$[39] have been developed as effective co-catalysts for activating metallocene and related metal alkyls, thereby yielding highly efficient olefin polymerization catalysts.

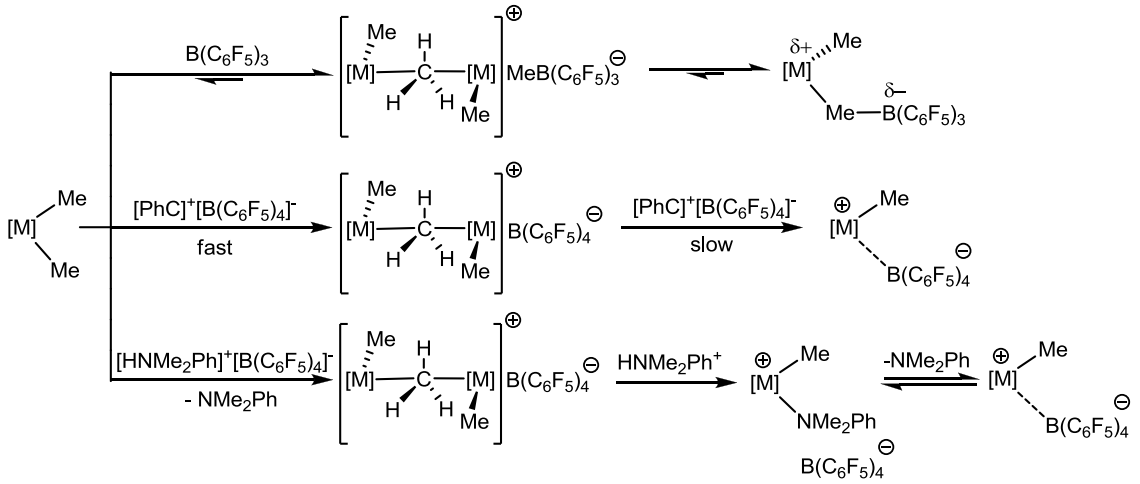

Scheme 1.7. Principal Activation Pathways for Metal Methyl Catalyst Precursors.

Although $[B(C_6F_5)_4]^-$ based activators have proven to be highly effective for olefin polymerization, they suffer from poor solubility in hydrocarbons and especially poor thermal stability and crystallizability of the cationic complexes derived therefrom, which results in very short catalytic lifetimes and limits the useful tools to characterize these species.[40]

1.3 Intramolecular hydroamination of aminoalkenes

The catalytic synthesis of organic building blocks from cheap and available starting materials is one of the main research targets of chemists, especially in the field of applied organic and industrial chemistry. The majority of industrially important catalytic reactions involve transformation of olefins exemplified by C-C or C-H bond forming reactions such as hydrogenations, hydroformylations, oligomerizations, polymerization, telomerizations and hydrocyanations. Apart from oxidation of olefins (C-O bond formation), reductive amination reactions and catalytic aminations of aryl halides (C-N bond formation), other catalytic carbon-heteroatom bond forming reactions are rarely used in industrial laboratories for a practical organic synthesis.

Amines and their derivatives are of great importance in almost all fields of chemistry, particularly as natural products, pharmaceuticals, as well as fine or bulk chemicals.[41] Many natural products (mainly alkaloids) and/or biologically active molecules contain an amino group. In industry, amines are used as solvents or starting materials for the bulk synthesis of various pharmaceuticals, antifoaming agents, corrosion inhibitors, detergents, colors and paints. The classical and established synthetic methods of amine preparation, either in the laboratory or on industrial scale, include aminations of alchools or alkyl halides, reductive amination of carbonyl compounds, aminoalkylation and reduction of amides, nitriles, azides or nitrocompounds.[42]

One of the most elegant and chemically efficient synthetic approaches towards amines-hydroamination appeared with the advent of transition metals catalysis.[43] As previously said, a major part of the organometallic chemistry is primarily focused on the C-C bond formation (including C-H bond activation), while catalytic methods leading to carbon-heteroatom bond formation have been less studied. The methods for the formation of C-N bond under catalytic conditions are even rarer, thus there is a clear need for simple, yet efficient synthetic approaches leading to amine. In this context, the catalytic hydroamination of olefins and alkynes emerges as an extremely powerful methodology. Due to its obviously "atom-economical" nature, hydroamination fulfills criteria of "green chemistry"[44] which is certainly not the case for metal-catalyzed aminations of organohalides[45] (due to unwanted salts formation). From both ecological and economical point of view, the direct addition of N-H group across the C=C bond of olefin is an ideal transformation, which delivers target amine in a single synthetic step starting from simple substrate.[46]

Although the direct addition of amines to alkenes is a thermodynamically feasible process, hydroamination reactions usually require the presence of a catalyst for the following reasons:

- An electrostatic repulsion between the nitrogen lone pair of the approaching amine and the π-bond of the electron-rich olefin results in high activation barrier;
- A concerted [2+2] addition of the N-H bond to the alkene is an orbital-symmetry forbidden process and is unfavourable due to large difference in energy between the carbon-carbon π-bond and the N-H σ-bond;
- At elevated temperatures the equilibrium is shifted towards the starting materials due to the negative reaction entropy.

For these reasons, the uncatalyzed addition of amine to double/triple carbon-carbon bond is usually observed only in hydroaminations of activated, electron-deficient alkenes or alkynes, 1,3-dienes or strained alkenes (norbornene).[43] On the other hand, an operationally simple and chemically efficient synthetic methodology of hydroamination of unactivated alkenes still remains one of the challenges of contemporary organometallic catalysis.[47] The hydroamination of alkenes is more difficult compared to that of alkynes because of the lower reactivity and electron density of C=C bonds.[48] Since hydroamination is a thermodynamically feasible process,[43] it is desirable to lower the activation barrier in order to increase the rate of cyclization of less reactive aminoalkenes. One of the efficient technique serving this purpose is the utilization of the so-called Thorpe-Ingold or gem-dialkyl effect.[49] In both cases, the beneficial conformational changes of the substrate are achieved by suitable substitution (with alkyl/aryl) of a carbon chain resulting in close spatial proximity of reacting functional groups (**Scheme 1.8**).[50]

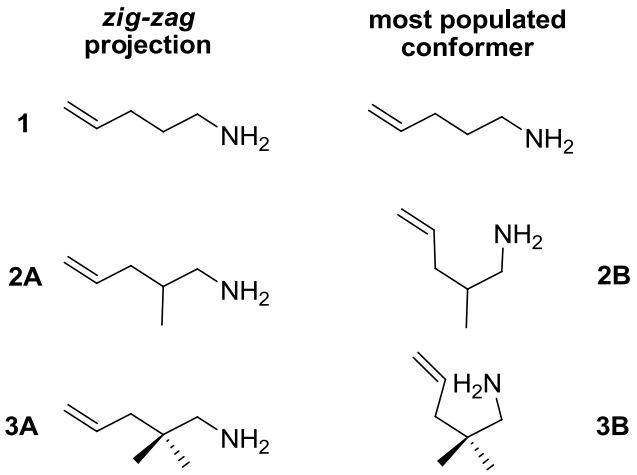

Scheme 1.8.

The higher population of the "more reactive" conformer results in a substantial rate increase in hydroamination of activated substrate in comparison with the structurally unmodified starting compound. However it is rather difficult to find an useful application of *gem*-disubstituted alkenylamines in the total synthesis of natural products or other structurally strictly define targets. In fact, although the activating Torpe-Ingold and/or *gem*-dialkyl effect is extremely beneficial for the hydroamination, its application must be carefully and thoroughly devised. While the utilization of such an activation strategy in the methodology development is useful and justified, one pays the price of limited scope of the reaction, *i.e.* in target-oriented syntheses.

Huge efforts have been performed in the last 60 years to develop these hydroamination reactions and numerous catalysts have been discovered belonging to alkali bases, but also to the class of alkaline earth metals, rare-earth, Group IV (and V) elements, late transition metals, and organocatalysts.

Transition metals have been initially devoted to promote the intermolecular hydroamination reaction. Pd and Pt salts were proven to allow the intermolecular[51] or intramolecular[52] reaction to occur when used in a stoichiometric quantity.

The first catalytic transformation was described with rhodium salts[53] and further with iridium complexes.[54] Numerous attempts have subsequently flourished in the presence of various transition metals associated with several ligands, and Togni et al. described the first enantioselective intermolecular hydroamination of olefins promoted by a chiral iridium complex.[55]

Meanwhile, the group of Marks discovered the ability of lanthanocenes to promote this transformation in the late 1980s, essentially in intramolecular procedure.[56] A few years later, they further reported the corresponding asymmetric version of this reaction in the presence of methyl-derived lanthanocenes;[57] thus they paved the way to further developments of the rare-earth-based chemistry.

Over the years, distinct modes of activation of the reagents have emerged according to the nature of the metal element involved in the catalytic cycle. As a general trend, Group I-V metal based catalysts have been proposed to proceed by activation of the amine through a rapid protonolysis reaction thanks to the presence of a strongly Brønsted basic moiety (X= alkyl or amido) on the metal and the ionic character of the M-X bond (**Scheme 1.9, B.1**). The activation of the amine functionality by this deprotonation pathway leads to the formation of a metal amido (or imido) complex that will further react trough a σ-insertive, or [2+2] mechanism to subsequently deliver the hydroamination product.[56,58,59,60,61,62]

With regard to hydroamination reaction by late transition metals, two antagonist activation modes by the metal center have been suggested. On one hand, oxidative addition of the N-H bond on a late transition metal in low oxidation state may occur to give birth to a metal hydride complex (**Scheme 1.9, B.2**).[54,63] Subsequent insertion of the carbon-carbon double bond into the metal-amido or metal-hydride bond and

reductive elimination will afford the hydroamination product. On the other hand, π-activation of the alkene by a Lewis acid late transition metal may precede the nucleophilic attack of the lone electron pair of the nitrogen on the coordinated alkene (**Scheme 1.9, A**).[64,65] Ensuing cleavage of the resulting carbon-metal bond by a protonolysis reaction will liberate the hydroamination product.

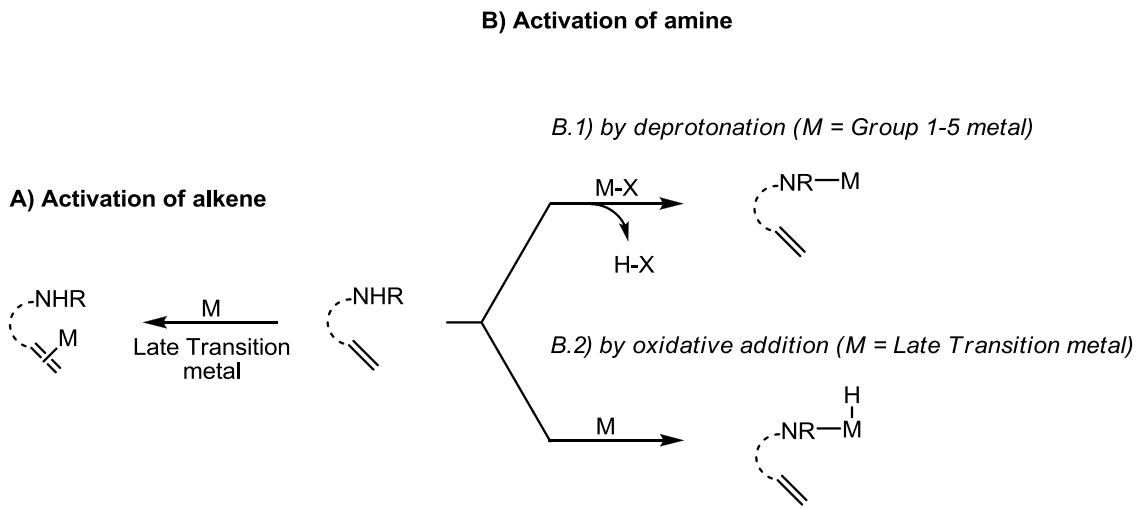

Scheme 1.9. Schematic representation of the activation mode of the substrate(s) in the metal-catalyzed hydroamination reaction depending on the nature of the metal: (M = metal, X = alkyl or amido group, R = H, alkyl or protecting group).

Rare-earth metal complexes are highly efficient catalysts for intramolecular hydroamination of various C-C unsaturations such as alkenes, alkynes, allenes and dienes, but reduced rates are observed in intermolecular hydroaminacion processes. Attractive features of rare-earth metal catalysts include very high turnover frequencies and excellent stereo-selectivities, rendering this methodology applicable to concise synthesis of naturally occurring alkaloids and other polycyclic azacycles.

Recent developments in catalytically active Group IV metal complexes have resulted in significant improvements in their reactivity towards aminoalkenes, and the first highly enantio-selective examples using chiral catalysts have been reported. Similar to rare-earth metals, Group IV metal complexes are very oxophilic, which reduces their functional group tolerance. Nevertheless, Group IV metal catalysts have been applied to

the synthesis of a range of biologically active molecules of relevance to pharmaceutical industry.

Group IV metals are less sensitive, generally easier to prepare than rare-earth metal complexes. Following the developments made in the lanthanide chemistry, in the 1990s, initial reports of Bergman[66] and Livinghouse[67] demonstrated the efficient use of titanium and zirconium complexes as catalysts for hydroamination of alkynes and allenes. Research concerning the transformation of alkenes is more recent and was initially based on the statement that cationic Group IV metal complexes are isoelectronic to lanthanocene compounds. In this context, Hultzsch et al. proved that cationic alkylzirconocene complexes afforded hydroaminacion/cyclization of secondary aminoalkenes with a mechanism similar to that described for rare-earth metals.[68] Neutral Group IV complexes were then demonstrated to be also active catalysts, through the formation of an imido intermediate, leading after [2+2] cycloaddition to the olefin to the formation of an azametallacyclobutane.[69]

Bergman and co-workers have proposed the *in-situ* synthesis of chiral bis(phosphinicamido) zirconium complexes that delivered scalemic pyrrolidines and piperidines with up 80% *e.e.*, albeit the reaction temperature could reach 135 °C.[70] One year later the group of Schafler prepared chiral amidate complexes of Group IV, with the zirconium complex leading to high enantio-selectivity values for a range of aminopentene derivatives.[71]

Other reports appeared in the last years with various successes in terms of enantio-selectivity, for which nonetheless the reaction had always to be conducted at very high temperature.[72] The group of Sadow recently described a tangible innovation in the transformation by preparing optically pure zirconium derivatives active at room

temperature.[61] This catalyst reacted easily with a wide range of primary aminoalkene derivatives at room temperature to provide the target pyrrolidines with *e.e.* values of up 98%. Kinetic studies led to the proposal of a new mechanism involving a reversible substrate–catalyst interaction that precedes the rate-determining step. This key and stereochemistry decisive step should occur through a six-membered transition species in which the zirconium center possesses two substrates as amido ligands (**Scheme 1.10**); the N-H transfer from one amide group to the terminal methylene unit of the other amidoalkene is concerted with intraligand C-N bond formation.

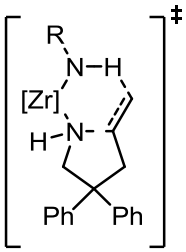

Scheme 1.10. Six-membered transition state proposed by Sadow for intramolecular hydroamination.

1.4 References

1 a) H. G. Alt, A. Köppl, *Chem. Rev.* **2000**, *100*, 1205; b) G. W. Coates, *Chem. Rev.* **2000**, *100*, 1223; c) S. D. Ittel, L. K. Johnson, M. Brookhart, *Chem. Rev.* **2000**, *100*, 1169.

2 E. Y. Chen, J. T. Marks *Chem. Rev.* **2000**, *100*, 1391.

3 K. Ziegler, E. Holzkamp, H. Martin, H. Breil, *Angew. Chem.* **1955**, *67*, 451.

4 G. Natta *Angew. Chem.* **1956**, *68*, 393.

5 M. Covezzi, *Macromol. Symp.* **1995**, *89*, 577.

6 G. Natta, P. Pino, G. Mazzanti, U. Giannini *J. Am. Chem. Soc.* **1957**, *79*, 2975.

7 D. S. Breslow, N. R. Newburg J. *Am. Chem. Soc.* **1957**, *79*, 5072.

8 W. Kaminsky, M. Miri, H. Sinn, R. Woldt *Makromol. Chem. Rapid. Commun.* **1983**, *4*, 417.

9 W. Kaminsky *Macromol. Chem Phys.* **1996**, *197*, 3907 (and references therein).

10 H. H. Brintzinger, D. Fischer, R. Mulhaupt, B. Rieger, R. Waymouth *Angew. Chem. Int. Ed. Engl.* **1995**, *34*, 1143.

11 L. Resconi, L. Cavallo, A. Fait, F. Piemontesi *Chem Rev.* **2000**, *100*, 1253.

12 a) W. Keim, F. H. Kowaldt, R. Goddard, C. Kruger *Angew. Chem. Int. Ed. Engl.* **1978**, *17*, 466-467; b) K. A. O. Starzewski, J. Witte *Angew. Chem. Int. Ed. Engl.* **1985**, *24*, 599-601; C) U. Klabunde, S. D. Ittel *J. Mol. Catal.* **1987**, *41*, 123; d) U. Klabunde, R. Mulhaupt, T. Herskovitz, A. H. Janowicz, J. Calabrese, S. D. Ittel *J. Polym. Sci. Polym. Chem.* **1987**, *25*, 1989.

13 L. K. Johnson, C. M. Killian, M. Brookhart *J. Am. Chem. Soc.* **1995**, *117*, 6414.

14 a) L. K. Johnson, S. Mecking, M. Brookhart *J. Am. Chem. Soc.* **1996**, *118*, 267; b) C. M. Killian, D. J. Tempel, L. K. Johnson, M. Brookhart *J. Am. Chem. Soc.* **1996**, *118*, 11664; c) L. K. Johnson, C. M. Killian, S. D. Arthur, J. Feldman, E. McCord, S. J. McLain, K. A. Kreutzer, A. M. A. Bennett, e. B. Coughlin, S. D. Ittel, A. Parthasarathy, D. J. Tempel, M. Brookhart (DuPont) WO 96/23010, **1996**; d) C. M. Killian, L. K. Johnson , M. Brookhart *Organomet.* **1997**, *16*, 2005; e) S. Mecking, L. K. Johnson, L. Wang, M. Brookart *J. Am. Chem. Soc.* **1998**, *120*, 888; f) S. A. Svejda, L. K. Johnson, M. Brookhart *J. Am. Chem. Soc.* **1999**, *121*, 10634; g) S. D. Ittel, L. K. Johnson, M. Brookhart, *Chem. Rev.* **2000**, *100*, 1169; h) D. P. Gates, A. A. Svejda, E Oñate, C. M. Killian, L. K. Johnson, P. S. White, M. Brookart *Macromolecules* **2000**, *33*, 2320; i) L. H. Shultz, D. J. Tempel; M. Brookhart *J. Am. Chem. Soc.* **2001**, *123*, 11539; j) L. H. Shultz; M. Brookhart *Organomet.* **2001**, *20*, 3975; k) A. C. Gottfried, M. Brookhart *Macromolecules* **2001**, *34*, 1140; l) M. D. Leatherman, S. A. Svejda, L. K. Johnson, M. Brookhart *J. Am. Chem. Soc.* **2003**, *125*, 3068.

15 W. G. Coates, P. D. Hustad, S. Reinartz *Angew. Chem. Int. Ed.* **2002**, *41*, 2237.

16 a) T. R. Boussie, G. M. Diamond, C. Goh, K. A. Hall, A. M. LaPointe, M. K. Leclerc, C. Lund, V. Murphy U.S. Patent Appl. **2006**/0135722A1; b) . R. Boussie, G. M. Diamond, C. Goh, K. A. Hall, A. M. LaPointe, M. K. Leclerc, C. Lund, V. Murphy U.S. Patent Appl. **2006**/7,018,949; c) . R. Boussie, G. M. Diamond, C. Goh, A. M. LaPointe, M. K. Leclerc, C. Lund, V. Murphy U.S. Patent Appl. **2004**/6,750,345; d) . R. Boussie, G. M. Diamond, C. Goh, K. A. Hall, A. M. LaPointe, M. K. Leclerc, C. Lund, V. Murphy U.S. Patent Appl. **2004**/6,713,577; e) . R. Boussie, G. M. Diamond, C. Goh, K. A. Hall, A. M. LaPointe, M. K. Leclerc, C. Lund, V. Murphy U.S. Patent Appl. **2004**/6,706,829; f) R. Boussie, G. M. Diamond, C. Goh, K. A. Hall, A. M. LaPointe, M. K. Leclerc, C. Lund, V. Murphy PCT Int. Appl. **2002**/WO038628.

17 R. Boussie, G. M. Diamond, C. Goh, K. A. Hall, A. M. LaPointe, M. K. Leclerc, C. Lund, V. Murphy, J. A. W. Shoemaker, U. Tracht, H. Turner, J. Zhang, T. Uno, R. K. Rosen, J. C. stevens *J. Am Chem. Soc.* **2003**, *125*, 4306.

18 R. Boussie, G. M. Diamond, C. Goh, K. A. Hall, A. M. LaPointe, M. K. Leclerc, C. Lund, V. Murphy,J. A. W. Shoemaker, H. Turner, R. K. Rosen, J. C. Stevens, F. Alfano, V. Busico, R. Cipullo, G. Talarico *Angew. Chem. Int. Ed.* **2006**, *45*, 3278.

19 a) D. J. Arriola, M. Bokota, F. J. Timmers PCT Int. Appl. **2004**/WO026925A1; b) K. A. Frazier, H. Boone, P. C. Vosejpka, J. C. Stevens U.S. Patent Appl. **2004**/0220050; c) L.-M. Tau, Y. W. Cheung, C. F. Diehl, L. G. Hazlitt U.S. Patent Appl. **2004**/0087751A1; d) L.-M. Tau, Y. W. Cheung, C. F. Diehl, L. G. Hazlitt U.S. Patent Appl. **2004**/0242784A1; e) J. N. Coalter, J. W. Van Egmond, L. J. Jr. Fouts, R. B. Painter, P. C. Vosejpka PCT Int. Appl. **2003**/040195A1; f) J. C. Stevens, D. D. Vanderlende PCT Int. Appl. **2003**/040201A1.

20 D. J. Arriola, E. M. Carnahan, P. D. Hustad, R. L. Kuhlman, T. T. Wenzel *Science* **2006**, *312*, 714.

21 C. Bianchini, G. Giambastiani, I. Guerrero Rios, G. Mantovani, A. Meli, A. M. Sagarra *Coord. Chem. Rev.* **2006**, *250*, 1391.

22 C. Bianchini, G. Giambastiani, L. Luconi, A. Meli *Coord. Chem. Rev.* **2010**, *254*, 431.

23 H. Sinn, W. Kaminky *Angew. Chem. Int. Ed.* **1980**, *19*, 390.

24 M. Hackmann, B. Rieger CATTECH 1 **1997**, 79 and references therein.

25 H. Sinn, W. Kaminky, H. Hoker (Eds) *Alumoxanes*; *Macromolecular Symposya 97*; Hutig & Wepf: Heidelberg, Germany, **1995**.

26 S. S. Reddy, S. Sivaram *Prog. Polym. Sci.* **1995**, *20*, 309.

27 P. L. Bryant, C. R. Harwell, A. A. Mrse, E. F. Emery, Z. Gan, T. Caldwell, A. P. Reyes, P. Kuhns, D. W. Hoyt, L. S. Simeral, R. W. Hall, L. G. Butler J. *Am. Chem. Soc.* **2001**, *123*, 12009.

28 H. Sinn Macromol. Symp. **1995**, *97*, 27.

29 M. R. Mason, J. M. Smith, S. G. Bott, A. R. Barron *J. Am. Chem. Soc.* **1993**, *115*, 4971.

30 V. Busico, R. Cipullo, F. Cutillo, N. Friederichs, S. Ronca, B. Wang *J. Am. Chem .Soc.* **2003**,*125*,12402.

31 T. Tsutsui, K. Yoshitsugu, T. Ueda Eur. Pat. Appl. 452,920 to Mitsui PC, **1991**.

32 L. Resconi, M. Galimberti, F. Piemontesi, F. Guglielmi, E. Albizzati U.S. Patent 5,910,464 to Montell Technology Co. **1998**.

33 a) L. Resconi, U. Giannini, T. Dall'Occo In *Metallocene-Based Polyolefins*; b) J. Scheirs, W. Kaminky Eds.; Wiley **1999**; Vol. *1*, p 69.

34 T. Dall'Occo, M. Galimberti, L. Resconi, E. Albizzati, G. Pennini U.S. Patent 5,849,653 to Montell Technology Co. **1998**.

35 V. E. Pires *Adv. Organomet. Chem.* **2004**, *52*, 1.

36 J. C. W Chien, W.-M. Tsai, M. D. Rausch J. *Am. Chem. Soc.* **1991**, *113*, 8570.

37 J. A. Ewen, M. J. Elder Eur. Patent Appl. 0,426,637, **1991**.

38 (a) G. G. Hlatky, D. J. Upton, H. W. Turner PCT Int. Appl.WO91/09882 **1991**. (Exxon Chemical Co.); (b) H. W. Turner Eur Pat. Appl. EP 0 277 004 A1, **1988** (Exxon Chemical Co.).

39 M. J. Elder, J. A. Ewen Eur. Pat. Appl. 0,573,403, **1993**.

40 L. Jia, X. Yang, A. Ishihara, T. Marks *J.Organometallics* **1995**, *14*, 3135.

41 a) J. March *Adv. Org. Chem.*, 4th ed., Wiley, New York, **1992**, 768-770 and references therein; b) J. P. Collman, B. M. Trost, T. R. Veroeven, in *Comprehensive Organometallic Chemistry*, Vol. 8 (Eds.: G. Wilkinson, F. G. A. Stone), Pergamon Press, Oxford, **1982**, 892-895 and references therein; c) M. S. Gibson, in *The Chemistry of Amino Group* (Ed.: S. Patai), Interscience, New York, **1968**, 61.

42 (a) S. A. Lawrence *Amines. Synthesis, Properties and Applications*; Cambridge University Press: Cambridge, United Kingdom, **2004**. (b) T. C. Nugent *Ed. Chiral Amine Synthesis: Methods, Developments and Applications*; Wiley-VCH: Weinheim, Germany, **2010**.

43 (a) K. C. Hultzsch *Org. Biomol. Chem.* **2005**, *3*, 1819. (b) K. C. Hultzsch *Adv. Synth. Catal.* **2005**, *347*, 367. (c) T. E. Müller, K. C. Hultzsch, M. Yus, F. Foubelo, M. Tada *Chem. Rev.* **2008**, *108*, 3795.

44 I. Aillaud, J. Collin, J. Hannedouche, E. Schulz *Dalton Trans.* **2007**, 5105.

45 T. E. Müller, M. Beller *Chem. Rev.* **1998**, *98*, 675.

46 C. Quinet, P. Jourdain, C. Hermans, A. Ates, I. Lucas, I. E. Markó, *Tetrahedron* **2008**, *64*, 1077.

47 R. A. Widenhoefer, X. Han *Eur. J. Org. Chem.* **2006**, 4555.

48 J. Haggins *Chem. Eng. News* **1993**, *71*(22), 23.

49 a) P. G. Sammes, D. Weller *J. Synthesis* **1995**, 1205; b) M. E. Jung, G. Piizzi, *Chem. Rev.* **2005**, *105*, 1735.

50 F. Mathia, P. Zálupský, P. Szolcsányi in Metal-Catalyzed Intramolecular Hydroamination of Unsaturated Amines With Terminal Double Bond - Part 1#

51 a) E. W. Stern, M. L. Spector, *Proc. Chem. Soc.* **1961**, 370; b) B. Akermark, J. E. Backvall, L. S. Hegedus, K. Zetterberg, K. Siirala-Hansén, K. Sjoberg, *J. Organomet. Chem.* **1974**, *72*, 127-138; C) A. Panunzi, A. De renzi, R. Palumbo, G. Pairo, *J. Am. Chem. Soc.* **1969**, *91*, 3879.

52 J. Ambuehl, P. S. Pregosin, L. M. Venanzi, G. Consiglio, F. Bachechi, L. Zambonelli *J. Organomet. Chem.* **1971**, *12*, 429.

53 D. R. Coulson *Tetrahedron Lett.* **1971**, *12*, 429.

54 A. L. Casalnuovo, J. C. Calabrese, D.Milstein *J.Am.Chem.Soc.***1988**, *110*, 6738.

55 R. Dorta, P. Egli, F. Zurcher, A. Togni J.*Am.Chem.Soc.* **1997**, *119*, 10857.

56 a) M. R. Gagne, T. J. Marks *J. Am. Chem. Soc.* **1989**, *111*, 4108–4109; b) M. R. Gagne, S. P. Nolan, T. J. Marks *Organometallics* **1990**, *9*, 1716; c) M. R. Gagne, C. L. Stern, T. J. Marks *J. Am. Chem. Soc.* **1992**, *114*, 275; d) V. M. Arredondo, F. E. McDonald, T. J. Marks *Organometallics* **1999**, *18*, 1949.

57 a) M. R. Gagne, L. Brard, V. P. Conticello, M. A. Giardello, C. L. Stern, T. J. Marks *Organometallics* **1992**, *11*, 2003; b) M. A. Giardello, V. P. Conticello, L. Brard, M. Sabat, A. L. Rheingold, C. L. Stern, T. J. Marks *J. Am. Chem. Soc.* **1994**, *116*, 10212; c) M. A. Giardello, V. P. Conticello, L. Brard, M. R. Gagne, T. J. Marks *J. Am. Chem. Soc.* **1994**, *116*, 10241.

58 a) B. D. Stubbert, T. J. Marks *J. Am. Chem. Soc.* **2007**, *129*, 6149; b) D. C. Leitch, R. H. Platel, L. L. Schafer *J. Am. Chem. Soc.* **2011**, *133*, 15453; c) L. E. N. Allan, G. J. Clarkson, D. J. Fox, A. L. Gott, P. Scott *J. Am. Chem. Soc.* **2010**, *132*, 15308.

59 For examples of computational mechanistic studies of aminoalkene hydroamination, see a) S. Tobisch *Dalton Trans.* **2012**, *41*, 9182; b) A. Motta,G. Lanza, I. L. Fragala,T. J. Marks *Organometallics* **2004**, *23*,4097.

60 K. Manna, M. L. Kruse, A. D. Sadow *ACS Catal.* **2011**, *1*, 1637.

61 K. Manna, S. Xu, A. D. Sadow *Angew. Chem.* **2011**, *123*, 1905; *Angew. Chem. Int. Ed.* **2011**, *50*, 1865.

62 M. Arrowsmith, M. R. Crimmin, A. G. M. Barrett, M. S. Hill, G. Kociok-Kçhn, P. A. Procopiou *Organometallics* **2011**, *30*, 1493.

63 C. S. Sevov, J. S. Zhou, J. F. Hartwig *J. Am. Chem. Soc.* **2012**, *134*, 11960.

64 K. D. Hesp, S. Tobisch, M. Stradiotto *J. Am. Chem. Soc.* **2010**, *132*, 413.

65 B. M. Cochran, F. E. Michael *J. Am. Chem. Soc.* **2008**, *130*, 2786.

66 a) P. J. Walsh, A. M. Baranger, R. G. Bergman *J. Am. Chem. Soc.* **1992**, *114*, 1708; b) A. M. Baranger, P. J. Walsh, R. G. Bergman *J. Am. Chem. Soc.* **1993**, *115*, 2753; c)J. L. Polse, R. A. Andersen, R. G. Bergman *J. Am. Chem. Soc.* **1998**, *120*, 13405.

67 a) P. L. McGrane, T. Livinghouse *J. Am. Chem. Soc.* **1993**, *115*, 11485; b) P. L. McGrane, T. Livinghouse *J. Org. Chem.* **1992**, *57*, 1323; c) D. Duncan,T. Livinghouse *Organometallics* **1999**, *18*, 4421.

68 D. V. Gribkov, K. C. Hultzsch *Angew.Chem.* **2004**, *116*, 5659; *Angew. Chem. Int. Ed.* **2004**, *43*, 5542.

69 a) J. A. Bexrud, J. D. Beard, D. C. Leitch, L. L .Schafer *Org. Lett. 2005*, *7*, 1959; b) H. Kim, P. H. Lee, T. Livinghouse *Chem. Commun.* **2005**, 5205; c) C. Müller, C. Loos, N. Schulenberg, S. Doye *Eur. J. Org. Chem.* **2006**, 2499.

70 D. A. Watson, M. Chiu, R. G. Bergman *Organometallics* **2006**, *25*, 4731.

71 M. C. Wood, D. C. Leitch, C. S. Yeung, J. A. Kozak, L. L. Schafer *Angew. Chem.* **2006**, *119*, 358; *Angew.Chem.Int.Ed.* **2006**, *46*, 354.

72 a) A. L. Gott, A. J. Clarke, G. J. Clarkson, P. Scott *Chem. Commun.* **2008**, 1422; b) G. Zi, F. Zhang, L. Xiang, Y. Chen, W. Fang, H. Song *Dalton Trans.* **2010**, *39*, 4048; c) A. L. Reznichenko, K. C. Hultzsch *Organometallics* **2010**, *29*, 24.

2

Facing Unexpected Reactivity Paths with Group IV Pyridylamido Polymerization Catalysts

2.1 Abstract

This work provides original insights to the better understanding of the complex structure-activity relationship of M^{IV}-pyridylamido-based (M = Zr, Hf) olefin polymerization catalysts highlighting the importance of the metal precursor choice [$M^{IV}(NMe_2)_4$ *vs.* $Zr^{IV}(Bn)_4$] while preparing precatalysts of unambiguous identity. A temperature-controlled and reversible σ-bond metathesis/protonolysis reaction is found to take place on the M^{IV}-amido complexes in the 298-383 K temperature range, changing the metal coordination sphere dramatically [from five-coordinated tris-amido species stabilized by bidentate monoanionic $\{N,N^-\}$ ligands to six-coordinated bis-amido-mono-amino complexes featured by tridentate dianionic $\{C^-,N,N^-\}$ ones]. Well-defined neutral Zr^{IV}-pyridylamido complexes have been prepared from $Zr(Bn)_4$ as a metal source. Their cationic derivatives $[Zr^{IV}\{C^-,N,N^-\}]^+B(C_6F_5)_4^-$ have been successfully applied to the room-temperature polymerization of 1-hexene with productivities up to one order of magnitude higher than those reported for the related Hf^{IV} state-of-the-art systems. Most importantly, a linear increase of the poly(1-hexene) M_n values (from 30 to 250 kg mol^{-1}) has been observed upon catalyst aging. According to that, the major active species (responsible for the increased M_n polymer values), in the aged catalyst solution, has been identified.

2.2 Introduction

In the past decades, "nonmetallocene" or "postmetallocene" complexes have attracted considerable attention in α-olefin polymerization chemistry. Group IV metal alkyls or amides, in combination with a number of nitrogen-containing ligands, are the basis of non-conventional, highly efficient and selective catalyst precursors of great promise for polyolefin production.

One of the most exciting classes of catalysts recently discovered by researchers at Symyx Technologies and The Dow Chemical Company followed by a fruitful collaboration between industry and academia is based on the C_1-symmetric arylcyclometallated pyridylamido Hf^{IV}-systems,[1] whose optimization was made possible by the use of high-throughput parallel screening techniques. This class of compounds has been successfully applied to the production of highly isotactic and high molecular weight polypropylenes in high-temperature solution processes[2] and olefin-based block copolymers through chain-shuttling polymerization.[3] Due to the utility of these complexes in the production of specialty polyolefins, many research efforts have been devoted to ascertain the identity of the true active species involved in the polymerization process, as well as to provide reliable mechanistic understandings of the polymerization processes.[2b,c] Overall, these studies have provided fundamental insights into the wealth of organometallic chemistry of nitrogen-based early transition metal complexes, highlighting at the same time their unique polymerization characteristics.

An unquestionable identification of the catalyst precursor along with the knowledge of the true active species involved in the process is of crucial importance for the design of improved catalytic structures and the study of novel catalytic processes. Tetrakis(dimethylamide) $M^{IV}(NMe_2)_4$ (M = Zr, Hf) are commonly used metal

precursors in the synthesis of organometallic derivatives by transamination reactions. In addition, Group IV amido-metal complexes are known to undergo intramolecular σ-bond metathesis,[1] providing unconventional cyclometallated frameworks.

Studies conducted on differently substituted aminopyridine ligands in the presence of $M^{IV}(NMe_2)_4$ (M = Zr, Hf) led to systems that revealed the presence of interconverting pyridylamido tautomers. One distinguishing structural feature of these species is the formation of a temperature-induced and reversible Zr^{IV}-C_{Aryl} bond, which makes the comprehension of their activation and polymerization mechanisms less evident. In the first part of this work we report a full account on the σ-bond metathesis/protonolysis process as observed by the combination of a series of 6-aryl substituted aminopyridine ligands with $M^{IV}(NMe_2)_4$ (M = Zr, Hf).

Aimed at highlighting the central role of the metal precursor choice in the production of well-defined molecular catalysts, a direct comparison between $M^{IV}(NMe_2)_4$ and $Zr^{IV}(Bn)_4$ has been systematically carried out. In particular, while studying the 1-hexene polymerization upon activation of selected dibenzyl catalyst precursors with strong Lewis acids, we came across an unusual effect of the catalyst aging time on both polymer molecular mass (M_n) and mass distribution (M_w/M_n) modality. An in-depth investigation of the activated catalytic species present in solution at different aging times (and in the absence of the monomer) has highlighted a progressive active species modification. If broad molecular weight distributions are reasonably consistent with polymers produced by multiple active sites (the latter being typically generated by permanent monomer-ligand modifications of the originally activated species), a catalyst modification occurring *before the monomer addition* adds additional layers of complexity to the identification of the active species operating in these polymerization processes.

2.3 Results and Discussions

2.3.1 Synthesis of aryl or heteroaryl aminopyridinate ligands.

While iminopyridyl ligands are well suited for stabilizing late transition metal complexes, early metals are much more electrophilic and prone to react at the amine moiety. Thus, the chemistry of early- and some mid-transition metals is more widely described by amidoalkylpyridyl ligation.

With regard to that we have synthetized a series of aminopyridinate ligands, bearing different aryl or heteroaryl substituents on the six position of the pyridine ring. The 6-aryl or heteroaryl-substituted ligands (**11a-11d**) were straightforwardly prepared, in fairly good yields (78-90% of isolated product), by simply imine reduction of the related iminopyridines (**6a, 6b, 10a, 10b**) by treatment with $NaCNBH_3/AcOH$[4] (**Scheme 2.1**).

All aminopyridinate lygands appears as off-white oils after extractive workup and solvent evaporation. Recrystallization from hot MeOH gave the pure compounds as white crystals with melting points ranging from 55 to 88 °C.

Palladium catalyzed C-C bond coupling is a widely used approach for the introduction of aryl or heteroaryl moieties on the 6-position of the pyridine ring. Consequently, a Suzuki reaction[5,6], between **3** and phenylboronic acid, or Stille protocol[6,7], between α-Br-pyridine derivative (**7**) and furan-2-yltrimethylstannane (**8)** or trimethyl(thiophen-2-yl)stannane (**9**) has been conveniently adopted for preparing 6-aryl or heteroaryl-2-iminopyridyl ligands (**6a, 6b, 10a** and **10b**) in multigram scale according to the procedures reported in the literature[8] or with slight modification.[9]

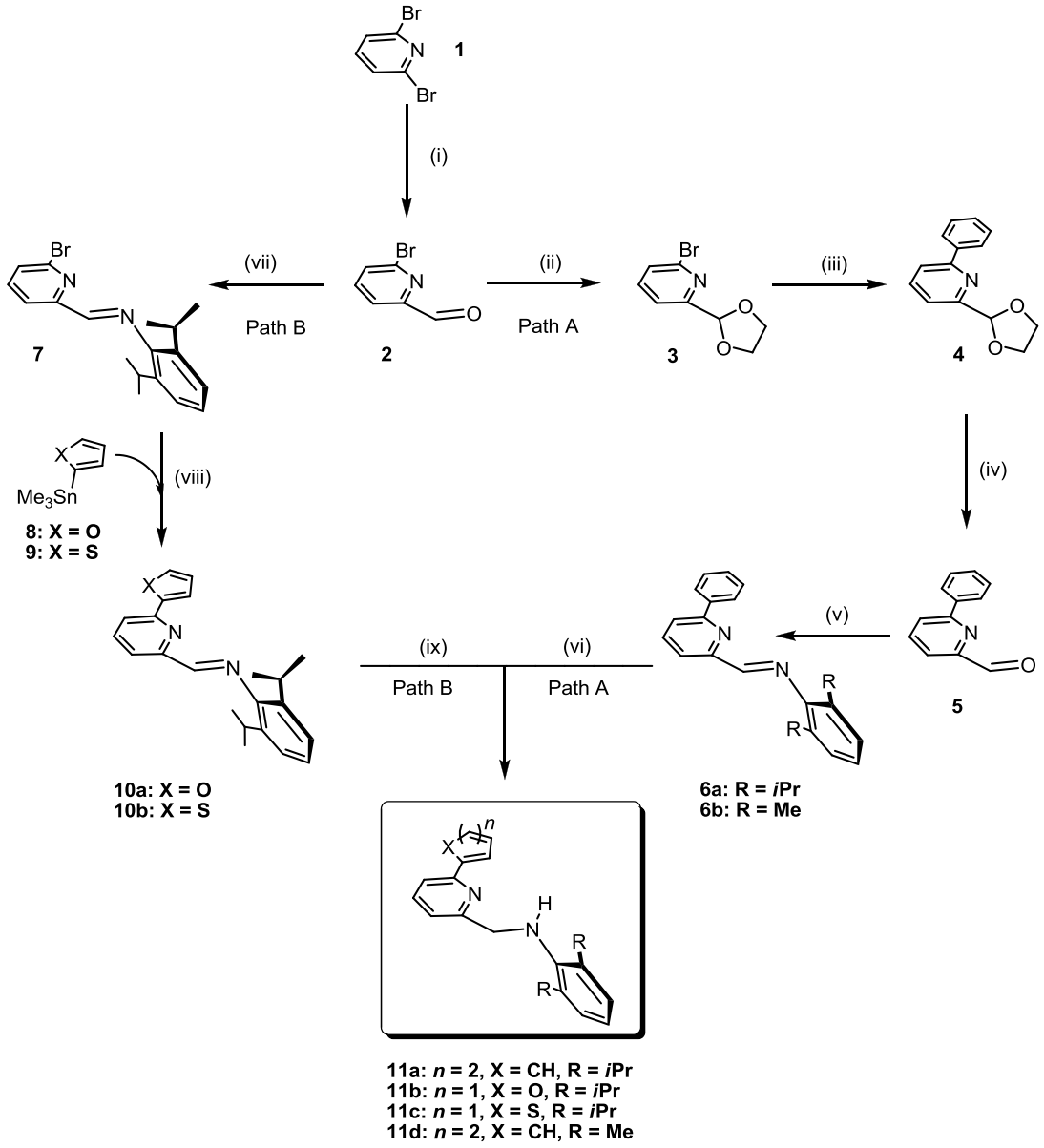

Scheme 2.1. Synthesis of the ligands (**11a**-**11d**). Reaction conditions: (i) tBuLi, DMF, Et_2O, -78 °C; (ii) 1,2-etandiolo, PTSA *cat.*, benzene, reflux; (iii) $PhB(OH)_2$, $Pd(dba)_2/PPh_3$ *cat.*, Na_2CO_3, toluene, MeOH, H_2O, 80 °C; (iv) 2M HCl, H_2O, 85 °C; (v) 2,6-diisopropylaniline or 2,6-dimethylaniline, HCOOH *cat.*, MeOH, r.t; (vi) $NaBH_3CN$, AcOH, THF,MeOH, 0 °C; (vii) 2,6-diisopropylaniline, HCOOH *cat.*, MeOH, r.t; (viii) furan-2-yltrimethylstannane (**8**) or trimethyl(thiophen-2-yl)stannane (**9**), $Pd(dba)_2/PPh_3$ *cat.*, toluene, reflux; (ix) $NaBH_3CN$, AcOH, THF,MeOH, 0 °C.

2.3.2 Synthesis of Zr^{IV}-Hf^{IV}-pyridylamido complexes from $M^{IV}(NMe_2)_4$ (M = Zr, Hf) as metal precursors.

As part of continuing interest in developing early-transition-metal based systems for efficient and selective olefin upgrade,[8] we have studied the reactivity of a series of aminopyridinate ligands (**11a**, **11b**, **11c**), bearing different aryl or heteroaryl

substituents on the six position of the pyridine ring, in combination with $M^{IV}(NMe_2)_4$ (M = Zr, Hf) as metal precursors.

The transamination reaction between $M^{IV}(NMe_2)_4$ (M = Zr, Hf) and the aminopyridinate ligands **11a**, **11b** and **11c** proceeded smoothly already at room temperature in toluene or benzene, with loss of only one dimethylamine molecule. In a typical procedure, the reaction course was followed by sampling mixtures at different reaction times until complete ligand consumption and analyzing the crude product obtained after solvent removal by ^{1}H NMR spectroscopy. The reaction workup lead to the tris-amido complexes $\mathbf{12_{Ph(Zr)}}$ and $\mathbf{13_{Fu(Zr)}}$ as air and moisture-sensitive, dark-yellow, microcrystalline solids in more than 90% yield with **11a** and **11b** respectively, while for the reactions with **11c** and Zr^{IV}- or $Hf^{IV}(NMe_2)_4$, the reaction workup lead to pale-yellow solids, whose 1H NMR (toluene-d_8, 298 K) revealed the coexistence of two distinct isomeric forms (tautomers $\mathbf{14_{Th(Zr)}}$/$\mathbf{14'_{Th(Zr)}}$ and $\mathbf{15_{Th(Hf)}}$/$\mathbf{15'_{Th(Hf)}}$) in about 70:30 and 80:20 ratios respectively, with the minorities being unambiguously attributed to the hexacoordinated cyclometallated $N_2{}^{Th}Zr^{IV}(NMe_2)_2(\eta^1\text{-}HNMe_2)$ and $N_2{}^{Th}Hf^{IV}(NMe_2)_2(\eta^1\text{-}HNMe_2)$ species ($\mathbf{14'_{Th(Zr)}}$ and $\mathbf{15'_{Th(Hf)}}$) with a dimethylamine ligand as part of the metal coordination sphere (**Scheme 2.2**).

The ^{1}H NMR spectra at room temperature (298 K) showed very similar patterns for the systems $\mathbf{12_{Ph(Zr)}}$ and $\mathbf{13_{Fu(Zr)}}$; only one broad resonance for the Zr-NMe_2 methyl protons was observed [δ = 2.85 ppm ($\mathbf{12_{Ph(Zr)}}$); 2.86 ppm ($\mathbf{13_{Fu(Zr)}}$)], indicating a rapid equilibration of the NMe_2 ligands on the NMR time scale. The most relevant spectral features were given by a pair of diastereotopic isopropyl methyl resonances [two doublets at 1.42 and 1.58 ppm ($\mathbf{12_{Ph(Zr)}}$) and 1.32 and 1.48 ppm ($\mathbf{13_{Fu(Zr)}}$)] with a single –C*H*Me_2 septet [3.82 ppm ($\mathbf{12_{Ph(Zr)}}$) and 3.73 ppm ($\mathbf{13_{Fu(Zr)}}$)] and a single resonance for the bridging PyCH_2N moiety [4.92 ppm ($\mathbf{12_{Ph(Zr)}}$) and 4.77 ppm ($\mathbf{13_{Fu(Zr)}}$)]. 1D variable-

temperature ^{1}H NMR spectroscopy (toluene-d_8, 298-383 K) of $\mathbf{12_{Ph(Zr)}}$ and $\mathbf{13_{Fu(Zr)}}$ showed the coexistence of two distinct isomeric forms in solution at high temperature, with the minor component being unambiguously attributed to the hexacoordinated cyclometallated $N_2^{Ar}Zr(NMe_2)_2(\eta^1\text{-}HNMe_2)$ species $\mathbf{12'_{Ph(Zr)}}$ and $\mathbf{13'_{Fu(Zr)}}$ with a dimethylamine ligand as part of the metal coordination sphere (**Scheme 2.2**). In contrast with the thienyl-containing system, where the two equilibrating tautomers were already present at room temperature in a 70:30 ($\mathbf{14_{Th(Zr)}/14'_{Th(Zr)}}$) and 80:20 ($\mathbf{15_{Th(Hf)}/15'_{Th(Hf)}}$) molar ratios, $\mathbf{12_{Ph(Zr)}}$ and $\mathbf{13}_{\mathbf{Fu(Zr)}}$ represented almost the only detectable species in solution at room temperature.

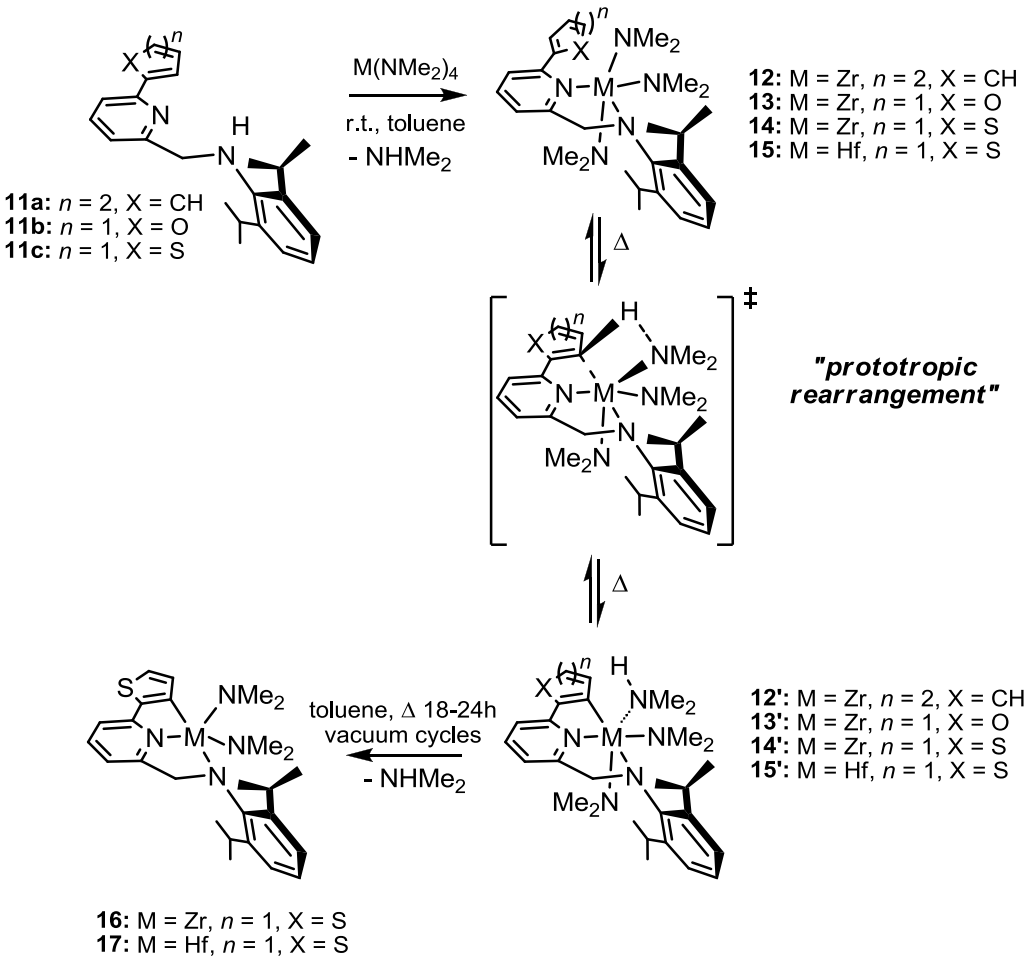

Scheme 2.2. Synthesis of Group IV amido complexes stabilized by nitrogen-containing ligands capable to undergo reversible and temperature-controlled σ-bond metathesis/protonolysis.

Varying the temperature from 298-383 K an inter-conversion of the isomeric mixtures from the initial 99:1 ratio to 58:42 (**12**$_{Ph(Zr)}$/**12'**$_{Ph(Zr)}$) and 38:62 (**13**$_{Fu(Zr)}$/**13'**$_{Fu(Zr)}$) took place (**Figure 2.2**).

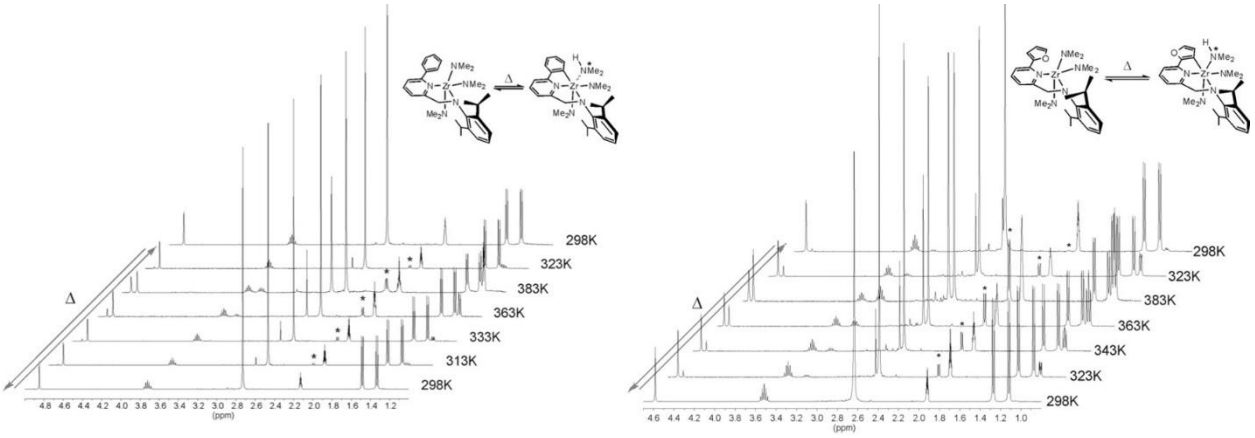

Figure 2.2. Selected VT ^{1}H NMR (400 MHz, C_7D_8, $5 \geq \delta$ (ppm) ≥ 1) spectra of **12**$_{Ph(Zr)}$/**12'**$_{Ph(Zr)}$ (left) and **13**$_{Fu(Zr)}$/**13'**$_{Fu(Zr)}$ (right).

The ^{1}H NMR spectra for the systems **14**$_{Th(Zr)}$/**14'**$_{Th(Zr)}$ and **15**$_{Th(Hf)}$/**15'**$_{Th(Hf)}$ at room temperature (298 K) showed two broad resonance for the M^{IV}-NMe_2 (M = Zr, Hf) methyl protons [2.80 ppm (**14**$_{Th(Zr)}$), 2.84 ppm (**14'**$_{Th(Zr)}$) and 2.77 ppm (**15**$_{Th(Hf)}$), 2.82 ppm (**15'**$_{Th(Hf)}$)] that integrated respectively 18 and 12 protons. The doublet centered at 2.22 for **14'**$_{Th(Zr)}$ and at 2.18 for **15'**$_{Th(Hf)}$ was assigned instead to the methyl of the dimethylamine strongly coordinated to the metal center. The signals for the isopropyl groups and for the bridging PyCH_2N moiety were all split for the concomitant presence of the two isomers **14**$_{Th(Zr)}$/**14'**$_{Th(Zr)}$ and **15**$_{Th(Hf)}$/**15'**$_{Th(Hf)}$ at room temperature (298 K). Varying the temperature from 238 to 373 K resulted in the inter-conversion of the isomeric mixture of **14**$_{Th(Zr)}$/**14'**$_{Th(Zr)}$ from 94/6 to 25/75 ratio and from 298 to 373 K for **15**$_{Th(Hf)}$/**15'**$_{Th(Hf)}$ from 83:17 to 11:89, respectively (from ^{1}H-NMR signal integration, **Figure 2.3**).

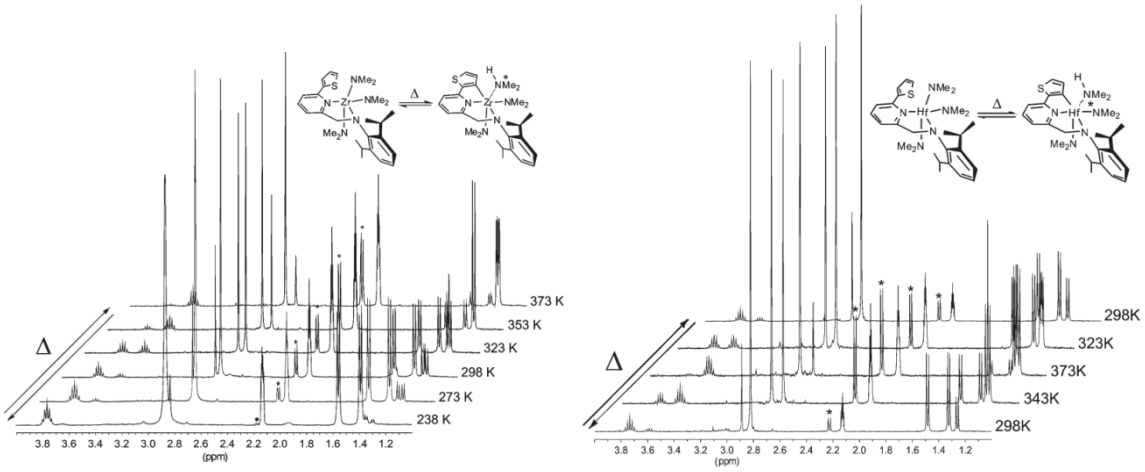

Figure 2.3. Selected VT ^{1}H NMR (400 MHz, C_7D_8, $4 \geq \delta$ (ppm) ≥ 1) spectra of $\mathbf{14_{Th(Zr)}/14'_{Th(Zr)}}$ (left) and $\mathbf{15_{Th(Hf)}/15'_{Th(Hf)}}$ (right).

From a careful process analysis, it appears that the Me_2N-H/C_β^{Ar}-M protonolysis competes with the C_β^{Ar}-H/M-NMe_2 σ-bond metathesis (M = Zr, Hf), the latter being predominant at high temperature.

Noteworthy, in all systems studied under variable temperature, a complete reversibility of the process was maintained throughout several thermal cycles with no apparent mixture decomposition.

Moreover, the dimethylamine generated upon the cyclometallation reaction strongly coordinates the metal center[10] as a non-innocent ligand, ultimately acting as a temperature-controlled proton shuttle for the M-C_{Ar} bond protonolysis.[11]

Consequently, the reversible σ-bond metathesis/protonolysis reaction, controlled by the temperature, changes the metal coordination sphere dramatically [from five-coordinated tris-amido species stabilized by bidentate monoanionic *{N,N⁻}* ligands to six-coordinated bis-amido-mono-amino complexes featured by tridentate dianionic *{C⁻,N,N⁻}* ones].

No example of controlled methathesis/protonolysis has been reported in the literature so far. Moreover, it is generally accepted that C-H bond activations on early-transition-

metal species are irreversibly inhibited in the presence of protic groups like alcohols or amines.[11]

Finally, a prolonged heating (18-24 h) of the mixture of the thienyl derivatives $\mathbf{14}_{\mathbf{Th(Zr)}}/\mathbf{14'}_{\mathbf{Th(Zr)}}$ and $\mathbf{15}_{\mathbf{Th(Hf)}}/\mathbf{15'}_{\mathbf{Th(Hf)}}$ in refluxing toluene, combined with static vacuum cycles, yielded the amine-free species $N_2^{Th}M^{IV}(NMe_2)_2$ (M = Zr, Hf) **16** and **17** as analytically pure yellow-brown and dark-brown microcrystalline solids in 93% and 95% yield, respectively (**Scheme 2.2**).[12]

Contrary to the previous cases, a prolonged heating (24-48 h) of both mixtures $\mathbf{12}_{\mathbf{Ph(Zr)}}/\mathbf{12'}_{\mathbf{Ph(Zr)}}$ and $\mathbf{13}_{\mathbf{Fu(Zr)}}/\mathbf{13'}_{\mathbf{Fu(Zr)}}$ did not eliminate the metal-coordinated $NHMe_2$ but a progressive system decomposition took place instead.

Thermodynamic standard parameters for the tautomeric interconversions of $\mathbf{12}_{\mathbf{Ph(Zr)}}/\mathbf{12'}_{\mathbf{Ph(Zr)}}$, $\mathbf{13}_{\mathbf{Fu(Zr)}}/\mathbf{13'}_{\mathbf{Fu(Zr)}}$, $\mathbf{14}_{\mathbf{Th(Zr)}}/\mathbf{14'}_{\mathbf{Th(Zr)}}$ and $\mathbf{15}_{\mathbf{Th(Hf)}}/\mathbf{15'}_{\mathbf{Th(Hf)}}$ were calculated from the respective linear van't Hoff fits (**Figure 2.4** and **Figure 2.5**). The linearity of van't Hoff plots indicates no appreciable heat capacity changes for all the processes over the 313-363 K temperature range; their calculated thermodynamics at 298 K are reported in **Table 2.1**.

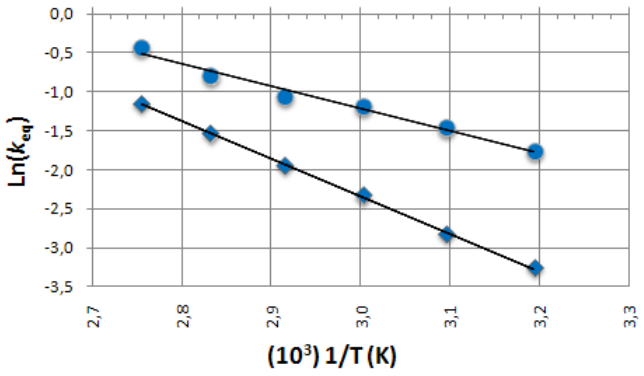

Figure 2.4. The van't Hoff plots for $\mathbf{12}_{\mathbf{Ph(Zr)}}/\mathbf{12'}_{\mathbf{Ph(Zr)}}$ (♦) and $\mathbf{13}_{\mathbf{Fu(Zr)}}/\mathbf{13'}_{\mathbf{Fu(Zr)}}$ (●) tautomeric equilibration.

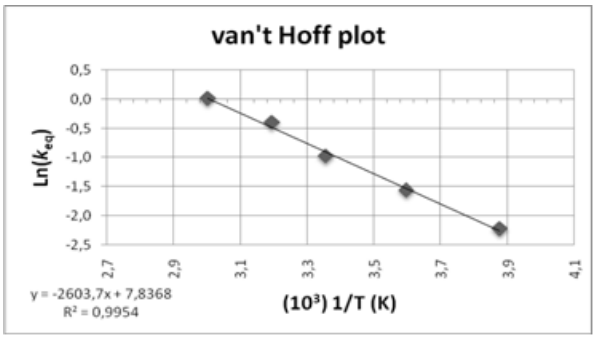

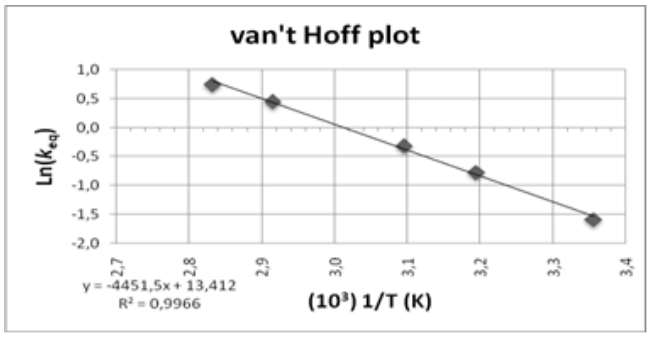

Figure 2.5. The van't Hoff plots for $\mathbf{14_{Th(Zr)}/14'_{Th(Zr)}}$ (left) and $\mathbf{15_{Th(Hf)}/15'_{Th(Hf)}}$ (right) tautomeric equilibration.

	ΔH^0 kcal mol^{-1}	ΔS^0 cal K^{-1} mol^{-1}	ΔG^0 kcal mol^{-1}
$\mathbf{12_{Ph(Zr)}/12'_{Ph(Zr)}}$	9.53 ± 0.2	23.93 ± 0.5	2.39 ± 0.08
$\mathbf{13_{Fu(Zr)}/13'_{Fu(Zr)}}$	5.66 ± 0.2	14.57 ± 0.6	1.32 ± 0.06
$\mathbf{14_{Th(Zr)}/14'_{Th(Zr)}}$	5.17 ± 0.2	15.56 ± 0.6	0.53 ± 0.02
$\mathbf{15_{Th(Hf)}/15'_{Th(Hf)}}$	8.84 ± 0.3	26.63 ± 1	0.90 ± 0.02

Table 2.1. Calculated thermodynamic parameters for the tautomeric equilibration of $\mathbf{12_{Ph(Zr)}/12'_{Ph(Zr)}}$, $\mathbf{13_{Fu(Zr)}/13'_{Fu(Zr)}}$, $\mathbf{14_{Th(Zr)}/14'_{Th(Zr)}}$ and $\mathbf{15_{Th(Hf)}/15'_{Th(Hf)}}$.

Density functional theory calculations carried out on all the real systems at the M06/6-31G* level of theory (toluene, *Polarizable Continuum Model* - PCM) have contributed to elucidate the mechanism of the observed tautomerism and to confirm (whenever possible) the calculated thermodynamics. All the processes present positive ΔE profiles associated with the formation of the cyclometallated species [$\Delta E(\mathbf{12_{Ph(Zr)}/12'_{Ph(Zr)}})$ = +8.8 kcal mol^{-1}; $\Delta E(\mathbf{13_{Fu(Zr)}/13'_{Fu(Zr)}})$ = +4.8 kcal mol^{-1} and $\Delta E(\mathbf{14_{Th(Zr)}/14'_{Th(Zr)}})$ = +6.1 kcal mol^{-1}, **Figure 2.6** (left) and **Figure 2.7**], with higher energy barriers for $\mathbf{12_{Ph(Zr)}/12'_{Ph(Zr)}}$ and $\mathbf{13_{Fu(Zr)}/13'_{Fu(Zr)}}$ (equal to 28.7 kcal mol^{-1}, 26.5 kcal mol^{-1} for $\mathbf{TS_{12/12}}$, and $\mathbf{TS_{13/13}}$, respectively) compared with that calculated for the thiophene analogue $\mathbf{14_{Th(Zr)}/14'_{Th(Zr)}}$ (19.2 kcal mol^{-1}). In the optimized geometry of $\mathbf{13_{Fu(Zr)}}$ or $\mathbf{14_{Th(Zr)}}$, the heteroaryl substituent is not coordinated to the metal center [final d(Zr-O) = 3.21 Å and d(Zr-S) = 3.76 Å], the heterocyclic ring being tilted away with respect to the pyridine central core [$\theta(N_{Py}\text{-C-C-O}_{Fu})$ = 26° and $\theta(N_{Py}\text{-C-C-O}_{Th})$ = 47°]. This suggests that the presence of the three amido groups on zirconium is enough to satisfy the electronic requirements of the electron-poor early-transition-metal ion. The

computational results match reasonably well with the experimental ΔH° values calculated from the vant'Hoff plots (9.53, 5.66 and 5.17 kcal mol^{-1} for the phenyl, furanyl and thiophenyl system, respectively). At odds with the thiophene-containing complex, where in line with the experimental results an extra energy of 15.6 kcal mol^{-1} is required in order to obtain the amine-free complex **16**, the internal energy levels of the {**12**'' + $NHMe_2$} or {**13**'' + $NHMe_2$} systems obtained after dimethylamine loss (and concomitant formation of the corresponding diamido derivative) lie *below* that of $\mathbf{TS_{12/12'}}$ or $\mathbf{TS_{13/13'}}$. Such a result does not mirror the experimental findings.

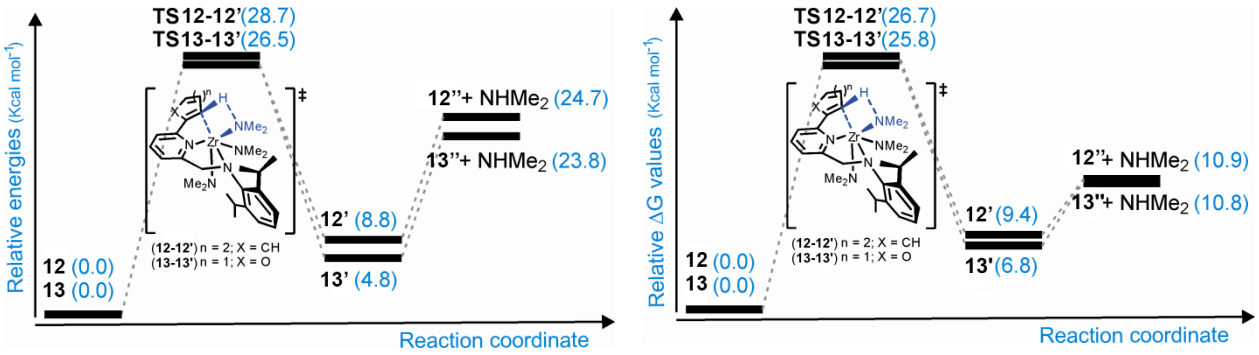

Figure 2.6. Calculated internal energies (Δ*E*, toluene) (left) and Gibbs free energy (Δ*G*, gas phase) values (right) for the $\mathbf{12_{Ph(Zr)}/12'_{Ph(Zr)}}$, $\mathbf{13_{Fu(Zr)}/13'_{Fu(Zr)}}$ tautomeric equilibrations and amine loss with generation of the diamido complex **12''** and **13''**. Refer to the ESI for the structures of the corresponding optimized geometries.

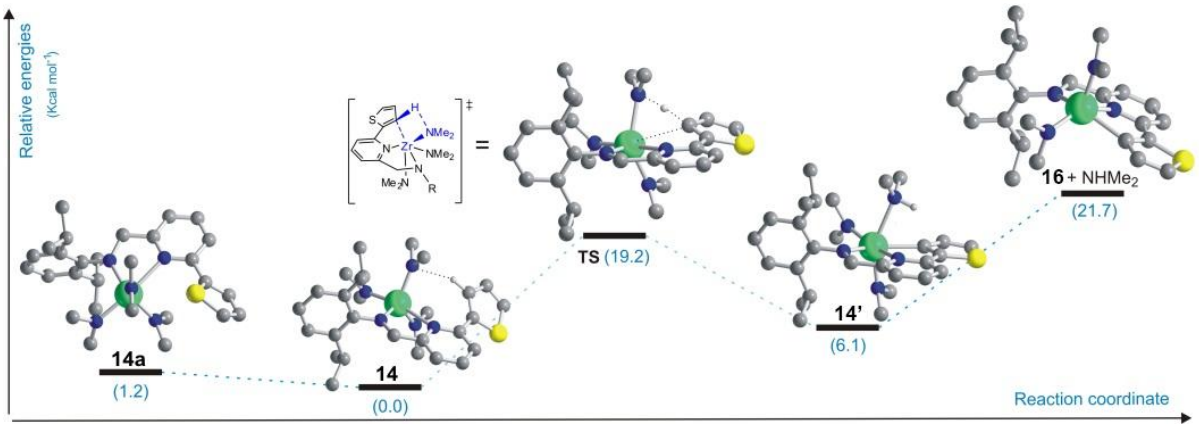

Figure 2.7. Energy profile in toluene for the C-H bond activation of the thiophene ring of $\mathbf{14a_{Th(Zr)}}$ and optimized structures for $\mathbf{14a_{Th(Zr)}}$, $\mathbf{14_{Th(Zr)}}$, **TS**, $\mathbf{14'_{Th(Zr)}}$ and **16**.

Different entropic factors in the gas phase and in solution are expected (S^{gas} *vs.* S^{sol}), mainly because of solvation phenomena that cannot be taken into account properly in

the computation. According to this, the Gibbs (*G*) rather than the internal (*E*) energy differences should be evaluated for this step. In fact, in the real sample the solvent molecules surrounding the metal complex severely limit the translational/rotational freedom of molecular fragments. This ultimately translates into significant ΔG^{gas} / ΔG^{solv} differences. The ΔG^{gas} values related to the formation of the {diamido complex + $NHMe_2$} ensemble reveal that the amine loss is only slightly endothermic [ΔG^{gas}(**12**' // **12**'' + $NHMe_2$) = + 1.5 kcal mol^{-1}; ΔG^{gas}(**13**' // **13**'' + $NHMe_2$) = + 4.0 kcal mol^{-1}, **Figure 2.6** (right)]. Smaller ΔG^{gas} than ΔE^{gas} values are in line with the positive entropy variation during the amine loss. Unfortunately, the evaluation of ΔG^{solv} is not trivial; no general procedure is given to assign a precise value to ΔG^{solv} within the continuum PCM approach.[13]

These results constitute a useful reference to gain additional insights into C-H bond functionalization reactions of early-transition-metal complexes, highlighting at the same time unexpected reactivity paths in the field of polymerization catalysis. Indeed, the well-established efficiency of Group IV pyridylamido catalysts (in high-temperature solution processes, in particular) for the production of specialty polyolefins[1,3,14,15] invariably relies on distinctive structural features of these catalyst precursors. In recent papers Macchioni *et al*. have developed a detailed understanding of the polymerization mechanisms with a series of arylcyclometallated Hf^{IV} pyridylamido complexes.[2b,c] These studies provide clear evidence of the fundamental role played by the unusual Hf-C^{Ar} bonds, emphasizing the importance of the true identification of the active species while studying new catalytic processes or designing improved catalytic structures. On this ground, a reliable identification of the *catalyst precursor* is also of crucial importance; in this context, the reactivity outlined above (temperature-induced tautomeric interconversions) is expected to add further layers of complexity to the

understanding of both activation and polymerization mechanisms. Indeed, the temperature-induced change occurring at the metal coordination sphere of the M^{IV} pyridylamido precatalysts [from five-coordinated species (**12**$_{Ph(Zr)}$, **13**$_{Fu(Zr)}$, **14**$_{Th(Zr)}$ and **15**$_{Th(Hf)}$) stabilized by bidentate monoanionic $\{N,N^-\}$ ligands to six-coordinated complexes (**12'**$_{Ph(Zr)}$, **13'**$_{Fu(Zr)}$, **14'**$_{Th(Zr)}$ and **15'**$_{Th(Hf)}$) with tridentate dianionic $\{C^-,N,N^-\}$ ones] limits the complete understanding of the structure-activity relationship.

Ethylene polymerization tests have been carried out with pre-catalysts **12**$_{Ph(Zr)}$/**12'**$_{Ph(Zr)}$, **13**$_{Fu(Zr)}$/**13'**$_{Fu(Zr)}$, **14**$_{Th(Zr)}$/**14'**$_{Th(Zr)}$ and **16**, using methylaluminoxane (MAO) as activator (Al/Zr > 1000) in the 40-80°C range of temperature. TOFs and GPC profiles for the HDPEs produced suggest that only the *ortho*-metallated species are responsible for the generation of catalytically active forms. The TOFs observed with (**14**$_{Th(Zr)}$/**14'**$_{Th(Zr)}$) are in fact comparable to those obtained with **16** when only the molar percentage of **14'**$_{Th(Zr)}$, at the corresponding temperature, is taken into account (**Table2.2**). Finally, perfectly matching gel permeation chromatography (GPC) traces for the HDPEs produced by the two catalyst precursors, imply identical active species at work.

Table 2.2. Ethylene Polymerization tests with **14**$_{Th(Zr)}$/**14'**$_{Th(Zr)}$ and **16** catalyst precursors[a]

Entry	pre-catalyst[a]	*T*(°C)	PE yield[b] (g)	TOF[c]	% of cyclometallated compound (3 or 4)[d]	T_m (°C)[e]	TOF_{cyclom}[f]
1	**14**$_{Th(Zr)}$/**14'**$_{Th(Zr)}$	40	-	-	40 (**14'**$_{Th(Zr)}$)	-	-
2	**16**	40	-	-	100 (**16**)	-	-
3	**14**$_{Th(Zr)}$/**14'**$_{Th(Zr)}$	50	0.26	1854	45 (**14'**$_{Th(Zr)}$)	121.7	4436
4	**16**	50	0.62	4420	100 (**16**)	122.0	4420
5	**14**$_{Th(Zr)}$/**14'**$_{Th(Zr)}$	70	0.68	4848	59 (**14'**$_{Th(Zr)}$)	122.4	8218
6	**16**	70	1.42	10124	100 (**16**)	122.3	10124
7	**14**$_{Th(Zr)}$/**14'**$_{Th(Zr)}$	80	0.87	6203	61 (**14'**$_{Th(Zr)}$)	120.9	10169
8	**16**	80	1.71	12192	100 (**16**)	121.4	12192

[a] Reaction conditions: catalyst precursor, 20 μmol; MAO equiv. 1000; C_2H_4 pressure, 15 bar; final volume, 50 mL; reaction time, 30 min; 1700 rpm. [b] Average value over three runs. [c] In units of mol of C_2H_4 converted (mol of Zr)$^{-1}$ h^{-1}. [d] The percentage of **14'**$_{Th(Zr)}$ in (**14**$_{Th(Zr)}$/**14'**$_{Th(Zr)}$) mixture, has been determined via ^{1}H-NMR at the corresponding temperature. [e] Determined by DSC. [f] In units of mol of C_2H_4 converted (mol of $Zr_{cylom.}$)$^{-1}$ h^{-1}.

Instead, ethylene polymerization tests conducted with both **12**$_{Ph(Zr)}$/**12'**$_{Ph(Zr)}$/MAO and **13**$_{Fu(Zr)}$/**13'**$_{Fu(Zr)}$/MAO catalytic systems between 298 and 343 K [where the

bidentate monoanionic $\{N,N^-\}$ forms $\mathbf{12_{Ph(Zr)}}$ and $\mathbf{13_{Fu(Zr)}}$ largely prevail over the tridentate dianionic $\{C^-,N,N^-\}$ ones ($\mathbf{12'_{Ph(Zr)}}$ and $\mathbf{13'_{Fu(Zr)}}$)] resulted in only moderately active to almost inactive catalytic systems.[16]

2.3.3 Synthesis of the pyridylamido $Zr^{IV}(Bn)_2$ complexes (18-21) from $Zr^{IV}(Bn)_4$ as alternative metal precursor.

Aiming at the development of tailored catalytic structures active as polymerization catalysis, we have investigated the reactivity of the aminopyridine ligands **11a-d** with $Zr^{IV}(Bn)_4$ as an alternative Zr^{IV} metal precursor (**Scheme 2.3**).

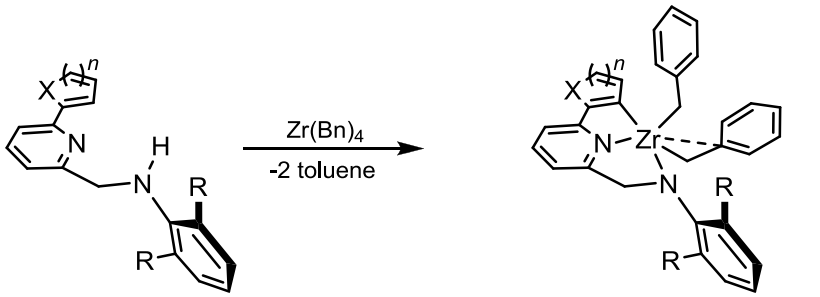

11a: *n* = 2, X = CH, R = ^{i}Pr
11b: *n* = 1, X = O, R = ^{i}Pr
11c: *n* = 1, X = S, R = ^{i}Pr
11d: *n* = 2, X = CH, R = Me

18: *n* = 2, X = CH, R = ^{i}Pr
19: *n* = 1, X = O, R = ^{i}Pr
20: *n* = 1, X = S, R = ^{i}Pr
21: *n* = 2, X = CH, R = Me

Scheme 2.3. Synthesis of the $M^{IV}(Bn)_2$ (M = Zr, Hf) complexes **18-21** stabilized by tridentate dianionic $\{C^-,N,N^-\}$ pyridylamido ligand.

The addition of $Zr^{IV}(Bn)_4$ to a toluene solution of the ligand (**11a-11d**) at room temperature did not generate any product, even after several hours under stirring. This was confirmed by the ^{1}H NMR spectra of the mixture recorded at different reaction times, which showed distinctive signals of the unreacted reagents. On the other hand, progressive ligand consumption took place upon heating the mixture at 70 °C for 12-48 h. The ^{1}H NMR spectroscopic analysis revealed the direct formation of a Zr^{IV}-dibenzyl cyclometallated compound as a unique species with no evidence of putative tribenzyl intermediate generation. Such a result indicates that at higher temperature ligand's N-H

deprotonation and *N,N* chelation of the metal center facilitate the immediate and irreversible *ortho*-metallation step, with concomitant elimination of a second toluene molecule. The ligands' ability to undergo intramolecular C-H bond activation provides clear evidence of the importance of the metal precursor choice for the preparation of well-defined catalysts.

Complexes **18-21**, isolated as air- and moisture-sensitive yellow-brown solids and less light sensitive than the parent tetrabenzyl complexes, were completely characterized by spectroscopic data and X-ray diffraction analyses. The most relevant ^{1}H NMR data for complexes containing isopropyl moieties (**18-20**) are two sets of methyl groups which appear as two well-separated doublets[17] centered at δ = 1.17/1.32 (**18**), 1.05/1.22 (**19**), and 1.15/1.32 (**20**), while a singlet at δ = 2.35 ppm is observed for the resonance of the methyl groups of the *m*-xylyl fragment in **21**. Methylene protons of the residual benzyl groups bound to the metal show an AB pattern[18] centered at δ = 1.91 ppm (**18**, $^{2}J_{HH}$ = 10.0 Hz), 1.53 ppm (**19**, $^{2}J_{HH}$ = 9.6 Hz), 1.74 ppm (**20**, $^{2}J_{HH}$ = 9.6 Hz), and 1.78 ppm (**21**, $^{2}J_{HH}$ = 9.8 Hz). In the ^{13}C{^{1}H} NMR spectra, only one carbon resonance around δ = 68 ppm (for **18-21**) is present for the two methylene groups directly bound to the metal, consistent with two isochronous benzyl groups in solution; ^{1}H and ^{13}C{^{1}H} NMR patterns indicate that all complexes possess C_s-symmetry in solution. Moreover, ^{13}C{^{1}H} NMR spectra of the methylene carbons attached to the metal ion show a $J_{C\text{-}H}$ value of 129-131 Hz (for **18-21**), typical of a weighted average value between a η^1- (120 Hz) and η^2-coordination mode (143 Hz).[19,20] These data confirm the existence of a rapid exchange in solution[21] between η^1- and η^2-coordinated benzyl groups.[22] The ^{1}H and ^{13}C{^{1}H} resonances for the CH_2 groups related to the pyridylamido framework appear at lower field when compared to those of the corresponding free ligands, thus confirming ligand coordination to the zirconium center.

Finally, the M-C^{Ar} bonds generated upon intramolecular cyclometallation are evidenced by a remarkable resonance shift to lower fields of the aromatic carbon directly bound to the metal (189.8, 168.0, 195.4, and 189.7 ppm for **18**-**21**).

All complexes are highly soluble in aromatic and aliphatic hydrocarbons, while they are only sparingly soluble in diethyl ether. Crystals suitable for X-ray analysis were isolated from concentrated solutions of toluene (**18** and **21**) or diethyl ether (**19** and **20**). ORTEP diagrams of the crystal structures of **18**-**21** are given in **Figures 2.6**-**2.9** and **Table 2.3** lists all the main crystal and structural refinement data, whereas selected bond lengths and angles are summarized in **Table 2.4**.

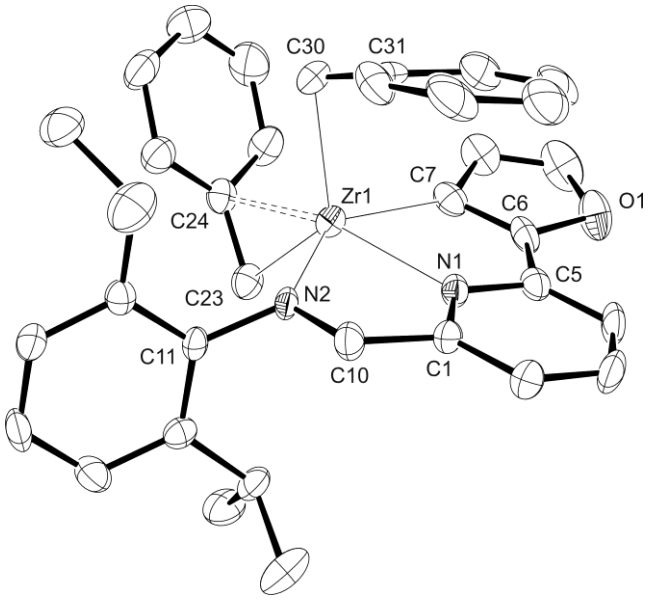

Figure 2.6. Crystal structure of $\mathbf{N_2^{Ph}Zr^{IV}(CH_2Ph)_2}$ (**18**). Thermal ellipsoids are drawn at the 40% probability level. Hydrogen atoms are omitted for clarity.

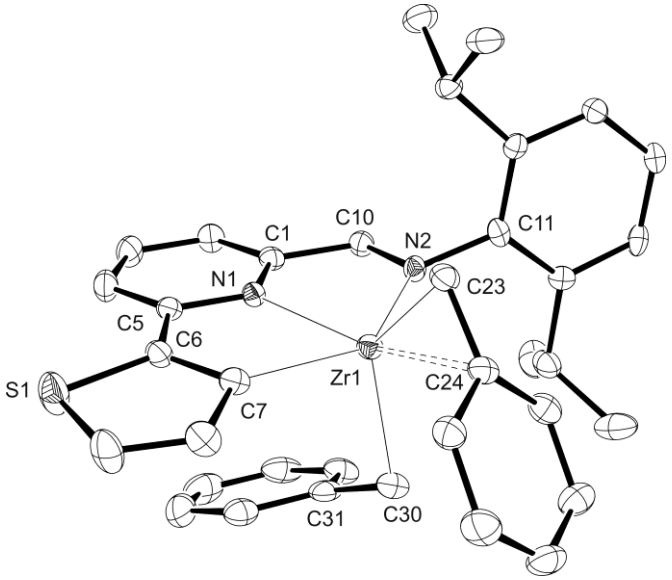

Figure 2.7. Crystal structure of $\mathbf{N_2^{Fu}Zr^{IV}(CH_2Ph)_2}$ (**19**). Thermal ellipsoids are drawn at the 40% probability level. Hydrogen atoms are omitted for clarity.

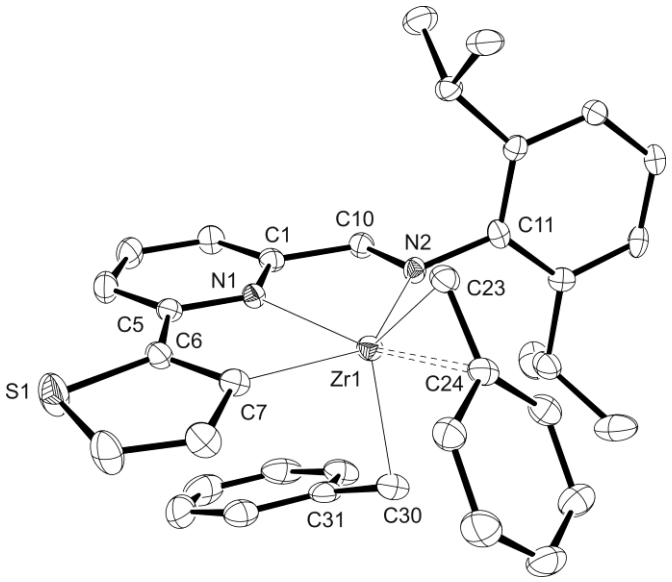

Figure 2.8. Crystal structure of $\mathbf{N_2^{Th}Zr^{IV}(CH_2Ph)_2}$ (**20**). Thermal ellipsoids are drawn at the 40% probability level. Hydrogen atoms and diethyl ether as crystallization solvent are omitted for clarity.

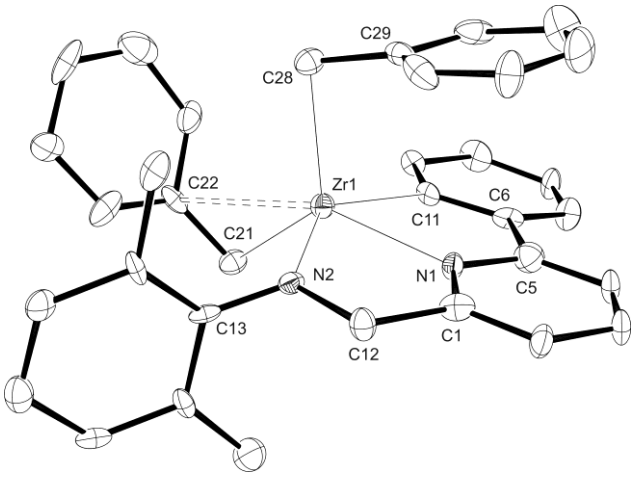

Figure 2.9. Crystal structure of $\mathbf{N_{2(xylyl)}^{ph}Zr^{IV}(CH_2Ph)_2}$ (**21**). Thermal ellipsoids are drawn at the 40% probability level. Hydrogen atoms and toluene as crystallization solvent are omitted for clarity.

The coordination environment at the metal center consists of two nitrogen atoms and one carbon atom from the dianionic tridentate *{C⁻,N,N⁻}* pyridylamido ligand (k^3-coordination) and two benzyl groups. All complexes show a (distorted) trigonal bipyramidal coordination geometry, where the three donor atoms from each ligand occupy the axial positions and the two residual benzyl fragments are placed at the equatorial positions. The k^3- pyridylamido fragments are almost planar, with an average deviation of the metal center from the *{C⁻,N,N⁻}* plane of 0.289 Å (**18**: 0.360(3) Å, **19**: 0.243(4) Å, **20**: 0.257(3) Å, **21**: 0.296(3) Å). The final coordination number at the metal is six, due to a close contact between the zirconium and the *ipso*-carbon of one benzyl group (η^2-coordination). For all complexes, the Zr-N(1) [2.315(2)Å ÷ 2.329(3)Å, **18-21**] and Zr-N(2) [2.090(2)Å ÷ 2.103(2)Å, **18-21**] distances are comparable to those measured for similar Zr^{IV}- pyridylamido systems[14] and the Zr-C^{Ar} bonds [2.313(3)Å ÷ 2.325(4)Å, **18-21**] also fall in the range observed for related structures.[22, 23] As clearly shown by the X-ray study, in the solid state one benzyl group is η^2-coordinated [**18**: Zr···C(26), 2.634(4)Å; Zr-C(25), 2.271(3)Å; Zr-C(25)-C(26), 86.9(2)°. **19**: Zr···C(24), 2.583(4)Å; Zr-C(23), 2.270(4)Å; Zr-C(23)-C(24), 85.0(2)°. **20**: Zr···C(24), 2.599(3)Å;

Zr-C(23), 2.268(3)Å; Zr-C(23)-C(24), 85.70(18)°. **21**: Zr···C(22), 2.687(3)Å; Zr-C(21), 2.289(3)Å; Zr-C(21)-C(22), 88.59(18)°], while the other approaches η^1-coordination to the metal centre (**18**: Zr–C(32), 2.280(3)Å; Zr-C(33), 3.006(4)Å; Zr-C(32)-C(33), 104.4(2)°. **19**: Zr–C(30), 2.279(4)Å; Zr-C(31), 2.878(3)Å; Zr-C(30)-C(31), 98.0(3)°. **20**: Zr–C(30), 2.284(3)Å; Zr-C(31), 2.977(2)Å; Zr-C(30)-C(31), 102.40(19)°. **21**: Zr–C(28), 2.272(3)Å; Zr-C(29), 2.906(4)Å; Zr-C(28)-C(29), 99.4(2)°).[24]

2.3.4 In Situ generation and characterization of cationic monobenzyl pyridylamido Zr^{IV}(Bn) complexes upon activation by either $B(C_6F_5)_3$ or $[Ph_3C][B(C_6F_5)_4]$.

Cationic zirconium complexes **18a-21a** and **18b-21b** were obtained by treatment of the dibenzyl precursors **18-21** with $B(C_6F_5)_3$ or $[Ph_3C][B(C_6F_5)_4]$, respectively. The reaction of **18-21** with one equivalent of $B(C_6F_5)_3$ in benzene-d_6 at room temperature resulted in the clean abstraction of one benzyl group from each complex,[25] with the rapid formation of red-orange zwitterionic species **18a-21a** (**Scheme 2.4**).

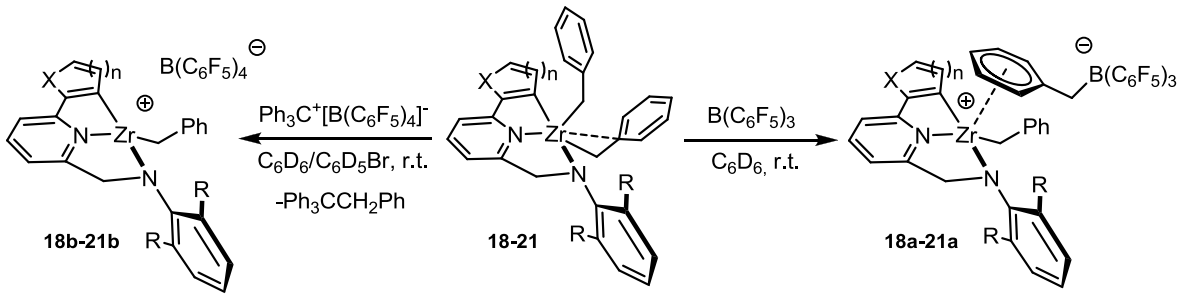

18 and **18a,b**: *n* = 2, X = CH, R = ^{i}Pr
19 and **19a,b**: *n* = 1, X = O, R = ^{i}Pr
20 and **20a,b**: *n* = 1, X = S, R = ^{i}Pr
21 and **21a,b**: *n* = 2, X = CH, R = Me

Scheme 2.4. Synthesis of the cationic **18a,b-21a,b** Zr^{IV}(Bn) complexes from activation of the dibenzyl precursors with either $B(C_6F_5)_3$ or $[Ph_3C][B(C_6F_5)_4]$.

Table 2.3. Crystal data and structure refinement for complexes **18-21**.

	18	**19**	**20 • 0.25 Et_2O**	**21 • 0.5 toluene**
CCDC number	829625	829624	829626	829623
Empirical formula	$C_{38}H_{40}N_2Zr$	$C_{36}H_{38}N_2OZr$	$C_{36}H_{38}N_2SZr$ ¼($C_4H_{10}O$)	$C_{34}H_{32}N_2Zr$ ½(C_7H_8)
Formula weight	614.22	605.90	640.49	605.90
Temperature [K]	100(2)	120(2)	120(2)	120(2)
Wavelength [Å]	0.71069	0.71069	0.71069	0.71069
Crystal system,	Monoclinic,	Triclinic,	Tetragonal,	Monoclinic,
space group	*P* $2_1/n$	*P -1*	*P 4/n*	*C 2/c*
a [Å]	9.522(7)	9.842(3)	26.133(9)	38.208(3)
b [Å]	21.178(14)	12.628(6)	26.133(9)	7.982(4)
c [Å]	16.076(17)	24.285(11)	9.573(5)	19.880(1)
α [°]	90	89.928(4)	90	90
β [°]	106.769(10)	87.846(3)	90	101.145(6)
γ [°]	90	83.873(3)	90	90
V [$Å^3$]	3104(4)	2999(2)	6538(7)	5949(5)
Z, D_c [g m^{-3}]	4, 1.318	4, 1.342	8, 1.301	8, 1.353
Absorption coefficient [mm^{-1}]	0.383	0.397	0.428	0.398
F(000)	1288	1264	2676	2520
Crystal size [mm]	0.01 × 0.05 × 0.05	0.02 × 0.02 × 0.05	0.05 × 0.10 × 0.20	0.05 × 0.05 × 0.1
Θ Range for data collection [°]	3.85 ÷ 26.46	4.14 ÷ 25.44	4.26 ÷ 26.47	4.16 ÷ 27.68
Limiting indices	$-11 \le h \le 10$	$-11 \le h \le 11$	$-27 \le h \le 29$	$-48 \le h \le 49$
	$-22 \le k \le 26$	$-14 \le k \le 14$	$-30 \le k \le 30$	$-10 \le k \le 9$
	$-18 \le l \le 15$	$-29 \le l \le 27$	$-11 \le l \le 11$	$-24 \le l \le 25$
Reflections collected/unique	14873/4629	20708/8633	49810/ 6084	31602/ 6173
GOF on F^2	0.979	0.836	0.809	0.926
Data/restraints/parameters	4629 / 0 / 370	5684 / 0 / 410	6084/0/382	6173/0/361
Final *R* indices [I>2σ(*I*)]	*R*1=0.0382,	*R*1=0.0442,	*R*1= 0.0379,	*R*1= 0.0404,
	w*R*2= 0.0822	w*R*2= 0.0766	w*R*2= 0.0670	w*R*2= 0.0976
R indices (all data)	*R*1=0.0626,	*R*1=0.0932,	*R*1= 0.1060,	*R*1= 0.0708,
	w*R*2= 0.0884	w*R*2= 0.0839	w*R*2= 0.0747	w*R*2= 0.1032
Largest diff. peak and hole [e $Å^{-3}$]	0.391 and –0.392	0.519 and –0.409	0.629 and –0.460	1.189 and –0.466

Table 2.4. Selected bond distances (Å) and angles (°) for complexes **18**-**21**.

	18	**19**	**20**	**21**
Zr-N(1)	2.321(4)	2.329(3)	2.315(2)	2.322(2)
Zr-N(2)	2.090(2)	2.095(3)	2.103(2)	2.097(2)
Zr-C(7)	-	2.321(5)	2.319(3)	-
Zr-C(11)	2.325(4)	-	-	2.313(3)
Zr-C(21)	-	-	-	2.289(3)
Zr-C(22)	-	-	-	2.687(3)
Zr-C(23)	-	2.270(4)	2.268(3)	-
Zr-C(24)	-	2.583(4)	2.599(3)	-
Zr-C(25)	2.271(3)	-	-	-
Zr-C(26)	2.634(4)	-	-	-
Zr-C(28)	-	-	-	2.272(3)
Zr-C(29)	-	-	-	2.906(4)
Zr-C(30)	-	2.279(4)	2.284(3)	-
Zr-C(31)	-	2.878(3)	2.977(2)	-
Zr-C(32)	2.280(3)	-	-	-
Zr-C(33)	3.006(4)	-	-	-
C(21)-C(22)	-	-	-	1.465(4)
C(23)-C(24)	-	1.444(5)	1.450(4)	-
C(28)-C(29)	-	-	-	1.479(4)
C(30)-C(31)	-	1.468(5)	1.481(4)	-
C(25)-C(26)	1.460(5)	-	-	-
C(32)-C(33)	1.473(5)	-	-	-
N(1)-Zr-N(2)	70.96(11)	70.08(14)	70.87(9)	70.76(9)
N(1)-Zr-C(7)	-	70.81(15)	70.45(10)	-
N(1)-Zr-C(11)	68.98(11)	-	-	69.60(10)
C(21)-Zr-C(28)	-	-	-	122.93(11)
C(22)-Zr-C(21)	-	-	-	33.03(10)
C(23)-Zr-C(24)	-	33.86(12)	33.80(9)	-
C(23)-Zr-C(30)	-	124.39(15)	126.07(11)	-
C(25)-Zr-C(26)	33.61(11)	-	-	-
C(25)-Zr-C(32)	124.67(13)	-	-	-
Zr-C(28)-C(29)	-	-	-	99.4(2)
Zr-C(30)-C(31)	-	98.0(3)	102.40(19)	-
Zr-C(32)-C(33)	104.4(2)	-	-	-
N(1)-C(1)-C(10)-C(7)	-	9.4(5)	–2.0(4)	-
N(1)-C(5)-C(6)-C(7)	-	1.1(6)	–2.6(4)	-
N(1)-C(5)-C(6)-$X_{(O,S)}$(1)	-	174.0(3)	–174.4(2)	-
N(1)-C(1)-C(12)-N(2)	–9.8(4)	-	-	–0.15(4)
N(1)-C(5)-C(6)-C(11)	–3.4(4)	-	-	6.04(4)

All the zwitterionic compounds were slightly soluble in benzene or toluene and separated as dark-red semi-solid products upon standing within a few hours. The limited solubility of ion pairs **18a-21a** in aromatic solvents is suggestive of weak ion pairing.[26] The ^{1}H NMR spectrum of **18a** $[N_2^{Ph}Zr^{IV}(CH_2Ph)]^+[B(CH_2Ph)(C_6F_5)_3]^-$ shows the presence of four non-equivalent Me groups from the two ^{i}Pr fragments; such a reduced symmetry of the activated complex is due to an η^6-coordination of the benzyl-tris(pentafluorophenyl)borate anion to the metal center. Noteworthy, two sets of diastereotopic methylene protons (AB systems) from the residual ZrCH_2Ph and PyCH_2N fragments appeared at δ = 2.55 and 4.44 ppm, respectively. Finally, the existence of non-equivalent proton signals of the methylene group at the BCH_2Ph moiety (two broad signals at δ = 3.54 and 3.09 ppm) suggests the presence of a close contact between the borate anion and the metal center. As a matter of fact, the ^{19}F NMR spectrum of complex **18a** shows a large Δδ[(*para*F)-(*meta*F)] value of 4.08 ppm which is typical for the borate anions tightly bound to the metal center.[27] In the ^{13}C NMR spectrum of complex **18a** the methylene carbon signal of ZrCH_2Ph appears at δ = 79.76 ppm with a $J_{C\text{-}H}$ value of 131 Hz, indicative of a η^2-coordination of the residual benzyl fragment in the cationic species. Finally, the ^{13}C{^{1}H} NMR signal for the BCH_2Ph carbon appears, as expected, as a broad multiplet centered at δ = 35.49 ppm. Similarly to the procedure reported above, the zwitterionic complexes **19a-21a** were prepared by reacting complexes **19-21** with 1 eq. of $B(C_6F_5)_3$. The activation chemistry of **19-21** is similar to that described for **18**, leading to highly unsymmetrical species (**19a-21a**) characterized by four non-equivalent Me groups (from the two ^{i}Pr fragments) and well defined AB systems for all residual methylene moieties [ZrCH_2Ph: 2.28 ppm (**19a**), 2.46 ppm (**20a**), 2.44 ppm (**21a**); PyCH_2N: 4.37 ppm (**19a**), 4.39 ppm (**20a**), 4.02 ppm (**21a**); BCH_2Ph 3.51 ppm (**19a**), 3.59 ppm (**20a**), 3.35 ppm (**21a**)].

The cationic monobenzyl complex **18b** was prepared by reacting a benzene solution of the dibenzyl precursor **18** with one equivalent of $[Ph_3C][B(C_6F_5)_4]$ (**Scheme 2.4**). The reaction occurs rapidly and quantitatively at room temperature producing dark-green crystals which precipitate within a few minutes. Due to the weaker coordinating character of the $B(C_6F_5)_4^-$ anion, the ^1H NMR spectrum of **18b** (C_6D_5Br) shows the formation of a C_s symmetric system characterized by only two non-equivalent Me pairs from the ^{i}Pr fragments and two well-defined singlets at δ = 2.84 and 5.04 ppm, assigned to ZrCH_2Ph and to PyCH_2N, respectively. Although poorly soluble in aromatic hydrocarbons such as benzene or toluene, the activated complex is stable in these solvents for days with no apparent decomposition. On the other hand, **18b** is highly soluble in polar aromatics such as mono- or di-halobenzene (halo: Cl, Br) where it forms a deep-orange solution. Unfortunately, polar solvents cause the catalyst decomposition within a few minutes resulting in the separation of rubbery/untreatable dark-brown semi-solid materials. The low solubility of the activated complex **18b** in benzene-d_6 or toluene-d_8, together with its rapid decomposition in polar aromatics, did not allow the complete spectroscopic characterization of this species. Cationic complexes **19b-21b** were prepared similarly by reacting **19-21** in benzene-d_6 with one equivalent of $[Ph_3C][B(C_6F_5)_4]$. ^1H NMR (benzene-d_6) spectra of the supernatants show signals almost exclusively attributed to the benzyltriphenylmethane derivative while those recorded on the solid residues (in either C_6D_5Br or C_6D_5Cl) show similar ^1H NMR patterns to those recorded for **18b** [δ(ZrCH_2Ph) = 2.73 ppm (**19b**), 2.76 ppm (**20b**), 2.72 ppm (**21b**); PyCH_2N: 4.90 ppm (**19b**), 4.98 ppm (**20b**), 2.69 ppm (**21b**)].

2.3.5 1-Hexene polymerization by activated pyridylamido Zr^{IV} complexes.

After the synthesis and characterization of the activated forms **18a-21a** and **18b-21b,** we studied their polymerization activity in the presence of 1-hexene as the monomer (**Table 2.5**). Catalysts derived from $B(C_6F_5)_3$ activation (**18a-21a**) showed very low catalytic

activity, providing only traces of polymer products. This very low activity is likely due to the strong η^6-binding of the $[B(CH_2C_6H_5)(C_6F_5)_3]^-$ anion to the cationic Zr^{IV} center, which hampers monomer access to the metal center.[1b, 28]

Table 2.5. 1-Hexene polymerization by activated pyridylamido complexes **18b-21b** [a]

Entry	Catalyst	*t* (min)	*T* (°C)	Yield (g)	Conv (%)[b,c]	Activity (10^{-3}) [d]	Activity [e]
1	**18b**	5	23	1.3	99.9	19.18	17.70
2	**18b**	2	23	1.1	81.4	39.07	36.05
3	**18b**	5	0 [f]	n.d.[g]	1.8	0.35	0.32
4	**18b**	1	50 [f]	0.6	46.2	44.35	40.92
5	**19b**	30	23	0.2	14.7	0.47	0.43
6	**20b**	30	23	0.1	9.2	0.29	0.27
7	**21b**	5	23	1.2	90.3	17.34	16.00

[a] Reaction conditions: catalyst precursor 10 μmol, $[Ph_3C][B(C_6F_5)_4]$ 10 μmol, 1-hexene 2 mL (16 mmol), toluene 8 mL. [b] Determined by GC. [c] Average values calculated over three independent runs. [d] Mol of 1-hexene converted (mol of Zr)$^{-1}$ h^{-1}. [e] Kg of 1-hexene converted (g of Zr)$^{-1}$ h^{-1}. [f] Precatalyst activation was run at room temperature for 5 min. prior to setting the final reaction temperature. [g] Not determined.

On the other hand, catalysts prepared using $[Ph_3C][B(C_6F_5)_4]$ as activator lead from moderately active (**19b** and **20b: Table 2.5**, entries 5 and 6) or highly efficient catalytic species (**18b** and **21b: Table 2.5**, entries 1 and 7) for the 1-hexene polymerization. It is noteworthy that catalyst **18b** gave poly(1-hexene) with complete monomer conversion in a few minutes and productivities which are over one order of magnitude higher than those previously reported in the literature for related Hf^{IV} pyridylamido systems.[1b] Although higher polymerization temperatures (**Table 2.5**, entry 4) were not found to affect the catalyst activity significantly, runs conducted at 0 °C revealed almost complete deactivation of the catalytic processes. All poly(1-hexene)s produced by **18b** showed moderate isotacticities (m^4 = 0.47) with approximately 5-6 mol % of regioerrors as evidenced by their $^{13}C\{^1H\}$ NMR spectra. While the observed isotacticity can be rationalized on the basis of an *in situ* ligand modification resulting from the monomer insertion into the Zr^{IV}-Ar bond (that translates into a lowering of the symmetry of the active species),[1b,2a-e] there is no apparent reason to explain the dramatic activity decrease observed in the case of heteroaryl-containing systems **19b** and **20b**.[2a,c] Experimental evidence for the olefin insertion into the Zr^{IV}-Ar bond was gathered by

reacting the two representative activated species **18b** and **19b** with a stoichiometric amount of 1-hexene at room temperature. The GC-MS analysis of the hydrolyzed reaction mixtures revealed the presence of two main peaks (*m*/*z* = 344 and *m*/*z* = 428 from **18b**/1-hexene; *m*/*z* = 334 and *m*/*z* = 418 from **19b**/1-hexene) in a 78:22 and 39:61 ratio, attributed to the unmodified ligands and the hexyl-substituted ligands **22** and **23**, respectively (**Figure 2.10**).

To gain additional information on the olefin insertion path, the GC-MS analysis was ultimately conducted on the solutions obtained from the sub-stoichiometric runs (6 equivalents of 1-hexenes) with **18b** and **19b**. The presence of a monomer excess did not change the ligand/modified-ligand ratio significantly (71:29 for **18b** and 28:72 for **19b**); no detectable amount of differently modified ligands (resulting from the possible chain-growth continuation between the metal and the aryl fragment) was found.[2a]

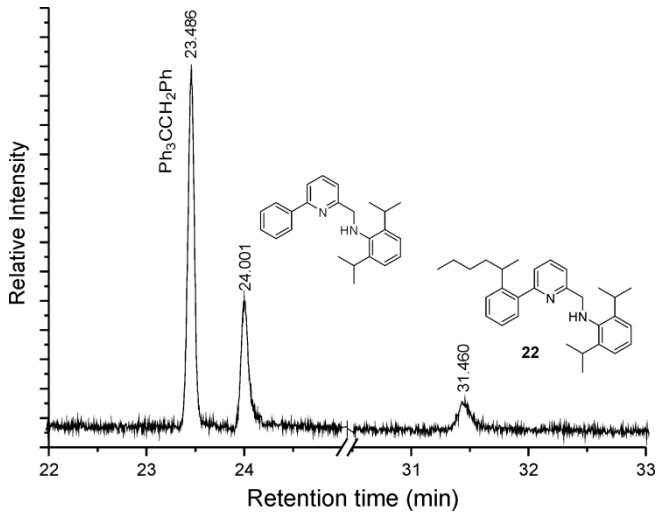

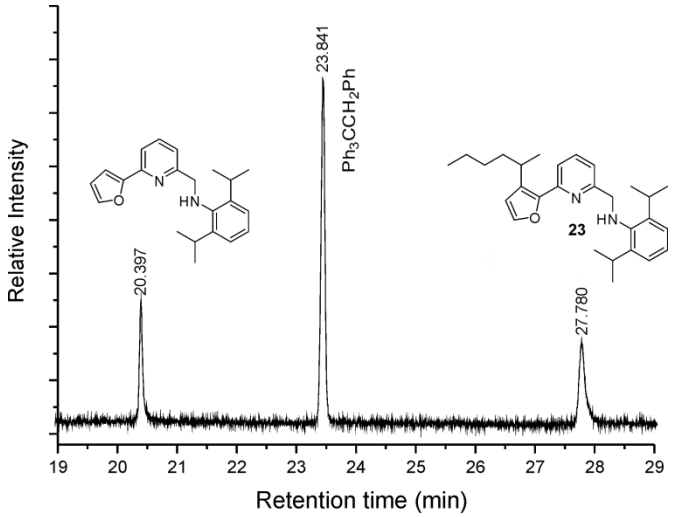

Figure 2.10. GC traces of reaction solutions obtained from the reaction of **18b** (top) and **19b** (bottom) with one equivalent of 1-hexene after quenching with MeOH (GC program: 40°C/1min, 15°C/min, 250°C/20min).

If the idea that the monomer insertion into the Zr-Ar bond of **18b** generates either inactive or slow polymerization species can be reasonably discarded on the basis of its high catalytic performance (**18b** shows productivities up to 41 kg of poly(1-hexene) per g of Zr per h), a deactivation path associated to the Zr-Ar monomer insertion cannot be definitively ruled out for **19b** and **20b**. On the contrary, it is evident that minor differences in the ligand frameworks (**11a,d** *vs.* **11b,c**) would influence the final catalysts performance dramatically.

2.3.6 Poly(1-hexene)s characterization and study on the effect associated to catalysts aging.

The effect of the catalyst aging in solution *before the monomer introduction* was investigated for the most efficient catalyst **18b**, aiming at a better understanding of its polymerization ability. Despite moderate solubility in aromatic solvents (benzene or toluene), compound **18b** maintains its catalytic activity virtually unchanged even after prolonged aging times (**Table 2.6**, entries 1-4).[1b] All poly(1-hexene)s produced by **18b** were isotactically enriched, as evidenced by the $^{13}C\{^1H\}$ NMR spectra, with no appreciable influence of the catalyst aging time on the isotacticity degree (m^4). The observed

isoselectivity from C_s-symmetric precursors can be explained by an *in situ* ligand modification brought about by monomer insertion into the Zr^{IV}-C^{Ph} bond.[2a]

Table 2.6. Poly(1-hexene) materials from catalysts **18b** and **21b** at different catalyst aging times [a]

Entry	Catalyst	t_{age} (h)	t (min)[b]	Yield (g)	conv (%)[c,d]	M_n vis[e] (10^{-3})	$[\eta]$[f] dL/g	M_n rel[g] (10^{-3})	M_w/M_n
1	**18b**	0	2	1.1	81.4	31	0.76	45	4.9
2	**18b**	1	5	1.3	97.8	60	1.04	82	5.2
3	**18b**	5	30	1.1	82.7	86	1.18	129	4.3
4	**18b**	16	30	0.5	37.6	258	0.98	265	2.5[h]
5	**21b**	0	5	1.23	90.3	127	1.33	137	3.4
6	**21b**	5	30	0.24	17.7	107	1.43	127	3.6

[a] Reaction conditions: catalyst precursor 10 μmol, $[Ph_3C][B(C_6F_5)_4]$ 10 μmol, 1-hexene 2 mL (16 mmol), toluene 8 mL, 23 °C. [b] Polymerization time. [c] Determined by GC. [d] Average values calculated over three independent runs. [e] Determined from viscosimetric elaboration. [f] Intrinsic viscosity. [g] Relative to polystyrene calibration. [h] Calculated on the main GPC curve corresponding to M_n value of 265 kDa.

Finally, relatively broad polydispersity indices (PDI) and the molecular weight distribution profiles (from monomodal to polymodal) measured for all polymer samples were consistent with a nonliving character of the catalytic active species; living species were previously reported by Coates *et al*. for related pyridylamido Hf^{IV} systems.[1b]

Worthy of note, the prolonged catalyst aging resulted in unexpected and almost linear increases of the M_n values from 30 to 250 kg mol^{-1} (**Table 2.6**, entries 1-4 and **Figure 2.11a**). In addition, a slight decrease of both r^4 and *mrrm* pentads, together with an increase of regioerrors in the polymer microstructure (up to 8 mol%) were also observed (**Table 2.7**, entries 1-4 and **Figure 2.11b**).

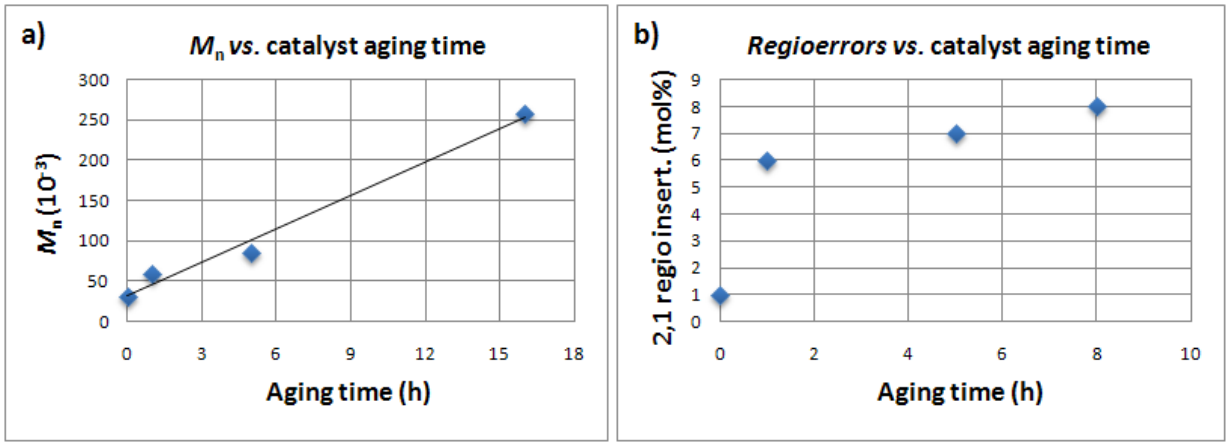

Figure 2.9. a) M_n of poly(1-hexene)s prepared at different **18b** aging time. b) Increased polymer microstructure regioerrors (2,1 regio insertion) in the poly(1-hexene)s obtained at different **18b** aging times.

Table 2.7. Microstructures of poly(1-hexene)s prepared from **18b** at different catalyst aging times [a]

Entry	t_{age} (h)	t (min)[b]	[mmmm][c]	[rrrr] + [mrrr] + [rmrm][c]	[mrrm][c]	2- hexenyl group (mol%)[c]	2,1 regio-insertion (mol%)[d]
1	0	2	0.47	0.27	0.08	0.017	1
2	1	5	0.47	0.27	0.08	0.007	6
3	5	30	0.47	0.24	0.09	n.d.	7
4	8	30	0.48	0.26	0.06	0.004	8

[a] Reaction conditions: catalyst **18b** (10 μmol), $[Ph_3C][B(C_6F_5)_4]$ (10 μmol), 1-hexene (2 mL, 16 mmol), toluene (8 mL), 23 °C. [b] Polymerization time. [c]Determined by ^{1}H NMR. [d]Terminal groups determined by $^{13}C\{^1H\}$ NMR.

The relative areas of the methine pentads were analyzed with theoretical statistical equations by using either the chain-end-controlled mechanism or the enantiomorphic site control, predicted by the site epimerization mechanism. The best fit with the experimental areas was found by using the site epimerization mechanism that confirmed the possibility of the growing polymer chain to migrate from one site to the other of the C_1-symmetric active species. All these data taken together suggested the generation of *new active forms* throughout the catalyst aging time. Accordingly, the GPC profiles of the polymeric materials prepared from catalyst **18b** at different catalyst aging times displayed either monomodal (for unaged catalyst) or bimodal (for any aged catalyst species) molecular weight and composition distributions. In order to shed light on this unusual polymerization trend, we were particularly interested in characterizing the nature of the active specie(s) responsible for the linear increase of the polymer M_n *vs.* aging time. Noteworthy, stirring a suspension of

18b in toluene prior to the monomer addition led to the formation of the one major soluble species **24b** (**Scheme 2.5**).

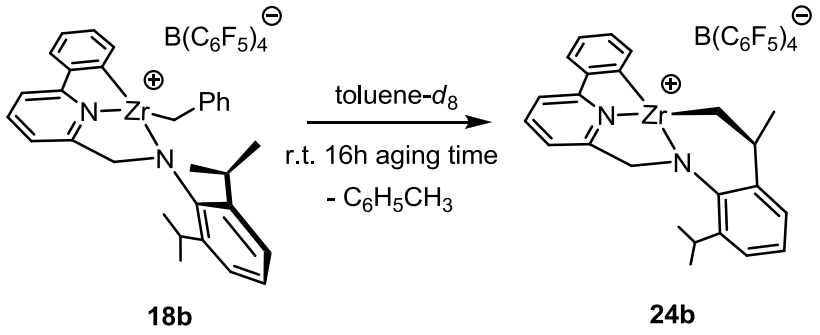

18b **24b**

Scheme 2.5. Evolution of the activated species **18b** into **24b** upon simple catalyst aging.

The key mechanism responsible for the generation of **24b** consists in the metallation of an isopropyl fragment with concomitant elimination of one molecule of toluene, a behavior which is not without precedent in the literature.[2b] The ^{1}H-NMR spectrum of **24b** exhibits two well-separated doublets attributed to the unmodified isopropyl fragment at δ = 1.18 ppm and 1.36 ppm, while the metallated alkyl moiety gives rise to two doublets (each integrating for one proton) centered at δ = 1.22 and 1.25 ppm, corresponding to diastereotopic methylene protons and the methyl group which appears as a doublet at δ = 1.02 ppm. The two ^{1}H NMR resonances from the Zr^{IV}-activated methyl group show a scalar coupling with the methine residue centered at δ = 3.43 ppm and correlate with the same carbon resonance at δ = 84.8 ppm (**Figure 2.10**). The metallation of the isopropyl fragment accounts for lower symmetry of the resulting species; as a matter of fact, the methylene bridging group PyCH_2N gives rise to a well-defined AB system centered at 4.98 ppm which correlates with a single carbon resonance at 63.79 ppm (**Figure 2.10**). Unfortunately, the limited solubility of **18b** in apolar aromatics and its rapid decomposition in polar aromatic solvents (C_6D_5Br or C_6D_5Cl) did not allow for an exact quantification of the **18b**/**24b** ratio at different catalyst aging times. It is

evident, however, that the soluble fraction of **18b** is quantitatively converted into the more soluble and stable cationic species **24b** after 16 hours.[29]

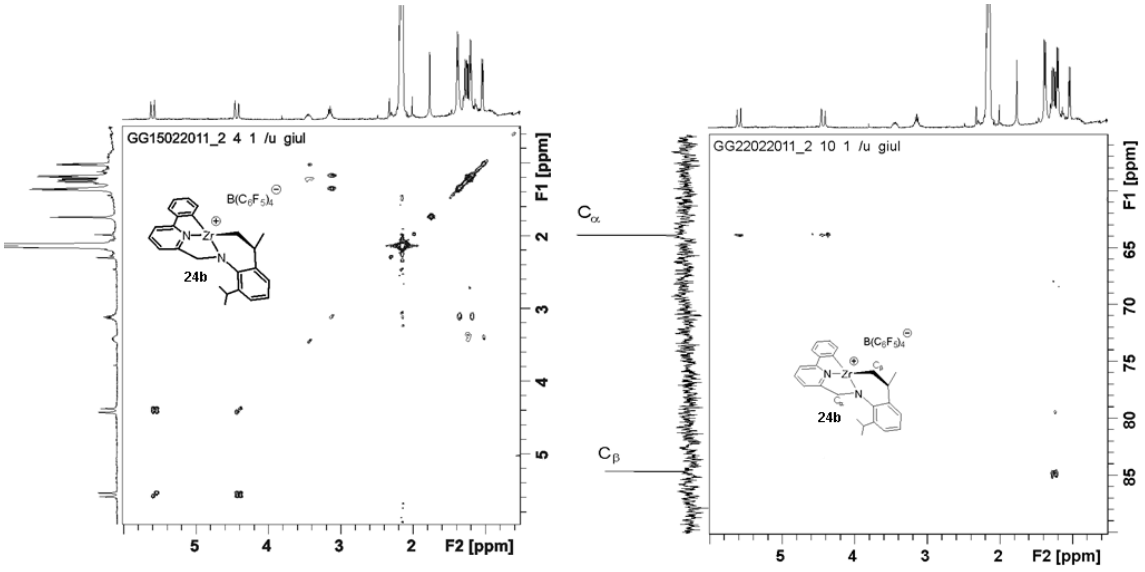

Figure 2.10. [^{1}H-^{1}H] COSY spectrum (400 MHz, C_7D_8, 298K, 0.5 ≥ δ (ppm) ≥ 6) (left) and [^{1}H-^{13}C] HETCOR spectrum [400 MHz, C_7D_8, 298K, (^{1}H; 0.5 ≥ δ (ppm) ≥ 6. ^{13}C; 55 ≥ δ (ppm) ≥ 90) of **24b** as obtained from an aged (12 h) solution of **18b**.

The increasing M_n values measured for the poly(1-hexene)s produced at different **18b** aging times, the reduction of the degree of regioerrors in the polymer microstructure, and the changes occurring on the polymer molecular weight distributions (from monomodal to bimodal) all together seem to offer a reasonable explanation of the observed activated species evolution (from **18b** to **24b**).

Indirect supporting evidence of the role played by **24b** in the catalytic performance of the aged **18b** was given by the analysis of the poly(1-hexene)s produced by the xylyl derivative **21b**, where further intramolecular activation paths cannot take place. As **Table 2.6** shows, the catalytic activity of **21b** rapidly decreases upon catalyst aging (**Table 2.6**, entries 5 *vs.* 6). Most importantly, the M_n values and molecular weight distributions of the poly(1-hexene)s produced by **21b** at different catalyst aging times did not show any relevant variation.

2.3.7 High-temperature polymerization studies.

To get further details about the catalytic performance of the newly prepared $Zr^{IV}(Bn)_2$ complexes, high-temperature polymerization and co-polymerization tests have also been carried out. In addition to the polymerization study with selected $Zr^{IV}(Bn)_2$ complexes (**18**, **19** and **21**), the highly optimized C_1-symmetric Zr^{IV}-pyridylamido complex **25** (**Figure 2.11**), recently proposed by us,[2g] has been included for comparison.

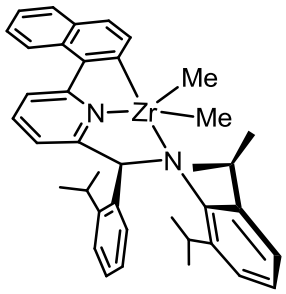

25

Figure 2.11. Schematic drawing of the C_1-symmetric Zr^{IV}-pyridylamido complex **25**.

Overall, the $Zr^{IV}(Bn)_2$ complexes scrutinized under high-temperature conditions (90-120 °C), exhibited similar reactivity trends to those measured in the 1-hexene polymerization reactions conducted at room temperature (productivities for **18** and **21** higher than that of **19**). The catalytic activity measured for the **18**/**19**/**21** group, under these harsher reaction conditions, was moderate (15% at the highest) compared with that obtained with **25**. Finally, the highest polymer stereo regularity (see polypropylene section) was obtained with the C_1-symmetric complex **25**, as expected. This set of data is in line with other previous studies, indicating how selected structural parameters (*i.e.* the amido nitrogen and/or the bridging methylene substitution and the nature of the 2-aryl substituent) and precatalyst symmetry, play a major role in controlling both catalyst activity and stereo regularity of the resulting polymers.

2.3.8 Ethylene/1-octene copolymerization study.

Ethylene/1-octene copolymerizations were conducted at 120 ^{o}C in a 2 L batch reactor filled with ethylene (460 psi) and 1-octene (250 g). All precatalysts were activated *in-situ* with 1.2 equivalents (relative to precatalyst) of $[HNMe(C_{18}H_{37})_2][B(C_6F_5)_4]$ as activator. Polymerization tests were carried out for 10 min. and stopped by venting the ethylene pressure. As shown in **Table 2.8**, complexes **18**, **19** and **21** were moderately active under these reaction temperature conditions, leading to very high molecular weight ethylene/1-octene copolymers ranging from 268 KDa for **19** to 542 KDa for **18**. 1-Octene incorporation, as measured by IR spectroscopy, ranged from 4.2-6.6 mol% and was somewhat lower than that found in copolymers produced by **25** (8.4 mol%).[30]

In all cases, complexes **18**, **19** and **21** form copolymers with higher polydispersities than those coming from the most active **25**; the least active precatalyst **19** produced copolymers with the highest polydispersity.

Table 2.8. Ethylene/1-octene copolymerization data.[a]

Entry	Catalyst (μmol)	Yield (g)	Activity (10^{-3}) [b]	M_w (10^{-3})	M_w/M_n	Octene content (mol%)
1	**18** (10)	16.7	10.02	542	2.4	4.2
2	**19** (10)	3.3	1.94	268	21.8	6.6
3	**21** (10)	11.5	6.90	377	2.5	6.4
4	**25** (0.7)	12.3	105.43	2010[2g]	1.6	8.4

[a] Polymerization conditions: temp = 120 ^{o}C; 533 mL of Isopar-E; 250 g of 1-octene; ethylene pressure = 460 psi; precatalyst:activator:MMAO = 1:1.2:10; activator: $[HNMe(C_{18}H_{37})_2][B(C_6F_5)_4]$; hydrogen = 10 mmol; polymerization time 10 min. [b] g of polymer (mmol of Zr)$^{-1}$ h^{-1}.

2.3.9 Propylene polymerization study.

Propylene polymerization reactions were conducted at 90 ^{o}C in a 1.8 L reactor filled with 180 g of propylene in 700 mL of solvent. The data summarized in **Table 2.8** indicate that Zr^{IV} complexes **18** and **21** exhibit (among the C_s-symmetric precatalysts) the highest catalytic activities while complex **19** shows moderate performance (**Table 2.8**, entries 1 and

3 *vs.* 2). Overall, the C_s precursors show about 15% of the catalytic activity measured for **25**, at the highest. The polydispersity *vs.* catalytic activity trend is almost identical to that described above for the ethylene/1-octene copolymerization tests (see **Table 2.7** *vs.* **Table 2.8**). Finally, the precatalyst **21**, bearing the xylyl substituent on the amido nitrogen atom, gave polypropylene with the lowest stereoregularity, as expected.[1e]

Table 2.8. Propylene polymerization data.[a]

Entry	Catalyst (μmol)	Yield(g)	Activity (10^{-3}) [b]	T_m (°C)	M_w (10^{-3})	M_w/M_n	[mmmm]
1	**6** (10)	11.9	7.14	144.9	282	4.1	0.48
2	**7** (10)	1.9	1.14	146.2	389	8.1	0.75
3	**9** (10)	7.8	4.68	146.8	230	4.0	0.19
4	**13** (1)	8.0	48.00	147.7	1052	2.5	0.91

[a]Polymerization conditions: temp = 90 °C; 700 mL of Isopar-E; propylene = 180 g; precatalyst:activator:MMAO = 1:1.2:10 activator: $[HNMe(C_{18}H_{37})_2][B(C_6F_5)_4]$; reaction time 10 min. [b] g of polymer (mmol of Zr)$^{-1}$ h^{-1}.

Although isotactically enriched polypropylenes can be obtained from C_s symmetric complexes as a result of an *in-situ* catalyst modification (olefin insertion into the Zr-aryl bond), the highest isotacticity is obtained with the C_1-symmetric precursor **25** (**Table 2.8**, entries 1-3 vs. 4).

2.4 Conclusions

Understanding the importance of the metal precursor choice as well as highlighting unexpected organometallic paths for selected classes of polymerization catalysts is a more important achievement than a mere chemical curiosity to be addressed. In the last few years, the organometallic chemistry and polymerization catalysis associated with Group IV pyridylamido complexes have offered an excellent ground for discussion to many research groups from industry and academia around the world; under this perspective, the present contribution is thought to shed further light on this topical subject. In the first part of the work, we present a full account on the temperature-controlled σ-bond

metathesis/protonolysis reaction occurring at Group IV amido complexes, an original outcome that highlights how the chemistry of well-known metal precursors such as $M^{IV}(NMe_2)_4$ (M = Zr, Hf) may deserve unexpected reactivity paths. More importantly, this issue provides a better understanding of the complex structure-activity relationships of Group IV amido-based olefin polymerization catalysts. With the aim at emphasizing the role of the metal precursor choice in the production of tailored catalyst systems, a direct comparison between $Zr^{IV}(NMe_2)_4$ and $Zr^{IV}(Bn)_4$ has been carried out. Irrespective of the unique nature of the newly synthesized $Zr^{IV}\{C^-,N,N^-\}(Bn)_2$ precatalysts, and the unambiguous identity of their activated forms (cationic $[Zr^{IV}\{C^-,N,N^-\}]^+B(C_6F_5)_4^-$ and zwitterionic $[Zr^{IV}\{C^-,N,N^-\}]^+BnB(C_6F_5)_3^-$ species), the wealth of the organometallic chemistry associated to this class of compounds has unveiled unexpected catalytic outcomes. Room temperature polymerizations of 1-hexene using the cationic Zr^{IV}-complexes have provided poly(1-hexene) with productivities up to one order of magnitude higher (as high as 44 10^3 kg of poly(1-hexene) (mmol of Zr)$^{-1}$ h^{-1}) than those previously reported in the literature for related Hf^{IV} pyridylamido systems. Most importantly, catalyst aging tests (conducted prior to the monomer addition) resulted into catalytic species capable of generating polymers featured by increased M_n values (from 30 to 250 kg mol^{-1}) and increased regioerrors in the polymer microstructure (up to 8 mol%). An in-depth investigation of the catalyst aging in solution (in the absence of monomer) has unambiguously demonstrated its progressive evolution towards the formation of (at least) one major novel active form with reduced symmetry; this finding adds additional layers of complexity to the identification of the true active species operating in the polymerization process.

Finally, high-temperature polymerization studies have shown that the cationic Zr^{IV}-complexes of the present study are moderately active catalysts for propene polymerization and ethylene/1-octene copolymerization.

2.5 Experimental Section

General Considerations. All air- and/or moisture-sensitive reactions were performed under inert atmosphere in flame-dried flasks using standard Schlenk-type techniques or in a dry-box filled with nitrogen. Benzene and toluene were purified by distillation from sodium/triglyme benzophenone ketyl and stored over 4Å molecular sieves or were obtained by means of an MBraun Solvent Purification Systems. Benzene-d_6 and toluene-d_8 were dried over sodium/benzophenone ketyl and condensed *in vacuo* over activated 4Å molecular sieves prior to use. 1-hexene was purified prior to use by distillation over Na, stored at room temperature under nitrogen atmosphere over activated 4Å molecular sieves and used within 2 days. All the other reagents and solvents were used (unless otherwise stated) as purchased from commercial suppliers without further purification. The amino-pyridinate ligands **11a-d** were obtained on a multigram scale according to standard procedures reported in the literature[31] or with slight modifications.[32] 1D (^{1}H and ^{13}C{^{1}H}) and 2D (COSY H,H, HETCOR H,C) NMR spectra of all organometallic species were obtained on either a Bruker Avance DRX-400 spectrometer (400.13 and 100.61 MHz for ^{1}H and ^{13}C, respectively) or a Bruker Avance 300 MHz instrument (300.13 and 75.47 MHz for ^{1}H and ^{13}C, respectively). Chemical shifts are reported in ppm (δ) relative to TMS, referenced to the chemical shifts of residual solvent resonances (^{1}H and ^{13}C). The multiplicities of the ^{13}C{^{1}H} NMR spectra were determined on the basis of the ^{13}C{^{1}H} JMOD sequence and quoted as: CH_3, CH_2, CH and C for primary, secondary, tertiary and quaternary carbon atoms, respectively. The C, H, N, S elemental analyses were made using a Thermo FlashEA 1112 Series CHNS-O

elemental analyzer with an accepted tolerance of ± 0.4 units on carbon (C), hydrogen (H) and nitrogen (N). *X-ray data measurements.* Single crystal X-Ray data were collected at low temperature (100 or 120 K) on an Oxford Diffraction XCALIBUR 3 diffractometer equipped with a CCD area detector using Mo Kα radiation (λ = 0.7107 Å). The program used for the data collection was CrysAlis CCD 1.171.[33] Data reduction was carried out with the program CrysAlis RED 1.171[34] and the absorption correction was applied with the program ABSPACK 1.17. Direct methods implemented in Sir97[35] were used to solve the structures and the refinements were performed by full-matrix least-squares against F^2 implemented in SHELX97.[36] All the non-hydrogen atoms were refined anisotropically (with the exception of those of the disordered diethyl ether and toluene solvent molecules in **20** and **21**, respectively), while the hydrogen atoms were fixed in calculated positions and refined isotropically with the thermal factor depending on the one of the atom to which they are bound (riding model). The presence of large accessible voids (107 $Å^3$) in the lattice of **20** is due to the presence of disordered Et_2O molecules that cannot be located precisely in the Fourier difference density maps. Molecular plots were produced by the program ORTEP3.[37]

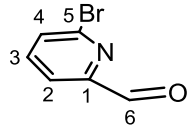

Synthesis of 6-bromopicolinaldehyde (2). To a stirred solution of 2,6-dibromopyridine (**1**) (3.00 g, 12.6 mmol), in Et_2O (55 mL) at -78 °C were added 7.8 mL (13.2 mmol) of a 1.7 M solution of ^{t}BuLi within 5 min. After 30 min of stirring at -78 °C, N,N-dimethylformamide (1.02 mL, 13.2 mmol) was added and the reaction was maintened under stirring for other 1.5 h. The resulting mixture was allowed to warm to room temperature and treated with water (30 mL). The formed layers were separated. The organic layer was washed with water (2 x 15 mL). The aqueous layer was extracted with Et_2O (3 x 15 mL). The combined organic layers were dried over Na_2SO_4. Removal of the solvent under reduced pressure gave a yellow solid that was dissolved in petroleum ether and cooled to -20 °C. After 6 h, white crystals were separated by filtration

(2.15 g, yield 92%). ^{1}H NMR (300 MHz, $CDCl_3$, 293K): δ 7.68-7.75 (2H, C*H*, $H^{2,3}$), 7.90 (m, 1H, C*H* Ar, H^4), 9.96 (s, 1H, C*H*O, H^6). $^{13}C\{^{1}H\}$ NMR (75 MHz, $CDCl_3$, 293 K): δ 120.3 (C^4), 132.6 (C^2), 139.3 (C^9), 153.7 (C), 161.3 (C).

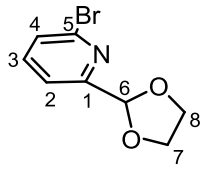

Synthesis of 2-bromo-6-(1,3-dioxolan-2-yl)pyridine (3). A solution of 6-bromopicolinaldehyde (**2**) (1.0 g, 5.37 mmol), 0.36 mL (6.45 mmol) of 1,2-ethanediol, and 0.1 g (0.53 mmol) of 4-toluensulfonic acid in 20 mL of distilled benzene was heated to reflux for 24 h in a Dean-Stark apparatus. The mixture was cooled at room temperature and then treated with 7 mL of 0.5 M aqueous NaOH solution. The formed layers were separated. The aqueous phase was washed with Et_2O (2 x 10 mL), and the combined organic extracts were dried over Na_2SO_4. After removal of the solvent under reduced pressure a yellow-brown oil (1.14 g) was obtained (yield 92.2%) that was used directly for the next step without other purification. ^{1}H NMR (300 MHz, CD_2Cl_2, 293K): δ 3.94-4.08 (4H, CH_2, $H^{7,8}$), 5.67 (s, 1H, C*H*, H^6), 7.40-7.41 (m, 1H, C*H* Ar, H^4), 7.42–7.43 (m, 1H, C*H* Ar, H^2), 7.55 (t, $^{3}J_{HH}$ = 7.8 Hz, 1H, C*H* Ar, H^3).

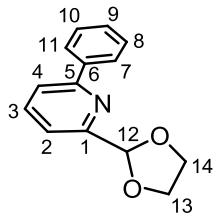

Synthesis of 2-(1,3-dioxolan-2-yl)-6-phenylpyridine (4). To a degassed solution of 2-bromo-6-(1,3-dioxolan-2-yl)pyridine (**3**) (1.1 g, 4.78 mmol) in toluene (20 mL), 5 mL of a 4.4 M aqueous solution of Na_2CO_3 were added, followed by a solution of phenylboronic acid (0.7 g, 5.73 mmol) in 5 mL of MeOH and a solution of $Pd(dba)_2$ (0.082 g, 0.14 mmol) and PPh_3 (0.3 g, 1.14 mmol) in 5 mL of toluene. The reaction mixture was heated to 80°C and maintained at that temperature under stirring for 20 h. the resulting solution was allowed to cool to room temperature and a solution of 9.5 mL of concentrated aqueous NH_3 in 24 mL of saturated aqueous Na_2CO_3 was added. The mixture was extracted with CH_2Cl_2 (3 x 15 mL). The combined organic layers were washed with water (70 mL) and brine solution (70 mL), and

dried over Na_2SO_4. Removal of the solvent under reduced pressure gave 1.5 g of crude product. Chromatographic separation using silica gel (petroleum ether: AcOEt = 80:20) gave a yellow pale oil (0.84 g, yield 81%). ^{1}H NMR (300 MHz, CD_2Cl_2, 293K): δ 4.00-4.15 (4H, C*H*$_2$, H^{13,14}), 5.80 (s, 1H, C*H*, H^{12}), 7.35-7.44 (4H, C*H* Ar, H^{2,8,9,10}), 7.68 (dd, $^3J_{HH}$ = 7.8 Hz, 1H, C*H* Ar, H^4), 7.75 (pt, $^3J_{HH}$ = 7.8 Hz, 1H, C*H* Ar, H^3), 7.97 (dd, $^3J_{HH}$ = 8.1 Hz, 2H, C*H* Ar, H^{7,11}). ^{13}C{^{1}H} NMR (75 MHz, CD_2Cl_2, 293 K): δ 65.6 (C^{13,14}), 104.1 (C^{12}), 118.8 (C^4), 120.5 (C^2), 126.8 (C^{7,11}), 128.6 (C^{8,10}), 129.0 (C^9), 137.5 (C^3), 138.9 (C^6), 156.5 (C^5), 157.3 (C^1).

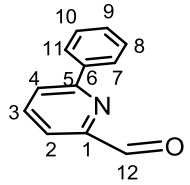

Synthesis of 6-phenylpicolinaldehyde (5). The 2-(1,3-dioxolan-2-yl)-6-phenylpyridine (**4**) (0.84 g, 3.86 mmol) was suspended in HCl 2M (15 mL) and stirred at 80-85 °C for 2h. The resulting mixture was then cooled in an ice bath, diluted with iced water (15 mL) and neutralized portion wise with solid $NaHCO_3$. A standard extractive work-up with AcOEt (3 x 30 mL) gave, after removal of the solvent under reduced pressure, a yellow pale oil product (0.69 g, yield 90.3%). ^{1}H NMR (300 MHz, CD_2Cl_2, 293K): δ 7.50-7.59 (3H, C*H* Ar, H^{8,9,10}), 7.91 (dd, $^3J_{HH}$ = 7.8 Hz, 1H, C*H* Ar, H^4), 7.96-8.05 (2H, C*H* Ar, H^{2,3}), 8.13-8.16 (2H, C*H* Ar, H^{7,11}), 10.17 (s, 1H, C*H*O, H^{12}). ^{13}C{^{1}H} NMR (75 MHz, CD_2Cl_2, 293 K): δ 119.6 (C^4), 124.4 (C^2), 126.9 (C^{7,11}), 128.8 (C^{8,10}), 129.5 (C^9), 137.8 (C^3), 138.1 (C^6), 152.7 (C^1), 157.6 (C^5), 193.8 (C^{12}).

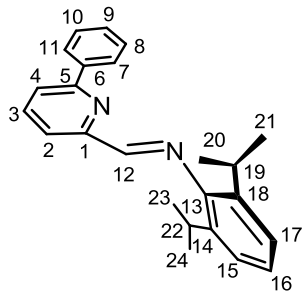

Synthesis of (2,6-diisopropyl-N-((6-phenylpyridin-2-yl)methylene)aniline (6a). To a solution of 6-phenylpicolinaldehyde (**5**) (0.69 g, 3.76 mmol) in methanol (20 mL) were added in sequence an excess of distilled 2,6-diisopropyl-aniline (1.77 mL, 9.40 mmol) and four drops of formic acid. The resulting mixture was stirred at r.t for 12 h. The resulting solution was allowed to cool at 4°C

and after a few hours yellow microcrystals of the pure product were isolated by filtration (0.95 g, yield 73.7%). Mp: 96°C. IR (KBr): $\nu_{(C=N)}$ 1648 cm^{-1}. MS *m/z* (%): 342 (M^+, 76); 377 (M^+ +1, 19); 327 (M^+ -15, 100). ^1H NMR (300 MHz, CD_2Cl_2, 293K): δ 1.21 (d, $^3J_{HH}$ = 6.8 H_Z, 12H, CH(C*H*$_3$), $H^{20, 21, 23, 24}$), 3.03 (sept, $^3J_{HH}$ = 6.8 Hz, 2H, C*H*(CH_3), $H^{19,22}$), 7.12-7.23 (3H, C*H* Ar, $H^{15,16,17}$), 7.45-7.57 (3H, C*H* Ar, $H^{8,9,10}$), 7.92 (dd, $^3J_{HH}$ = 7.8 Hz, 1H, C*H* Ar, H^2), 7.97 (pt, $^3J_{HH}$= 7.8 Hz, 1H, C*H* Ar, H^3), 8.11-8.15 (2H, C*H* Ar, $H^{7,11}$), 8.26 (dd, $^3J_{HH}$ = 7.8 Hz, 1H, C*H* Ar, H^4), 8.41 (s, 1H, C*H*N, H^{12}). $^{13}C\{^1H\}$ NMR (75 MHz, CD_2Cl_2, 293 K): δ 23.1 (CH(*C*H_3)$_2$, $C^{20,21,23,24}$), 27.9 (*C*H(CH_3)$_2$, $C^{19,22}$), 119.3 (C^4), 121.8 (C^2), 122.9 ($C^{15,17}$), 124.3 (C^{16}), 126.8 ($C^{7,11}$), 128.7 ($C^{8,10}$), 129.2 (C^9), 137.2 ($C^{14,18}$), 137.4 (C^3), 138.7 (C^6), 148.6 (C^{13}), 154.3 (C^1), 157.0 (C^5), 163.6 (C^{12}). Anal. Calcd (%) for $C_{24}H_{26}N_2$ (342.48): C 84.17, H 7.65, N 8.18; found C 84.32, H 7.60, N 8.08.

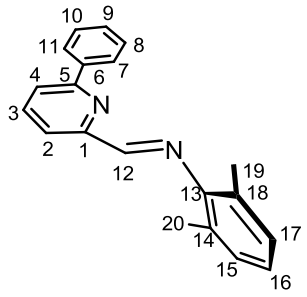

Synthesis of 2,6-dimethyl-N-((6-phenylpyridin-2-yl)methylene)aniline (6b). To a solution of 6-phenylpicolinaldehyde (**5**) (0.50 g, 2.73 mmol) in methanol (15 mL) were added in sequence an excess of distilled 2,6-dimethyl-aniline (0.43 mL, 3.55 mmol) and four drops of formic acid. The resulting mixture was stirred at r.t for 12 h. Removal of the solvent under reduced pressure gave the crude product as dark-yellow oil that was used directly for the next step without other purification.

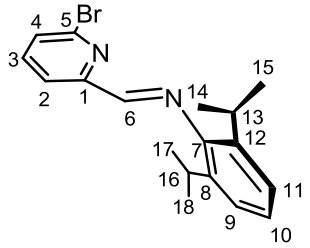

Synthesis of N-((6-bromopyridin-2-yl)methylene)-2,6-diisopropylaniline (7). To a solution of 6-phenylpicolinaldehyde (**5**) (1.50 g, 8.06 mmol) in methanol (50 mL) were added in sequence an excess of distilled 2,6-diisopropyl-aniline (1.97 mL, 10.48 mmol) and four drops of formic acid. The resulting mixture was stirred at r.t for 12 h.

Then the mixture was concentrated approximately to 1/3 of its initial volume and stored at 4 °C and after a few hours yellow microcrystals of the pure product were isolated by filtration (2.51 g, yield 90.5 %). ^{1}H NMR (300 MHz, CD_2Cl_2, 293K): δ 1.20 (d, $^{3}J_{HH}$ = 6.8 H_Z, 12H, CH(CH_3), H^{14,15,17,18}), 2.97 (sept, $^{3}J_{HH}$ = 6.8 Hz, 2H, CH(CH_3), H^{13,16}), 7.13-7.23 (3H, CH Ar, H^{9,10,11}), 7.65 (d, $^{3}J_{HH}$ = 7.8 Hz, 1H, CH Ar, H^{2}), 7.76 (pt, $^{3}J_{HH}$= 7.8 Hz, 1H, CH Ar, H^{3}), 8.25-8.29 (2H, H^{4,6}). ^{13}C{^{1}H} NMR (75 MHz, CD_2Cl_2, 293 K): δ 23.1 (CH(CH_3)$_2$, C^{14,15,17,18}), 27.9 (CH(CH_3)$_2$, C^{13,16}), 119.9 (C^{4}), 123.0 (C^{9,11}), 124.6 (C^{10}), 129.8 (C^{2}), 137.1 (C^{8,12}), 139.1 (C^{3}), 141.7 (C^{7}), 148.1 (C), 155.4 (C), 161.6 (C^{6}). Anal. Calcd (%) for $C_{18}H_{21}BrN_2$ (345.28): C 62.61, H 6.13, N 8.11; found C 62.70, H 6.20, N 8.15.

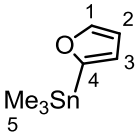

Synthesis of furan-2-yltrimethylstannane (8). A solution of furan (2.13 mL, 29.37 mmol) in 70 mL of Et_2O was cooled at -78 °C and treated dropwise with a 1.7 M solution of ^{t}BuLi in pentane (19.0 mL, 32.31 mmol). The reaction mixture was allowed to stir at that temperature for 30 min then a solution of Me_3SnCl (6.63 g, 33.31 mmol) in Et_2O (30 mL) was added dropwise within 10 min. The mixture was allowed to stand at -78 °C for 1 h then was slowly warmed until -35 °C and quenched with 50 mL of a saturated $NaHCO_3$ aqueous solution. The aqueous layer was extracted with Et_2O (3 x 25 mL). The combined organic layers were dried over Na_2SO_4. Removal of the solvent under reduced pressure gave the stannane product as crude slurry oil. The product was purified by fractional distillation under reduced pressure to afford a colorless oil (yield 95 %). ^{1}H NMR (300 MHz, CD_2Cl_2, 293K): δ 0.36 (s, 9H, Sn(CH_3)$_3$, H^{5}), 6.45 (m, 1H, CH Ar, H^{2}), 6.63 (m, 1H, CH Ar, H^{3}), 7.75 (m, 1H, CH Ar, H^{1}). ^{13}C{^{1}H} NMR (75 MHz, CD_2Cl_2, 293 K): δ -9.6 (C^{5}), 109.2 (C^{2}), 120.3 (C^{3}), 146.8 (C^{1}), 160.6 (C^{4}).

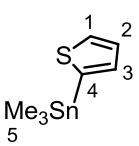

Synthesis of trimethyl(thiophen-2-yl)stannane (9). A solution of thiophene (1.9 mL, 23.7 mmol) in 70 mL of Et_2O was cooled at -78 °C and treated

dropwise with a 1.7 M solution of ^{t}BuLi in pentane (15.3 mL, 26.0 mmol). The reaction mixture was allowed to stir at that temperature for 30 min then a solution of Me_3SnCl (7.08 g, 35.5 mmol) in Et_2O (30 mL) was added dropwise within 10 min. The mixture was allowed to stand at -78 °C for 1 h then was slowly warmed until -35 °C and quenched with 50 mL of a saturated $NaHCO_3$ aqueous solution. The aqueous layer was extracted with Et_2O (3 x 25 mL). The combined organic layers were dried over Na_2SO_4. Removal of the solvent under reduced pressure gave the stannane product as crude slurry oil. The product was purified by fractional distillation under reduced pressure to afford a colorless oil (yield 93 %). ^{1}H NMR (300 MHz, CD_2Cl_2, 293K): δ 0.46 (s, 9H, Sn(C*H*$_3$)$_3$, H^5), 7.30-7.35 (2H, C*H* Ar, H^{2,3}), 7.72 (m, 1H, C*H* Ar, H^1). ^{13}C{^{1}H} NMR (75 MHz, CD_2Cl_2, 293 K): δ -7.7 (C^5), 128.6 (C^2), 131.4 (C^3), 135.7 (C^1), 137.8 (C^4).

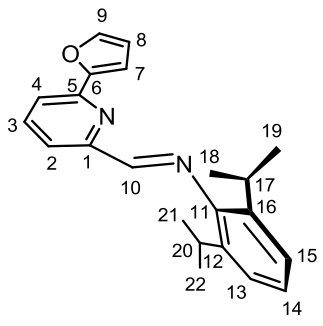

Synthesis of N-((6-(furan-2-yl)pyridin-2-yl)methylene)-2,6-diisopropylaniline (10a). A solution of N-((6-bromopyridin-2-yl)methylene)-2,6-diisopropylaniline (**7**) (1 g, 2.9 mmol) and furan-2-yltrimethylstannane (1.0 g, 4.3 mmol) in 15 mL of toluene was treated with a solution of $Pd(dba)_2$ (0.05 g, 0.08 mmol) and PPh_3 (0.182 g, 0.7 mmol) in toluene (5 mL). The reaction mixture was refluxed for 20 h, then cooled at room temperature and treated with water (20 mL). The formed layers were separated, the aqueous phase extracted with CH_2Cl_2 (3 x 15 mL) and then dried over Na_2SO_4. The collected organic layers were evaporated under reduced pressure to give yellow oil. The product was purified by recrystallization from hot MeOH, by cooling the resulting solution at 4°C overnight to afford yellow crystals (0.85 g, yield 88.3%). Mp: 110°C. IR (KBr): $\nu_{(C=N)}$ 1637 cm^{-1}. MS *m/z* (%): 332 (M$^+$, 56); 317 (M$^+$ -15, 77); 146 (100). ^{1}H NMR (300 MHz, CD_2Cl_2, 293K): δ 1.10 (d, $^3J_{HH}$ = 6.8 Hz, 12H, CH(C*H*$_3$), H$^{18, 19, 21, 22}$), 2.90 (sept, $^3J_{HH}$ = 6.8 Hz, 2H, C*H*(CH$_3$), H^{17,20}), 6.51 (dd, $^3J_{HH}$ = 3.4 Hz, $^4J_{HH}$= 1.8 Hz, 1H, C*H* Ar, H^8)

7.02-7.12 (4H, C*H* Ar, $H^{7,13,14,15}$), 7.52 (m, 1H, C*H* Ar, H^{9}), 7.73 (dd, $^{3}J_{HH}$ = 7.8 Hz, $^{4}J_{HH}$= 1.14 Hz, 1H, C*H* Ar, H^{2}), 7.82 (pt, $^{3}J_{HH}$ = 7.8 Hz, 1H, C*H* Ar, H^{3}), 8.08 (dd, $^{3}J_{HH}$ = 7.8 Hz, $^{4}J_{HH}$= 1.11 Hz, 1H C*H* Ar, H^{4}), 8.23 (s, 1H, C*H*N, H^{10}). $^{13}C\{^{1}H\}$ NMR (75 MHz, CD_2Cl_2, 293 K): δ 23.1 ($CH(CH_3)_2$, $C^{18,19,21,22}$), 27.8 ($CH(CH_3)_2$, $C^{17,20}$), 109.0 (C^{7}), 112.0 (C^{8}), 119.1 (C^{4}), 119.8 (C^{2}), 122.9 ($C^{13,15}$), 124.3 (C^{14}), 137.1 ($C^{12,16}$), 137.3 (C^{3}), 143.5 (C^{9}), 148.5 (C^{11}), 149.2 (C^{11}), 153.3 (C^{1}), 154.2 (C^{5}), 163.2 (C^{10}). Anal. Calcd (%) for $C_{22}H_{24}N_2O$ (332.44): C 79.48, H 7.28, N 8.43, O 4.81; found C 79.52, H 7.31, N 8.40, O 4.77.

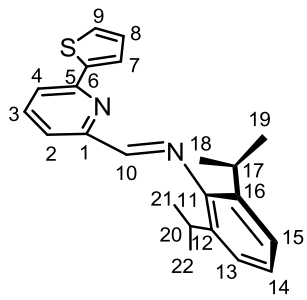

Synthesis of 2,6-diisopropyl-N-((6-(thiophen-2-yl)pyridin-2-yl)methylene)aniline (10b). A solution of N-((6-bromopyridin-2-yl)methylene)-2,6-diisopropylaniline (**7**) (0.7 g, 2.0 mmol) and trimethyl(thiophen-2-yl)stannane (0.75 g, 3.0 mmol) in 15 mL of toluene was treated with a solution of $Pd(dba)_2$ (0.035 g, 0.06 mmol) and PPh_3 (0.127 g, 0.487 mmol) in toluene (5 mL). The reaction mixture was refluxed for 20 h, then cooled at room temperature and treated with water (20 mL). The formed layers were separated, the aqueous phase extracted with CH_2Cl_2 (3 x 20 mL) and then dried over Na_2SO_4. The collected organic layers were evaporated under reduced pressure to give yellow oil. The product was purified by recrystallization from hot MeOH, by cooling the resulting solution at 4°C overnight to afford yellow crystals (0.67 g, yield 94.4%). Mp: 123°C. IR (KBr): $\nu_{(C=N)}$ 1646 cm^{-1}. MS *m/z* (%): 378 (M^+, 76); 379 (M^+ +1, 20); 333 (M^+ -15, 100). ^{1}H NMR (300 MHz, CD_2Cl_2, 293K): δ 1.17 (d, $^{3}J_{HH}$ = 6.8 H_Z, 12H, $CH(CH_3)$, $H^{18, 19, 21, 22}$), 2.97 (sept, $^{3}J_{HH}$ = 6.8 Hz, 2H, C*H*(CH_3), $H^{17,20}$), 7.08-7.19 (4H, C*H* Ar, $H^{8,13,14,15}$), 7.43 (dd, $^{3}J_{HH}$= 5.05 Hz, $^{4}J_{HH}$= 1.14 Hz, 1H, C*H* Ar, H^{7}), 7.68 (dd, $^{3}J_{HH}$ = 3.69 Hz, $^{4}J_{HH}$= 1.14 Hz, 1H, C*H* Ar, H^{9}), 7.78 (dd, $^{3}J_{HH}$ = 7.8 Hz, $^{4}J_{HH}$= 1.11 Hz, 1H, C*H* Ar, H^{2}), 7.84 (t, $^{3}J_{HH}$ = 7.8 Hz, 1H, C*H* Ar, H^{3}), 8.14 (dd, $^{3}J_{HH}$ = 7.8 Hz, $^{4}J_{HH}$= 1.11 Hz, 1H C*H* Ar, H^{4}), 8.29 (s, 1H, C*H*N, H^{10}). $^{13}C\{^{1}H\}$ NMR (75 MHz, CD_2Cl_2, 293 K): δ 23.1

($CH(CH_3)_2$, $C^{18,19,21,22}$), 27.9 ($CH(CH_3)_2$, $C^{17,20}$), 119.0 (C^4), 120.2 (C^2), 122.9 ($C^{13,15}$), 124.3 (C^{14}), 125.0 (C^9), 127.8 (C^7), 128.0 (C^8), 137.1 ($C^{12,16}$), 137.3 (C^3), 144.2 (C^6), 148.6 (C^{11}), 152.4 (C^1), 154.2 (C^5), 163.1 (C^{10}). Anal. Calcd (%) for $C_{22}H_{24}N_2S$ (348.50): C 75.82, H 6.94, N 8.04, S 9.20; found C, 75.90, H 6.98, N, 8.00, S, 9.12.

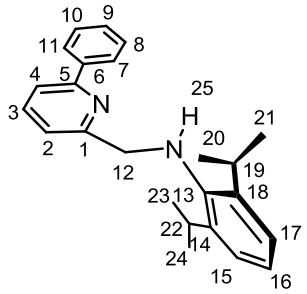

Synthesis of 2,6-diisopropyl-N-((6-phenylpyridin-2-yl)methyl)aniline (11a). To a solution of 2,6-diisopropyl-N-((6-phenylpyridin-2-yl)methylene)aniline (**6a**) (1.5 g, 4.35 mmol), in a 1:1 mixture of dry and degassed MeOH (15 mL) and THF (15 mL), was added, under nitrogen at 0°C, $NaBH_3CN$ (0.82 g, 13.06 mmol) and acetic acid (0.75 mL, 13.06 mmol). The resulting solution was stirred at 0°C for 2.5 h and then a saturated solution of Na_2CO_3 was added and the reaction allowed coming to room temperature. The aqueous layer was extracted with AcOEt (3 x 20 mL), the organic layers were combined and dried over Na_2SO_4. Filtration, removal the solvent *in vacuo* and drying gave the crude product which was crystallized from MeOH, by cooling the resulting solution at -20°C overnight to afford white crystals (1.20 g, yield 80.4 %). Mp: 88°C. IR (KBr): $\nu_{(N-H)}$ 3355, $\nu_{(C-N)}$ 1261 cm^{-1}. MS *m/z* (%): 344 (M^+, 55); 301 (M^+ -43, 41); 176 (100). ^1H NMR (300 MHz, CD_2Cl_2, 293K): δ 1.18 (d, $^3J_{HH}$ = 6.8 H_Z, 12H, $CH(CH_3)$, $H^{20,21,23,24}$), 3.43 (sept, $^3J_{HH}$ = 6.8 Hz, 2H, $CH(CH_3)$, $H^{19,22}$), 4.17 (s, 2H, CH_2N, H^{12}), 6.95-7.06 (3H, C*H* Ar, $H^{15,16,17}$), 7.17 (dd, $^3J_{HH}$ = 7.8 Hz, 1H, C*H* Ar, H^2), 7.37-7.47 (3H, C*H* Ar, $H^{8,9,10}$), 7.63 (dd, $^3J_{HH}$ = 7.8 Hz, 1H, C*H* Ar, H^4), 7.69 (t, $^3J_{HH}$= 7.8 Hz, 1H, C*H* Ar, H^3), 8.03-8.06 (2H, C*H* Ar, $H^{7,11}$). $^{13}C\{^1H\}$ NMR (75 MHz, CD_2Cl_2, 293 K): δ 23.9 ($CH(CH_3)_2$, $C^{20,21,23,24}$), 27.7 ($CH(CH_3)_2$, $C^{19,22}$), 56.4 (C^{12}), 118.5 (C^4), 120.4 (C^2), 123.4 ($C^{15,17}$), 123.5 (C^{16}), 126.7 ($C^{7,11}$), 128.6 ($C^{8,10}$), 128.9 (C^9), 137.2 (C^3), 139.1 (C^6), 142.6 ($C^{14,18}$), 143.8 (C^{13}), 156.2 (C^5), 158.4 (C^1). Anal. Calcd (%) for $C_{24}H_{28}N_2$ (344.49): C 83.68, H 8.19, N, 8.13; found C 83.75, H 8.20, N 8.05.

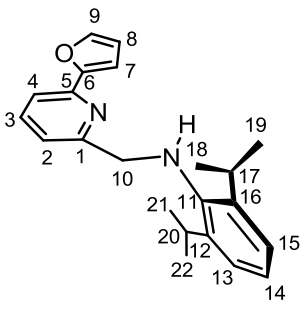

Synthesis of N-((6-(furan-2-yl)pyridin-2-yl)methyl)-2,6-diisopropylaniline (11b). To a solution of N-((6-(furan-2-yl)pyridin-2-yl)methylene)-2,6-diisopropylaniline (**10a**) (0.57 g, 1.71 mmol), in a mixture of dry and degassed MeOH (5 mL) and THF (7 mL), was added, under nitrogen at 0°C, $NaBH_3CN$ (0.32 g, 5.14 mmol) and acetic acid (0.30 mL, 5.14 mmol). The resulting solution was stirred at 0°C for 2.5 h and then a saturated solution of Na_2CO_3 was added and the reaction allowed coming to room temperature. The aqueous layer was extracted with AcOEt (3 x 10 mL), the organic layers were combined and dried over Na_2SO_4. Filtration, removal the solvent *in vacuo* and drying gave the crude product which was crystallized from MeOH, by cooling the resulting solution at -20°C overnight to afford white crystals (0.400 g, yield 70.0 %). Mp: 55°C. IR (KBr): $\nu_{(N-H)}$ 3342, $\nu_{(C-N)}$ 1254 cm^{-1}. MS *m/z* (%): 334 (M^+, 50); 291 (M^+ -43, 38); 176 (100). ^1H NMR (300 MHz, $CDCl_3$, 293K): δ 1.27 (d, $^3J_{HH}$ = 6.8 H_Z, 12H, CH(C*H*$_3$), $H^{18,19,\ 21,22}$), 3.46 (sept, $^3J_{HH}$ = 6.8 Hz, 2H, C*H*(CH_3), $H^{17,20}$), 4.21 (s, 2H, *CH*$_2$N, H^{10}), 4.52 (bs, 1H, CH_2N*H*, H^{23}), 6.55 (dd, $^3J_{HH}$ = 3.3 Hz, $^4J_{HH}$= 1.7 Hz, 1H, C*H* Ar, H^8), 7.05-7.15 (5H, C*H* Ar, $H^{2,7,13,14,15}$), 7.54 (m, 1H, C*H* Ar, H^9), 7.61 (d, $^3J_{HH}$ = 7.8 Hz, 1H, C*H* Ar, H^4), 7.68 (pt, $^3J_{HH}$= 7.8 Hz, 1H, C*H* Ar, H^3). $^{13}C\{^1H\}$ NMR (75 MHz, $CDCl_3$, 293 K): δ 24.2 (CH(*C*H_3)$_2$, $C^{18,19,21,22}$), 27.7 (*C*H(CH_3)$_2$, $C^{17,20}$), 56.2 (C^{10}), 108.5 (C^7), 112.0 (C^8), 116.8 (C^4), 120.1 (C^2), 123.5 ($C^{13,15}$), 123.6 (C^{14}), 137.0 (C^3), 142.4 ($C^{12,16}$), 143.2 (C^9), 143.6 (C^{11}), 148.7 (C^5), 153.8 (C^1), 158.3 (C^6). Anal. Calcd (%) for $C_{22}H_{26}N_2O$ (334.45): C 79.00, H 7.84, N 8.38, O 4.78; found C 79.05, H 7.90, N 8.32, O 4.73.

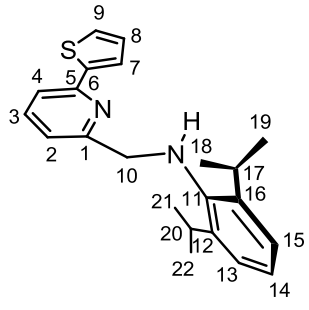

Synthesis of 2,6-diisopropyl-N-((6-(thiophen-2-yl)pyridin-2-yl)methyl)aniline (11c). To a solution of 2,6-diisopropyl-N-((6-(thiophen-2-yl)pyridin-2-yl)methylene)aniline (**10b**) (1.0 g, 2.87

mmol), in a mixture of dry and degassed MeOH (8 mL) and THF (12 mL), was added, under nitrogen at 0°C, $NaBH_3CN$ (0.54 g, 8.61 mmol) and acetic acid (0.50 mL, 8.61 mmol). The resulting solution was stirred at 0°C for 2.5 h and then a saturated solution of Na_2CO_3 and water was added and the reaction allowed coming to room temperature. The aqueous layer was extracted with AcOEt (3 x 15 mL), the organic layers were combined and dried over Na_2SO_4. Filtration, removal the solvent *in vacuo* and drying gave the crude product which was crystallized from MeOH, by cooling the resulting solution at -20°C overnight to afford white crystals (0.9 g, yield 89.1 %). Mp: 80°C. IR (KBr): $\nu_{(N-H)}$ 3355, $\nu_{(C-N)}$ 1253 cm^{-1}. MS *m/z* (%): 350 (M^+, 48); 307 (M^+ -43, 41); 176 (100). ^1H NMR (300 MHz, $CDCl_3$, 293K): δ 1.32 (d, $^3J_{HH}$ = 6.8 H_Z, 12H, CH(CH_3), $H^{18,19,21,22}$), 3.56 (sept, $^3J_{HH}$ = 6.8 Hz, 2H, CH(CH_3), $H^{17,20}$), 4.23 (s, 2H, CH_2N, H^{10}), 4.68 (bs, 1H, CH_2NH, H^{23}), 7.10-7.19 (5H, CH Ar, $H^{2,8,13,14,15}$), 7.43 (dd, $^3J_{HH}$ = 5.0 Hz, $^4J_{HH}$= 1.0 Hz, 1H, CH Ar, H^7), 7.59 (d, $^3J_{HH}$ = 7.5 Hz, 1H, CH Ar, H^4), 7.57-7.69 (2H, CH Ar, $H^{3,9}$). $^{13}C\{^1H\}$ NMR (75 MHz, $CDCl_3$, 293 K): δ 24.3 (CH(CH_3)$_2$, $C^{18,19,21,22}$), 27.8 ($CH(CH_3)_2$, $C^{17,20}$), 56.1 (C^{10}), 117.0 (C^4), 120.1 (C^2), 123.5 ($C^{13,15}$), 123.6 (C^{14}), 124.5(C^9), 127.6 (C^7), 127.9 (C^8), 137.1 (C^3), 143.6 ($C^{12,16}$), 143.6 (C^{11}), 145.0 (C^5), 152.0 (C^1), 158.1 (C^6). Anal. Calcd (%) for $C_{22}H_{26}N_2S$ (350.52): C 75.38, H 7.48, N 7.99, S 9.15; found C, 75.40, H 7.53, N 7.96, S 9.11.

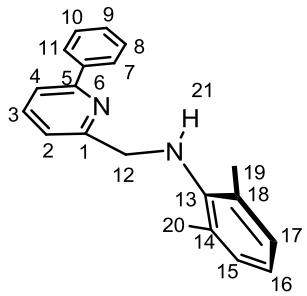

Synthesis of 2,6-dimethyl-N-((6-phenylpyridin-2-yl)methyl)aniline (11d). To a solution of 2,6-dimethyl-N-((6-phenylpyridin-2-yl)methylene)aniline (**6b**) (0.70 g, 2.44mmol), in a 1:1 mixture of dry and degassed MeOH (7 mL) and THF (7 mL), was added, under nitrogen at 0°C, $NaBH_3CN$ (0.46 g, 7.33 mmol) and acetic acid (0.42 mL, 7.33 mmol). The resulting solution was stirred at 0°C for 2.5 h and then a saturated solution of Na_2CO_3 was added and the reaction allowed coming to room temperature. The aqueous layer was extracted with AcOEt (3 x 20 mL), the organic layers

were combined and dried over Na_2SO_4. Filtration, removal the solvent *in vacuo* and drying gave the crude product which was crystallized from MeOH, by cooling the resulting solution at -20°C overnight to afford white crystals (0.55 g, yield 78.0 %). ^{1}H NMR (300 MHz, CD_2Cl_2, 293K): δ 2.40 (s, 6H, C*H*$_3$, H^{19,20}), 4.39 (s, 2H, *CH*$_2$N, H^{12}), 4.73 (brs, 1H, *C*H$_2$N*H*, H^{21}), 6.82 (m, 1H, C*H* Ar, H^{16}), 7.04 (m, 2H, C*H* Ar, H^{15,17}), 7.17 (m, 1H, C*H* Ar, H^{2}), 7.47-7.56 (3H, C*H* Ar, H^{8,9,10}), 7.69-7.78 (m, 2H, C*H* Ar, H^{3,4}), 8.11-8.15 (2H, C*H* Ar, H^{7,11}). ^{13}C{^{1}H} NMR (75 MHz, CD_2Cl_2, 293 K): δ 18.6 (*C*H$_3$, C^{19,20}), 53.5 (C^{12}), 118.5 (C^4), 120.3 (C^2), 121.3 (C^{16}), 126.7 (C^{7,11}), 128.6 (C^{15,17}), 128.7 (C^{8,10}), 128.9 (C^9), 128.9 (C^{13}), 137.2 (C^3), 139.2 (C^6), 146.6 (C^{14,18}), 156.3 (C^5), 158.7 (C^1). Anal. Calcd (%) for $C_{20}H_{20}N_2$ (288.39): C 83.30, H 6.99, N 9.71; found C 83.40, H 7.20, N 9.40.

General procedure for the synthesis of the M^{IV}-pyridylamido (M = Zr, Hf) tautomeric mixtures $\mathbf{12_{Ph(Zr)}/12'_{Ph(Zr)}}$, $\mathbf{13_{Fu(Zr)}/13'_{Fu(Zr)}}$, $\mathbf{14_{Th(Zr)}/14'_{Th(Zr)}}$ and $\mathbf{15_{Th(Hf)}/15'_{Th(Hf)}}$. To a solution of the proper aminopyridinate ligand N_2H^R (**11a, 11b** or **11c**) (0.150 g) in C_6H_6 (2 mL) a solution of M^{IV}(NMe$_2$)$_4$ (M = Zr, Hf) 99% (1 equiv.) in C_6H_6 (3 mL) was added dropwise. The reaction mixture was maintained at r.t. under stirring for 3 h and then concentrated *in vacuo* to afford a yellowish solid residue. The crude material was re-crystallized by layering a toluene solution with pentane and cooling down the mixture overnight to –30 °C (**$\mathbf{12_{Ph(Zr)}/12'_{Ph(Zr)}}$**: 0.230 g, yield 94%; **$\mathbf{13_{Fu(Zr)}/13'_{Fu(Zr)}}$**: 0.232 g, yield 93%; **$\mathbf{14_{Th(Zr)}/14'_{Th(Zr)}}$**: 0.211 g, yield 86%; **$\mathbf{15_{Th(Hf)}/15'_{Th(Hf)}}$**: 0.238 g, yield 84%). Products were isolated as tautomeric mixtures in a roughly 99:1 ratio (**$\mathbf{12_{Ph(Zr)}/12'_{Ph(Zr)}}$** and **$\mathbf{13_{Fu(Zr)}/13'_{Fu(Zr)}}$**) and 73:27 ratio (**$\mathbf{14_{Th(Zr)}/14'_{Th(Zr)}}$**), 83:17 ratio (**$\mathbf{15_{Th(Hf)}/15'_{Th(Hf)}}$**) at 298 K.

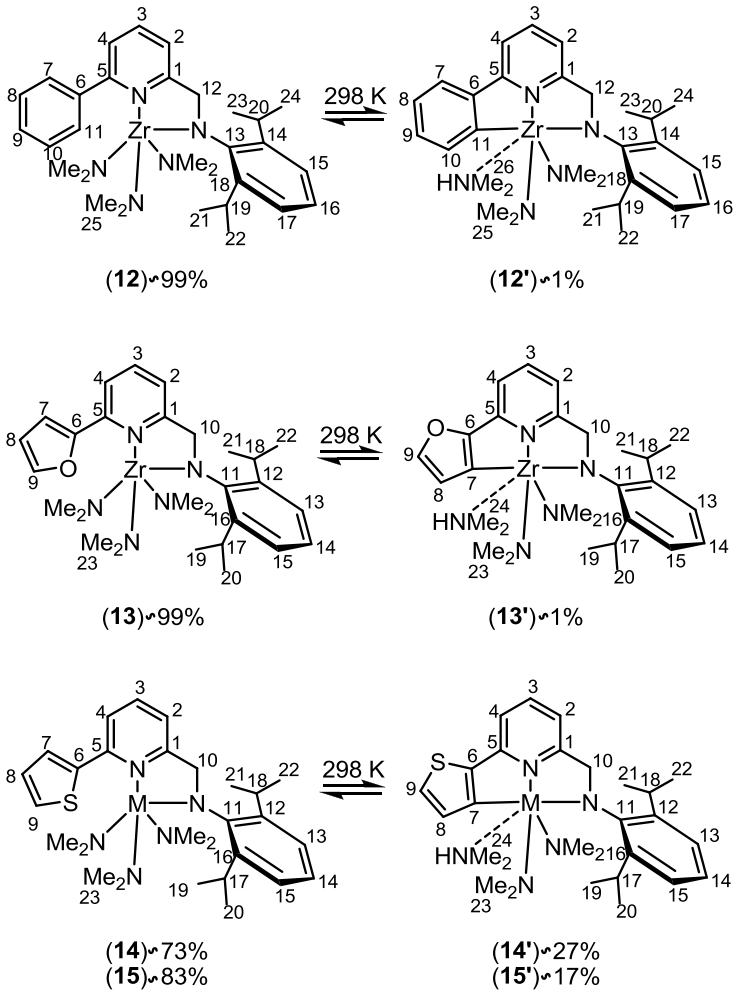

12$_{Ph(Zr)}$/12'$_{Ph(Zr)}$ (≈ 99:1): ^{1}H NMR (300 MHz, C_6D_6, 293 K, selected data): δ 1.33 (d, $^{3}J_{HH}$ = 6.9 Hz, 6H, CH(CH$_3^A$C*H*$_3^B$), H^{22,24}, **12**), 1.49 (d, $^{3}J_{HH}$ = 6.9 Hz, 6H, CH(C*H*$_3^A$CH$_3^B$), H^{21,23}, **12**), 2.74 (br, 18H, N(C*H*$_3$)$_2$, H^{25}, **12**), 3.73 (sept, $^{3}J_{HH}$ = 6.9 Hz, 2H, C*H*(CH$_3$)$_2$, H^{19,20}, **12**), 4.83 (s, 2H, *CH*$_2$N, H^{12}, **15**), 6.52 (m, 1H, C*H* Ar, H^{2}, **12**), 6.80 (m, 1H, C*H* Ar, H^{4}, **12**), 6.89 (t, $^{3}J_{HH}$ = 7.8 Hz, 1H, C*H* Ar, H^{3}, **12**), 7.14-7.19 (3H, C*H* Ar, H^{15,16,17}, **12**), 7.25-7.30 (3H, C*H* Ar, H^{8,9,10}, **12**), 7.44-7.47 (2H, C*H* Ar, H^{7,11}, **12**). ^{13}C{^{1}H} NMR (75 MHz, C_6D_6, 293 K, selected data): δ 23.9 (CH(CH$_3^A$*C*H$_3^B$), C^{21,23}, **12**), 26.8 (*C*H(*C*H$_3^A$CH$_3^B$), C^{22,24}, **12**), 28.2 (*C*H(CH$_3$)$_2$, C^{19,20}, **12**), 41.8 (N(*C*H$_3$), C^{25}, **12**), 65.4 (C^{12}, **12**), 119.3 (C^{4}, **12**), 123.1 (C^{2}, **12**), 123.2 (C^{15,17}, **15**), 123.9 (C^{16}, **12**), 127.6 (C^{8,10}, **12**), 128.4 (C^{9}, **12**), 128.5 (C^{7,11}, **12**), 137.2 (C^{3}, **12**), 140.0 (C, **12**), 144.6 (C, **12**), 150.5 (C, **12**), 160.9 (C, **12**), 164.6 (C, **12**). Anal.

Calcd (%) for $C_{30}H_{45}N_5Zr$ (566.94): C 63.56, H 8.00, N 12.35; found: C 63.32, H 7.92, N 12.47. **$13_{Fu(Zr)}$/$13'_{Fu(Zr)}$** (≈ 99:1)**:** ^{1}H NMR (300 MHz, C_6D_6, 293 K, selected data): δ 1.32 (d, $^3J_{HH}$ = 6.9 Hz, 6H, CH($CH_3^ACH_3^B$), $H^{20,22}$, **13**), 1.48 (d, $^3J_{HH}$ = 6.9 Hz, 6H, CH($CH_3^ACH_3^B$), $H^{19,21}$, **13**), 2.86 (br, 18H, N(CH_3)$_2$, H^{23}, **13**), 3.73 (sept, $^3J_{HH}$ = 6.9 Hz, 2H, C*H*(CH_3)$_2$, $H^{17,18}$, **13**), 4.77 (s, 2H, CH_2N, H^{10}, **13**), 6.26 (m, 1H, C*H* Ar, H^8, **13**), 6.42 (d, $^3J_{HH}$ = 7.8 Hz, 1H, C*H* Ar, H^2, **13**), 6.87 (t, $^3J_{HH}$ = 7.8 Hz, 1H, C*H* Ar, H^3, **13**), 7.09 (m, 1H, C*H* Ar, H^7, **13**), 7.16-7.20 (m, 1H, C*H* Ar, H^{14}, **13**), 7.25-7.28 (2H, C*H* Ar, $H^{13,15}$, **13**), 7.32 (m, 1H, C*H* Ar, H^9, **13**), 7.37 (d, $^3J_{HH}$ = 7.8 Hz, 1H, C*H* Ar, H^4, **13**). ^{13}C{^{1}H} NMR (75 MHz, C_6D_6, 293 K, selected data): δ 23.9 (CH($CH_3^AC H_3^B$), $C^{19,21}$, **13**), 26.8 (CH($CH_3^ACH_3^B$), $C^{20,22}$, **13**), 28.2 (*C*H(CH_3)$_2$, $C^{17,18}$, **13**), 42.7 (N(CH_3), C^{23}, **13**), 65.5 (C^{10}, **13**), 112.0 (C^9, **13**), 112.5 (C^8, **13**), 119.2 (C^2, **13**), 119.9 (C^4, **13**), 123.2 ($C^{13,15}$, **13**), 124.1 (C^{14}, **13**), 137.0 (C^3, **13**), 143.2 (C^7, **13**), 144.8 (C, **13**), 150.0 (C, **13**), 150.1 (C, **13**), 151.5 (C, **13**), 164.2 (C, **13**). Anal. Calcd (%) for $C_{28}H_{43}N_5OZr$ (556.90): C 60.39, H 7.78, N 12.58, O 2.87; found: C 60.20, H 7.52, N 12.43, O 2.95. **$14_{Th(Zr)}$/$14'_{Th(Zr)}$** (≈ 73:27)**:** ^{1}H NMR (400 MHz, C_7D_8, 293 K, selected data): δ 1.23 (d, $^3J_{HH}$ = 6.9 Hz, 6H, CH($CH_3^AC H_3^B$), $H^{20,22}$, **14'**), 1.26 (d, $^3J_{HH}$ = 6.9 Hz, 6H, CH($CH_3^ACH_3^B$), $H^{19,21}$, **14'**), 1.32 (d, $^3J_{HH}$ = 6.9 Hz, 6H, CH($CH_3^AC H_3^B$), $H^{20,22}$, **14**), 1.48 (d, $^3J_{HH}$ = 6.9 Hz, 6H, CH($CH_3^ACH_3^B$), $H^{19,21}$, **14**), 2.22 (d, $^3J_{HH}$ = 6.7 Hz, 6H, (CH_3)$_2^{24}$NH, **14'**), 2.80 (s, 18H, N(CH_3)$_2$, H^{23}, **14**), 2.84 (s, 12H, N(CH_3)$_2$, H^{23}, **14'**), 3.57 (sept, $^3J_{HH}$ = 6.9 Hz, 2H, C*H*(CH_3)$_2$, $H^{17,18}$, **14'**), 3.72 (sept, $^3J_{HH}$ = 6.9 Hz, 2H, C*H*(CH_3)$_2$, $H^{17,18}$, **14**), 4.80 (s, 2H, CH_2N, H^{10}, **14'**), 4.81 (s, 2H, CH_2N, H^{10}, **14**), 6.41 (m, 1H, C*H* Ar, H^2, **14'**), 6.55 (m, 1H, C*H* Ar, H^2, **14**), 6.84-6.97 (4H, C*H* Ar, $H^{3,4,7,8}$, **14**; 3H, C*H* Ar, $H^{3,4,8}$, **14'**), 7.12- 7.25 (3H, C*H* Ar, $H^{13,14,15}$, **14**, **14'**), 7.48-7.50 (m, 1H, C*H* Ar, H^9, **14**, **14'**). ^{13}C{^{1}H} NMR (100 MHz, C_7D_8, 293 K, selected data): δ 23.37 (CH($CH_3^AC H_3^B$), $C^{19,21}$, **14**), 23.43 (CH($CH_3^AC H_3^B$), $C^{19,21}$, **14'**), 25.91 (CH($CH_3^ACH_3^B$), $C^{20,22}$, **14'**), 26.27 (CH($CH_3^ACH_3^B$), $C^{20,22}$, **14**), 27.34 (*C*H(CH_3)$_2$, $C^{17,18}$, **14'**), 27.75 (*C*H(CH_3)$_2$, $C^{17,18}$, **14**), 38.10 (N(CH_3), C^{24},

14'), 39.96 (N(*C*H$_3$), C^{23}, **14**), 42.23 (N(*C*H$_3$), C^{23}, **14'**), 65.16 (C^{10}, **14**), 65.80 (C^{10}, **14'**), 114.04 (C^{2}, **14'**), 114.69 (C^{4}, **14'**), 118.87 (C^{2,4}, **14**), 122.72 (C, **14**), 122.83 (C, **14**), 122.99 (C, **14'**), 123.60 (C, **14**), 124.21 (C, **14'**), 126.29 (C^{8}, **14'**), 126.43 (C, **14**), 127.02 (C, **14**) 128.87 (C, **14**), 136.19 (C^{9}, **14**), 136.61 (C, **14**), 139.34 (C^{3}, **14'**), 140.77 (C, **14**), 144.35 (C, **14**), 145.87 (C^{12,16}, **14'**), 148.31 (C, **14'**), 149.84 (C, **14**), 153.88 (C, **14**), 158.58 (C, **14'**), 164.30 (C, **14'**), 164.58 (C, **14**), 193.79 (C^{7}, **14**). Anal. Calcd (%) for $C_{28}H_{43}N_5SZr$ (572.96): C 58.69, H 7.56, N 12.22, S 5.60; found: C 58.31, H 7.44, N 12.03, S 6.06. **15$_{Th(Hf)}$/15'$_{Th(Hf)}$** (≈ 83:17)**:** ^{1}H NMR (400 MHz, C_7D_8, 293 K, selected data): δ 1.21 (d, $^3J_{HH}$ = 6.9 Hz, 12H, CH(C*H*$_3^A$C*H*$_3^B$), H^{19,20,21,22}, **15'**), 1.27 (d, $^3J_{HH}$ = 6.9 Hz, 6H, CH(CH$_3^A$C*H*$_3^B$), H^{20,22}, **15**), 1.43 (d, $^3J_{HH}$ = 6.9 Hz, 6H, CH(C*H*$_3^A$CH$_3^B$), H^{19,21}, **15**), 2.18 (d, $^3J_{HH}$ = 6.4 Hz, 6H, (C*H*$_3$)$_2$^{24}NH, **15'**), 2.77 (s, 18H, N(C*H*$_3$)$_2$, H^{23}, **15**), 2.82 (s, 12H, N(C*H*$_3$)$_2$, H^{23}, **15'**), 3.54 (sept, $^3J_{HH}$ = 6.9 Hz, 2H, C*H*(CH$_3$)$_2$, H^{17,18}, **15'**), 3.69 (sept, $^3J_{HH}$ = 6.9 Hz, 2H, C*H*(CH$_3$)$_2$, H^{17,18}, **15**), 4.87 (s, 2H, C*H*$_2$N, H^{10}, **15'**), 4.89 (s, 2H, C*H*$_2$N, H^{10}, **15**), 6.37 (m, 1H, C*H* Ar, H^{2}, **15'**), 6.49 (m, 1H, C*H* Ar, H^{2}, **15**), 6.76-7.00 (4H, C*H* Ar, H^{3,4,7,8}, **15**; 3H, C*H* Ar, H^{3,4,8}, **15'**), 7.07- 7.21 (3H, C*H* Ar, H^{13,14,15}, **15**, **15'**), 7.45 (m, 1H, C*H* Ar, H^{9}, **15**), 7.48 (m, 1H, C*H* Ar, H^{9}, **15'**). ^{13}C{^{1}H} NMR (100 MHz, C_7D_8, 293 K, selected data): δ 24.20 (CH(CH$_3^A$*C*H$_3^B$), C^{19,21}, **15**), 24.26 (CH(CH$_3^A$*C*H$_3^B$), C^{19,21}, **15'**), 26.82 (CH(*C*H$_3^A$CH$_3^B$), C^{20,22}, **15'**), 27.21 (CH(*C*H$_3^A$CH$_3^B$), C^{20,22}, **15**), 28.10 (*C*H(CH$_3$)$_2$, C^{17,18}, **15'**), 28.45 (*C*H(CH$_3$)$_2$, C^{17,18}, **15**), 38.91 (N(*C*H$_3$), C^{24}, **15'**), 40.65 (N(*C*H$_3$), C^{23}, **15'**), 42.87 (N(*C*H$_3$), C^{23}, **15**), 65.95 (C^{10}, **15**), 66.77 (C^{10}, **15'**), 114.88 (C^{2}, **15'**), 115.55 (C^{4}, **15'**), 119.66 (C^{2,4}, **15**), 123.51 (C, **15**), 123.74 (C, **15'**), 124.16 (C, **15**), 124.50 (C, **15**), 124.98 (C, **15'**), 127.38 (C^{8}, **15'**), 127.67 (C, **15**), 127.91 (C, **15'**), 129.78 (C, **15**), 137.4 (C, **15**), 138.10 (C^{9}, **15'**), 140.22 (C^{3}, **15'**), 141.32 (C, **15**), 145.37 (C, **15**), 146.74 (C^{12,16}, **15'**), 149.55 (C, **15'**), 150.49 (C, **15**), 154.81 (C, **15**), 158.98 (C, **15'**), 165.42 (C, **15**), 165.47 (C, **15'**), 203.61 (C^{7}, **15'**).

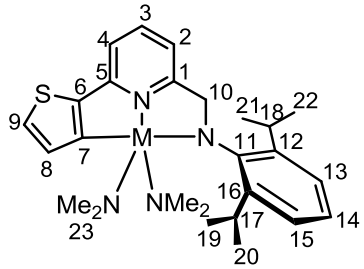

M^{IV} = Zr (**16**); Hf (**17**)

General procedure for the synthesis of 16 and 17. In a typical procedure, the tautomeric mixture of $\mathbf{14_{Th(Zr)}/14'_{Th(Zr)}}$ ($\mathbf{15_{Th(Hf)}/15'_{Th(Hf)}}$) (0.25 mmol) in C_7H_8 (3 mL) was refluxed for 24 h (18 h) and periodically evacuated as to maintain the reaction vessel under a low static vacuum. Afterwards, solvent evaporation gave the bis-amido complex **16** (**17**) as an air and moisture sensitive dark-yellow (dark-brown) microcrystalline solids in 93% yield (95% yield). **16**: ^{1}H NMR (400 MHz, C_7D_8, 293 K): δ 1.23 (d, $^3J_{HH}$ = 6.9 Hz, 6H, CH(CH$_3^A$C*H*$_3^B$), H^{20,22}), 1.26 (d, $^3J_{HH}$ = 6.9 Hz, 6H, CH(C*H*$_3^A$CH$_3^B$), H^{19,21}), 2.84 (s, 12H, N(C*H*$_3$)$_2$, H^{23}), 3.55 (sept, $^3J_{HH}$ = 6.9 Hz, 2H, C*H*(CH$_3$)$_2$, H^{17,18}), 4.80 (s, 2H, C*H*$_2$N, H^{10}), 6.41 (d, $^3J_{HH}$ = 7.8 Hz, 1H, C*H* Ar, H^2), 6.84 (d, $^3J_{HH}$ = 7.8 Hz, 1H, C*H* Ar, H^4), 6.88 (t, $^3J_{HH}$ = 7.8 Hz, 1H, C*H* Ar, H^3), 7.13-7.20 (4H, C*H* Ar, H^{8,13,14,15}), 7.50 (d, $^3J_{HH}$ = 4.5 Hz, 1H, C*H* Ar, H^9). ^{13}C{^{1}H} NMR (100 MHz, C_7D_8, 293 K): δ 23.79 (CH(CH$_3^A$*C*H$_3^B$), C^{19,21}), 26.35 (CH(*C*H$_3^A$CH$_3^B$), C^{20,22}), 27.66 (*C*H(CH$_3$)$_2$, C^{17,18}), 40.21 (N(*C*H$_3$), C^{23}), 66.05 (C^{10}), 114.41 (C^2), 115.19 (C^4), 123.33 (C^{13,15}), 124.57 (C^{14}), 126.74 (C^8), 136.67 (C^9), 139.78 (C^3), 146.14 (C^{12,16}), 148.05 (C), 148.34 (C), 158.81 (C), 164.63 (C), 193.72 (C^7). Anal. Calcd (%) for $C_{26}H_{36}N_4SZr$ (527.88): C 59.16, H 6.87, N 10.61, S 6.07; found: C 58.82, H 6.71, N 10.90, S 6.34. **17**: ^{1}H NMR (400 MHz, C_7D_8, 293 K): δ 1.21 (d, $^3J_{HH}$ = 6.9 Hz, 12H, CH(C*H*$_3$)$_2$, H^{19,20,21,22}), 2.82 (s, 12H, N(C*H*$_3$)$_2$, H^{23}), 3.54 (sept, $^3J_{HH}$ = 6.9 Hz, 2H, C*H*(CH$_3$)$_2$, H^{17,18}), 4.89 (s, 2H, C*H*$_2$N, H^{10}), 6.36 (d, $^3J_{HH}$ = 7.8 Hz, 1H, C*H* Ar, H^2), 6.76 (d, $^3J_{HH}$ = 7.8 Hz, 1H, C*H* Ar, H^4), 6.89 (t, $^3J_{HH}$ = 7.8 Hz, 1H, C*H* Ar, H^3), 7.08-7.21 (4H, C*H* Ar, H^{8,13,14,15}), 7.49 (d, $^3J_{HH}$ = 4.5 Hz, 1H, C*H* Ar, H^9). ^{13}C{^{1}H} NMR (100 MHz, C_7D_8, 293 K): δ 24.82 (CH(CH$_3^A$*C*H$_3^B$), C^{19,21}), 27.23 (CH(*C*H$_3^A$CH$_3^B$), C^{20,22}), 28.43 (*C*H(CH$_3$)$_2$, C^{17,18}), 40.90 (N(*C*H$_3$), C^{23}), 66.92 (C^{10}), 115.25 (C^2), 116.05 (C^4), 124.08 (C^{13,15}), 125.32 (C^{14}), 127.05 (C^8), 138.46 (C^9), 140.66 (C^3), 146.98 (C^{12,16}), 149.33 (C), 149.65 (C), 159.24 (C), 165.75 (C), 203.67 (C^7).

General procedure for the synthesis of Zr^{IV}-pyridylamido complexes 18, 19, 20 and **21.** To a solution of the proper aminopyridinate ligand N_2H^R (**11a-d**) (0.100 g) in dry and degassed C_6H_6 (2 mL) heated at 70 °C, a solution of tetrabenzylzirconium 95% (1 equiv.) in dry and degassed C_6H_6 (4 mL) was added dropwise. The reaction was maintained at the same temperature for several hours and the reaction course was periodically monitored by sampling the mixture at different times and following the ligand consumption *via* ^{1}H NMR (inside NMR capillary filled with C_6D_6) till completeness (**18**: 13h; **19**: 16h; **20**, 48h; **21**: 13h). Afterwards, the reaction mixture was concentrated in *vacuo* to afford red-brown solids. The crude materials were re-crystallized by layering a toluene solution with pentane and cooling down the mixtures overnight to –30 °C (**18**: 0.170 g, 95% yield; **19**: 0.155 g, 89% yield; **20**: 0.165 g, 91% yield; **21**: 0.180 g, 95% yield). Crystals suitable for X-ray diffraction analyses were obtained from concentrated solutions of each complex in: **18**: toluene at room temperature; **19** and **20**: Et_2O cooled to – 30°C; **21**: toluene cooled to – 30°C.

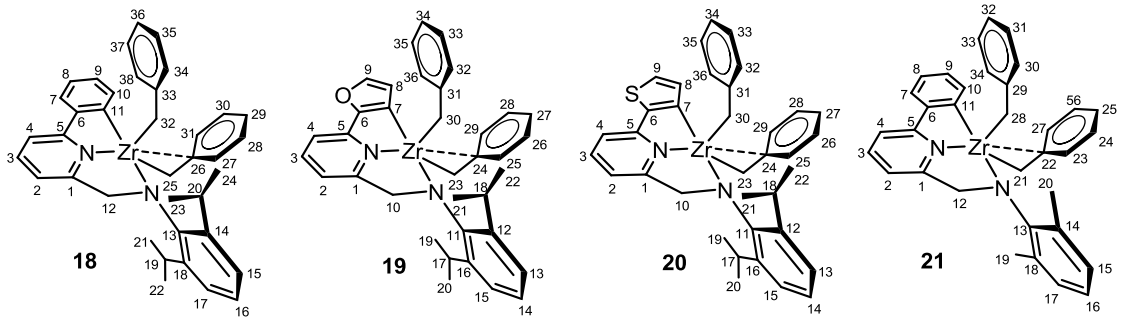

18: ^{1}H NMR (300 MHz, CD_2Cl_2, 293 K): δ 1.17 (d, $^3J_{HH}$ = 6.8 Hz, 6H, CH(CH_3), H^{22,24}), 1.32 (d, $^3J_{HH}$ = 6.8 Hz, 6H, CH(CH_3)$_2$, H^{21,23}), 1.59 (d, AB*q*, $^2J_{HH}$ = 10.0 Hz, 2H, ZrC*HH*Ph, H^{25,32}), 2.22 (d, AB*q*, $^2J_{HH}$ = 10.0 Hz, 2H, ZrC*HH*Ph, H^{25,32}), 3.59 (sept, $^3J_{HH}$ = 6.8 Hz, 2H, C*H*(CH$_3$), H^{19,20}), 4.87 (s, 2H, *CH$_2$*N, H^{12}), 6.38 (d, $^3J_{HH}$ = 7.4 Hz, 4H, *o*-Ph, H^{27,31,34,38}), 6.71 (t, $^3J_{HH}$ = 7.3 Hz, 2H, *p*-Ph, H^{29,36}), 6.88 (t, $^3J_{HH}$ = 7.6 Hz, 4H, *m*-Ph, H^{28,30,35,37}), 7.11 (d, $^3J_{HH}$ = 7.7 Hz, 1H, C*H* Ar, H^2), 7.22-7.27 (5H, C*H* Ar, H^{8,9,15,16,17}), 7.53-7.59 (2H, C*H* Ar,

$H^{4,10}$), 7.73 (t, $^3J_{HH}$ = 7.7 Hz, 1H, C*H* Ar, H^3), 7.80 (m, 1H, C*H* Ar, H^7). $^{13}C\{^1H\}$ NMR (75 MHz, CD_2Cl_2, 293 K): δ 22.6 ($CH(CH_3)_2$, $C^{21,23}$), 27.4 ($CH(CH_3)_2$, $C^{22,24}$), 27.8 ($CH(CH_3)_2$, $C^{19,20}$), 67.3 (C^{12}), 68.2 ($C^{25,32}$), 115.2 (C^4), 117.4 (C^2), 122.3 (C^{10}), 122.4 ($C^{29,36}$), 123.9 ($C^{15,17}$), 126.0 (C^{16}), 127.6 ($C^{28,30,35,37}$), 127.7 (C^8), 128.8 (C^9), 129.0 ($C^{27,31,34,38}$), 134.5 (C^7), 140.1 (C^3), 140.8 (C), 145.6 (C), 146.7 (C), 146.9 (C), 163.6 (C), 164.6 (C), 189.8 (C^{11}). Anal. Calcd (%) for $C_{38}H_{40}N_2Zr$ (615.96): C, 74.10; H, 6.55; N, 4.55. Found: C, 74.02; H, 6.49; N, 4.61. **19**: ^1H NMR (300 MHz, CD_2Cl_2, 293 K): δ 1.04-1.10 (8H, $CH(CH_3)$, ZrC*HH*Ph, $H^{20,22,23,30}$), 1.22 (d, $^3J_{HH}$ = 6.8 Hz, 6H, $CH(CH_3)$, $H^{19,21}$), 2.00 (d, AB*q*, $^2J_{HH}$ = 9.6 Hz, 2H, ZrC*HH*Ph, $H^{23,30}$), 3.44 (sept, $^3J_{HH}$ = 6.8 Hz, 2H, $CH(CH_3)_2$, $H^{17,18}$), 4.66 (s, 2H, CH_2N, H^{10}), 6.31-6.34 (5H, C*H* Ar, *o*-Ph, $H^{8,25,29,32,36}$), 6.69 (t, $^3J_{HH}$ = 7.3 Hz, 2H, *p*-Ph, $H^{27,34}$), 6.84-6.90 (5H, *m*-Ph, C*H* Ar, $H^{2,26,28,33,35}$), 6.95 (d, $^3J_{HH}$ = 7.7 Hz, 1H, C*H* Ar, H^4), 7.11-7.14 (3H, C*H* Ar, $H^{13,14,15}$), 7.28 (d, $^3J_{HH}$ = 1.4 Hz, 1H, C*H* Ar, H^9), 7.54 (t, $^3J_{HH}$ = 7.7 Hz, 1H, C*H* Ar, H^3). $^{13}C\{^1H\}$ NMR (75 MHz, CD_2Cl_2, 293 K): δ 22.5 ($CH(CH_3)_2$, $C^{19,21}$), 27.4 ($CH(CH_3)_2$, $C^{17,18}$), 27.8 ($CH(CH_3)_2$, $C^{20,22}$), 65.7 (C^{10}), 68.2 ($C^{23,30}$), 112.4 (C^4), 116.0 (C^2), 118.9 (C^8), 123.2 ($C^{27,34}$), 123.8 ($C^{13,15}$), 125.9 (C^{14}), 127.5 ($C^{26,28,33,35}$), 129.5 ($C^{25,29,32,36}$), 140.4 (C^3), 140.7 (C), 142.1 (C^9), 146.1 (C), 146.8 (C), 152.1 (C), 162.1 (C), 164.6 (C), 168.0 (C^7). Anal. Calcd (%) for $C_{36}H_{38}N_2OZr$ (605.92): C, 71.36; H, 6.32; N, 4.62; O, 2.64. Found: C, 71.22; H, 6.28; N, 4.45; O, 2.94. **20**: ^1H NMR (300 MHz, CD_2Cl_2, 293 K): δ 1.16 (d, $^3J_{HH}$ = 6.8 H_Z, 6H, $CH(CH_3)$, $H^{20,22}$), 1.31-1.33 (8H, $CH(CH_3)$, ZrC*HH*Ph, $H^{19,21,23,30}$), 2.16 (d, AB*q*, $^2J_{HH}$ = 9.6 Hz, 2H, ZrC*HH*Ph, $H^{23,30}$), 3.57 (sept, $^3J_{HH}$ = 6.8 Hz, 2H, $CH(CH_3)_2$, $H^{17,18}$), 4.82 (s, 2H, CH_2N, H^{10}), 6.39 (d, $^3J_{HH}$ = 7.5 Hz, 4H, *o*-Ph, $H^{25,29,32,36}$), 6.75 (t, $^3J_{HH}$ = 7.3 Hz, 2H, *p*-Ph, $H^{27,34}$), 6.92-7.00 (5H, *m*-Ph, C*H* Ar, $H^{2,26,28,33,35}$), 7.08 (d, $^3J_{HH}$ = 7.7 Hz, 1H, C*H* Ar, H^4), 7.13 (d, $^3J_{HH}$ = 4.5 Hz, 1H, C*H* Ar, H^8), 7.22-7.24 (4H, C*H* Ar, $H^{9,13,14,15}$), 7.62 (t, $^3J_{HH}$ = 7.7 Hz, 1H, C*H* Ar, H^3). $^{13}C\{^1H\}$ NMR (75 MHz, CD_2Cl_2, 293 K): δ 22.5 ($CH(CH_3)_2$, $C^{19,21}$), 27.4 ($CH(CH_3)_2$, $C^{17,18}$), 27.8 ($CH(CH_3)_2$,

$C^{20,22}$), 66.4 (C^{10}), 68.3 ($C^{23,30}$), 114.8 (C^{4}), 115.8 (C^{2}), 123.0 ($C^{27,34}$), 123.9 ($C^{13,15}$), 125.9 (C^{14}), 126.0 (C^{9}), 127.5 ($C^{26,28,33,35}$), 129.4 ($C^{25,29,32,36}$), 135.5 (C^{8}), 140.4 (C^{3}), 140.5 (C), 146.3 (C), 146.8 (C), 149.4 (C), 157.9 (C), 164.2 (C), 195.4 (C^{7}). Anal. Calcd (%) for $C_{36}H_{38}N_2SZr$ (621.99): C, 69.52; H, 6.16; N, 4.50; S, 5.16. Found: C, 69.25; H, 6.09; N, 4.43; S, 5.64. **21**: ^{1}H NMR (300 MHz, CD_2Cl_2, 293 K): δ 1.52 (d, AB*q*, $^{2}J_{HH}$ = 9.8 Hz, 2H, ZrC*HH*Ph, $H^{21,28}$), 2.05 (d, AB*q*, $^{2}J_{HH}$ = 9.8 Hz, 2H, ZrC*HH*Ph, $H^{21,28}$), 2.34 (s, 6H, CH_3, $H^{19,20}$), 4.85 (s, 2H, CH_2N, H^{12}), 6.32 (d, $^{3}J_{HH}$ = 7.2 Hz, 4H, *o*-Ph, $H^{23,27,30,34}$), 6.71 (t, $^{3}J_{HH}$ = 7.3 Hz, 2H, *p*-Ph, $H^{25,32}$), 6.86 (t, $^{3}J_{HH}$ = 7.4 Hz, 4H, *m*-Ph, $H^{24,26,31,33}$), 7.06-7.28 (6H, C*H* Ar, $H^{2,8,9,15,16,17}$), 7.50-7.57 (2H, C*H* Ar, $H^{4,10}$), 7.69 (t, $^{3}J_{HH}$ = 7.8 Hz, 1H, C*H* Ar, H^{3}), 7.78 (m, 1H, C*H* Ar, H^{7}). ^{13}C{^{1}H} NMR (75 MHz, CD_2Cl_2, 293 K): δ 19.0 (CH_3, $C^{19,20}$), 65.2 (C^{12}), 67.1 ($C^{21,28}$), 115.2 (C^{4}), 117.6 (C^{2}), 122.3 (C^{10}), 122.4 ($C^{25,32}$), 125.2 (C^{16}), 127.6 (C^{8}), 127.7 ($C^{23,27,30,34}$), 128.6 ($C^{15,17}$), 128.7 (C^{9}), 129.1 ($C^{24,26,31,33}$), 134.2 (C^{7}), 136.4 (C), 140.0 (C^{3}), 141.0 (C), 145.8 (C), 148.6 (C), 163.6 (C), 164.9 (C), 189.7 (C^{11}). Anal. Calcd (%) for $C_{34}H_{32}N_2Zr$ (559.86): C, 72.94; H, 5.76; N, 5.00. Found: C, 72.68; H, 5.65; N, 5.32.

General procedures for the synthesis of the zwitterionic pyridylamido complexes 18a, 19a, 20a and 21a upon $B(C_6F_5)_3$ activation of the dibenzyl precursors. To a dry and degassed C_6D_6 (0.5 mL) solution of the proper dibenzyl complex (**18, 19, 20** or **21**) (0.025 g), a C_6D_6 (0.5 mL) solution of $B(C_6F_5)_3$ (1 equiv.) was added in one portion. The addition of the Lewis acid causes the rapid change of the solutions' color from yellowish to dark-orange. The final mixtures are stirred at room temperature for 5 min. before being sealed in an NMR tube and spectroscopically characterized. Activation yields were assumed to be quantitative by ^{1}H NMR spectroscopy because of the absence of detectable amount of the signals attributed to the starting dibenzyl species.

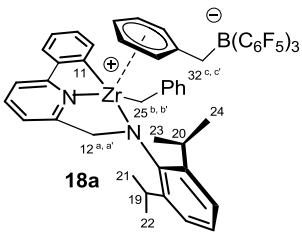

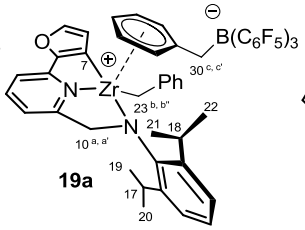

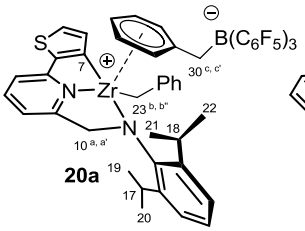

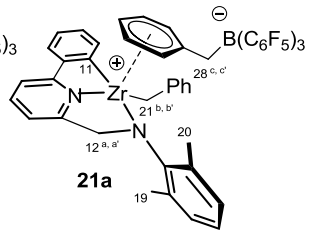

18a: ^{1}H NMR (400 MHz, C_6D_6, 293 K, selected data): δ 0.95 (d, $^{3}J_{HH}$ = 6.5 Hz, 3H, CH(CH_3), H^{22}), 1.00 (d, $^{3}J_{HH}$ = 6.5 Hz, 3H, CH(CH_3), H^{24}), 1.09 (d, $^{3}J_{HH}$ = 6.5 Hz, 3H, CH(CH_3), H^{21}), 1.33 (d, $^{3}J_{HH}$ = 6.5 Hz, 3H, CH(CH_3), H^{23}), 2.30-2.36 (2H, CH(CH$_3$)$_2$, ZrCHHPh, H^{19}, H^{25b}), 2.74 (d, $^{3}J_{HH}$ = 11.2 Hz, 1H, ZrCHHPh, H$^{25b'}$), 3.09 (m, 1H, BCHHPh, H^{32c}), 3.54-3.61 (2H, CH(CH$_3$)$_2$, BCHHPh, H^{20}, H$^{32c'}$), 4.13 (d, $^{3}J_{HH}$ = 19.9 Hz, 1H, CHHN, H^{12a}), 4.76 (d, $^{3}J_{HH}$ = 19.9 Hz, 1H, CHHN, H$^{12a'}$). ^{13}C{^{1}H} NMR (100 MHz, C_7D_8, 293 K, selected data): δ 21.5 (CH(*C*H$_3$), C^{23}), 23.2 (CH(*C*H$_3$), C^{24}), 26.2 (CH(*C*H$_3$), C^{22}), 27.3 (*C*H(CH$_3$), C^{20}), 27.4 (CH(*C*H$_3$), *C*H(CH$_3$), C$^{19, 21}$), 69.3 (*C*HHN, H^{12}), 79.6 (Zr*C*HHPh, C^{25}), 185.9 (C^{11}). **19a**: ^{1}H NMR (400 MHz, C_7D_8, 293 K, Selected data): δ 0.78 (d, $^{3}J_{HH}$ = 6.8 Hz, 3H, CH(CH_3), H^{20}), 0.91 (d, $^{3}J_{HH}$ = 6.8 Hz, 3H, CH(CH_3), H^{22}), 1.10 (d, $^{3}J_{HH}$ = 6.8 Hz, 3H, CH(CH_3), H^{19}), 1.27 (d, $^{3}J_{HH}$ = 6.8 Hz, 3H, CH(CH_3), H^{21}), 2.14 (m, 1H, ZrCHHPh, H^{23b}), 2.25 (sept, $^{3}J_{HH}$ = 6.8 Hz, 1H, CH(CH$_3$)$_2$, H^{17}), 2.41 (d, $^{3}J_{HH}$ = 11.5 Hz, 1H, ZrCHHPh, H$^{23b'}$), 3.37-3.47 (2H, CH(CH$_3$)$_2$, BCHHPh, H^{18}, H^{30c}), 3.58 (m, 1H, BCHHPh, H$^{30c'}$), 3.98 (d, $^{3}J_{HH}$ = 20.8 Hz, 1H, CHHN, H^{10a}), 4.74 (d, $^{3}J_{HH}$ = 20.8 Hz, 1H, CHHN, H$^{10a'}$). ^{13}C{^{1}H} NMR (100 MHz, C_7D_8, 293 K, selected data): δ 21.9 (CH(*C*H$_3$), C^{21}), 23.0 (CH(*C*H$_3$), C^{22}), 26.3 (CH(*C*H$_3$), C^{20}), 27.1 (*C*H(CH$_3$), C^{18}), 27.2 (CH(*C*H$_3$), C^{19}), 27.5 (*C*H(CH$_3$), C^{17}), 68.6 (*C*HHN, H^{10}), 80.4 (Zr*C*HHPh, C^{23}), 168.9 (C^{7}). **20a:** ^{1}H NMR (400 MHz, C_7D_8, 293 K, Selected data): δ 0.89 (d, $^{3}J_{HH}$ = 6.8 Hz, 3H, CH(CH_3), H^{20}), 0.93 (d, $^{3}J_{HH}$ = 6.8 Hz, 3H, CH(CH_3), H^{22}), 1.16 (d, $^{3}J_{HH}$ = 6.8 Hz, 3H, CH(CH_3), H^{19}), 1.40 (d, $^{3}J_{HH}$ = 6.8 Hz, 3H, CH(CH_3), H^{21}), 2.22-2.30 (2H, CH(CH$_3$)$_2$, ZrCHHPh, H^{17}, H^{23b}), 2.67 (d, $^{3}J_{HH}$ = 11.2 Hz, 1H, ZrCHHPh, H$^{23b'}$), 3.34 (m, 1H, BCHHPh, H^{30c}), 3.60 (sept, $^{3}J_{HH}$ = 6.8 Hz, 1H, CH(CH$_3$)$_2$, H^{18}), 3.85 (m, 1H, BCHHPh, H$^{30c'}$), 4.06 (d, $^{3}J_{HH}$ = 19.9 Hz, 1H, CHHN, H^{10a}),

4.87 (d, $^3J_{HH}$ = 19.9 Hz, 1H, CH*H*N, H$^{10a'}$). $^{13}C\{^1H\}$ NMR (100 MHz, C_7D_8, 293 K, selected data): δ 21.6 (CH(*C*H$_3$), C^{21}), 23.1 (CH(*C*H$_3$), C^{22}), 26.3 (CH(*C*H$_3$), C^{20}), 27.2 (*C*H(CH$_3$), C^{18}), 27.3 (CH(*C*H$_3$), *C*H(CH$_3$), C^{17,19}), 69.2 (*C*HHN, H^{10}), 81.6 (Zr*C*HHPh, C^{23}), 192.2 (C^7). **21a**: ^{1}H NMR (400 MHz, C_7D_8, 293 K, Selected data): δ 1.55 (s, 3H, C*H*$_3$, H^{19}), 2.23 (d, $^3J_{HH}$ = 11.0 Hz, 1H, ZrCH*H*Ph, H^{21b}), 2.33 (s, 3H, C*H*$_3$, H^{20}), 2.66 (d, $^3J_{HH}$ = 11.0 Hz, 1H, ZrCH*H*Ph, H$^{21b'}$), 3.25 (m, 1H, BCH*H*Ph, H^{28c}), 3.45 (m, 1H, BCH*H*Ph, H$^{28c'}$), 3.56 (d, $^3J_{HH}$ = 20.7 Hz, 1H, CH*H*N, H^{12a}), 4.49 (d, $^3J_{HH}$ = 20.7 Hz, 1H, CH*H*N, H$^{12a'}$). $^{13}C\{^1H\}$ NMR (100 MHz, C_7D_8, 293 K, selected data): δ 18.1 (*C*H$_3$, C^{20}), 21.0 (*C*H$_3$, C^{19}), 37.8 (B*C*HHPh, C^{28}), 67.7 (*C*HHN, C^{12}), 79.8 (Zr*C*HHPh, C^{21}), 185.2 (C^{11}).

General procedures for the synthesis of cationic pyridylamido complexes 18b, 19b, 20b and 21b upon $Ph_3C^+[B(C_6F_5)_4]^-$ activation of the dibenzyl precursors. All samples were prepared at room temperature in a dry-box filled with nitrogen. To a dry and degassed C_6D_6 (0.5 mL) solution of the proper dibenzyl complex (**18, 19, 20** or **21**) (0.025 g), a C_6D_6 (2 mL) solution of $Ph_3C^+[B(C_6F_5)_4]^-$ (1 equiv.) was added in one portion. Dark-green rubbery materials precipitate out upon addition of the tritylborate and were decanted from the supernatant. Afterwards, the solids were washed twice with C_6H_6 (2 x 2 mL) and dried under vacuum to constant weight before being characterized through ^{1}H NMR spectroscopy. Again, activation yields were assumed to be quantitative from ^{1}H NMR spectroscopy; the mother liquors contain an equimolar amount of the tritylbenzyl [Ph_3CCH_2Ph] species).

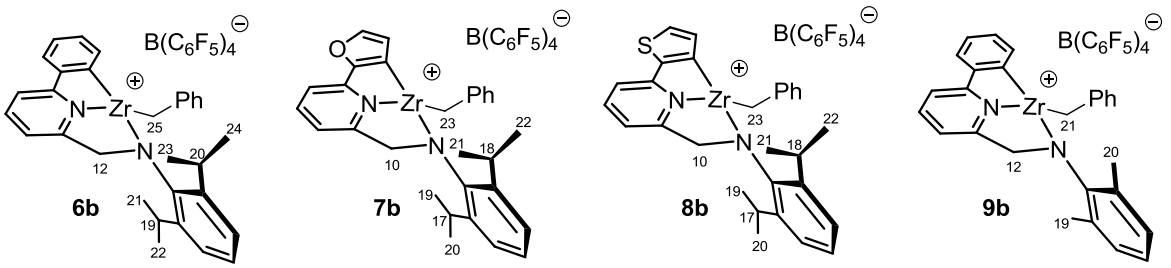

18b: ^{1}H NMR (400 MHz, C_6D_5Br, 293 K, Selected data): δ 1.11 (d, $^3J_{HH}$ = 6.8 Hz, 6H, CH(C*H*$_3$), H^{22,24}), 1.21 (d, $^3J_{HH}$ = 6.8 Hz, 6H, CH(C*H*$_3$), H^{21,23}), 2.84 (s, 2H, ZrC*H*$_2$Ph, H^{25}),

3.28 (m, 2H, C*H*(CH_3), $H^{19,20}$), 5.05 (s, 2H, *CH*$_2$N, H^{12}). **19b:** ^{1}H NMR (400 MHz, C_6D_5Br, 293 K, Selected data): δ 1.09 (d, $^3J_{HH}$ = 6.7 Hz, 6H, CH(C*H*$_3$), $H^{20,22}$), 1.22 (d, $^3J_{HH}$ = 6.7 Hz, 6H, CH(C*H*$_3$), $H^{19,21}$), 2.73 (s, 2H, ZrC*H*$_2$Ph, H^{23}), 3.22 (m, 2H, C*H*(CH_3), $H^{17,18}$), 4.90 (s, 2H, *CH*$_2$N, H^{10}).**20:** ^{1}H NMR (400 MHz, C_6D_5Br, 293 K, Selected data): δ 1.10 (d, $^3J_{HH}$ = 6.7 Hz, 6H, CH(C*H*$_3$), $H^{20,22}$), 1.22 (d, $^3J_{HH}$ = 6.7 Hz, 6H, CH(C*H*$_3$), $H^{19,21}$), 2.76 (s, 2H, ZrC*H*$_2$Ph, H^{23}), 3.28 (m, 2H, C*H*(CH_3), $H^{17,18}$), 4.98 (s, 2H, *CH*$_2$N, H^{10}). **21b:** ^{1}H NMR (400 MHz, C_6D_5Br, 293 K, Selected data): δ 2.15 (s, 6H, CH(C*H*$_3$), $H^{19.20}$), 2.72 (s, 2H, ZrC*H*$_2$Ph, H^{21}), 4.64 (s, 2H, *CH*$_2$N, H^{12}).

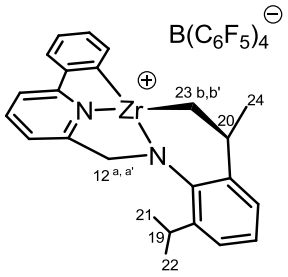

Synthesis of 24b. In a dry-box filled with nitrogen atmosphere, a solution of **18b** (0.025 g), in dry and degassed C_7D_8 (1 mL), was maintained under vigorous stirring, in the dark and at room temperature for 16h. The soluble fraction was isolated from the residual 6b fraction and analyzed by 1D and 2D NMR (see **Figure 2.10**) spectroscopy. ^{1}H NMR (400 MHz, C_7D_8, 293 K, Selected data): δ 1.02 (d, $^3J_{HH}$ = 6.7 Hz, 3H, CH(C*H*$_3$), H^{24}), 1.18 (d, $^3J_{HH}$ = 6.7 Hz, 3H, CH(C*H*$_3$), H^{22}), 1.22 (d, $^3J_{HH}$ = 6.7 Hz, 1H, ZrCH*H*CH, H^{23b}), 1.25 (d, $^3J_{HH}$ = 6.7 Hz, 1H, ZrCH*H*CH, $H^{23b'}$), 1.36 (d, $^3J_{HH}$ = 6.7 Hz, 3H, CH(C*H*$_3$), H^{21}), 3.12 (sept, 1H, C*H*(CH_3)$_2$, H^{19}), 3.43 (m, 1H, CH_2C*H*(CH_3), H^{20}), 4.40 (d, $^2J_{HH}$ = 20.0 Hz, 1H, CH*H*N, H^{12a}), 5.56 (d, $^2J_{HH}$ = 20.0 Hz, 1H, CH*H*N, $H^{12a'}$). ^{13}C{^{1}H} NMR (100 MHz, C_7D_8, 293 K, selected data)[29]: δ 15.3 (C), 22.7 (C), 23.9 (C), 28.7 (C), 63.7 (*C*HHN, C^{12}), 84.8 (CH(*C*H$_3$), C^{23}).

Polymerization Procedures and Polymer Characterizations.

Propylene polymerization. Propylene polymerizations were conducted in a 1.8 L SS batch reactor. This reactor was manufactured by Buchi AG and sold by Mettler, and is heated/cooled *via* the vessel jacket and reactor head. Syltherm 800 is the heat transfer fluid

used and is controlled by a separate heating/cooling skid. Both the reactor and the heating/cooling system are controlled and monitored by a Camile TG process computer. The bottom of the reactor is fitted with a large orifice bottom dump valve, which empties the reactor contents into a 6 L SS dump pot. The dump pot is vented to a 30 gal. blowndown tank, with both the pot and the tank N_2 purged. All chemicals used for polymerization or catalyst makeup were run through purification columns, to remove any impurities that may affect polymerization. Propylene, toluene, and IsoparE were passed through two columns, the first containing A2 alumina, and the second containing Q5 reactant. N_2 and H_2 were passed through a single Q5 reactant column. The reactor was cooled to 50 °C for chemical additions. The Camile controls the addition of IsoparE, using a micro-motion flowmeter to add the desired amount accurately. The accurate addition of H_2 was achieved by pressuring a 50 mL shot tank to 240 psi, and adding H_2 slowly until the desired decrease was reflected in the shot tank pressure. Propylene was then added through the micro-motion flow meter. After the additions, the reactor was heated to the polymerization temperature. The activator(s) and catalyst were handled in an inert dry-box, mixed together in a vial, drawn into a syringe and pressure transferred into the catalyst shot tank. The polymerizations were run for 10 min., then the agitator was stopped, the reactor pressured to ~500 psi with N_2, and the bottom dump valve opened to empty the reactor contents into the dump pot. The dump pot contents were poured into trays placed in a lab hood where the solvent was evaporated off overnight. The trays containing the polymeric residue were then transferred to a vacuum oven, where they were heated to 145 °C under vacuum to remove any residual solvent. After the trays cooled to ambient temperature, the polymers were weighed for yield/efficiencies, and submitted for polymer testing. *Polypropylene: material characterization*. Molecular weight distribution (M_w, M_n) information was determined by analysis on a custom Dow-built Robotic-Assisted Dilution High-Temperature Gel Permeation Chromatographer (RAD-GPC). Polymer samples were dissolved by stirring them for 90 minutes at 160 °C at a

concentration of 30 mg/mL in 1,2,4-trichlorobenzene (TCB) stabilized by 300 ppm BHT. They were then diluted to 1 mg/mL immediately before a 400 µL aliquot of the sample was injected. The GPC utilized two (2) Polymer Labs PLgel 10 µm MIXED-B columns (300 x 10mm) at a flow rate of 2.0 mL/min at 150 °C. Sample detection was performed using a PolyChar IR4 detector in concentration mode. A conventional calibration of narrow polystyrene (PS) standards was utilized, with apparent units adjusted to homo-polyethylene (PE) using known Mark-Houwink coefficients for PS and PE in TCB at this temperature. Absolute M_w information was calculated using a PDI static low-angle light scatter detector. Melting and crystallization temperatures of polymers were measured by differential scanning calorimetry (DSC 2910, TA Instruments, Inc.). Samples were first heated from room temperature to 210 °C at 10 °C/min. After being held at this temperature for 4 min, the samples were cooled to –40 °C at 10 °C/min and were then heated to 215 °C at 10 °C/min after being held at –40 °C for 4 min. *^{13}C NMR analysis of polypropylene samples.* The sample was prepared by adding approximately 2.7 g of stock solvent to a 0.21-1.2 g sample in a 10 mm NMR tube, and then purging in an N_2 box for 2 h. The stock solvent was made by dissolving 4 g of *para*-dichlorobenzene (PDCB) in 39.2 g of *ortho*-dichlorobenzene with 0.025 M chromium acetylacetonate (relaxation agent). The sample was dissolved and homogenized by heating the tube and its contents at 140-150°C. Samples were homogenized immediately prior to insertion into the heated (125 °C) NMR tube changer, and were allowed to thermally equilibrate in the probe for 7 minutes prior to data acquisition. The NMR polymer characterization was carried out on a Bruker 400 MHz spectrometer equipped with a Bruker Dual DUL high-temperature CryoProbe.[38] The ^{13}C NMR data were acquired using 320 transients per sample, a 7.3 sec pulse repetition delay (6 sec delay + 1.3 sec acq. time), 90 degree flip angles, and modified inverse gated decoupling[39] with a sample temperature of 120 °C. All measurements were made on non-spinning samples in locked mode.

1-Hexene polymerization by cationic pyridylamido complexes 18b, 19b, 20b and 21b. All polymerization tests were conducted under inert atmosphere in nitrogen filled dry-box. The catalyst precursor (10 μmol) was dissolved in 5 mL of toluene and treated with 2 mL (0.016 mol) of freshly distilled 1-hexene. To the resulting mixture, a solution of the activator ($Ph_3C^+[B(C_6F_5)_4]^-$ - 10 μmol) in 3 mL of toluene was added in one portion. The mixture was then maintained under vigorous stirring at room temperature for the desired reaction time. Afterwards, polymerization was stopped by quenching the mixture with 5 mL of MeOH. The mixture was maintained under vigorous stirring for three hours, while a sticky colorless solid separated off. The solid material was decanted, washed with methanol (3 X 5 mL) and dried at 50 °C under vacuum to constant weight. For the monomer conversion, *n*-heptane was used as the GC internal standard. Activities were calculated on the basis of the isolated poly(1-hexene) materials and expressed as mol of 1-hexene converted * (mol of Zr * h)$^{-1}$. Catalyst aging tests were carried out by adding the monomer (after the proper aging time) to the pre-activated catalyst. Catalytic 1-hexene polymerization experiments were performed in a dry-box filled with nitrogen, using a 50 mL Schlenk-type round flask equipped with a magnetic stirrer bar. *Poly(1-hexene)s: material characterization.* Melting (T_m) temperatures of the poly(1-hexene) materials were determined by differential scanning calorimetry (DSC) using a Perkin-Elmer DSC-7 instrument equipped with a CCA-7 cooling device and calibrated with the melting transition of indium and *n*-heptane as references (156.1 and –90.61 °C, respectively). The poly(1-hexene) sample mass was 10 mg and aluminum pans were used. Any thermal history in the polymers was eliminated by first heating of the specimen at a heating rate of 20 °C min^{-1} to 200 °C, cooling at 20 °C min^{-1} to -100 °C, and then recording the second scan from -100 °C to 200 °C. NMR characterization. For ^{13}C NMR about 100 mg of polymer was dissolved in $C_2D_2Cl_4$ in a 10 mm tube. HDMS (hexamethyldisiloxane) was used as internal chemical shift reference. The spectra were recorded on a Bruker NMR AVANCE 400 Spectrometer operating at 100.58 MHz (^{13}C) in the PFT mode working at 103

°C. The applied conditions were the following: 10 mm probe, 90° pulse angle; 64 K data points; acquisition time 5.56 s; relaxation delay 20 s; 3 – 4 K transient. Proton broadband decoupling was achieved with a 1D sequence using bi_waltz_16_32 power-gated decoupling. Chemical shifts for ^{1}H were referred to internal solvent resonances (5.86 ppm) and chemical shifts for ^{13}C were referred to hexamethyldisiloxane (HMDS). Molecular Weight Measurement. GPC measurements were performed on about 12 mg of product in tetrahydrofuran at 35 °C by a GPCV2000 high temperature size exclusion chromatography (SEC) system from Waters (Millford, MA, USA) equipped with two online detectors: a viscometer (DV) and a differential refractometer (DRI). The column set was composed of three mixed TSK-Gel GMHXL-XT columns from Tosohaas. Molar masses were based on polystyrene standards. The universal calibration was constructed from 18 narrow MMD polystyrene standards, with the molar mass ranging from 162 to 5.48 x.106 g/mol.

Stoichiometric and sub-stoichiometric reactions of 18b and 19b with 1-hexene. The catalyst precursor (**18** or **19**, 250 μmol) was dissolved in 8 mL of toluene and treated with either 35 μL or 210 μL (1 equiv or 6 equiv) of freshly distilled 1-hexene. To the resulting mixture, a solution of the activator ($Ph_3C^+[B(C_6F_5)_4]^-$ - 250 μmol) in 6 mL of toluene was added in one portion. The mixture was then maintained under vigorous stirring at room temperature for 1 h. Afterwards, the reaction mixture was treated with 3 mL of MeOH followed by 20 mL of saturated aqueous NaCl. The organic phase was separated and the mother liquor extracted with AcOEt (3 x 10 mL). The collected organic layers were concentrated to small volume and analyzed by GC/MS (GC program: 40 °C/1min, 15 °C/min, 250 °C/20min).

***Ethylene-1-octene copolymerization*.** A 2-liter Parr reactor was used in the copolymerization tests. All feeds were passed through columns of alumina and Q-5™ catalyst (available from Engelhard Chemicals Inc.) prior to introduction into the reactor.

Precatalyst and cocatalyst (activator) solutions were handled in a nitrogen filled dry-box. The reactor was charged with about 533 g of mixed alkanes solvent (Isopar^{TM} E) and 250 g of 1-octene comonomer. Hydrogen was added as a molecular weight control agent by differential pressure expansion from a 75 mL addition tank at 300 psi (2070 kPa). The reactor contents were heated to the polymerization temperature of 120 ^{o}C and saturated with ethylene at 460 psig (3.4 MPa). The catalysts and cocatalysts, as dilute solutions in toluene, were mixed and transferred to a catalyst addition tank and injected into the reactor. The polymerization conditions were maintained for 10 minutes with ethylene added on demand. Heat was continuously removed from the reaction vessel through an internal cooling coil. The resulting solution was removed from the reactor, quenched with isopropyl alcohol, and stabilized by addition of 10 mL of a toluene solution containing approximately 67 mg of a hindered phenol antioxidant (Irganox™ 1010 from Ciba Geigy Corporation) and 133 mg of a phosphorus stabilizer (Irgafos™ 168 from Ciba Geigy Corporation). Between polymerization runs, a wash cycle was conducted in which 850 g of mixed alkanes were added to the reactor and the reactor was heated to 150 °C. The reactor was then emptied of the heated solvent immediately before beginning a new polymerization run. Polymers were recovered by drying for about 12 h in a temperature-ramped vacuum oven with a final set point of 140°C. *Ethylene-1-octene copolymers: material characterization*. Melting and crystallization temperatures of ethylene-1-octene copolymers were measured by differential scanning calorimetry (DSC 2910, TA Instruments, Inc.). Samples were first heated from room temperature to 180 °C at 10 °C /min. After being held at this temperature for 2-4 min, the samples were cooled to –40 °C at 10 °C /min, held for 2-4 min, and were then heated to 160 °C. Weight average molecular weights (M_w) and polydispersity values (PDI) were determined by analysis on a Viscotek HT-350 Gel Permeation Chromatographer (GPC) equipped with a low-angle/right-angle light scattering detector, a 4-capillary inline viscometer and a refractive index detector. The GPC utilized three (3) Polymer Labs PLgel

10μm MIXED-B columns (300 x 7.5 mm) at a flow rate of 1.0 mL/minute in 1,2,4-trichlorobenzene at either 145 °C or 160 °C. To determine octene incorporation, 140 μL of each polymer solution was deposited onto a silica wafer, heated at 140 ^{o}C until the trichlorobenzene had evaporated and analyzed using a Nicolet Nexus 670 FTIR with 7.1 version software equipped with an AutoPro auto sampler.

Computational methodology. Density Functional Theory (DFT) calculations were performed using the M06[40] functional implemented within the *Gaussian09* program.[41] Structures were fully optimized using this functional. The theoretical study was carried out on the *real* system, with the full pyridylamido ligand. The starting geometries were obtained from the crystallographic atomic coordinates of **18** (L^{Ph}) and **19** (L^{Fu}) by replacing the benzyl substituents with three NMe_2 ligands and re-optimizing the resulting structures. Core electrons of the Zr atom were described using the pseudo-potentials of Hay-Wadt,[42] and their valence electrons were expressed through a LANL2DZ basis.[III] A 6-31G* basis set was chosen for all the other atoms. Transition states were characterized by a frequency calculation. Normal coordinate analysis on these stationary points was also performed by intrinsic reaction coordinate (IRC) calculations[43] in both directions to the correspondent minima. When the IRC calculations failed to reach the minima, geometry optimizations from the initial phase of the IRC path were performed. Finally, a continuum modeling of the reaction medium was also included in the computational treatment, using the same basis set. Bulk solvent effects (toluene, $\varepsilon = 2.38$) were expressed through the Polarizable Continuum Model (PCM-UA0 solvation spheres).[44]

2.6 References

1 (a) R. T Boussie, G. M. Diamond, C. Goh, K. A. Hall, A. M. LaPointe, M. K. Leclerc, V. Murphy, J. A. W. Shoemaker, H. Turner, R. K. Rosen, J. C. Stevens, F. Alfano, V. Busico, R. Cipullo, G. Talarico, *Angew. Chem. Int. Ed.* **2006**, *45*, 3278. (b) G. J. Domski, E. B. Lobkovsky, G. W. Coates, *Macromolecules*, **2007**, *40*, 3510. (c) V. Busico, R. Cipullo, R. Pellecchia, L. Rongo, G. Talarico, A. Macchioni, C. Zuccaccia, R. D. J. Froese, P. D. Hustad, *Macromolecules*, **2009**, *42*, 4369. (d) T. R. Boussie, G. M. Diamond, C. Goh, K. A. Hall, A. M. LaPointe, M. K. Leclerc, C. Lund, V. Murphy, (Symyx Technologies, Inc.) U.S. Pat. Appl. Publ. No. US **2006**/0135722 A1. (e) Boussie, T. R.; Diamond, G. M.; Goh, C.; LaPointe, A. M.; Leclerc, M. K.; Lund, C.; Murphy, V. (Symyx Technologies, Inc.) U.S. Pat. 6750345, **2004**.

2 (a) R. D. J. Froese, P. D. Hustad, R. L. Kuhlman, T. T. Wenzel, *J. Am. Chem. Soc.* **2007**, *129*, 7831. (b) C. Zuccaccia, A. Macchioni, V. Busico, R. Cipullo, G.Talarico, F. Alfano, H. W. Boone, K. A. Frazier, P. D. Hustad, , J. C. Stevens, P. C. Vosejpka, K. A. Abboud, *J. Am. Chem. Soc.* **2008**, *130*, 10354. (c) C. Zuccaccia, V. Busico, R. Cipullo, G. Talarico, R. D. J. Froese, P. C. Vosejpka, P. D. Hustad, A. Macchioni, *Organometallics* **2009**, *28*, 5445. (d) K. A. Frazier, H. W. Boone, P. C. Vosejpka, J. C. Stevens, (DOW Global Techologies Inc.), U.S. Pat. Appl. Publ. No. US **2004**/0220050 A1. (e) G. J. Domski, J. B. Edson, I. Keresztes, E. B. Lobkovsky, G. W. Coates, *Chem. Commun.* **2008**, 6137. (f) J. R. Hagadorn, (EXXONMOBIL Chemical Patents Inc.), WO **2009**/114209 A1. (g) K. A. Frazier, R. D. Froese, Y. He, J. Klosin, C. N. Theriault, P. C. Vosejpka, Z. Zhou, K. A. Abboud, *Organometallics* **2011**, *30*, 3318.

3 D. J. Arriola, E. M. Carnahan, P. D. Hustad, R. L. Kuhlman, T. T. Wenzel, *Science* **2006**, *312*, 714.

4 M. M. Salter, J. Kobayashi, Y. Shimizu, S. Kobayashi, *Org Lett.* **2006**, *8*, 3533.

5 P. Espinet, A. M. Echavarren, *Angew. Chem. Int. Ed.* **2004**, *43*, 4704.

6 J. Tsuji in Palladium reagents and catalysts: innovation in organic synthesis, Wiley, New York, **1996**.

7 N. Miyaura, A. Suzuky, *Chem. Rev.* **1995**, *95*, 2457.

8 a) D. M. Lyubov, G. K. Fukin, A. S. Shavyrin, A. A Trifonov, L. Luconi, C. Bianchini, A. Meli, G. Giambastiani, *Organometallics* **2009**, *28*, 1227. b) L. Luconi, D. M. Lyubov, C. Bianchini, A. Rossin, C. Faggi, G. K. Fukin, A. V. Cherkasov, A. S. Shavyrin, A. A Trifonov, G. Giambastiani, *Eur. J. Inorg. Chem.* **2010**, 608.

9 Ligand 11d containing the N-xylyl fragment was prepared according to the procedure described for the analogue 11a (see Ref. 2b, and references therein), by using 2,6-dimethylaniline instead of 2,6-diisopropylaniline as reactant.

10 (a) Y. Li, A. Turnas, J. T. Ciszewski, A. L. Odom, *Inorg. Chem*. **2002**, *41*, 6298. (b) P. N. Riley, P. E. Fanwick, I. P. Rothwell, *J. Chem. Soc*., *Dalton Trans*. **2001**, 181. (c) H. Fuhrmann, S. Brenner, P. Arndt, R. Kempe, *Inorg. Chem.* **1996**, *35*, 6742. (d) D. G. Black, D. C. Swenson, R. F. Jordan, *Organometallics* **1995**, *14*, 3539.

11 (a) T. Agapie, J. E. Bercaw, *Organometallics* **2007**, *26*, 2957. (b) J. A. Labinger, J. E. Bercaw, Nature **2002**, *417*, 507.

12 D. G. Black, D. C. Swenson, R. F. Jordan, *Organometallics* **1995**, *14*, 3539.

13 A. A. C. Braga, G. Ujaque, F. Maseras, *Organometallics* 2006, 25, 3647.

14 (a) F. Guérin, D. H. McConville, J. J. Vittal, G. A. P. Yap, *Organometallics* **1998**, *17*, 5172. (b) M. E. G. Skinner, Y. Li, P. Mountford, *Inorg. Chem.* **2002**, *41*, 1110. (c) Z. Ziniuk, I. Goldberg, M. Kol, Inorg. *Chem. Commun*. **1999**, *2*, 549. (d) M. E. G. Skinner, T. Toupance, D. A. Cowhig, B. R. Tyrrell, P. Mountford, *Organometallics* **2005**, *24*, 5586. (e) K. Nienkemper, G. Kehr, S. Kehr, R. Fröhlich, G. Erker, *J. Organomet. Chem.* **2008**, *693*, 1572.

15 G. Giambastiani, L. Luconi, R. L. Kuhlman, P. D. Hustad, in *Olefin Upgrading Catalysis by Nitrogen-based Metal Complexes I* (Eds. G. Giambastiani, J. Campora - ISBN 978-90-481-3814-2), Springer, London, **2011**, pp. 197-282.

16 Polymerization conditions used: catalyst precursor (**12$_{Ph(Zr)}$/12'$_{Ph(Zr)}$** and **13$_{Fu(Zr)}$/13'$_{Fu(Zr)}$**), 20 μmol; MAO equiv, 1000; C_2H_4 pressure, 15 bar; toluene, 50 mL; reaction time, 30 min; 1700 rpm; Productivity = 7.2 Kg (HDPE)/mol^{-1}h^{-1} at the highest.

17 All ligands showed four equivalent methyl groups for the isopropyl moiety: a doublet centered at δ = 1.27 (11a), 1.19 (11b) and 1.20 ppm (11c).

18 H. Tsurugi, Y. Matsuo, T. yamagata, K. Mashima, *Organometallics* **2004**, *23*, 2797.

19 (a) M. Bochmann, S. J. Lancaster, *Organometallics* **1993**, *12*, 633. (b) S. L. Latesky, A. K. McMullen, G. P. Niccolai, I. P. Rothwell, *Organometallics* **1985**, *4*, 902. (c) R. F. Jordan, R. E. LaPointe, N. Baenziger, G. D. Hinch, *Organometallics* **1990**, *9*, 1539. (d) R. F. Jordan, R. E. LaPointe, S. B. Chandrasekhar, S. F. Echols, R. Willett, *J. Am. Chem. Soc*. **1987**, *109*, 4111.

20 All dibenzyl complexes (18-21) show different M-Cα / M-Cipso distances at the "η2-coordinated" benzyl groups. The definition of "η2-coordination" has been conventionally adopted (according to the literature – see refs 14, 15) to allow one to distinguish among the differently coordinated -CH_2Ph groups in the solid state, η1- vs. η2-, although a "C-C α-agostic interaction" should be most properly invoked for the latter!

21 Attemps to freeze this rapid interconversion by 1H NMR at 193 K did not allow the authors to differentiate the two bonding modes.

22 B. Qian, W. J. Scanlon IV, M. R. Smith III, D. H. Motry, *Organometallics* **1999**, *18*, 1693.

23 (a) M. Bouwkamp, D. van Leusen, A. Meetsma, B. Hessen, *Organometallics* **1998**, *17*, 3645. (b) P. Shao, R. A. L. Gendron, D. J. Berg, G. W. Bushnell, *Organometallics* **2000**, *19*, 509. (c) M. C. W. Chan, S. C. F. Kui, J. M. Cole, G. J. McIntyre, S. Matsui, N. Zhu, K.-H. Tam, *Chem. Eur. J.* **2006**, *12*, 2607. (d) S. C. F. Kui, N. Zhu, M. C. W. Chan, *Angew. Chem. Int. Ed.* **2003**, *42*, 1628.

24 For similar distances (Å) and angles (°) see also refs. 12 and 22b

25 Conversion of the neutral $B(C_6F_5)_3$ to the anionic $B(CH_2Ph)(C_6F_5)_3^-$ is confirmed by the upfield shift of the ^{11}B resonance from +59.8 ppm to -12.9 (**18a**), -12.7 (**19a**), -12.4 (**20a**) and -13.0 (**21a**).

26 (a) S. Beck, M. H. Prosenc, H. H. Brintzinger, *J. Mol. Catal. A: Chem.* **1998**, *128*, 41-52. (b) R. A. Lee, R. J. Lachicotte, G. C. Bazan, *J. Am. Chem. Soc.* **1998**, *120*, 6037-6046. (c) S. Y. Desjardins, A. A. Way, M. C. Murray, D. Adirim, M. C. Baird, *Organometallics* **1998**, *17*, 2382-2384. (d) C. Pellecchia, A. Immirzi, A. Grassi, A. Zambelli, *Organometallics* **1993**, *12*, 4473-4478. (e) L. Jia, X. Yang, C. L. Stern, T. J. Marks, *Organometallics* **1997**, *16*, 842-857. (f) C. L. Beswick, T. J. Marks, *Organometallics* **1999**, *18*, 2410.

27 (a) A. D. Horton, J. de With, *Chem. Commun.* **1996**, 1375. (b) A. D. Horton, J. de With, A. J. van der Linden, H. van de Weg, *Organometallics* **1996**, *15*, 2672.

28 (a) J. Sassmanhausen, A. K. Powell, C. E. Anson, S. Wocadlo, M. Bochmann, *J. Organomet. Chem.***1999**, *592*, 84. (b) A. Noor, W. P. Kretschmer, G. Glatz, A. Meetsma, R. Kempe, R. *Eur. J. Inorg. Chem.* **2008**, 5088.

29 The complete $^{13}C\{^1H\}$ NMR assignment for complex **24b** was hampered by the partial signals overlap caused by the intense residual solvent resonances.

30 During this study the precatalysts **25** was employed under identical experimental conditions to those previously described in ref. 2g except for the use of hydrogen to control the polymer molecular weights.

31 L. Luconi, D. M. Lyubov, C. Bianchini, A. Rossin, C. Faggi, G. K. Fukin, A. V. Cherkasov, A. S. Shavyrin, A. A. Trifonov, G. Giambastiani, *Eur. J. Inorg. Chem,* **2010**, 608 and refs cited therein.

32 Ligand **11d** containing the *N*-xylyl fragment was prepared according to the procedure described for the analogue **11a** using 2,6-dimethyl-aniline instead of 2,6-^{i}Pr-aniline as reactant.

33 CrysAlisCCD 1.171.31.2 (release 07-07-2006), CrysAlis171 .NET, Oxford Diffraction Ltd.

34 CrysAlis RED 1.171.31.2 (release 07-07-2006), CrysAlis171 .NET, Oxford Diffraction Ltd.

35 A. Altomare, M. C. Burla, M. Camalli, G. L. Cascarano, C. Giacovazzo, A. Guagliardi, A. G. Moliterni, G. Polidori, R. Spagna, *J. Appl. Crystallogr.* **1999**, *32*, 115.

36 Sheldrick, G. M. SHELXL (**1997**).

37 L. J. Farrugia, *J. Appl. Crystallogr.* **1997**, *30*, 565.

38 Z. Zhou, R. Küemmerle, J. C. Stevens, D. Redwine, Y. He, X. Qiu, R. Cong, J. Klosin, N. Montanez, G. Roof, *J. Magn. Reson.* **2009**, *200*, 328.

39 Z. Zhou, R. Küemmerle, X. Qiu, D. Redwine, R. Cong, A. Taha, D. Baugh, B. Winniford, *J. Magn. Reson.* **2007**, *187*, 225.

40 Y. Zhao, D. G. Truhlar, *Theor. Chem. Account* **2008**, *120*, 215.

41 M. J. Frisch *et al.*, *Gaussian09*, Revision A.02, Gaussian Inc., Wallingford CT, **2009**.

42 (a) P. J. Hay, W. R. Wadt, *J. Chem. Phys.* **1985**, *82*, 270. (b) W. R. Wadt, P. J. Hay, *J. Chem. Phys.* **1985**, *82*, 284.

43 K. Fukui, *Acc. Chem. Res.* **1981**, *14*, 363.

44 (a) S. Miertus, E. Scrocco, J. Tomasi, *J. Chem. Phys.* **1981**, *55*, 117. (b) V. Barone, M. Cossi, J. Tomasi, *J. Chem. Phys.* **1997**, *107*, 3210.

3

Intramolecular Hydroamination Reactions Catalyzed by Neutral and Cationic Group IV Pyridylamido Complexes

3.1 Abstract

Zr^{IV} and Hf^{IV} benzyl (neutral or cationic) and amido catalysts stabilized by pyridylamido ligands are found to be good candidates for the intramolecular hydroamination/cyclization of primary and secondary aminoalkenes. In particular, cationic monobenzyl derivatives have shown remarkable catalytic activity for the production of five and six-membered N-containing heterocycles from secondary amino alkenes. In addition, Zr^{IV} and Hf^{IV} amido derivatives that are produced by a temperature-controlled prototropic rearrangement have provided evidence of the central role played by the metal coordination sphere in promoting such catalytic transformations efficiently.

3.2 Introduction

Group IV amidopyridinate complexes are among the most studied and successfully employed post-metallocene catalysts for the efficient upgrading of non-activated olefin substrates.[1] Many of these systems have recently played an essential role in the development of new polyolefin materials [1,2] and in the elucidation of knotty and original organometallic aspects.[1,3,4] Widening the application range of exceptional C-C bond-forming catalyst precursors is a challenging research issue of great interest for both academia and industry. To this aim, metal-mediated and selective C-N bond formation reactions represent a stimulating research area for the production of N-containing compounds of potential application in the pharmaceutical and fine chemical synthesis. Although there are many synthetic routes to C-N bonds, the hydroamination reaction,[5] a formal N-H addition to unsaturated C-C bonds, provides a convenient pathway and easy access to a variety of N-containing compounds. In the last two decades, the number of publications on hydroamination reactions has sharply grown and early studies on alkali[6] and rare-earth[7] metal catalysts have set the way to the development of highly efficient and selective *d*-block transition metal complexes.[8,9,10,11,12] Recent achievements in the field have stressed the importance of rethinking molecular frameworks in Group IV metal catalysts to obtain active and selective systems for the intramolecular hydroamination reaction starting from either primary or secondary aminoalkenes. Similar to the story of polymerization catalysts, there have been rapid developments to the Group IV metal complexes to make them easily tunable, highly active and selective catalysts from the constraint geometry (CGCs), half-sandwich and cyclopentadienyl-free series. This choice also satisfies fundamental thermodynamic requirements for the catalytic hydroamination of primary aminoalkenes.[10,11]

Our interest in hydroamination reaction stems from previous studies on cationic monobenzyl pyridylamido cyclometallated M^{IV}-complexes (M = Zr, Hf) of general formula $[N_2^{Ph}M(CH_2Ph)]^+[B(C_6F_5)_4]^-$ (**2**, **Scheme 3.1** left), which readily engage in highly efficient α-olefin polymerization (C-C bond formation).[4b] In accordance with this, we became intrigued in addressing whether such coordinatively unsaturated cationic species **2** (as well as their neutral dibenzyl precursors **1**, **Scheme 3.1**, left) could also promote intramolecular hydroamination efficiently (C-N bond formation) in the presence of either primary or secondary aminoalkenes.

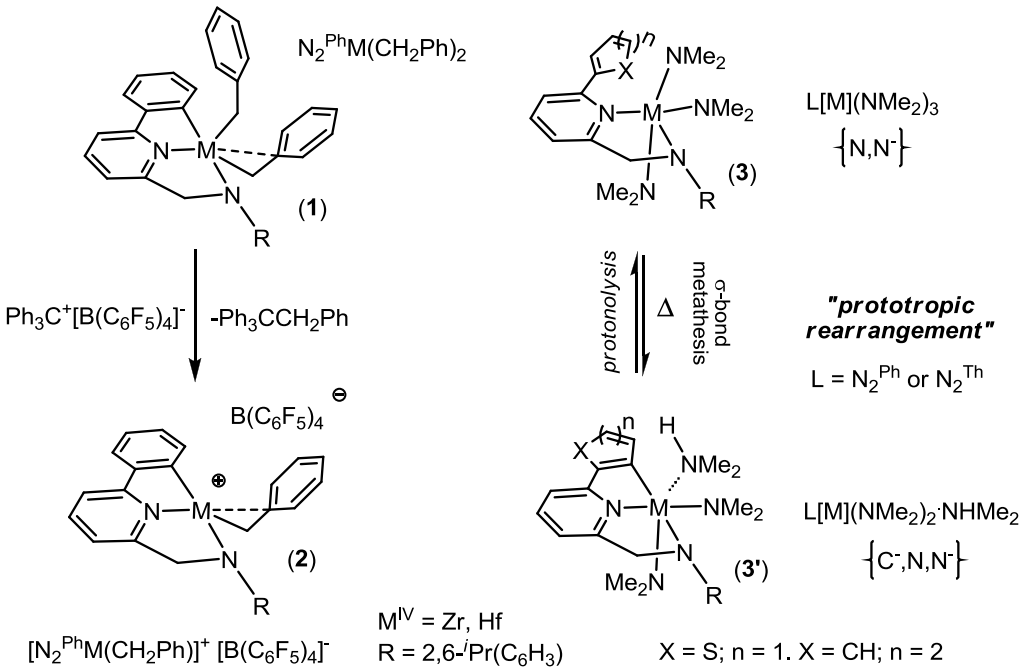

Scheme 3.1. Left: dibenzyl (**1**) and cationic monobenzyl (**2**) pyridylamido cyclometallated M^{IV}-complexes (M = Zr, Hf). Right: prototropic rearrangement of Group IV amido complexes stabilized by nitrogen-containing ligands capable to undergo reversible and temperature-controlled σ-bond metathesis/protonolysis.

Recently, we highlighted the unusual organometallic behavior of related Group IV amido species (**Scheme 3.1**, right **3** and **3'**),[4] in which a temperature controlled σ-bond metathesis/protonolysis took place reversibly over a wide temperature range (238-373 K). The metal coordination sphere was found to change dramatically: from five-coordinated tris-amido species stabilized by bidentate monoanionic $\{N,N^-\}$ ligands (**3**)

to six-coordinated bis-amido-mono-amino complexes featured by tridentate dianionic {C^-,*N*,N^-} systems (**3'**).[4a] Unlike amido precursors, tailored neutral (**1**) and cationic (**2**) M^{IV}-amidopyridinate benzyl complexes were prepared from $M^{IV}(Bn)_4$ (M = Zr, Hf; Bn = $CH_2(C_6H_5)$) as a metal source (**Scheme 3.1**, left – **1** and **2**).

In this work, we report the catalytic performance of selected complexes from both series in the hydroamination reaction of either primary or secondary aminoalkene substrates. In addition, the present study has also contributed to elucidate the central role of the metal coordination environment (*N*,N^- *vs.* C^-,*N*,N^- ligated species) on the final catalyst performance.

3.3 Results and Discussions

We have recently developed bidentate/tridentate pyridylamido ligands, of the type shown in **Scheme 3.1**, bearing aryl or heteroaryl pendant arms as olefin polymerization catalysts in combination with early and rare-earth metals.[1,4,13] Ligand treatment under relatively mild conditions (70 °C, 12-48 h) with $M^{IV}(Bn)_4$ (M = Zr, Hf; Bn = $CH_2(C_6H_5)$) as metal precursor resulted into M^{IV}-dibenzyl cyclometallated compounds as unique species (**1**, **Scheme 3.1**).[4b] The reaction did not show any evidence for the generation of intermediates, due to the ligand ability to rapidly and quantitatively undergo intramolecular *ortho*-metallation. Complexes $\mathbf{1_{Zr}}$ and $\mathbf{1_{Hf}}$ were prepared in 95% and 93% isolated yield, respectively.[4b] X-ray diffraction analysis performed on both isolated species unambiguously showed dianionic tridentate {C^-,*N*,N^-} ligating systems. Whereas crystals of $\mathbf{1_{Zr}}$ for X-ray analysis were straightforwardly obtained by standing a concentrated toluene solution of the complex at room temperature,[4b] suitable X-ray crystals of $\mathbf{1_{Hf}}$ were grown by cooling at –35 °C in a concentrated toluene solution of the complex and layering this with cold drops of *n*-hexane. After maintaining the

system at −35 °C for several days, yellow pale microcrystals of $\mathbf{1_{Hf}}$ were separated off. ORTEP representation of the crystal structure of $\mathbf{1_{Hf}}$ is now given in **Figure 3.1**. **Table 3.1** lists all the main crystal and structural refinement data, while selected bond lengths and angles are summarized in **Table 3.2**

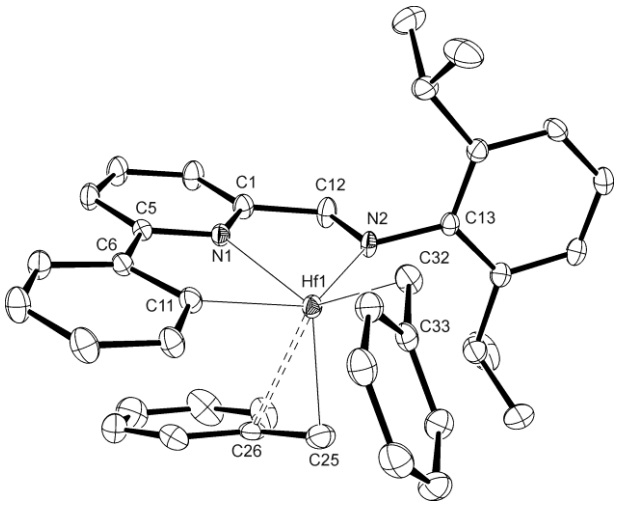

Figure 3.1. Crystal structure of $N_2^{Ph}Hf(CH_2Ph)_2$ ($\mathbf{1_{Hf}}$). Thermal ellipsoids are drawn at the 40% probability level. Hydrogen atoms and one toluene molecule as crystallization solvent are omitted for clarity.

$\mathbf{1_{Hf}}$ crystallizes in the triclinic *P –1* space group and the asymmetric unit contains one toluene molecule; no special feature is to be underlined, and the main structural parameters (**Table 3.2**) are very similar to those obtained for the previously reported Zr^{IV} analogue.[4b] The ligand coordination mode and its κ^3-{*C*$^-$,*N*,*N*$^-$} hapticity are also of the same kind. As seen for the Zr^{IV} complex, one of the two benzyl groups in the crystal is η^2-bound to the metal ion {d[Hf-C(25)] = 2.233(3) Å; d[Hf-C(26)] = 2.771(3) Å; α[Hf-C(25)-C(26)] = 94.18(2)°}, while the other shows η^1-coordination {d[Hf-C(32)] = 2.235(3) Å; d[Hf-C(33)] = 3.161(2) Å; α[Hf-C(32)-C(33)] = 114.75(2)°}.

π-π interactions between the η^2-bound benzyl group and the pyridine ligand are present: the distance between the C_6H_5 group centroid and the plane of the pyridine ring is 3.485 Å, and an angle of 22.0(2)° is formed between the benzyl and pyridine planes.

Table 3.1. Crystal data and structure refinement for complexes $\mathbf{1_{Hf}}$, $\mathbf{3_{Ph(Zr)}}$, $\mathbf{4_{Th(zr)}}$ and $\mathbf{4_{Th(Hf)}}$.

	$\mathbf{1_{Hf}}$• $\mathbf{C_7H_8}$	$\mathbf{3_{Ph(Zr)}}$	$\mathbf{4_{Th(zr)}}$	$\mathbf{4_{Th(Hf)}}$
CCDC number	882101	882103	882102	882104
Empirical formula	$C_{38}H_{40}HfN_2$ C_7H_8	$C_{30}H_{45}N_5Zr$	$C_{26}H_{36}N_4SZr$	$C_{26}H_{36}HfN_4S$
Formula weight	795.34	566.93	527.87	615.14
Temperature [K]	120(2)	120(2)	120(2)	120(2)
Wavelength [Å]	0.71069	0.71069	0.71079	0.71069
Crystal system, space group	Triclinic, *P -1*	*Ortorombic*, *Pbca*	monoclinic, *P* $2_1/n$	Triclinic, *P* $2_1/n$
a [Å]	9.841(3)	21.994(2)	19.016(5)	10.687(5)
b [Å]	9.888(3)	15.315(1)	14.169(5)	18.284(9)
c [Å]	19.767(6)	35.931(3)	19.964(5)	13.563(6)
α [°]	87.794(2)	90	90	90
β [°]	98.871(2)	90	91.854	96.169(4)
γ [°]	74.050(2)	90	90	90
V [$Å^3$]	1848.0(9)	12103(2)	5376(3)	2634.9(2)
Z, D_c [g m^{-3}]	2, 1.249	16, 1.245	8, 1.304	4, 1.551
Absorption coefficient [mm^{-1}]	2.856	0.389	0.506	4.058
F(000)	808	4800	2208	1232
Crystal size [mm]	0.05×0.05×0.01	0.01×0.01×0.01	0.04×0.05×0.05	0.01×0.013×0.02
Θ Range for data collection [°]	4.24 ÷ 32.87	4.10 ÷ 26.99	4.09 ÷ 29.15	4.12 ÷ 29.37
Limiting indices	$-14 \le h \le 14$	$-24 \le h \le 26$	$-25 \le h \le 25$	$-14 \le h \le 14$
	$-14 \le k \le 14$	$-18 \le k \le 17$	$-18 \le k \le 18$	$-24 \le k \le 24$
	$-30 \le l \le 28$	$-44 \le l \le 40$	$-25 \le l \le 26$	$-18 \le l \le 17$
Reflections collected/unique	29941/12333	89972/11350	57569/12789	33738/6402
GOF on F^2	1.059	0.943	1.032	1.078
Data/restraints/ parameters	12333/0/448	11350/0/663	12789/0/617	6402/0/297
Final *R* indices [I>2σ(*I*)]	*R*1=0.0331, w*R*2= 0.0724	*R*1=0.0851, w*R*2= 0.1599	*R*1=0.0540, w*R*2= 0.0986	*R*1=0.0409, w*R*2= 0.0888
R indices (all data)	*R*1=0.0390 w*R*2= 0.0762	*R*1=0.2551, w*R*2= 0.02232	*R*1=0.1119, w*R*2= 0.1216	*R*1=0.0589, w*R*2= 0.1021
Largest diff. peak and hole [e $Å^{-3}$]	1.956/–1.497	2.146/–0.707	0.736/–0.721	2.998/–1.652

Cationic monobenzyl derivatives $\mathbf{2_{Zr}}$ and $\mathbf{2_{Hf}}$ were prepared *in-situ* upon treatment of $\mathbf{1_{Zr}}$ and $\mathbf{1_{Hf}}$ with an equimolar amount of $[Ph_3C]^+[B(C_6F_5)_4]^-$.[4b] Although these cationic complexes have limited solubility in aromatic hydrocarbons such as benzene or toluene at room temperature,[4b] $\mathbf{2_{Zr}}$ and $\mathbf{2_{Hf}}$ gave stable dark-green solutions at higher temperatures (solvent boiling points).

Table 3.2. Selected bond distances (Å) and angles (°) for complexes $\mathbf{1^{Hf} \cdot C_7H_8}$, $\mathbf{3_{Ph(Zr)}}$, $\mathbf{4_{Th(Zr)}}$ and $\mathbf{4_{Th(Hf)}}$.

	$\mathbf{1_{Hf} \bullet C_7H_8}$	$\mathbf{3_{Ph(Zr)}}$	$\mathbf{4_{Th(Zr)}}$	$\mathbf{4_{Th(Hf)}}$
M-N(1)	2.277(2)	2.478(6)	2.344(3)	2.308(4)
M-N(2)	2.088(2)	2.085(6)	2.136(3)	2.094(4)
M-N(3)		2.066(7)	2.028(3)	2.011(5)
M-N(4)		2.061(7)	2.017(3)	2.042(4)
M-N(5)		2.026(7)	-	-
M-C(7)	-	2.321(5)	2.324(3)	-
M-C(11)	2.279(3)	-	-	-
M-C(25)	2.233(3)	-	-	-
M-C(26)	2.771(3)	-	-	-
M-C(32)	2.235(3)	-	-	-
M-C(33)	3.161(2)	-	-	-
C(25)-C(26)	1.485(4)	-	-	-
C(32)-C(33)	1.488(3)	-	-	-
N(1)-M-N(2)	71.66(7)	71.4(2)	69.89(10)	70.43(15)
N(1)-M-N(3)			111.25(11)	130.20(16)
N(1)-M-N(4)			139.03(11)	148.52(17)
N(1)-M-N(5)			-	-
N(2)-M-N(3)			108.17(12)	106.94(18)
N(2)-M-N(4)			109.97(11)	109.00(17)
N(2)-M-N(5)			-	-
N(2)-M-C(7)			137.70(12)	137.72(17)
N(1)-M-C(7)	-	-	69.49(11)	70.71(17)
N(1)-M-C(11)	70.88(8)	-	-	-
C(25)-M-C(26)	32.32(10)	-	-	-
C(25)-M-C(32)	108.02(11)	-	-	-
M-C(32)-C(33)	114.75(18)	-	-	-
N(1)-C(5)-C(6)-C(7)	-	117.10(11)	-5.3(5)	-1.9(7)
N(6)-C(35)-C(36)-C(41)	-	134.4(9)	-	-
N(1)-C(5)-C(6)-S(1)	-	-	174.8(2)	179.7(4)
N(1)-C(1)-C(12)-N(2)	-3.7(3)	-15.0(12)	-	-
N(1)-C(5)-C(6)-C(11)	-1. 6(3)	-66.8(12)	-	-

Before investigating these systems (neutral and cationic species) in catalytic hydroamination reactions, the stability of the cyclometallated forms in the presence of model primary aminoalkenes were properly addressed. Indeed, permanent catalyst modifications in the presence of plain α-olefins, resulting from alkene insertion into the reactive C^{Ar}-M bond, have been extensively claimed by the scientific community as factors that add layers of complexity to the identification of the active species operating in polymerization catalysis.[3,4b,14] Unlike plain olefin systems, aminoalkenes **I** and **II** (**Scheme 3.2**) did not show any ligand/complex modification on both neutral and

cationic forms (**1** and **2**), even after their prolonged heating in toluene under reflux. Experimental evidence was given by the analysis of the GC-MS traces of the hydrolyzed reaction mixtures resulting from either stoichiometric (complex:substrate = 1:1) or sub-stoichiometric (complex:substrate = 1:3) cyclization test. Three main peaks from selected trials [$(m/z - 1)_{aminoalkene}$ = 236, $(m/z = 237)_{pyrrolidine}$ and $(m/z = 344)_{ligand}$ from $\mathbf{1_{Zr}}$/**I**; $(m/z - 1)_{aminoalkene}$ = 112, $(m/z)_{pyrrolidine}$ = 113 and $(m/z)_{ligand}$ = 343 from $\mathbf{2_{Hf}}$/**II**] were unambiguously attributed to the expected hydroamination products, the residual aminoalkenes and the totally unmodified ligand, respectively. Although a definitive explanation of the different chemical behavior of aminoalkenes from plain olefins has yet to be provided in a straightforward manner (it would also beyond the scope of this work), it seems reasonable that amido/imido cyclization intermediates sterically prevent olefin insertion into the C^{Ar}-M bond. Accordingly, the ability of complexes $\mathbf{1_{Zr}}$ and $\mathbf{1_{Hf}}$ to promote the hydroamination/cyclization of primary and secondary amines tethered to monosubstituted alkenes have been systematically scrutinized (**Scheme 3.2**, **Table 3.3**).

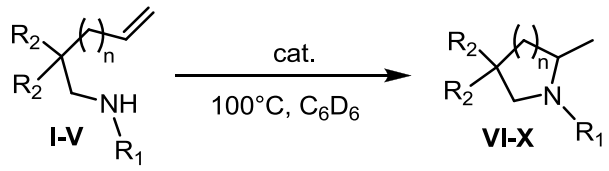

I n=1 R_2 = Ph R_1 = H
II n=1 R_2 = CH_3 R_1 = H
III n=1 R_2 = Ph R_1 = Me
IV n=1 R_2 = -$(CH_2)_5$- R_1 = H
V n=2 R_2 = CH_3 R_1 = Me

Scheme 3.2. Intramolecular hydroamination of primary and secondary amines.

As shown in **Table 3.3**, both neutral complexes are active catalysts for the hydroamination reaction of primary aminoalkenes (**Table 3.3**, entries 1-6). Indeed, 10 mol% of $\mathbf{1_{Zr}}$ allows the almost complete (> 95%) and total regioselective cyclization of the *gem*-diphenyl aminopentene **I** after 2h at 100 °C (entry 1). Slightly longer reaction

times are required to complete the cyclization of the less Thorpe–Ingold-activated substrate **IV** (entry 3). Similarly to other literature preceding,[10] the activity of the zirconium complex (**1$_{Zr}$**) results markedly superior to that measured for the hafnium counterpart (**1$_{Hf}$**) with both primary aminoalkenes investigated (entries 4-6); over ten-fold longer reaction times were required to completely convert **I** into the corresponding pyrrolidine derivative while passing from **1$_{Zr}$** to **1$_{Hf}$** (entry 5 *vs*. entry 1). At odds with primary aminoalkenes, both neutral dibenzyl complexes show rather scarce activities in the presence of substrates containing secondary amine groups. As a matter of fact, the most active **1$_{Zr}$** provides only 45% conversion of **III** into the desired pyrrolidine derivative (entry 2) after 20h reaction time under the same catalytic conditions used for the primary amino substrates **I** and **IV**. Additionally, over 20 mol% of by-products arising from a ß-hydride elimination path is detected by ^{1}H-NMR spectroscopy. Such a competitive side-reaction has been earlier observed in Group IV metal-catalyzed intramolecular hydroamination with secondary aminoalkenes.[10c]

Table 3.3. Intramolecular hydroamination of primary and secondary aminoalkenes catalyzed by neutral and cationic Zr^{IV} and Hf^{IV} complexes.[a]

Entry	Catalyst	Substrate	Product	Time (h)	Conv.(%)[b]
1	**1$_{Zr}$**	**I**	**VI**	2	>95
2	**1$_{Zr}$**	**III**	**VIII**	20	45[c]
3	**1$_{Zr}$**	**IV**	**IX**	3	>97
4	**1$_{Hf}$**	**I**	**VI**	2	77
5	**1$_{Hf}$**	**I**	**VI**	20	92
6	**1$_{Hf}$**	**IV**	**IX**	23	86
7	**2$_{Zr}$**	**I**	**VI**	2	>97
8	**2$_{Zr}$**	**III**	**VIII**	0.25	>98
9[c]	**2$_{Zr}$**	**IV**	**IX**	8	93
10	**2$_{Zr}$**	**V**	**X**	0.25	>98
11	**2$_{Hf}$**	**I**	**VI**	2	>98
12[c]	**2$_{Hf}$**	**III**	**VIII**	0.25	>98
13[c]	**2$_{Hf}$**	**IV**	**IX**	16	93
14	**2$_{Hf}$**	**V**	**X**	025	>98

[a] Reactions were performed in C_6D_6 at 100 °C under argon with 10 mol% of catalyst, unless otherwise stated. [b] Determined by *in-situ* ^{1}H NMR spectroscopy. [c] In the presence of over 20 mol% of byproduct.

On the other hand, cationic monobenzyl complexes **2$_{Zr}$** and **2$_{Hf}$** (prepared *in-situ* upon treatment of neutral precursors with an equimolar amount of $[Ph_3C][B(C_6F_5)_4]$ are

capable of catalyzing the hydroamination of primary and secondary aminoalkenes efficiently (**Table 3.3**, entries 7-14). Although both cationic species are scarcely soluble in aromatic hydrocarbons at room temperature, they turn out to be completely soluble at the final reaction temperature (100 °C). Both $\mathbf{2_{Zr}}$ and $\mathbf{2_{Hf}}$ catalysts give a complete conversion of **I** into the corresponding pyrrolidine derivative within 2h (entries 7 and 11), in line with the catalytic activities measured for the neutral compounds $\mathbf{1_{Zr}}$ and $\mathbf{1_{Hf}}$ (entry 7 *vs*. entry 1 and entry 11 *vs*. entry 4). However, the less activated primary aminoalkene **IV** undergoes cyclization less efficiently in the presence of cationic promoters (entry 9 *vs*. entry 3). Overall, neutral and cationic Hf^{IV} derivatives are less efficient in the cyclization of primary aminoalkenes compared to their Zr^{IV} counterparts; they require longer reaction times to drive the reaction to completeness (entry 6 *vs*. entry 3 and entry 13 *vs*. entry 9).

Notably, the hydroamination of the secondary aminoalkene **III** with both $\mathbf{2_{Zr}}$ and $\mathbf{2_{Hf}}$ resulted into considerably improved reaction rates. Indeed, an almost complete substrate conversion into the desired product was achieved in less than 20 minutes (entries 8 and 12). Additionally, the formation of a six-membered ring from the *gem*-dimethyl *N*-methylaminohexene **V** was conveniently and quantitatively achieved in 20 minutes with both cationic catalysts (entries 10 and 14).[15,16] No traces of hydroaminoalkylation[17] side-products was ever noted during the cyclization of **V**.[18] Overall, both cationic forms $\mathbf{2_{Zr}}$ and $\mathbf{2_{Hf}}$ present remarkable reactivity in the hydroamination reaction, particularly for the cyclization of secondary aminoalkenes. These results are even more interesting once compared with those based on other cationic Group IV metal complexes reported in the literature so far (referring to both five-[9] and six-membered[9a] cyclizations).

Only a few systems based on Group IV metals are effective catalysts for the hydroamination of both primary and secondary aminoalkenes.[9c,10g,j] As a general trend,

cationic Group IV metal complexes are restricted to the cyclization of secondary aminoalkenes, whereas they are (with rare exceptions)[9c] almost inactive systems for the cyclization of primary amino substrates.[9a,b] Herein, cationic monobenzyl Zr^{IV} and Hf^{IV} complexes $\mathbf{2_{Zr}}$ and $\mathbf{2_{Hf}}$ have demonstrated their ability at promoting catalytic hydroamination of both primary and secondary amines with enhanced catalytic activity compared with those reported in the literature and based on Group IV metal catalysts.[9c]

In addition to neutral dibenzyl and cationic monobenzyl Zr/Hf complexes, amido derivatives of the type shown in **Scheme 3.1** (right) have also been investigated as hydroamination catalysts. In particular, the ability of these systems to undergo prototropic rearrangement over a wide temperature range (resulting into a relevant change of the metal coordination sphere) was taken into account in order to elucidate the role of the active site environment on the catalytic performance.

The amido complexes shown in **Scheme 3.3** have already been exploited by us as polymerization catalysts for the production of high-density polyethylene (HDPE).[4a] The results of this study have demonstrated that only the *ortho*-metallated forms were responsible for the generation of catalytically active species in polymerization catalysis.

For hydroamination tests, only the thienyl-containing systems ($\mathbf{3_{Th(Zr)}}$/$\mathbf{3'_{Th(Zr)}}$ and $\mathbf{3_{Th(Hf)}}$/$\mathbf{3'_{Th(Hf)}}$) were selected, according to their higher ability at undergoing intramolecular σ-bond metathesis and thus providing higher molar fractions of the cyclometallated forms ($\mathbf{3'_{Th(M)}}$) in high temperature solution processes.[19] In addition, the phenyl derivative $\mathbf{3_{Ph(Zr)}}$/$\mathbf{3'_{Ph(Zr)}}$ (for which the tris-amido form was always the most abundant in solution even at high temperatures)[19] was also selected for the sake of comparison. To assess the influence of the metal coordination sphere in catalytic hydroamination tests, unique Hf^{IV} and Zr^{IV}- bisamido derivatives ($\mathbf{4_{Th(M)}}$) were

synthesized. According to literature procedures, prolonged heating of the tautomeric mixtures (**3**$_{Th(M)}$/**3'**$_{Th(M)}$) in toluene under reflux, combined with static vacuum cycles, allowed for the isolation of the bisamido derivatives **4**$_{Th(Zr)}$ and **4**$_{Th(Hf)}$ in 93% and 95% yield, respectively. Single crystals suitable for X-ray diffraction studies were straightforwardly grown from concentrated 1:1 toluene/*n*-hexane mixtures of **4**$_{Th(Zr)}$ and **4**$_{Th(Hf)}$.

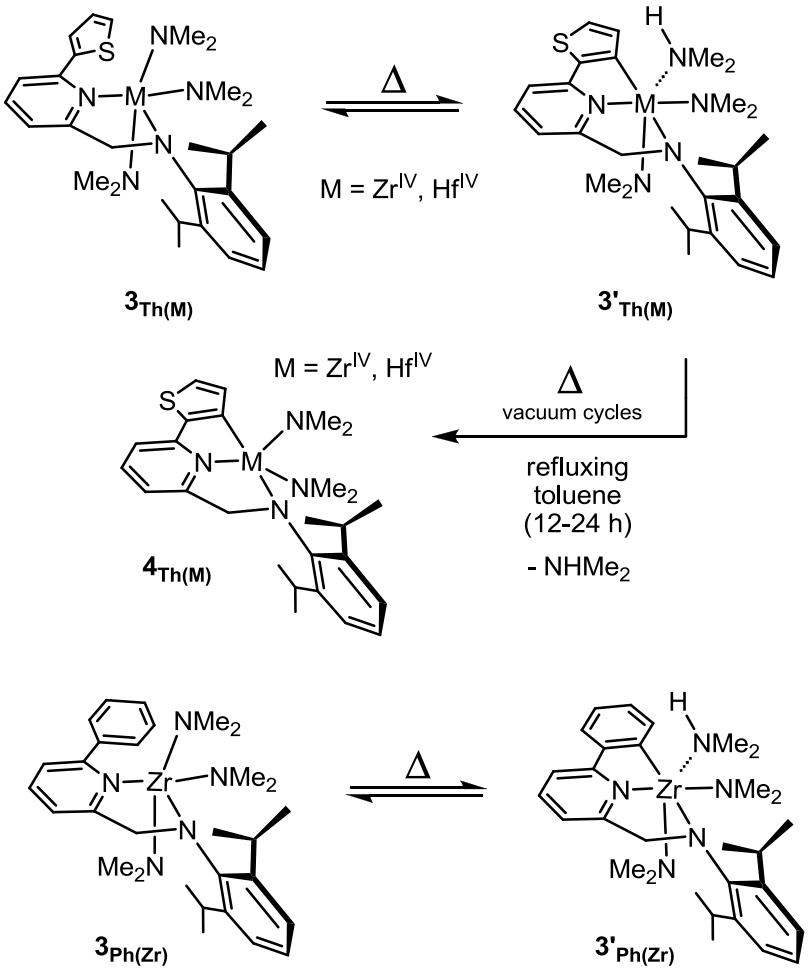

Scheme 3.3. Zr^{IV} and Hf^{IV} pyridyl-amido catalysts scrutinized in hydroamination processes.

ORTEP drawings of the crystal structures obtained from **4**$_{Th(Zr)}$ and **4**$_{Th(Hf)}$ are given in **Figures 3.2** and **3.3**, respectively, while **Table 3.1** lists all the main crystal and structural refinement data.

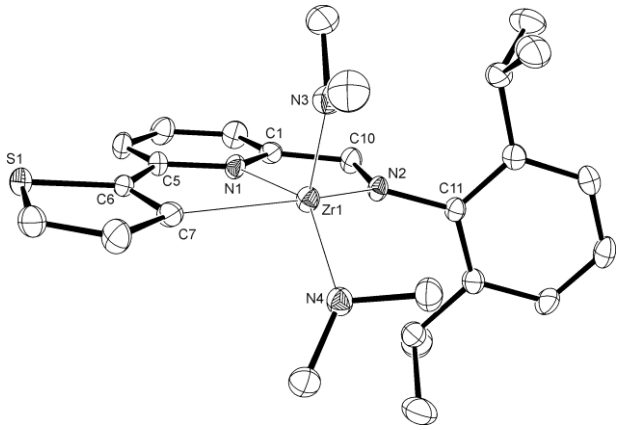

Figure 3.2. Crystal structure of $\{C^{-},N,N^{-}\}N_2^{Th}Zr(NMe_2)_2$ [$\mathbf{4_{Th(Zr)}}$]. Thermal ellipsoids are drawn at the 40% probability level. Hydrogen atoms are omitted for clarity. Selected bond lengths and angles are summarized in **Table 3.2**.

The two compounds are isostructural; they both crystallize in the monoclinic $P2_1/n$ space group. The coordination geometry around the metal centre is similar to that observed in the benzyl analogues.[4b] In the $\mathbf{4_{Th(Zr)}}$, two almost identical molecules are present in the asymmetric unit; they are related to each other through a C_2 pseudo-symmetry axis along the *b* direction. Consequently, the same chemical species is "seen" as two structurally different molecules.[20] The unit cell volume and Z in $\mathbf{4_{Th(Zr)}}$ are doubled with respect to those of $\mathbf{4_{Th(Hf)}}$, while maintaining the same structural features.

While preparing crystals from cyclometallated forms, we also succeeded in the isolation of crystals of $\mathbf{3_{Ph(Zr)}}$. Upon standing for weeks, yellow pale microcrystals suitable for X-ray diffraction analysis were separated off from a cooled (– 50°C) and highly diluted toluene solution of $\mathbf{3_{Ph(Zr)}/3'_{Ph(Zr)}}$.

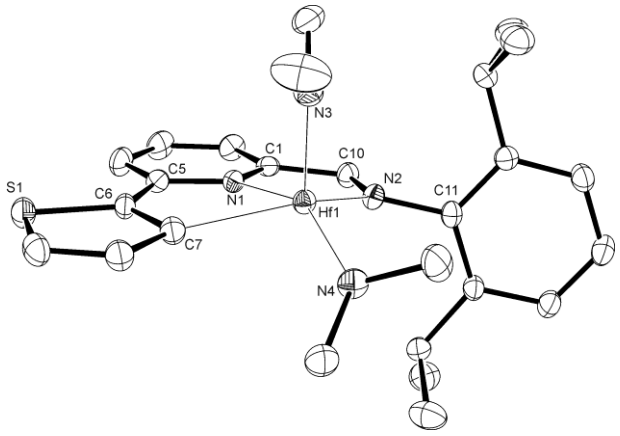

Figure 3.3. Crystal structure of $\{C^-,N,N^-\}N_2{}^{Th}Hf(NMe_2)_2$ [$\mathbf{4_{Th(Hf)}}$]. Thermal ellipsoids are drawn at the 40% probability level. Hydrogen atoms are omitted for clarity. Selected bond lengths and angles are summarized in **Table 3.2**.

Previous attempts to isolate single-crystals for X-ray analysis from the tautomeric mixture under milder conditions (diluted or concentrated solutions in the –35 °C ÷ 0 °C temperature range), failed.[21] An ORTEP drawing of the trisamido-Zr^{IV} species is shown in **Figure 3.4**. The compound crystallizes in the orthorhombic *Pbca* space group. The coordination number and geometry of the Zr^{IV} ion are the same as those of the corresponding bis(amido) analogues; the ligand phenyl ring is dangling, and two molecules with a different Py-Ph dihedral angle are present in the asymmetric unit [equal to 117.0(11)° and 134.4(9)°, respectively].

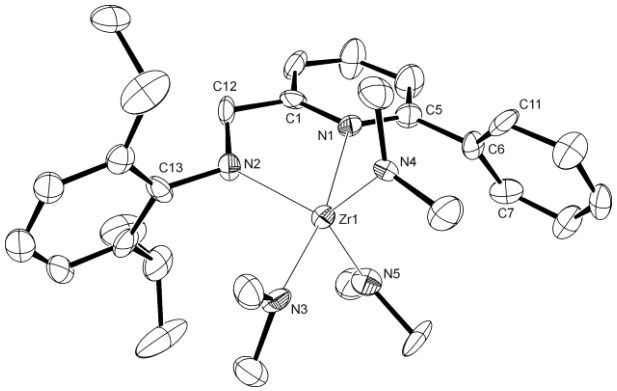

Figure 3.4. Crystal structure of $\{N,N^-\}N_2{}^{Ph}Zr(NMe_2)_3$ [$\mathbf{3_{Ph(Zr)}}$]. Thermal ellipsoids are drawn at the 40% probability level. Hydrogen atoms are omitted for clarity. Selected bond lengths and angles are summarized in **Table 3.2**.

The low energy barrier for the phenyl ring rotation around the C(5)-C(6) bond allows for the presence of two different conformers within the same crystal lattice. As a consequence, the unit cell volume [12103(2) $Å^3$] and Z value (16) for $\mathbf{3_{Ph(Zr)}}$ are unusually high (four times as much) if compared with those of its cyclometallated benzyl analogue $\{C^-,N,N^-\}N_2{}^{Ph}Zr(CH_2Ph)_2$.[4b] Refer to **Table 3.2** for the most relevant crystallographic parameters.

All isolated compounds and tautomeric mixtures were used as catalysts for the intramolecular hydroamination of the aminoalkene **I** as model substrate. Unlike the previous catalytic studies carried out in a J-Young NMR tube [see experimental section for neutral (alkyl) and cation Zr^{IV} and Hf^{IV} complexes], catalytic tests with amido compounds were conducted in a glove-box, under inert atmosphere. The reactions were set-up in a two-necked round flask equipped with a magnetic stirrer-bar and a septum for the ongoing syringe substrate addition. By this method, the aminoalkene **I** was added to a pre-heated catalyst(s) solution at the final reaction temperature. These conditions were used to achieve a better control of the molar fraction of the cyclometallated species to be put in contact with the substrate; this procedure was of major importance for catalytic tests carried out in the presence of temperature sensitive tautomeric mixtures such as $\mathbf{3_{Th(M)}/3'_{Th(M)}}$ and $\mathbf{3_{Ph(Zr)}/3'_{Ph(Zr)}}$. Catalyst(s) content was fixed to 5 mol % and the reaction temperature (unless otherwise stated) was set at 100 °C. **Table 3.4** summarizes the catalytic assays obtained with different Zr/Hf amido catalysts. All complexes showed from moderate to high efficiency in the cyclo-hydroamination reaction of the primary aminoalkene **I**.[22] In particular $\mathbf{4_{Th(Zr)}}$ gave complete substrate conversion to the corresponding pyrrolidine in 1h (**Table 3.4**, entry 4).

Table 3.4. Intramolecular hydroamination of **I** (and **III**) by pyridylamido complexes $\mathbf{3_{Th(M)}/3'_{Th(M)}}$, $\mathbf{3_{Ph(Zr)}/3'_{Ph(Zr)}}$ and $\mathbf{4_{Th(M)}}$.[a]

Entry	Catalyst	3/3' molar ratio[b]	Substrate	Product	time (h)	Conversion[c] (isolated yield)[d] (%)
1	$\mathbf{3_{Th(Zr)}/3'_{Th(Zr)}}$	25:75	**I**	**VI**	2	92 (87)
2	$\mathbf{3_{Th(Hf)}/3'_{Th(Hf)}}$	11:89	**I**	**VI**	2	25 (19)[e]
3	$\mathbf{3_{Ph(Zr)}/3'_{Ph(Zr)}}$	62:38	**I**	**VI**	2	59 (52)
4	$\mathbf{4_{Th(Zr)}}$	-	**I**	**VI**	1	>99 (98)
5	$\mathbf{4_{Th(Zr)}}$	-	**III**	**VIII**	5	n.d.
6	$\mathbf{4_{Th(Zr)}}^{f}$	-	**I**	**VI**	3	94 (90)
7	$\mathbf{4_{Th(Zr)}}^{f}$	-	**I**	**VI**	4	>99 (98)
8	$\mathbf{4_{Th(Zr)}}^{g}$	-	**I**	**VI**	3	6 (n.d.)[e]
9[c]	$\mathbf{4_{Th(Hf)}}$	-	**I**	**VI**	1	19 (16)[e]
10	$\mathbf{4_{Th(Hf)}}$	-	**III**	**VIII**	5	n.d
11	$\mathbf{4_{Th(Hf)}}^{f}$	-	**I**	**VI**	3	29 (26)[e]
12[c]	$\mathbf{4_{Th(Hf)}}^{f}$	-	**I**	**VI**	72	89 (85)
13[c]	$\mathbf{4_{Th(Hf)}}^{g}$	-	**I**	**VI**	3	<1 (n.d.)

[a] Hydroaminaton conditions: toluene solvent (3 mL), Substrate (0.632 mmol), T = 100 °C, 5 mol% catalyst. [b] Calculated from the ^{1}H NMR spectrum at the final reaction temperature; see ref. 4. [c] Determined by GC-MS. [d] Calculated from the weight of the isolated product after chromatographic purification of the crude mixture. [e] Average values calculated over three independent runs. [f] T = 80 °C. [g] r.t. Not determined = n.d.

Notably, the comparison of tautomeric catalytic mixtures (**3/3'**) with the pure bisamido cyclometallated form (**4**) has contributed to shedding light on important structure-activity relationships for this class of Group IV amido-based systems.[4] In particular, pre-catalysts $\mathbf{3_{Th(Zr)}/3'_{Th(Zr)}}$ and $\mathbf{4_{Th(Zr)}}$ were the most active systems under the selected cyclization conditions. Apparently, the metal coordination environment was the most relevant factor influencing the measured catalytic activities. Unlike **4**, the $\mathbf{3_{Th(Zr)}/3'_{Th(Zr)}}$ mixture was present in 75% as bisamido {*C*$^-$,*N*,*N*$^-$} cyclometallated form, at 100 °C (**Table 3.4**, entry 1).[4]

Accordingly, the $\mathbf{3_{Ph(Zr)}/3'_{Ph(Zr)}}$ mixture, whose maximum cyclometallated content (**3'**) at 100 °C was estimated to be the 38%, gave lower substrate conversions (**Table 3.4**, entries 3 *vs.* 1). In spite of a higher percentage of the cyclometallated form in the $\mathbf{3_{Th(Hf)}/3'_{Th(Hf)}}$ counterparts (**Table 3.4**, entry 2), worse substrate conversions were (usually) reached when switching from Zr^{IV}-amido to Hf^{IV}-amido pre-catalysts (**Table 3.4**, entries 2 *vs.* 1 and entries 4, 6, 8 vs. 9, 11, 13).[10] According to these data, it is evident that both the metal type (Zr *vs.* Hf) and their coordination environment play a

crucial role in the final catalyst performance. Similarly to our previous studies on polymerization catalysis,[4] cyclometallated Group IV pyridylamido systems gave higher substrate conversions. Although a real comparison between unique trisamido {*N*,*N*$^-$} and bisamido cyclometallated {*C*$^-$,*N*,*N*$^-$} forms was hampered by the ability of the former to undergo intramolecular cyclometallation (σ-bond metathesis) at high temperature, the observed reactivity trend (**3/3'** mixtures *vs.* **4** bisamido systems) confirmed the major contribution of the cyclometallated species (**4**). The ability of the latter to perform intramolecular hydroamination was then investigated under different temperature conditions. Whereas $\mathbf{4_{Th(Zr)}}$ gave complete conversion of **I** in 1h at 100 °C, lowering the temperature to 80 °C resulted into high conversion after 3 h and complete cyclization of **I** after 4 h (**Table 3.4**, entries 4 *vs*. 6 *vs*. 7). The Hf^{IV} analogue $\mathbf{4_{Th(Hf)}}$ showed only moderate substrate conversions; lowering the reaction temperature to 80 °C required long reaction times to get satisfactory pyrrolidine yields (**Table 3.4**, entries 9 *vs*. 11 *vs*. 12). Preliminary kinetic investigations on complexes $\mathbf{3_{Th(Zr)}/3'_{Th(Zr)}}$ and $\mathbf{4_{Th(Zr)}}$ confirmed the first order kinetics in substrate with both catalytic systems (**Figure 3.5**).

To get a better comparison of the activity at 100°C for the two catalytic systems, the kinetic profile resulting from substrate consumption/conversion as obtained from 5 mol% of the $\mathbf{3_{Th(Zr)}/3'_{Th(Zr)}}$ was compared with that recorded in the presence of 3.75 mol% of $\mathbf{4_{Th(Zr)}}$.[19,23]

As it can be appreciated from **Figure 3.5**, there are no significant differences on the catalysts half-lives measured with both catalytic systems [$t_{½}$ $\mathbf{3_{Th(Zr)}/3'_{Th(Zr)}}$ = 28 min; $t_{½}$ $\mathbf{4_{Th(Zr)}}$ = 30 min]. In addition, the hydroamination reaction performed with the pure $\mathbf{4_{Th(Zr)}}$ catalyst was determined to be first order in catalyst concentration. A first order in

catalyst and substrate concentration was previously reported for other neutral zirconium catalysts.[10,24]

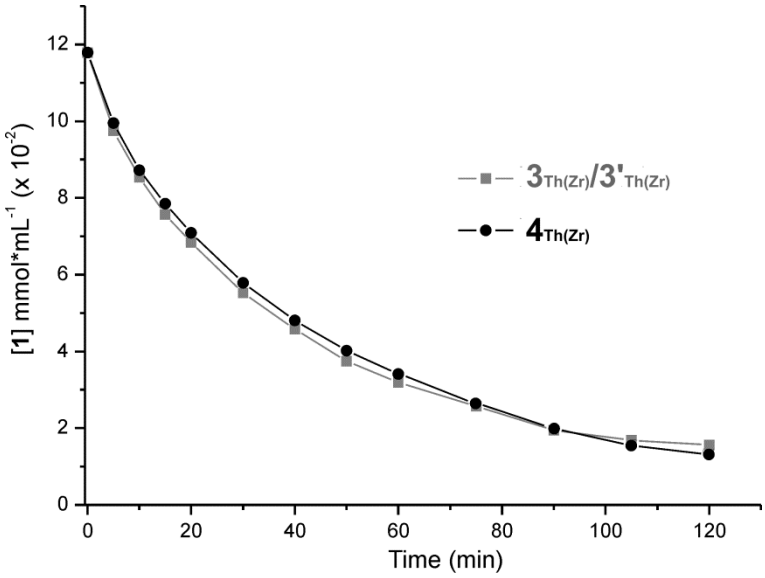

Figure 3.5. Plot of first-order substrate (**I**) conversion by $\mathbf{3}_{\mathbf{Th(Zr)}}/\mathbf{3'}_{\mathbf{Th(Zr)}}$ and $\mathbf{4}_{\mathbf{Th(Zr)}}$ using 5 mol% and 3.75 mol%, respectively.[23]

Normalized Ln[substrate] *vs.* time plots measured for three different catalyst [$\mathbf{4}_{\mathbf{Th(Zr)}}$] concentrations are shown in **Figure 3.6**, the inset demonstrates the linearity of the observed *k* values *vs.* catalyst concentration. All these data taken together lead to the conclusion that the two catalytic systems [$\mathbf{3}_{\mathbf{Th(Zr)}}/\mathbf{3'}_{\mathbf{Th(Zr)}}$ and $\mathbf{4}_{\mathbf{Th(Zr)}}$] share a common catalytically active species. Even if a catalytic role of the tris-amido species $\mathbf{3}_{\mathbf{Th(Zr)}}$ in the $\mathbf{3}_{\mathbf{Th(Zr)}}/\mathbf{3'}_{\mathbf{Th(Zr)}}$ mixture cannot be fully discarded,[23] it is apparent that its contribution is kinetically negligible under the cyclization conditions applied in these trials. Hydroamination of secondary aminoalkenes with bisamido systems **4** did not take place even after prolonged heatings (**Table 3.4**, entries 5 and 10), which is in agreement with most previous studies on neutral Group IV metal complexes in hydroamination reaction.[10,25] This observation supports the hypothesis of imido species as intermediates in the catalytic cycle.[5,10]

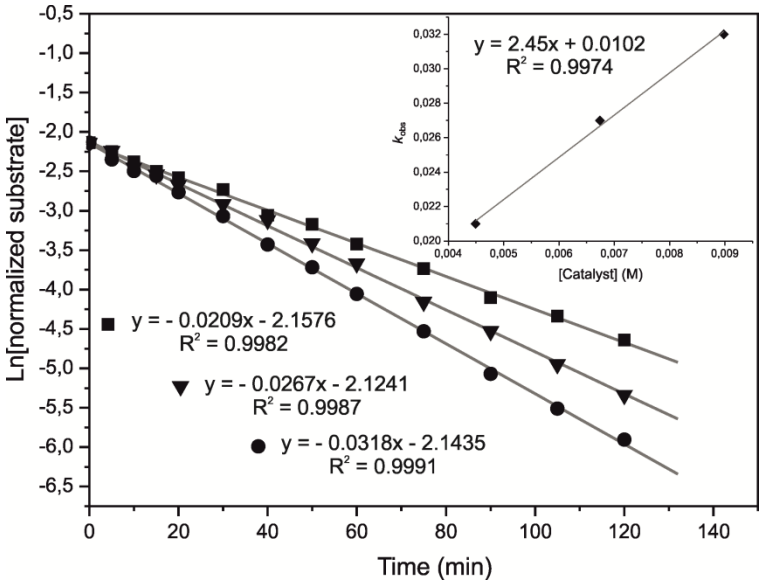

Figure 3.6. Plot of first-order catalyst dependence for intramolecular hydroamination of **I** at different $\mathbf{4_{Th(Zr)}}$ concentrations (■ = 4 mol%; ▼ = 6 mol%; ● = 8 mol%). Inset refers to the linearity of the observed *k* values vs. catalyst concentration.

3.4 Conclusions

In summary, a number of Zr^{IV} and Hf^{IV} benzyl and amido polymerization catalysts of the state-of-the-art are found to be good candidates (in either neutral or cationic form) for the intramolecular hydroamination/cyclization of either primary or secondary aminoalkenes. In particular, cationic monobenzyl derivatives prepared upon treatment of their neutral counterpart with $[Ph_3C][B(C_6F_5)_4]$ have shown remarkable catalytic activity for the production of five and six-membered N-containing heterocycles starting from secondary amino alkenes. In addition, Zr^{IV} and Hf^{IV} amido derivatives featured by a temperature controlled prototropic rearrangement capable of a deep "redrawing" of the metal coordination sphere have been investigated with the specific aim of elucidating the role of the active site environment on the final catalyst's performance. To fulfill the latter aspect, unique Zr^{IV} and Hf^{IV} bisamido cyclometallated species have been isolated and completely characterized. Their catalytic behavior in the hydroamination reaction combined with preliminary kinetic investigations, have provided evidence of the central

role played by the metal coordination sphere in promoting such catalytic transformations, efficiently. Overall, this study demonstrates the applicability of pyridylamido Group IV metal complexes in the intramolecular hydroamination reaction, widening the scope of exceptional polymerization catalyst of the-state-of-the-art. These findings pave the way to the development of original early-transition metal complexes based on C_1 symmetric N-containing ligands for stereoselective hydroamination catalysis.

3.5 Experimental Section

General Considerations. All air- and/or moisture-sensitive reactions were performed under inert atmosphere in flame-dried flasks using standard Schlenk-type techniques or in a dry-box filled with nitrogen or argon. Benzene and toluene were purified by distillation from sodium/triglyme benzophenone ketyl and stored over activated 4Å molecular sieves or were obtained by means of a MBraun Solvent Purification Systems. Benzene-d_6 and toluene-d_8 were dried over sodium/benzophenone ketyl and condensed *in vacuo* over activated 4Å molecular sieves prior to use. All other reagents and solvents were used (unless otherwise stated) as purchased from commercial suppliers without further purification. The amino-pyridinate ligands were synthesized according to standard procedures reported in the literature.[13] Literature methods were used to synthesize the corresponding Zr^{IV}/Hf^{IV}-benzyl (neutral, **1** and cationic, **2**) and/or amido complexes **3**/**3'** and **4**[4] 1D (^{1}H and ^{13}C{^{1}H}) and 2D (COSY H,H, HETCOR H,C) NMR spectra of all organometallic species were obtained on either a Bruker Avance DRX-400 spectrometer (400.13 and 100.61 MHz for ^{1}H and ^{13}C, respectively) or a Bruker Avance 300 MHz instrument (300.13 and 75.47 MHz for ^{1}H and ^{13}C, respectively). Chemical shifts are reported in ppm (δ) relative to TMS,

referenced to the chemical shifts of residual solvent resonances (^{1}H and ^{13}C). The multiplicities of the $^{13}C\{^{1}H\}$ NMR spectra were determined on the basis of the $^{13}C\{^{1}H\}$ JMOD sequence and quoted as: CH_3, CH_2, CH and C for primary, secondary, tertiary and quaternary carbon atoms, respectively. Deuterated solvents for NMR measurements were dried over molecular sieves. The C, H, N, S elemental analyses were made on a Thermo FlashEA 1112 Series CHNS-O elemental analyzer with an accepted tolerance of ± 0.4 units on carbon (C), hydrogen (H) and nitrogen (N). *X-ray data measurements.* Single crystal X-Ray data were collected at low temperature (120 K) on an Oxford Diffraction XCALIBUR 3 diffractometer equipped with a CCD area detector using Mo Kα radiation (λ = 0.7107 Å). The program used for the data collection was CrysAlis CCD 1.171.[26] Data reduction was carried out with the program CrysAlis RED 1.171[27] and the absorption correction was applied with the program ABSPACK 1.17. Direct methods implemented in Sir97[28] were used to solve the structures and the refinements were performed by full-matrix least-squares against F^2 implemented in SHELX97.[29] All the non-hydrogen atoms were refined anisotropically, while the hydrogen atoms were fixed in calculated positions and refined isotropically with the thermal factor depending on the one of the atom to which they are bound (riding model). In the refinement of **3$_{Ph(Zr)}$**, restraints on some Anisotropic Displacement Parameters of C atoms had to be introduced, due to the bad crystal data quality (R_{int} = 0.30) generated by the existence of different conformers in the same lattice (see the Results and Discussion section) and by the disorder of the dimethylamido ligands even at 120 K. Molecular plots were produced by the program ORTEP3.[30] Catalytic reactions were performed under inert atmosphere in either a J-Young NMR tube or in a 10 mL round bottom flask and the reaction course was followed by ^{1}H NMR spectroscopy and GC/MS analysis, respectively. All substrates were dried overnight over activated 4Å molecular sieves with a few drops of benzene-d_6 prior to use.

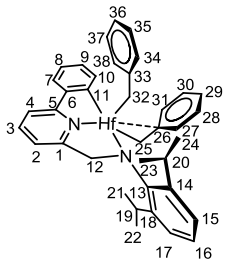

Synthesis and characterization of the pyridylamido $Hf^{IV}(Bn)_2$ complex $\mathbf{1_{Hf}}$. To a heated (60 °C) solution of N_2H^{Ph} (0.100g, 0.29 mmol) in dry and degassed C_6H_6 (2 mL), a solution of tetrabenzylhafnium (0.158g, 0.29 mmol) in dry and degassed C_6H_6 (4 mL) was added dropwise. The resulting reaction mixture was heated at 60°C for 2 h and then it was concentrated *in vacuo* to give a yellow-brown solid. Recrystallization of the mixture from a concentrated toluene solution gave yellow crystals of the analytically pure compound $\mathbf{1_{Hf}}$ (0.190 g, 93% yield). Crystals suitable for X-ray diffraction analysis were grown by cooling a concentrated complex solution in toluene at –35 °C and layering it with cold drops of *n*-hexane. ^{1}H NMR (300 MHz, CD_2Cl_2, 293K): δ 1.26 (d, $^3J_{HH}$ = 6.8 Hz, 6H, CH(C*H*$_3$), H^{22,24}), 1.38 ((d, $^3J_{HH}$ = 6.8 HZ, 6H, CH(C*H*$_3$), H^{21,23}), 1.74 (d, AB*q*, $^3J_{HH}$ = 11.4 Hz, 2H, HfC*HH*Ph, H^{25,32}), 2.21 (d, AB*q*, $^3J_{HH}$ = 11.4 Hz, 2H, HfC*HH*Ph, H^{25,32}), 3.71 (sept, $^3J_{HH}$ = 6.8 Hz, 2H, C*H*(CH$_3$), H^{19,20}), 5.05 (s, 2H, *CH*$_2$N, H^{12}), 6.52 (d, $^3J_{HH}$ = 7.4 Hz, 4H, *o*-Ph, H^{27,31,34,38}), 6.70 (t, $^3J_{HH}$ = 7.3 Hz, 2H, *p*-Ph, H^{29,36}), 6.91 (t, $^3J_{HH}$ = 7.6 Hz, 4H, *m*-Ph, H^{28,30,35,37}), 7.14 (d, $^3J_{HH}$ = 7.7 Hz, 1H, C*H* Ar, H^2), 7.23-7.34 (4H, C*H* Ar, H^{9,15,16,17}), 7.45 (t, $^3J_{HH}$ = 6.6 Hz, 1H, C*H* Ar, H^8), 7.56 (d, $^3J_{HH}$ = 7.7 Hz, 1H, C*H* Ar, H^4), 7.69-7.76 (2H, C*H* Ar, H^{3,10}), 8.01 (d, $^3J_{HH}$ = 6.6 Hz, 1H, C*H* Ar, H^7). ^{13}C{^{1}H} NMR (75 MHz, CD_2Cl_2, 293 K): δ 23.5 (CH(*C*H$_3$)$_2$, C^{21,23}), 27.7 (CH(*C*H$_3$)$_2$, C^{22,24}), 28.2 (*C*H(CH$_3$)$_2$, C^{19,20}), 67.7 (C^{12}), 81.0 (C^{25,32}), 115.8 (C^4), 117.9 (C^2), 122.6 (C^{29,36}), 123.2 (C^{10}), 124.5 (C^{15,17}), 126,2 (C^{16}), 128.3 (C^{28,30,35,37}), 128.4 (C^8), 128.5 (C^{27,31,34,38}), 129.9 (C^9), 137.4 (C^7), 140.7 (C^3), 141.2 (C), 147.2 (C), 147.3 (C), 147.8 (C), 163.5 (C), 165.2 (C), 201.6 (C^{11}). Anal. Calcd (%) for $C_{38}H_{40}N_2Hf$ (703.23): C 64.90, H 5.73, N 3.98; found: C 64.75, H 5.80, N 4.06.

General Procedure for Intramolecular Hydroamination of Aminoalkenes. Two different cyclization conditions were used depending on the employed catalytic system.

Both procedures were set-up under inert atmosphere using N_2 or Ar-filled dry-box. **Procedure A:** Neutral (alkyl) and cationic Group-IV amidopyridinate complexes were tested as catalyst precursors in the intramolecular hydroamination reaction using a sealed J-Young NMR tube. **For neutral complexes $\mathbf{1_{Zr}}$ and $\mathbf{1_{Hf}}$**: In an Ar-filled dry-box, a solution of isolated $\mathbf{1_{Zr}}$ or $\mathbf{1_{Hf}}$ (0.016 mmol) in C_6D_6 (0.6 mL) was slowly added to a vial containing the corresponding aminoalkene ($0.16 \cdot 10^{-3}$ mol) at room temperature. The homogeneous reaction mixture was then introduced into a J-Young-tap NMR tube and placed in an oil bath heated to100°C. The conversion of the reaction was monitored by comparative integration of the signal relative to the olefinic protons of the substrate and the signal relative to the protons of the product. A similar procedure was used for kinetic measurements with precatalysts $\mathbf{3_{Th(Zr)}}$/$\mathbf{3'_{Th(Zr)}}$ and $\mathbf{4_{Th(Zr)}}$. **For cationic complexes $\mathbf{2_{Zr}}$ and $\mathbf{2_{Hf}}$**: In an Ar-filled dry-box, $[Ph_3C][B(C_6F_5)_4]$ was slowly added to a solution of $\mathbf{1_{Zr}}$ or $\mathbf{1_{Hf}}$ (0.016 mmol) in C_6D_6 (0.6 mL) at room temperature. The solution was stirred a few minutes and transferred into a vial containing the corresponding aminoalkene (0.16 mmol). The heterogeneous reaction mixture was then introduced into a J. Young-tap NMR tube and placed in an oil bath heated at 100°C. The conversion of the reaction was monitored by comparative integration of the signal relative to the olefinic protons of the substrate and the signal relative to the protons of the product. **Procedure B:** Amido precursors $\mathbf{3_{Th(M)}}$/$\mathbf{3'_{Th(M)}}$ and $\mathbf{4_{Th(M)}}$ (M = Zr, Hf) were tested as catalysts in the intramolecular hydroamination reaction using a two-necked 10 mL round bottom flask equipped with a magnetic stir bar, a reflux condenser and a septum. In a typical procedure, a solution of the pre-catalyst (5 mol%) in dry and degassed toluene (2.5 mL) was heated at 100 °C. After keeping the pre-heated catalyst solution under stirring for 10 min, a pre-heated (80 °C) solution of the aminoalkene **I** (0.150 g, 0.632 mmol) in dry and degassed toluene (0.5 mL) was added *via* syringe in one portion. Afterwards, the reaction course was periodically monitored by sampling the

reaction mixture and analyzing it via GC/MS, till completeness. Finally, the reaction mixture was concentrated under reduced pressure and the crude material was purified by flash-chromatography (CH_2Cl_2 + 5% MeOH) to give the final pure pyrrolidine.

Kinetic measurements on $\mathbf{3_{Th(Zr)}}$/$\mathbf{3'_{Th(Zr)}}$ and $\mathbf{4_{Th(Zr)}}$. Kinetic studies were performed for the conversion of **I**, using either variable catalyst's concentration (4, 6 or 8 mol%) or different catalyst precursors ($\mathbf{3_{Th(Zr)}}$/$\mathbf{3'_{Th(Zr)}}$ *vs.* $\mathbf{4_{Th(Zr)}}$), for all runs using constant initial concentration of **I**. All measurements were carried out in a sealed J-Young NMR tube and the course of the process was monitored via ^{1}H NMR spectra recorded at constant times using ferrocene as internal standard. Both catalyst precursors $\mathbf{3_{Th(Zr)}}$/$\mathbf{3'_{Th(Zr)}}$ and $\mathbf{4_{Th(Zr)}}$ showed a first order dependence in substrate consumption/cyclization. To better compare the two catalyst precursors, 5 mol% of $\mathbf{3_{Th(Zr)}}$/$\mathbf{3'_{Th(Zr)}}$ were compared with 3.75 mol% of the pure $\mathbf{4_{Th(Zr)}}$. Previous studies from some of us showed a 25:75 ratio of $\mathbf{3_{Th(Zr)}}$/$\mathbf{3'_{Th(Zr)}}$ at the target reaction temperature (100 °C). According to that, equal amounts of the cyclometallated species $\mathbf{3'_{Th(Zr)}}$ and $\mathbf{4_{Th(Zr)}}$ were then taken into account. In a typical procedure, stock solutions of catalyst precursors $\mathbf{3_{Th(Zr)}}$/$\mathbf{3'_{Th(Zr)}}$ and $\mathbf{4_{Th(Zr)}}$ were prepared by dissolving 20 mg of each complex in 0.5 mL of toluene-d_8. 20 mg of **I** and 5 mg (26.34 μmol) of ferrocene 98% (internal standard) [10j] were weighted into a 1 mL volumetric flask and dissolved in approximately 0.2 mL of toluene-d_8. Afterwards, a proper amount of the stock solution of the catalyst precursor [0.06 mL of $\mathbf{3_{Th(Zr)}}$/$\mathbf{3'_{Th(Zr)}}$; 0.04 mL of $\mathbf{4_{Th(Zr)}}$] was added to the 1 mL volumetric flask and the volume was topped to 1 mL with toluene-d_8. The as prepared solution was shaken and 0.8 mL were rapidly transferred into the J-Young NMR tube. The tube was placed into a pre-heated (100 °C) 300 MHz NMR probe and the system was allowed to thermally equilibrate for 5 minutes prior starting to collect the t = 0 ^{1}H NMR spectrum. The ^{1}H NMR spectra (8 scans) were collected every 5/10 minutes up to the almost complete

substrate conversion (at least 90%). Comparison of the integration of product and substrate peaks with internal standard peaks was used to calculate the relative percentage of substrate and product at any given time.

First order in catalyst concentration for the pure $\mathbf{4_{Th(Zr)}}$ was determined using a similar procedure to that described above. Three different catalyst concentrations (4, 6 and 8 mol% of $\mathbf{4_{Th(Zr)}}$) were used in the presence of a constant concentration of **I**. In a typical procedure, the proper amount of $\mathbf{4_{Th(Zr)}}$ in toluene-d_8 (stock solution) was added to a solution of **I** (20 mg, 84.27 μmol) and ferrocene (5 mg, 26.34 μmol – internal standard) and the volume was raised up to 1 mL with toluene-d_8. The solution was shaken and 0.8 mL were rapidly transferred into the J-Young NMR tube. The reaction course was monitored via ^{1}H NMR spectra, similarly to the procedure described above.

5.6 References

1 For a comprehensive review on the topic see: G. Giambastiani, L. Luconi, R. L. Kuhlman, P. D. Hustad in *Imino- and amido-pyridinate d-Block Metal Complexes in Polymerization/ Oligomerization Catalysis*, Vol. 35 – *Catalysis by Metal Complexes* series (Eds: G. Giambastiani, J. Cámpora), Springer, London, **2011**, pp. 197-281.

2 D. J. Arriola, E. M. Carnahan, P. D. Hustad, R. L. Kuhlman, T. T. Wenzel, *Science*, **2006**, *312*, 714.

3 a) C. Zuccaccia, A. Macchioni, V. Busico, R. Cipullo, G.Talarico, F. Alfano, H. W. Boone, K. A. Frazier, P. D. Hustad, , J. C. Stevens, P. C. Vosejpka, K. A. Abboud, *J. Am. Chem. Soc.* **2008**, *130*, 10354. b) C. Zuccaccia, V. Busico, R. Cipullo, G. Talarico, R. D. J. Froese, P. C. Vosejpka, P. D. Hustad, A. Macchioni, *Organometallics* **2009**, *28*, 5445.

4 a) L. Luconi, G. Giambastiani, A. Rossin, C. Bianchini, A. Lledós, *Inorg. Chem.*, **2010**, *49*, 6811-6813. b) L. Luconi, A. Rossin, G. Tuci, I. Tritto, L. Boggioni, J. J. Klosin, C. N. Theriault, G. Giambastiani, *Chem. Eur. J.*, **2012**, *18*, 671.

5 For general and more specialized reviews on hydroamination and its asymmetric version: a) K. D. Hesp, M. Stradiotto, *Chem.Cat.Chem.* **2010**, *2*, 1192; b) G. Zi, *Dalton Trans.* **2009**, 9101; c) S. C. Chemler, *Org. Biomol. Chem.* **2009**, 3009; d) T. E. Müller, K. C. Hultzsch, M. Yus, F. Foubelo, M. Tada, *Chem. Rev.* **2008**, *108*, 3795; e) I. Aillaud, J. Collin, J. Hannedouche, E. Schulz, *Dalton Trans.* **2007**, 5105; f) R. Severin, S. Doye, *Chem. Soc. Rev*. **2007**, *36*, 1407; g) K. C. Hultzsch, *Adv. Synth. Catal.* **2005**, *347*, 367; h) K. C. Hultzsch, *Org. Biomol. Chem.* **2005**, *3*, 1819; i) S. Hong, T. J. Marks, *Acc. Chem. Res.* **2004**, *37*, 673; j) P. W. Roesky, T. E. Müller, *Angew. Chem.* **2003**, *115*, 2812; *Angew. Chem., Int. Ed.* **2003**, *42*, 2708; k) T. E. Müller, M. Beller, *Chem. Rev.* **1998**, *98*, 675.

6 For a selection of early and more recent reports on alkali-metal-catalyzed inter- and intramolecular hydroamination on unactivated alkenes, see: a) B. W. Howk, E. L. Little, S. L.Scott, G. M. Whitman, *J. Am. Chem. Soc.* **1954**, *76*, 1899; b) R. Stroh, J. Ebersberger, H. Haberland,W. Hahn, *Angew. Chem.* **1957**, *69*, 124; c) B. E. Evans, P. S. Anderson, M. E. Christy, C. D. Colton, D. C. Remy, K. E. Rittle, E. L. Engelhardt, *J. Org. Chem.* **1979**, *44*, 3127; d) V. Khedkar, A. Tillack, C. Benisch, J.-P. Melder, M. Beller, *J. Mol. Catal. A* **2005**, *241*, 175; e) H. Fujita, M. Tokuda, M. Nitta, H. Suginome, *Tetrahedron Lett.* **1992**, *33*, 6359; f) A. Ates, C. Quinet, *Eur. J. Org. Chem.* **2003**, 1623; g) C. Quinet, L. Sampoux, I. E. Markó, *Eur. J. Org. Chem.* **2009**, 1806. For enantioselective lithium-catalyzed hydroamination, see: h) P. H. Martinez, K. C. Hultzsch, F. Hampel, *Chem. Commun.* **2006**, 2221; i) T. Ogata, A. Ujhara, S. Tsuchida, T. Shimizu, A. Kaneshige, K. Tomioka, *Tetrahedron Lett.* **2007**, *48*, 6648; j) J. Deschamp, C. Olier, E. Schulz, R. Guillot, J. Hannedouche, J. Collin, *Adv. Synth. Catal.* **2010**, *352*, 2171; k) J. Deschamp, J. Collin, J. Hannedouche, E. Schulz, *Eur. J. Org. Chem.* **2011**, 3329.

7 For seminal work in this field, see: a) M. R. Gagné, T. J. Marks, *J. Am. Chem. Soc.* **1989**, *111*, 4108; b) M. R. Gagné, S. P. Nolan, T. J. Marks, *Organometallics* **1990**, *9*, 1716; c) M. R. Gagné, C. L. Stern, T. J. Marks, *J. Am. Chem. Soc.* **1992**, *114*, 275; d) M. R. Gagné, L. Brard, V. P. Conticello, M. A. Giardello, C. L. Stern, T. J. Marks, *Organometallics* **1992**, *11*, 2003. For a selection of rare-earth catalyzed (enantioselective) intra- and intermolecular hydroamination reaction, see: e) Y. Li, T. J. Marks, *Organometallics* **1996**, *15*, 3770; f) J. – S. Ryu, G. Y. Li, T. J. Marks, *J. Am. Chem. Soc.* **2003**, *125*, 12584; g) S. Hong, S. Tian, M. V. Metz, T. J. Marks, *J. Am. Chem. Soc*. **2003**, *125*, 14768; h) P. N. O'Shaughnessy, P. D. Knight, C. Morton, K. M. Gillespie, P. Scott, *Chem. Commun*. **2003**, 1770; i) J. Y. Kim, T. Livinghouse, *Org. Lett.* **2005**, *7*, 1737; j) N. Meyer, A. Zulys, P. W. Roesky, *Organometallics* **2006**, *25*, 4179; k) D. V. Gribkov, K. C. Hultzsch, F. Hampel, *J. Am. Chem. Soc.* **2006**, *128*, 3748; l) I. Aillaud, J. Collin, C. Duhayon, R. Guillot, D. Lyubov, E. Schulz, A. Trifonov, *Chem. Eur. J.* **2008**, *14*, 2189; m) G. Zi, L. Xiang, H. Song, *Organometallics* **2008**, *27*, 1242; n) Y. Chapurina, J. Hannedouche, J. Collin, R. Guillot, E. Schulz, A. Trifonov, *Chem. Commun.* **2010**, *46*, 6918; o) A. L. Reznichenko, H. N.

Nguyen, K. C. Hultzsch, *Angew. Chem., Int. Ed.* **2010**, *49*, 8984; p) Y. Chapurina, H. Ibrahim, R. Guillot, E. Kolodziej, J. Collin, A. Trifonov, E.; Schulz, J. Hannedouche, *J. Org. Chem.* **2011**, *76*, 10163; q) D. V. Vitanova F. Hampel, K. C. Hultzsch, *J. Organomet. Chem.* **2011**, *696*, 321; r) P. Benndorf, J. Jenter, L. Zielke, P. W. Roesky, *Chem. Commun*. **2011**, 2574; s) H. M. Lovick, D. K. An, T. S. Livinghouse, *Dalton Trans*. **2011**, *40*, 7697.

8 For a selection of late transition metal-catalyzed hydroamination, see: a) R. Dorta, P. Egli, F. Zurcher, A. Togni, *J. Am. Chem. Soc.* **1997**, *119*, 10857; b) M. Kawatsura, J. F. Hartwig, *J. Am. Chem. Soc*. **2000**, *122*, 9546; c) O. Löber, M. Kawatsura, J. F. Hartwig, *J. Am.Chem. Soc.* **2001**, *123*, 4366; d) M. Utsunomiya, J. F. Hartwig, *J. Am. Chem. Soc.* **2003**, *122*, 14286; e) C. F. Bender, R. A. Widenhoefer, *J. Am. Chem. Soc*. **2005**, *127*, 1070; f) R. L. LaLonde, B. D. Sherry, E. J. Kang, F. D Toste, *J. Am. Chem. Soc.* **2007**, *129*, 2452; g) G. L. Hamilton, E. J. Kang, M. Mba, F. D. Toste, *Science* **2007**, 317, 496; i) Z. Zhang, C. F. Bender, R. A. Widenhoefer, *J. Am. Chem. Soc.* **2007**, *129*, 14148; j) J. (S.) Zhou, J. F. Hartwig, *J. Am. Chem. Soc.* **2008**, *130*, 12220; k) Z. Liu, J. F. Hartwig, *J. Am. Chem. Soc*. **2008**, *130*, 1570; l) C. F. Bender, W. B. Hudson, R. A. Widenhoefer, Organometallics **2008**, *27*, 2356; m) M. Ohmiya, T. Moriya, M. Sawamura, *Org. Lett*. **2009**, *11*, 2145; n) Z. Zhang, S. D. Lee, R. A. Widenhoefer, *J. Am. Chem. Soc.* **2009**, *131*, 5372; o) K. D. Hesp, S. Tobisch, M. Stradiotto, *J. Am. Chem. Soc*. **2010**, *132*, 413; p) X. Shen, S. L. Buchwald, *Angew. Chem., Int. Ed*. **2010**, *49*, 564; q) Z. Liu, H. Yamamichi, S. Madrahimov, J. F. Hartwig, *J. Am. Chem. Soc*. **2011**, *133*, 2772; r) O. Kanno, W. Kuriyama, Z. Wang, J. F. D. Toste, *Angew. Chem., Int. Ed.* **2011**, *50*, 9919.

9 For cationic Group 4 metal-catalyzed hydroamination of aminoalkenes, see: a) P. D. Knight, I. Munslow, P. N. O'Shaughnessy, P. Scott, *Chem. Commun*. **2004**, 894; b) D. V. Gribkov, K. C. Hultzsch, *Angew. Chem., Int. Ed*. **2004**, *43*, 5542 c) X. Wang, Z. Chen, X.-L. Sun, Y. Tang, Z. Xie, *Org. Lett*., **2011**, *13*, 4758; d) A. Mukherjee, S. Nembenna, T. K. Sen, S. Pillai Sarish, P. Kr. Ghorai, H. Ott, D. Stalke, S. K. Mandal, H. W. Roesky, *Angew. Chem., Int. Ed.* **2011**, *50*, 3968.

10 For neutral Group IV metal-catalyzed hydroamination of aminoalkenes, see: a) R. K. Thomson, J. A. Bexrud, L. L. Schafer, *Organometallics* **2006**, *25*, 4069; b) M. C. Wood, D. C. Leitch, C. S. Yeung, J. A. Kozak, L. L. Schafer, *Angew. Chem., Int. Ed*. **2007**, *46*, 354; c) S. Majumder, A. L. Odom, *Organometallics* **2008**, *27*, 1174; d) A. L. Gott, A. J. Clarke, G. J. Clarkson, P. Scott, *Chem. Commun.*, **2008**, 1422; e) C. Müller, W. Saak, S. Doye, *Eur. J. Org. Chem*. **2008**, 2731; f) J. Cho, T. K. Hollis, T. R. Helgert, E. J. Valente, *Chem. Commun*. **2008**, 5001; g) D. C. Leitch, P. R. Payne, C. R. Dunbar, L. L. Schafer, *J. Am. Chem. Soc*. **2009**, *131*, 18246; h) A. L. Reznichenko, K. C. Hultzsch, *Organometallics* **2010**, *29*, 24; i) J. A. Bexrud, L. L. Schafer, *Dalton Trans*. **2010**, *39*, 361; j) Y.-C. Hu, C.-F. Liang, J.-H. Tsai, G. P. A. Yap, Y.-T. Chang, T.-G. Ong, *Organometallics* **2010**, *29*, 3357; k) J. Cho, T. K. Hollis, E. J. Valente, J. M. Trate, *J. Organomet. Chem.* **2011**, *696*, 373; l) R. O. Ayinla, L. L. Schafer, *Dalton Trans.* **2011**, *40*, 7769; m) H. Kim, P. H. Lee, T. Livinghouse, *Chem. Commun*. **2005**, 5205; n) J. A. Bexrud, J. D. Beard, D. C. Leitch, L. L. Schafer, *Org. Lett.* **2005**, *7*, 1959; o) H. Kim, Y. K. Kim, J. H. Shim, M. Kim, M. Han, T. Livinghouse, P. H. Lee, *Adv. Synth. Catal.* **2006**, *348*, 2609; p) D. A. Watson, M. Chiu, R. G. Bergman, *Organometallics* **2006**, *25*, 4731; q) A. L. Gott, A. J. Clarke, G. J. Clarkson, P. Scott, *Organometallics* **2007**, *26*, 1729; r) X. Li, S. Haibin, G. Zi, *Eur. J. Inorg. Chem.* **2008**, 1135. s) G. Zi, Q. Wang, L. Xiang, H. Song, *Dalton Trans*. **2008**, 5930; t) G. Zi, X. Liu, L. Xiang, H. Song *Organometallics* **2009**, *28*, 1127; u) G. Zi, F. Zhang, L. Xue, L. Ai, H. Song, *J. Organomet. Chem.* **2010**, *695*, 730; v) G. Zi, F. Zhang, L. Xiang, Y. Chen, W. Fang, H. Song, *Dalton Trans*. **2010**, *39*, 4048; w) B. D. Stubbert, T. J. Marks, *J. Am. Chem. Soc*. **2007**, *129*, 6149; x) see also refs. 9c,d.

11 For zwitterionic Group 4 metal-catalyzed hydroamination of aminoalkenes, see: a) K. Manna, A. Ellern, A. D. Sadow, *Chem. Commun*. **2010**, *46*, 339; b) K. Manna, S. Xu, A. D. Sadow, *Angew. Chem., Int. Ed*. **2011**, *50*, 1865.

12 For significant contributions on Group 2- and 5-based catalysts for hydroamination: a) X. Zhang, T. J. Emge, K. C. Hultzsch, *Angew. Chem., Int. Ed.* **2012**, *51*, 394; b) S. R. Neal, A. Ellern, A. D. Sadow, *J. Organomet. Chem.* **2011**, *696*, 228; c) J. S. Wisey, B. D. Ward, *Chem. Commun*. **2011**, 5449; d) J. S. Wisey, B. D. Ward, *Dalton Trans* **2011**, *40*, 7693; e) P. Horrillo-Martínez, K. C. Hultzsch, *Tetrahedron Lett.* **2009**, *50*, 2054; f) F. Buch, S. *Z.* Harder, *Naturforsch. B* **2008**, *63*, 169; g) B. Liu, T. Roisnel, J.-F. Carpentier, Y. Sarazin *Angew. Chem., Int. Ed.* **2012**, *51*, 4943; h) A. L. Reznichenko, T. J. Emge, S. Audörsch, E. G. Klauber, K. C. Hultzsch, B. Schmidt, *Organometallics* **2011**, *30*, 921; i) K. E. Near, B. M. Chapin, D. C. McAnnally-Linz, A. R. Johnson, *J. Organomet. Chem.* **2011**, *696*, 81; j) M. C. Hansen, C. A. Heusser, T. C. Narayan, K. E. Fong, N. Hara, A. W. Kohn, A. R. Venning, A. L. Rheingold, A. R. Johnson, *Organometallics* **2011**, *30*, 4616; k) F. Zhang, H. Song, G. Zi, Dalton Trans. **2011**, *40*, 1547.

13 L. Luconi, D. M. Lyubov, C. Bianchini, A. Rossin, C. Faggi, G. K. Fukin, A. V. Cherkasov, A. S. Shavyrin, A. A. Trifonov, G. Giambastiani, *Eur. J. Inorg. Chem*. **2010**, 608 and refs cited therein.

14 a) R. D. J. Froese, P. D. Hustad, R. L. Kuhlman, T. T. Wenzel, *J. Am. Chem. Soc.* **2007**, *129*, 7831. d) K. A. Frazier, H. W. Boone, P. C. Vosejpka, J. C. Stevens, (DOW Global Techologies Inc.), U.S. Pat. Appl. Publ. No. US 2004/0220050 A1. e) G. J. Domski, J. B. Edson, I. Keresztes, E. B. Lobkovsky, G. W. Coates, *Chem. Commun.* **2008**, 6137. f) G. J. Domski, E. B. Lobkovsky, G. W. Coates, *Macromolecules*, **2007**, *40*, 3510.

15 No detectable product formation was observed for this transformation with the use of commercially available $Zr^{IV}Bn_4$ and $Hf^{IV}Bn_4$ in a catalytic amount.

16 Although deeper investigations and kinetic studies are needed, this rate similarity for the formation of a five- and six-membered ring seems to be against the general trend for classical stereoelectronically controlled cyclization processes. This observation was previously noted in the field of Group IV-metal catalyzed hydroamination of aminoalkenes, for an example see ref. 9a.

17 For a selection of Group IV metal-catalyzed hydroaminoalkylation, see; a) W. A. Nugent ; D. W. Ovenall ; S. J. Holmes, *Organometallics* **1983**, *2*, 161; b) P. W. Roesky, *Angew. Chem. Int. Ed. Engl*. **2009**, *48*, 4892 ; c) J. A. Bexrud; P. Eisenberger; D. C. Leitch, P. R. Payne; L. L. Schafer *J. Am. Chem. Soc.* **2009,** *131*, 2116; d) R. Kubiak; I. Prochnow; S. Doye *Angew. Chem. Int. Ed. Engl*. **2009**, *48*, 1153; e) R. Kubiak; I. Prochnow; S. Doye *Angew. Chem. Int. Ed.* **2010**, *49*, 2626.

18 For an example of hydroamination side-reactivity using Group IV metal complexes see ref. 10f.

19 The molar fraction of the cyclometallated species in high temperature solutions was spectroscopically determined via ^{1}H-NMR (400 MHz, C_7D_8). For variable temperature VT NMR spectra of $\mathbf{3_{Th(Zr)}/3'_{Th(Zr)}}$, $\mathbf{3_{Th(Hf)}/3'_{Th(Hf)}}$ and $\mathbf{3_{Ph(Zr)}/3'_{Ph(Zr)}}$ see refs. 4.

20 This co-existence had already been noticed for the benzyl analogue $\{C,N,N\}N_2^{Fu}Zr(CH_2Ph)_2$,[4b] and in this case it is reasonably caused by the combination of three factors: (a) disorder present on the dimethylamido ligands; (b) the (very) low temperature data collection and (c) the employ of two-dimensional CCD X-ray detectors.

21 Although VT ^{1}H NMR spectra of $\mathbf{3_{Ph(Zr)}/3'_{Ph(Zr)}}$ showed the presence at room temperature of almost exclusively trisamido form ($\mathbf{3_{Ph(Zr)}}$) its isolation in crystals for X-Ray diffraction analysis required severe and controlled conditions.

22 For a comparison of the catalytic performance of our Zr^{IV} and Hf^{IV}-amido catalysts on the model hydroamination/cyclization reaction of **1** see also refs: 10b,c,g,k,l,m.

23 The molar fraction of the tris- and bis-amido (cyclometallated) species $\mathbf{3_{Th(Zr)}/3'}_{Th(Zr)}$, in toluene at 100°C was found 25/75 mol%.

24 A zero-order dependence of the hydroamination reaction rate on aminoalkene concentration was also observed with some Group IV-metal based catalytic systems, see refs: 10e,x.

25 For rare exceptions of neutral Group-IV catalyzed hydroamination of secondary aminoalkenes, see refs: 10h,k,x.

26 CrysAlisCCD 1.171.31.2 (release 07-07-2006), CrysAlis171 .NET, Oxford Diffraction Ltd.

27 CrysAlis RED 1.171.31.2 (release 07-07-2006), CrysAlis171 .NET, Oxford Diffraction Ltd.

28 A. Altomare, M. C. Burla, M. Camalli, G. L. Cascarano, C. Giacovazzo, A. Guagliardi, A. G. Moliterni, G. Polidori, R. Spagna, *J. Appl. Crystallogr.* **1999**, *32*, 115.

29 Sheldrick, G. M. SHELXL (**1997**).

30 L. J. Farrugia, *J. Appl. Crystallogr.* **1997**, *30*, 565.

4

Group IV Organometallic Compound Based on Dianionic "Pincer" Ligands: Synthesis, Characterization and Catalytic Activity in Intramolecular Hydroamination Reactions

4.1 Abstract

Neutral Zr^{IV} and Hf^{IV} diamido complexes stabilized by unsymmetrical dianionic *N,C,N'* pincer ligands have been prepared through the simplest and convenient direct metal-induced C_{Aryl}–H bond activation. Simple ligand modification has contributed to highlight the non-innocent role played by the donor atom set in the control of the cyclometallation kinetics. The as-prepared bis-amido catalysts have been found to be good candidates for the intramolecular hydroamination/cyclization of primary aminoalkenes. Their ability to promote such a catalytic transformation efficiently (providing in some cases fast and complete substrate conversions already at room temperature) constitutes a remarkable step forward towards catalytic systems capable of operating at relatively low catalyst loading and under milder reaction conditions. Kinetic studies and substrate scope investigations, in conjunction with preliminary DFT calculations on the real systems, have been used to elucidate the effects of the substrate substitution on the catalyst performance, as well as to support the most reliable mechanistic path operative in the hydroamination reaction.

4.2 Introduction

The control of single site catalysts efficiency by tailoring ligand frameworks is an ultimate goal and a challenging matter for many inorganic and organometallic chemists. Indeed, the ability to vary the steric and electronic properties of a given ligand provides a powerful tool to tune reactivity, stability, catalytic performance and other important features of the metal center. On this ground, aryl-based $\{E,C,E\}$-pincer transition metal complexes with anionic tridentate ligands have been widely applied in organic synthesis, organometallic catalysis and other related areas.[1] Their basic structure consists of a central σ-bonded aryl donor group (*C*) capable of forming robust M-C bonds with a given metal center, enforced by the synergic effect of both the coordination of peripheral donor groups (*E*) and the chelating rigid structure of the $\{E,C,E\}$ ligand framework. Such a combination typically results into systems featured by unique stability *vs*. reactivity balance. Synthetically, the simplest method for the construction of these complexes is the direct metal-induced C_{Aryl}–H bond activation, which can be fulfilled by choosing the appropriate neutral or anionic functional donor groups (*E*) at the two side arms of the pincer moiety. Transition metal organometallics featured by either monoanionic or trianionic $\{N,C^-,N;\ N^-,C^-,N^-\}$ pincer-type motifs have been extensively investigated in recent years revealing remarkable and to some extent unique catalytic properties in selected fields of organometallic catalysis.[1] Most importantly, the easy tuning of the N donors hardness has led to the isolation of a large variety of complexes with metals spanning from alkaline earths to those of the Group XII late transition series (Zn−Hg).[1,2] While a relatively large number of *NCN*-pincer-type complexes containing metals of the Groups VIII-X have been reported to date, much less work has been done for the synthesis and characterization of the early-based counterparts.[1a,3] In addition to that, most of the *NCN*-pincer complexes are symmetrical

with two identical N donors[1,4] (because of the easier synthetic protocols that can be adopted for their preparation), while unsymmetrical *NCN'*-systems are rather uncommon and limited (to the best of our knowledge) to an unique example based on palladium derivatives.[1i,5,6,7]

Research in our group has a long-lasting tradition in designing and synthesizing ligand systems that combine hard donating atoms (*N* and *C*) with additional coordinating donor groups.[8] Their combination with a large variety of transition metals and rare-earth metals has provided a number of catalyst precursors for the efficient olefin upgrading[8,9] (oligomerization, polymerization and co-polymerization) and aminoalkene hydroaminations.[10] If developing catalysts capable of operating efficiently under increasing temperature solution processes represents a key issue in catalysis, preparing robust and thermally stable systems is a challenging and highly desirable goal. Starting from our recent interest in Group IV pyridylamido catalysts,[9,10,11] a re-thinking of their molecular framework, while maintaining the same donor atom set, has resulted in a step-forward towards more thermally stable and catalytically active systems (**Figure 4.1**).

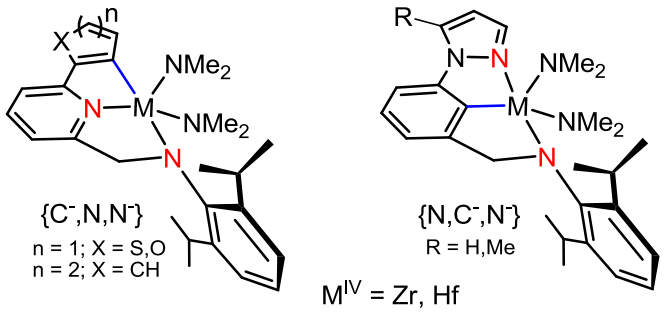

Figure 4.1. Left: Group IV Pyridylamido Complexes of the state of the art.[8,9,10] Right: Group IV *NCN'*-pincer complexes from this work.

Within this work we describe a new set of pincer ligands and their use for preparing non symmetrical Group IV complexes bearing dianionic {*N*,*C*⁻,*N*⁻} pincer fragments.

The donor atom set includes a pyridinic nitrogen from the poor π-acceptor pyrazole ring (as a harder donor site compared to classical pyridine units),[12] in conjunction with other two hard coordination sites form the aryl central unit (*C*⁻) and the amido pendant arm (*N*⁻), respectively. Using $Zr(NMe_2)_4$ and $Hf(NMe_2)_4$ as metal precursors, under mild reaction conditions, mono-substituted $M^{IV}\{\kappa\text{-}N\text{-}L\}(NMe_2)_3$ complexes bearing a "dangling" intact C-H aryl bond are isolated and completely characterized, as a result of a simple transamination reaction. Their prolonged heating in solution leads to the formation of thermally stable $M^{IV}\{\kappa^3\text{-}N,C,N\text{-}L\}(NMe_2)_2$ pincer species through a successive metal-ligand σ-bond metathesis (**Figure 4.1**, right). To the best of our knowledge, this is the first example of thermally stable, unsymmetrical dianionic *N,C,N'* Group IV metal complexes reported in the literature up to date.[13] Simple modifications of the ligand framework result into a remarkable increase of the cyclometallation kinetics, highlighting the non-innocent role played by the pyrazole moiety. The as-synthesized neutral pincer-diamido complexes are found to be good candidates for the intramolecular hydroamination/cyclization of primary aminoalkenes.[10,14,15] In particular, the $Zr^{IV}\{\kappa^3\text{-}N,C,N\text{-}L\}(NMe_2)_2$ derivative has shown a remarkable hydroamination activity with selected aminoalkenes, providing fast and complete substrate conversions already at room temperature. Kinetic measurements and substrate scope investigations, in conjunction with DFT calculations on the whole systems, have been used to elucidate the effects of the substrate substitution on the catalyst performance, as well as to support the most reliable mechanistic path operative for these systems.

4.3 Results and Discussions

4.3.1 Synthesis of N,C,N-pincer ligands H_2L 4 and H_2L^{Me} 12.

Scheme 4.1 illustrates the stepwise procedure developed to prepare the desired pincer ligands in fairly good yields. Since this synthesis work has not been technically trivial (at least for the methylated ligand H_2L^{Me}) and may be useful to design other related molecular architectures, a description of the most relevant reaction steps is given in the following section.

Two different strategies, summarized in **Scheme 4.1**, have been developed to prepare ligands **4** and **12**. Path A was followed to prepare **4** in a three-steps synthesis, while the introduction of a methyl group on the pyrazolyl moiety of **12** required a slightly more complex approach (see Path B on **Scheme 4.1**). According to Path A in **Scheme 4.1**, the 3-bromobenzaldehyde (**1**) was straightforwardly converted into the imine derivative (**2**) under classical condensation conditions in the presence of a catalytic amount of PTSA, using a Dean-Stark apparatus.[16]

The subsequent imine reduction by treatment with $NaCNBH_3/AcOH$[17] resulted into the formation of the corresponding secondary aniline derivative (**3**). A Cu-catalyzed Ullmann coupling between **3** and pyrazole under microwave irradiation/heating[18,19] gave the expected H_2L pincer ligand (**4**) after chromatographic purification in the form of off-white crystals in 68 % isolated yield, over three synthetic steps (see Experimental Section).

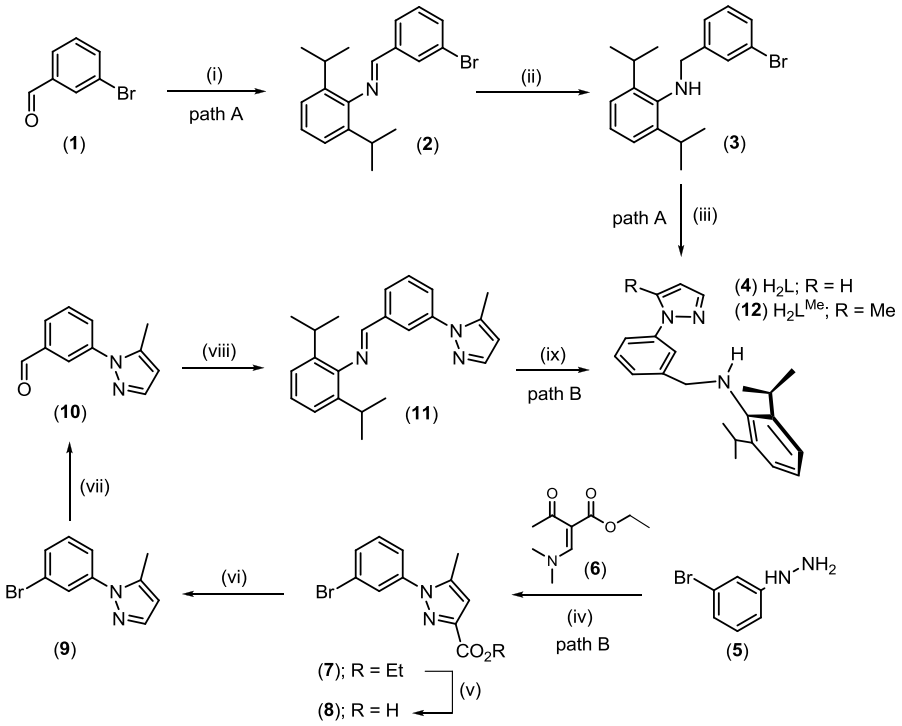

Scheme 4.1. Synthesis of the pincer ligands (**4**) and (**12**). Reaction conditions: Path A {H_2L}, (i) 2,6-diisopropyl aniline, p-TSA *cat*., toluene, reflux; (ii) $NaBH_3CN$, AcOH, THF/MeOH; (iii) Pyrazole, CuI, NMP, MW irrad., 210 °C, 5h, 250W; Path B {H_2L^{Me}}, (iv) (**6**), EtOH, reflux, 2h; (v) LiOH, EtOH/H_2O, 80 °C, 16h; (vi) neat (**8**), 215 °C, 60 h; (vii) HCOONa, DMF, $Pd(PPh_3)_2Cl_2$ *cat*., CO, 110 °C, 1h; (viii) = (i); (ix) = (ii).

Commercially available 3-bromophenyl-hydrazine (**5**) was used as starting material to synthesize the methylated pyrazolyl ligand **12** (H_2L^{Me}). The reaction of the ethyl 2-((dimethylamino)methylene)-methyl-3-oxobutanoate (**6**) with **5** gave the 3,5-disubstituted pyrazolyl (**7**) in fairly good yield.[20] Successive ethylester hydrolysis[21] followed by thermal decarboxylation afforded the desired 1-(3-bromophenyl)-5-methyl-1H-pyrazole (**9**) intermediate. Palladium-catalyzed formylation[22] followed by reductive amination[16,17] gave the desired pincer ligand **12** in 55 % isolated yield, over six synthetic steps (see Experimental Section).

4.3.2 Synthesis and Characterization of Group IV metal/amido complexes from {H_2L} and {H_2L^{Me}} ligands.

The reaction of both ligands with either $Zr^{IV}(NMe_2)_4$ or $Hf^{IV}(NMe_2)_4$ in toluene was followed by ^1H NMR spectroscopy till completeness. Ligand consumption took place already at room temperature with the progressive disappearance of distinctive signals attributed to the uncoordinated system. After 10 hours stirring at room temperature, unique tris-amido species were generated, irrespective of the ligand or metal precursor used (**Scheme 4.2**, path A). All the ^1H and $^{13}C\{^1H\}$ NMR spectra show similar patterns, with large superimposable spectral regions and no traces of low-field quaternary carbons ascribable to the presence of cyclometallated forms.[9,11] While the occurrence of a transamination reaction was evidenced by the disappearance of the typical ligand broad singlet at the aniline moiety, no unequivocal proof of the effective coordination of the pyrazole moiety to the metal center could be found.

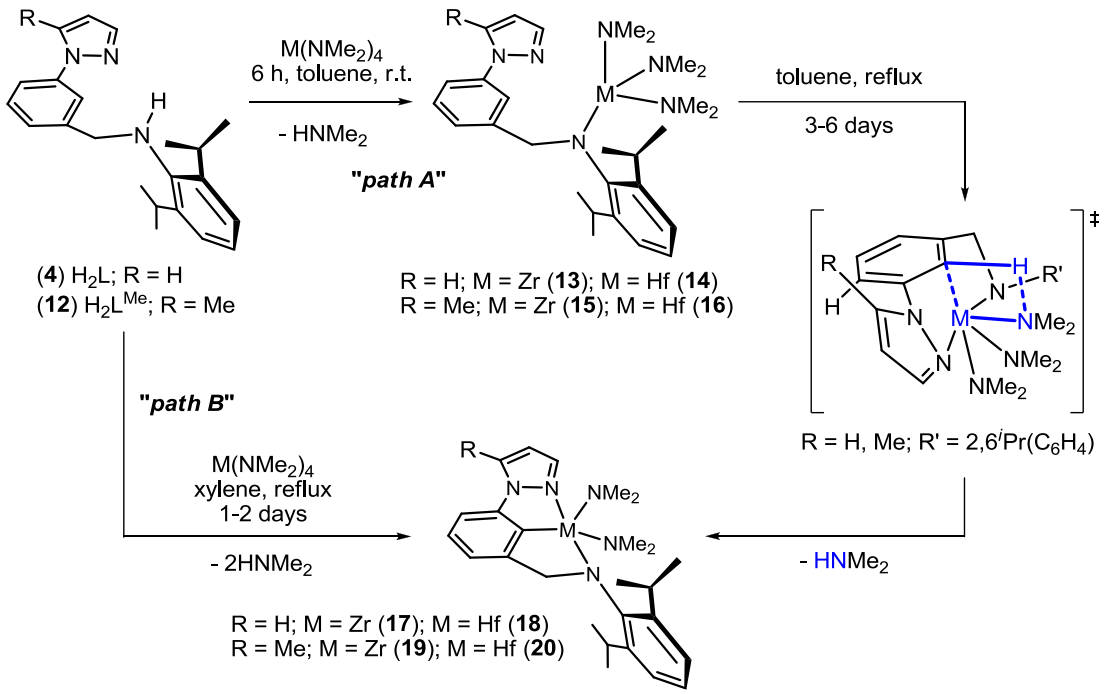

Scheme 4.2. Synthesis of the $M^{IV}\{\kappa\text{-}N\text{-}HL^R\}(NMe_2)_3$ (**13-16**) and $M^{IV}\{\kappa^3\text{-}N,C,N\text{-}L^R\}(NMe_2)_2$ (**17-20**) (M^{IV} = Zr or Hf) complexes.

X-ray diffraction analyses on **13** and **14** have contributed to clarify the metal coordination sphere of all the tris-amido complexes. A perspective view of both complexes is given in **Figures 4.2-4.3**, whereas selected bond lengths and angles are listed in **Table 4.2**. In both systems, the metal coordination environment appears as tetrahedral, with three dimethylamido groups and one amido moiety from the monoanionic $\{N,C,N^-\}$ ligand. The pyrazolyl moieties are tilted with respect to the central aryl unit [torsion angle (θ) C(1)–C(6)–N(2)–N(3): **13**, 30.9(2)°; **14**, -30.4(7)°] and point away from the metal coordination sphere. Such metal environments are likely due to the contribution of steric and electronic factors, the latter being mainly attributed to the reduced basicity of the pyrazole nitrogen[23] if compared to a classical pyridine units. For both compounds, two almost identical molecules are present in the asymmetric unit; they are related to each other through a C_2 pseudo-symmetry axis along the *b* direction. Consequently, the same chemical species is "seen" as two structurally different molecules.[24] **Table 4.1** reports all the main crystal and structural refinement data.

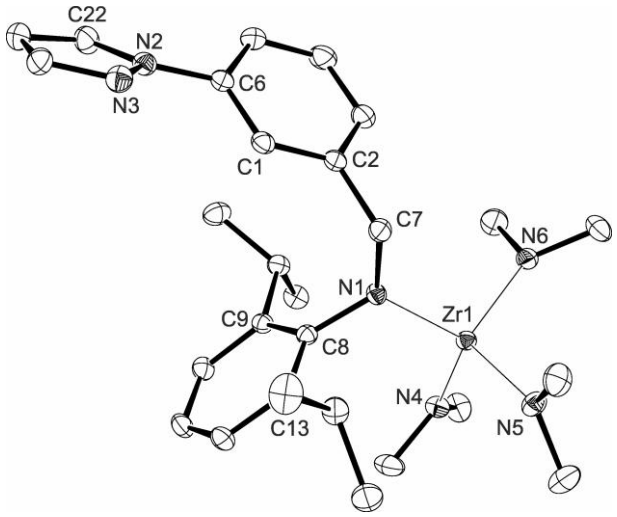

Figure 4.2. Crystal structure of **$Zr^{IV}\{\kappa$-*N*-HL$\}(NMe_2)_3$ (13)**. Thermal ellipsoids are drawn at the 40% probability level. Hydrogen atoms are omitted for clarity.

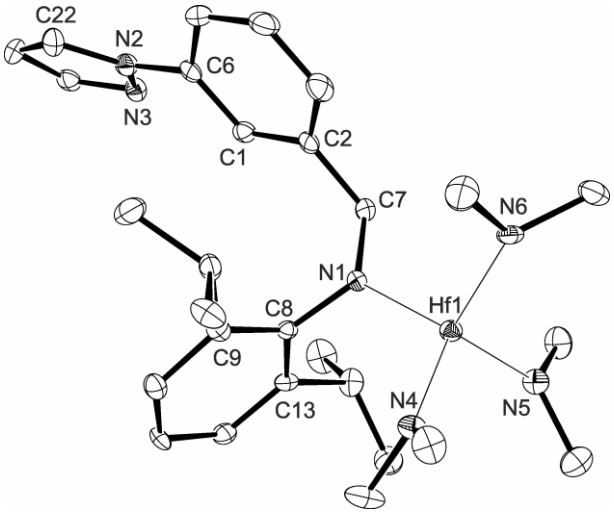

Figure 4.3. Crystal structure of $Hf^{IV}\{\kappa\text{-}N\text{-}HL\}(NMe_2)_3$ **(14)**. Thermal ellipsoids are drawn at the 40% probability level. Hydrogen atoms are omitted for clarity.

A prolonged heating of all the tris-amido species (**13**-**16**) in refluxing toluene provided the bis-amido derivatives (**17**-**20**), as a result of an intramolecular orthometallation/pyrazolyl coordination to the metal center (**Scheme 4.2**, path A). The as-synthesized pentacoordinate complexes are isolated as air- and moisture-sensitive microcrystals and completely characterized by spectroscopic data (see Supporting Information) and X-ray diffraction analyses. ^{1}H and $^{13}C\{^{1}H\}$ NMR patterns indicate that all complexes possess C_s-symmetry in solution. The most relevant ^{1}H NMR data and $^{13}C\{^{1}H\}$ NMR resonances related to the κ^3-coordinated ligand framework fall at lower field when compared to those observed in the tris-amido precursors (**13**-**16**). Notably, the $M\text{-}C^{Ar}$ bonds generated upon intramolecular cyclometallation are unambiguously evidenced by a remarkable resonance shift to lower fields of the aromatic carbon directly bound to the metal centre (174.0, 181.8, 175.5 and 183.1 ppm for **17**, **18**, **19** and **20**, respectively). All complexes are highly soluble in aromatic hydrocarbons, while they are only sparingly soluble in *n*-pentane. Accordingly, suitable crystals for X-ray analyses have been isolated from concentrated and cold *n*-pentane/toluene solutions. ORTEP representations of crystal structures of **17**-**20** are

given in **Figures 4.4-4.7**. **Table 4.1** lists all the main crystal and structural refinement data, while selected bond lengths and angles are summarized in **Table 4.2**.

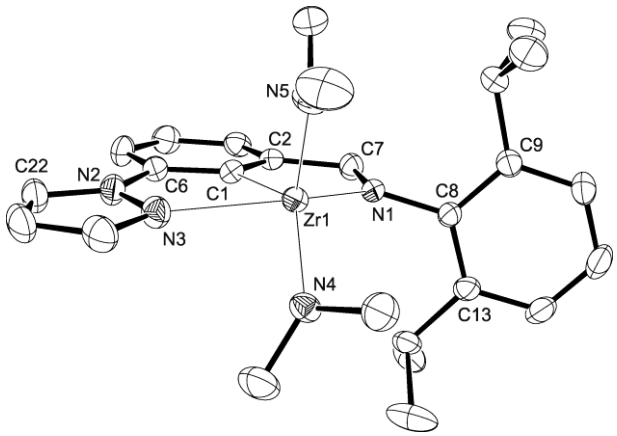

Figure 4.4. Crystal structure of $Zr^{IV}\{\kappa^3$-*N,C,N*-$L\}(NMe_2)_2$ **(17)**. Thermal ellipsoids are drawn at the 40% probability level. Hydrogen atoms are omitted for clarity.

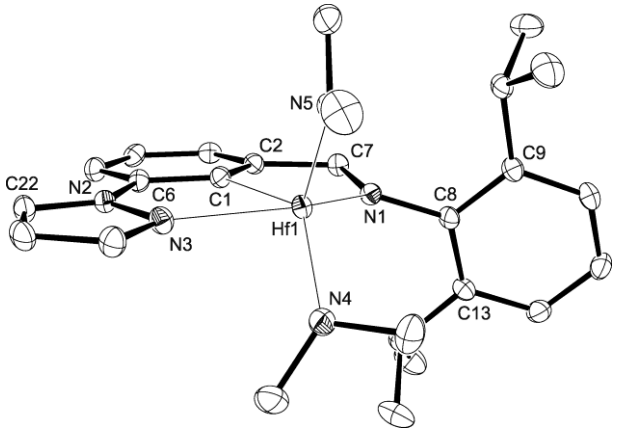

Figure 4.5. Crystal structure of $Hf^{IV}\{\kappa^3$-*N,C,N*-$L\}(NMe_2)_2$ **(18)**. Thermal ellipsoids are drawn at the 40% probability level. Hydrogen atoms and crystallization solvent (pentane) are omitted for clarity.[25]

For all the isolated species, the coordination environment at the metal center consists of two nitrogen atoms and one carbon atom from the dianionic tridentate *{N,C⁻,N⁻}* ligand (κ^3-coordination) and two dimethylamido fragments. All complexes show a distorted square pyramidal coordination geometry with the ligand donor atoms and one dimethylamido group lying equatorially and a residual $–NMe_2$ fragment occupying the axial position.[26]

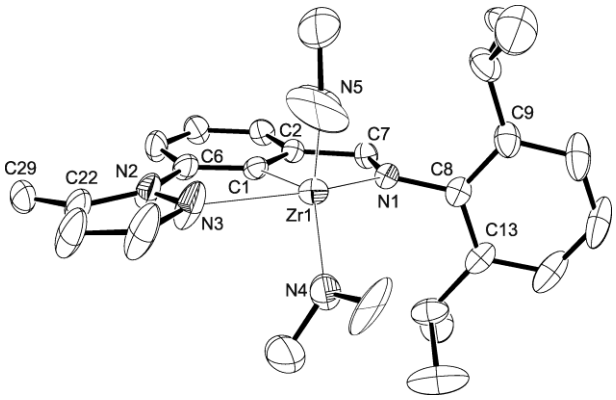

Figure 4.6. Crystal structure of $Zr^{IV}\{\kappa^3$-*N,C,N*-$L^{Me}\}(NMe_2)_2$ **(19)**. Thermal ellipsoids are drawn at the 40% probability level. Hydrogen atoms are omitted for clarity.

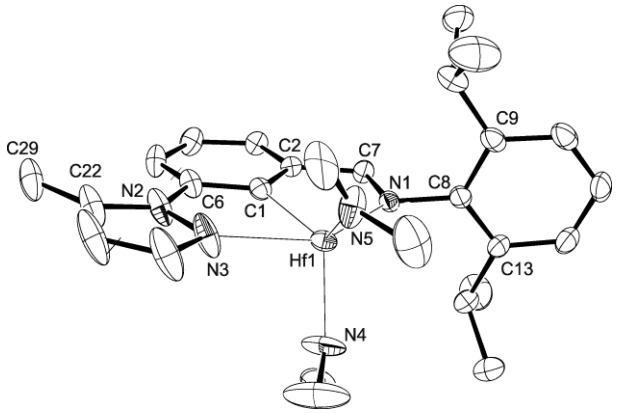

Figure 4.7. Crystal structure of $Hf^{IV}\{\kappa^3$-*N,C,N*-$L^{Me}\}(NMe_2)_2$ **(20)**. Thermal ellipsoids are drawn at the 40% probability level. Hydrogen atoms are omitted for clarity.

The κ^3-coordinated fragments are almost planar, with the pyrazolyl moieties slightly tilted away from the phenyl central core {**17**; θ[C(1)-C(6)-N(2)-N(3)] = -1,3(3)°, **18**; θ[C(1)-C(6)-N(2)-N(3)] = -3.9(4)°, **19**; θ[C(1)-C(6)-N(2)-N(3)] = 4.5(6)°, **20**; θ[C(1)-C(6)-N(2)-N(3)] = -4.2(5)°]. For all complexes, the M-N(1) [**17**: 2.1055(19)Å, **18**: 2.108(3)Å, **19**: 2.127(3)Å, **20**: 2.103(3)Å], M-N(3) [**17**: 2.365(2)Å, **18**: 2.328(3)Å, **19**: 2.308(4)Å, **20**: 2.292(4)Å] and M-C(1) [**17**: 2.238(2)Å, **18**: 2.229(3)Å, **19**: 2.247(4)Å, **20**: 2.220(4)Å] distances fall in a similar range to those measured for related structures.[27,28,29]

The as-synthesized pentacoordinated species showed a remarkable thermal stability, with no apparent decomposition even after six days under reflux in toluene. Noteworthy, precursors bearing a methyl-pyrazole fragment (**15** and **16**) showed faster orthometallation kinetics, with the complete generation of the cyclometallated species up to twice as fast as the counterparts containing plain pyrazole moieties (**Table 4.3**, entries 1 *vs.* 5 and 3 *vs.* 7). For all runs, the reaction course was periodically monitored by sampling the mixture at different times and following the precursor(s) consumption via ^{1}H NMR (inside NMR capillary filled with toluene-d_8) till completeness.

In the attempt of optimizing the reaction conditions and chemical yields, compounds **17**-**20** were prepared in a single step (**Scheme 4.2**, path B) from a ligand/metal precursor mixture, using xylene as solvent. As **Table 4.3** shows, isolated yields were improved for all runs. Additionally, increasing the reaction temperature of about 20°C (from refluxing toluene to refluxing xylene) resulted in a remarkable speed-up of the orthometallation kinetics (**Table 4.3**, even *vs*. odd entries). Compounds **19** and **20** were obtained as pure microcrystalline solids after 24-30 h of reflux, while the non-methylated counterparts (**17**, **20**) required over three fold longer reaction times to reach completeness. Such a result is reasonably due to the simultaneous occurrence of stereo-electronic factors.

In particular, the coordination of the free pyrazole nitrogen of the heteroaromatic moiety to the metal center is assumed to be crucial in assisting the subsequent cyclometallation step. Theoretical simulations carried out on the *real* systems **13** and **15** have shown a significant increase of the dihedral angle θ [C(1)-C(6)-N(2)-N(3)] for the latter optimized conformer (**Figure 4.8**).

Table 4.1. Crystal data and structure refinement for complexes **13**, **14**, **17-20**.

	13	**14**	**17**	**18 · ½C_5H_{12}**	**19**	**20**
CCDC number	897882	897880	897878	897881	897879	897883
Empirical formula	$C_{28}H_{44}N_6Zr$	$C_{28}H_{44}HfN_6$	$C_{26}H_{37}N_5Zr$	$C_{26}H_{37}HfN_5$½C_5H_{12}	$C_{27}H_{39}N_5Zr$	$C_{27}H_{39}HfN_5$
Formula weight	555.91	643.18	510.83	634.17	524.85	612.12
Temperature [K]	120(2)	120(2)	150(2)	120(2)	150(2)	120(2)
Wavelength [Å]	0.71069	0.71069	0.71079	0.71069	0.71069	0.71069
Crystal system, space group	Triclinic, *P -1*	Triclinic, *P -1*	Triclinic, *P -1*	Triclinic, *P -1*	Monoclinic, *P* $2_1/n$	Monoclinic, *P* $2_1/n$
a [Å]	9.292(3)	9.313(4)	8.722(4)	11.202(5)	12.512(2)	12.468(2)
b [Å]	16.458(6)	16.442(6)	9.077(5)	16.516(8)	15.094(2)	14.965(2)
c [Å]	19.607(6)	19.637(9)	18.248(8)	17.669(9)	14.823(3)	14.873(3)
α [°]	77.704(3)	77.568(3)	96.749(4)	64.542(5)	90	90
β [°]	82.857(3)	82.947(4)	101.692(4)	83.354(4)	99.818(18)	99.793(17)
γ [°]	86.290(3)	86.442(3)	109.978(4)	83.026(4)	90	90
V [$Å^3$]	2904.7(16)	2912.2(19)	1301.9(11)	2922.4(18)	2758.4(13)	2734.6(8)
Z, D_c [g m^{-3}]	4, 1.271	4, 1.467	2, 1.303	4, 1.441	4, 1.264	4, 1.487
Absorption coefficient [mm^{-1}]	0.404	3.608	0.444	3.593	0.421	3.837
F(000)	1176	1304	536	1284	1104	1232
Crystal size [mm]	0.04×0.04×0.06	0.01×0.01×0.02	0.01×0.01×0.02	0.01×0.015×0.03	0.05×0.05×0.07	0.03×0.03×0.05
Θ Range for data collection [°]	4.10 ÷ 32.58	4.19 ÷ 29.47	4.16 ÷ 29.37	4.14 ÷ 32.95	4.17 ÷ 29.25	4.18 ÷ 29.35
Limiting indices	$-13 \le h \le 13$ $-24 \le k \le 24$ $-29 \le l \le 29$	$-11 \le h \le 12$ $-22 \le k \le 21$ $-24 \le l \le 27$	$-11 \le h \le 11$ $-12 \le k \le 12$ $-24 \le l \le 24$	$-15 \le h \le 16$ $-24 \le k \le 24$ $-26 \le l \le 26$	$-15 \le h \le 15$ $-18 \le k \le 20$ $-19 \le l \le 19$	$-16 \le h \le 16$ $-19 \le k \le 19$ $-18 \le l \le 19$
Reflections collected/unique	55455/19200	23903/13346	28661/6277	44830/19269	47863/6845	35576/6694
GOF on F^2	0.962	1.000	1.041	1.074	1.041	1.048
Data/restraints/parameters	19200/0/651	13346/0/651	6277/0/297	19269/0/640	6845/0/307	6694/0/307
Final *R* indices [I>2σ(*I*)]	*R*1=0.0371, w*R*2= 0.0833	*R*1=0.0439, w*R*2= 0.0729	*R*1=0.0383, w*R*2= 0.0839	*R*1=0.0372, w*R*2= 0.0802	*R*1= 0.0664, w*R*2= 0.1464	*R*1= 0.0335, w*R*2= 0.0686
R indices (all data)	*R*1=0.0587 w*R*2= 0.0951	*R*1=0.0695, w*R*2= 0.0831	*R*1=0.0513, w*R*2= 0.0905	*R*1=0.0543, w*R*2= 0.0924	*R*1= 0.1054, w*R*2= 0.1691	*R*1= 0.0478, w*R*2= 0.0751
Largest diff. peak and hole [e $Å^{-3}$]	0.572 and –0.784	1.483 and –2.036	0.702 and –0.421	2.905 and –2.140	1.361 and –1.023	1.435 and –1.339

Table 4.2. Selected bond distances (Å) and angles (°) for complexes **13, 14, 17-20**.

	13[*]	**14**[*]	**17**	**18 · ½ C_5H_{12}**[*]	**19**	**20**
M-N(1)	2.0845(16)	2.067(4)	2.1055(19)	2.108(3)	2.127(3)	2.103(3)
M-N(3)	-	-	2.365(2)	2.328(3)	2.308(4)	2.292(4)
M-N(4)	2.0353(16)	2.020(4)	2.045(2)	2.032(3)	2.034(4)	2.013(4)
M-N(5)	2.0452(15)	2.031(4)	2.058(2)	2.040(3)	2.025(5)	2.024(4)
M-N(6)	2.0229(16)	2.015(4)	-	-	-	-
M-C(1)	-	-	2.238(2)	2.229(3)	2.247(4)	2.220(4)
N(2)-N(3)	1.352(2)	1.359(5)	1.367(3)	1.375(4)	1.360(6)	1.358(5)
N(1)-C(7)	1.470(2)	1.482(6)	1.470(3)	1.480(4)	1.461(5)	1.468(5)
N(1)-M-N(3)	-	-	139.75(7)	141.77(10)	140.11(14)	141.35(13)
N(1)-M-N(4)	114.83(6)	113.80(16)	112.12(7)	111.03(12)	111.92(16)	110.94(15)
N(1)-M-N(5)	109.78(6)	110.08(16)	107.45(8)	108.38(11)	108.08(18)	107.96(16)
N(1)-M-N(6)	108.30(6)	108.58(17)	-	-	-	-
N(1)-M-C(1)	-	-	72.86(8)	73.76(12)	72.98(13)	73.84(13)
N(3)-M-C(1)	-	-	68.22(8)	68.95(11)	67.71(15)	68.24(14)
N(4)-M-C(1)	-	-	130.11(8)	128.61(12)	127.34(16)	128.38(15)
N(5)-M-C(1)	-	-	111.93(9)	115.51(13)	114.8(3)	114.9(2)
N(4)-M-N(5)	105.85(6)	106.29(18)	112.99(8)	111.01(13)	112.8(3)	111.9(2)
C(1)-C(2)-C(7)-N(1)	103.21(18)	-103.5(5)	3.2(3)	9.6(4)	-1.4(5)	0.9(5)
C(1)-C(6)-N(2)-N(3)	30.9(2)	-30.4(7)	-1.3(3)	-3.9(4)	4.5(6)	-4.2(5)
C(7)-N(1)-C(8)-C(9)	106.63(17)	-106.3(5)	90.5(2)	-80.7(4)	89.4(4)	89.8(4)
C(29)-C(34)-N(8)-N(9)*	-23.0(2)	-22.4(8)	-	-	-	-
C(27)-C(32)-N(7)-N(8)*	-	-	-	-0.07(6)	-	-

M^{IV} = Zr, Hf; *selected dihedral angles of the second molecule in the asymmetric unit.

Table 4.3. Reaction times and isolated yields for compounds **17**-**20**.

Entry	Precursor(s)	Product	Reaction temperature (°C)	Reaction time (h)[a]	Isolated yield (%)
1[b]	**13**	**17**	110	145	85[e]
2[c]	**4** + $Zr(NMe_2)_4$ [d]	**17**	138	70	87
3[b]	**14**	**18**	110	135	77[f]
4[c]	**4** + $Hf(NMe_2)_4$ [d]	**18**	138	70	79
5[b]	**15**	**19**	110	70	86[g]
6[c]	**12** + $Zr(NMe_2)_4$ [d]	**19**	138	30	86
7[b]	**16**	**20**	110	65	83[h]
8[c]	**12** + $Hf(NMe_2)_4$ [d]	**20**	138	24	85

[a] The reaction course was followed by sampling mixtures at different reaction times till completeness and analyzing the crude products *via* ^{1}H NMR (inside NMR capillary filled with C_7D_8). [b] toluene as solvent. [c] xylene as solvent. [d] (ligand):(metal precursor) ratio: (1):(1.05).[e] 82 % isolated yield over two reaction steps. [f] 72 % isolated yield over two reaction steps. [g] 82 % isolated yield over two reaction steps. [h] 76 % isolated yield over two reaction steps.

The main source of the pyrazolyl-phenyl deviation from co-planarity is the presence of H-H eclipsing interactions between the proton atoms of the methyl group at the pyrazolyl fragment (**15** and **16**) and the hydrogen atom of the phenyl central unit (see **Scheme 4.2** for the supposed TS).

Although for precursors **13** and **14** no evidence of N-pyrazolyl coordination to the metal center before the cyclometallation step can be unambiguously provided, it seems reasonable that only a pyrazolyl assistance can be invoked to justify the increased cyclometallation kinetics for the methylated intermediates **15** and **16**.[30]

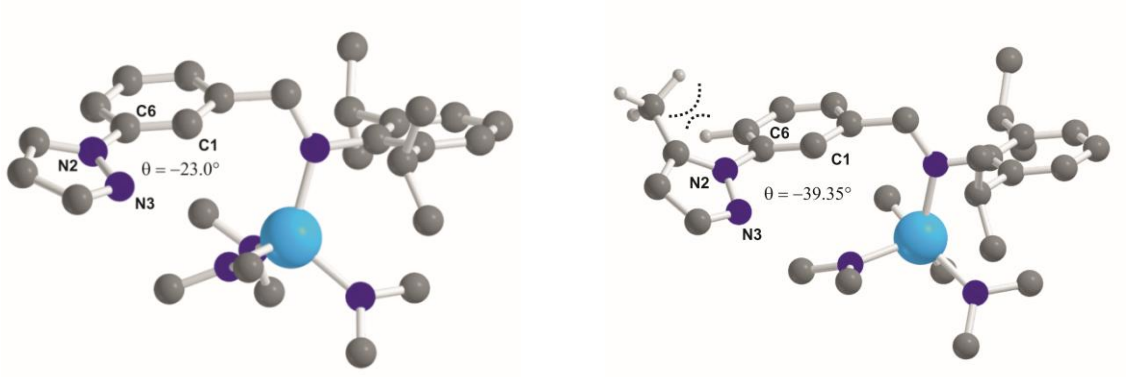

Figure 4.8. Gas-phase optimized structures (DFT//M06) of compounds **13** and **15**. Hydrogen atoms not relevant for the discussion omitted for clarity. Atom color code: gray, C; white, H; blue, N; light blue, Zr. The optimized θ [C(1)-C(6)-N(2)-N(3)] dihedral angles between the phenyl and the pyrazole rings are also reported.

Such an aspect, in combination with the coordination ability of the pyrazolyl moiety, represents a fundamental prerequisite to succeed in the central aryl C-H bond activation where other related synthetic approaches failed.[3d]

4.3.3 Catalytic performance of novel amido complexes in the intramolecular hydroamination of aminoalkenes.

All the isolated amido compounds were tested as catalysts for the intramolecular hydroamination/cyclization of primary and secondary amines tethered to monosubstituted alkenes (**Scheme 4.3**, **Table 4.4**).

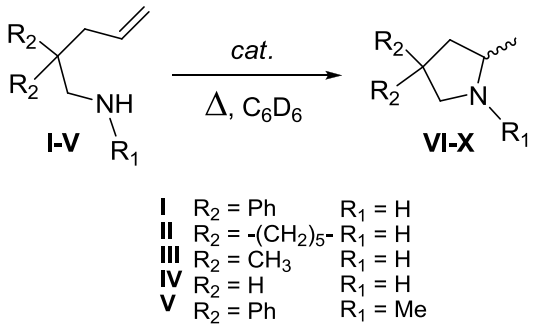

Scheme 4.3.Intramolecular hydroamination of primary and secondary aminoalkenes.

The catalytic tests were conducted in a glove-box, under inert atmosphere using a two-necked round flask equipped with a magnetic stirrer-bar and a septum for the progressive substrate addition *via* syringe. Benzene (unless otherwise stated) was used as reaction solvent and the catalyst content was fixed to 5 mol% for each run. Finally, the reaction temperature was systematically varied from room temperature (22 °C) to solvent reflux. As shown in **Table 4.4**, neutral systems **17-20** were found to be active catalysts for the intramolecular hydroamination reaction of model primary aminoalkenes providing, for selected issues, relatively fast and complete substrate conversions already at room temperature (**Table 4.4**, entries 2 and 5).

Notably, a dramatic Thorpe-Ingold effect on the kinetic of the intramolecular hydroamination reaction is apparent (entries 1 *vs.* 7 *vs.* 10). In particular, the diphenyl-substituted precursor **I** appears as the most suitable substrate capable of converting into the corresponding cyclization product **VI** quantitatively (entries 2 and 9), within 5 h under mild conditions. This result is certainly remarkable, because only a few examples based on Group IV amido complexes reported in the literature refer to the complete cyclization of **I** under these mild reaction conditions (reaction temperature and catalyst loading).[15k,l,x,31]

Table 4.4. Intramolecular hydroamination of primary and secondary aminoalkenes catalyzed by neutral amido complexes **13**, **14**, **17**-**20**.[a]

Entry	Catalyst	Substrate	Product	T (°C)	Time (h)	Conv. (%)[b]
1	**17**	**I**	**VI**	r.t.	3	96
2	**17**	**I**	**VI**	r.t.	5	>99
3	**17**	**I**	**VI**	50	1	98
4	**17**	**I**	**VI**	80	0,5	>99
5	**19**	**I**	**VI**	r.t.	5	>99
6	**19**	**I**	**VI**	50	1	96
7	**17**	**II**	**VII**	r.t.	48	40
8	**17**	**II**	**VII**	80	36	87
9[c]	**17**	**II**	**VII**	110	1,5	95
10	**17**	**III**	**VIII**	r.t.	48	9
11	**17**	**III**	**VIII**	80	36	45
12[c]	**17**	**III**	**VIII**	110	4	78
13[c]	**17**	**IV**	**IX**	110	10	31
14	**17**	**V**	**X**	80	96	--[d]
15	**13**	**I**	**VI**	r.t.	3	12
16	**13**	**I**	**VI**	80	1	6
17	**18**	**I**	**VI**	r.t.	3	15
18	**18**	**I**	**VI**	50	1	91
19	**18**	**I**	**VI**	80	0.75	>99
20	**20**	**I**	**VI**	r.t.	3	17
21	**20**	**I**	**VI**	50	1	87
22	**18**	**II**	**VII**	80	36	67
23	**18**	**III**	**VIII**	80	36	38
24[c]	**18**	**III**	**VIII**	110	6	66
25[c]	**18**	**IV**	**IX**	110	10	14
26	**18**	**V**	**X**	80	96	--[d]
27	**14**	**I**	**VI**	r.t.	3	<1
28	**14**	**I**	**VI**	80	1	2

[a] Reaction conditions: substrate: 0.63 mmol, catalyst: 5 mol%, solvent: benzene (2 mL). [b] Determined by *in-situ* ^{1}H NMR spectroscopy using ferrocene as internal standard. [c] Toluene (2 mL) as solvent. [d] Not appreciable amount of cyclization product observed.

With catalyst **17**, only geminally substituted substrates (**I**-**III**) undergo intramolecular hydroamination at room temperature with appreciable conversions

(entries 1, 7 and 10). On the contrary, prolonged heating in conjunction with higher reaction temperatures (refluxing toluene was used instead of benzene for selected issues) are required to give appreciable cyclization yield in the case of the unsubstituted substrate **IV** (entries 13 and 25).

While ligand modifications (**17** *vs.* **19** and **18** *vs.* **20**) did not show any appreciable difference in the catalyst's activity (entries 1 and 3 *vs.* 5 and 6; 17 and 18 *vs.* 20 and 21), experiments focused on comparing Zr^{IV} *vs*. Hf^{IV} analogues (**17** *vs.* **18**) highlighted the higher catalytic performance of the former. Indeed, an over six fold higher conversion of **I** was obtained with **17** instead of **18** (entries 1 *vs.* 17). Notably, increasing the reaction temperature translates into a significant reduction of the catalysts activity gap (entries 2-4 *vs.* 17-19). Accordingly, **17** and **18** showed remarkable and almost similar activities for the complete conversion of **I** into **VI** when the reaction temperature was raised to reflux of solvent (entries 4 *vs*. 19). Optimized reaction conditions are reported for the cyclization of the less sterically bulky aminoalkene precursors (**II**-**IV**). As **Table 4.4** shows, the highest the reaction temperature the highest the substrate cyclization and the lowest the reaction time (entries 7-9, 10-12, 17-19). Noteworthy, increasing the reaction temperature (from refluxing benzene to refluxing toluene) resulted in a dramatic decrease of the reaction time, together with significantly higher substrate conversions (entries 8 *vs*. 9, 11 *vs*. 12 and 23 *vs*. 24). For all the investigated runs, Zr^{IV} precursors displayed higher catalytic performances compared to Hf^{IV} ones, under similar reaction conditions. Aimed at highlighting the ligand's acceleration effects in hydroamination reactions, the catalyst performance of **17** and **18** were compared with those of tris-amido precursors **13** and **14**. As it can be appreciated from **Table 4.4**, **13** and **14** present a significantly reduced catalytic activity compared with that of the related cyclometallated bis-amido counterparts **17** and **18** (entries 1 *vs*. 15 and 17 *vs*.

27). Additionally, high reaction temperatures result in lowest substrate conversions probably due to a more rapid metal/ligand displacement *via* a substrate-induced transamination reaction (entries 4 *vs*. 16 and 19 *vs*. 28). Overall, these data highlight the outstanding substrate dependence on the catalytic performance of these novel pincer-type complexes. If it is generally accepted that reducing the substrate steric demand translates into reduced cyclization efficiencies (**IV** << **III** < **II** << **I**), such a trend is typically less marked than for the outcomes presented here. While **I** is rapidly and quantitatively transformed by **17** into the corresponding cyclization product **VI** at room temperature, either moderate conversions (for **II** and **III**) or no conversion at all (for **IV**) are given for the other substrates (*vide infra*) under similar conditions (**Table 4.4**, entries 1 *vs*. 7 *vs*. 10).

Finally, hydroamination of the secondary aminoalkene **V** does not take place, with both **17** and **18**, even after prolonged heating (**Table 4.4**, entries 14 and 26), which is in agreement with most of the previous studies on neutral Group IV metal complexes in hydroamination reaction.[15,32] This observation also supports the hypothesis of imido species as intermediates in the catalytic cycle[14,15] whose one most reliable representation is provided in **Scheme 4.4**.

In the attempt of shedding light on the marked substrate-dependence of catalyst **17** and looking for possible and favorable substrate-complex interactions capable to justify the observed outcomes (**Table 4.4**, entries 1 *vs*. 10), preliminary DFT calculations on the real systems **17**/**I** and **17**/**III** have been carried out. In both cases, simulations have been done on the whole systems assuming the formation of "imido species" (**Scheme 4.4**) as the most reliable mechanistic path (see also Experimental section).[14,15,33]

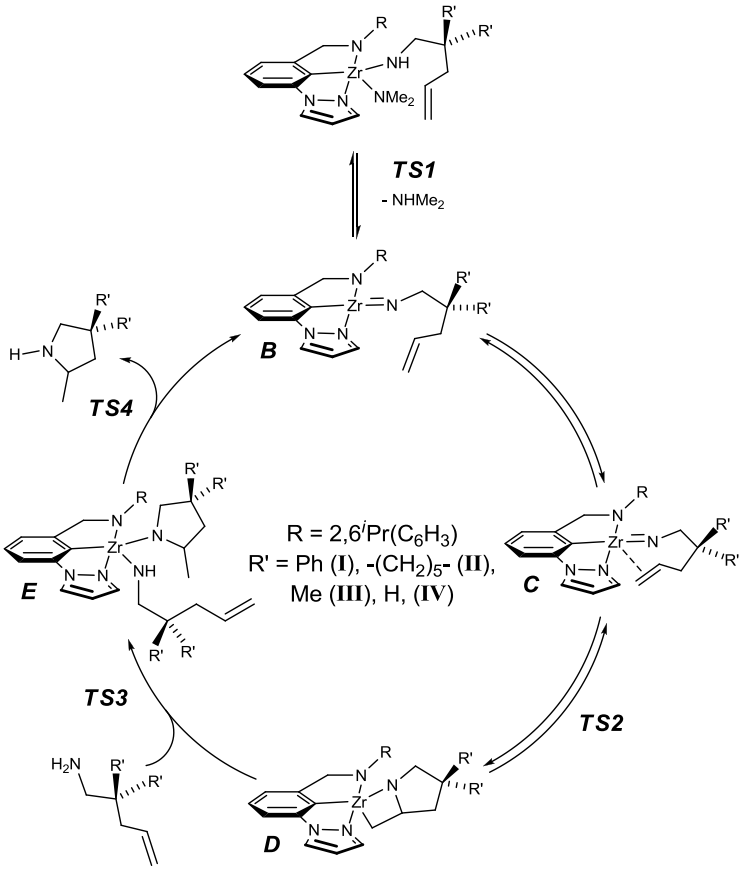

Scheme 4.4. [2+2]-cycloaddition mechanism for the intramolecular hydroamination of primary aminoalkenes catalyzed by neutral bisamido Group IV metal complexes.

Accordingly, the relative internal energy profiles ($\Delta E = \Delta H$) for the two processes[34] have been calculated and the energy values for intermediates and transition states are outlined in **Figure 4.9**. In both cases, the energy profiles show similar trends, the formation of the imido species (TS1 and TS4) being the highest endothermic steps (TS1: +33.4 and +35.2 kcal/mol for **I** and **III**, respectively; TS4: +37.3 and +38.1 kcal/mol for **I** and **III**, respectively).[35]

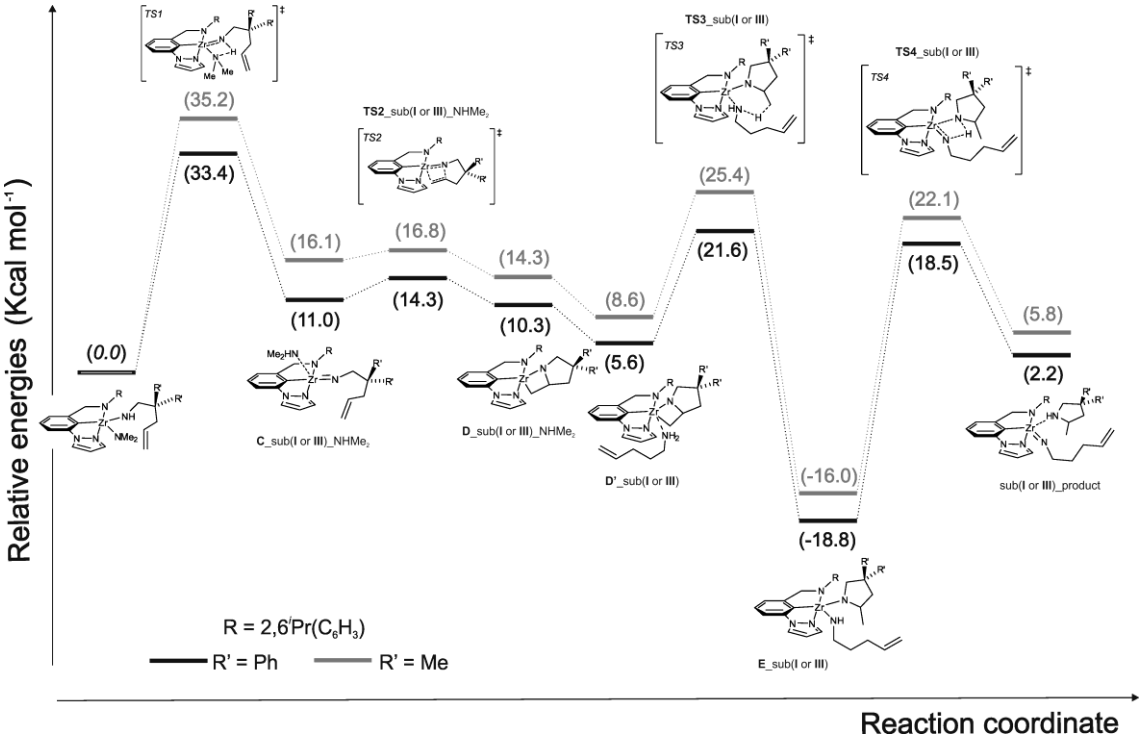

Figure 4.9. Calculated energetic profiles ($\Delta H = \Delta E$) for the hydroamination/cyclization of **I** and **III** catalyzed by **17**. Imido mechanism (**Scheme 4.4**) is assumed as the most realistic for the catalytic systems employed in the present study. Labeling refers to **Scheme 4.4** and provides labels to each intermediate and TS.

The subsequent [2+2]-cycloaddition (**Figure 4.10a**) leads to the metalla-azacycle D intermediate (**Scheme 4.4**) through a fully reversible process for both aminoalkene precursors (3.3 kcal/mol and 0.7 kcal/mol for **I** and **III**, respectively). The protonolysis step (**Figure 4.10b**) takes place after the approaching of a second molecule of substrate and it is considered an irreversible process, shifting the overall reaction to the products. Finally, an additional protonolysis takes place, leading to the cyclization product with the re-generation of a novel imido species capable to undergo further catalytic cycles (**Figure 4.10c**). It is worthy of note that all transition states associated with protonolysis events (and potentially eligible as rate limiting steps) are in line with the cyclization kinetics experimentally measured for precursor **I** and **III**, respectively [$\Delta(\Delta E^{\#})$ differences equal to 0.8 kcal/mol are calculated on both TS3 and TS4].

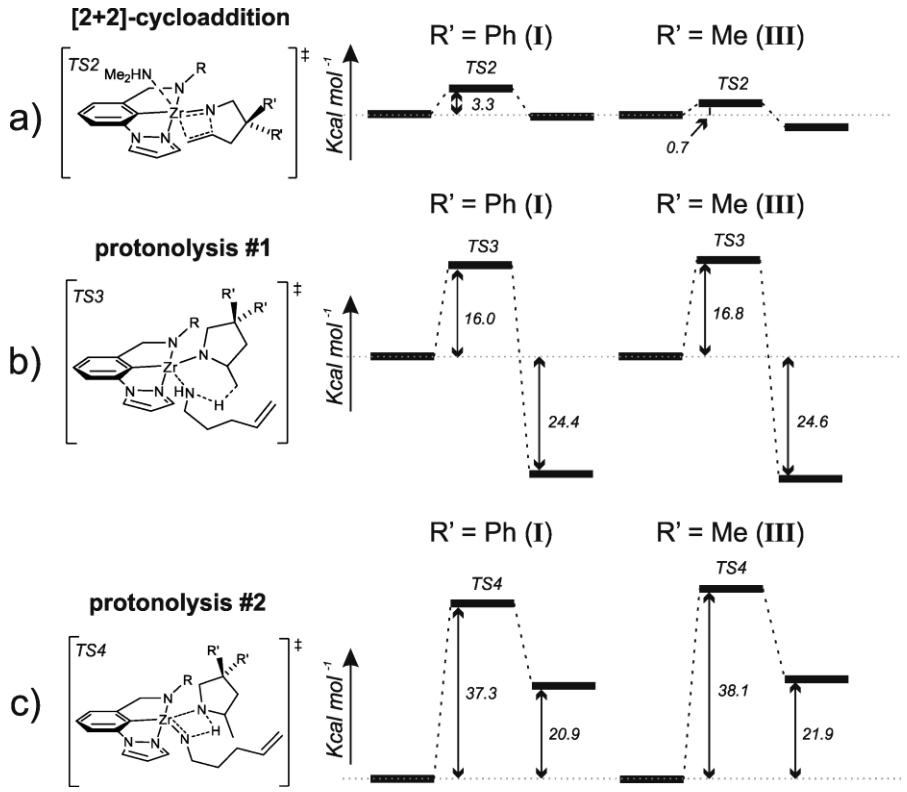

Figure 4.10. Calculated energetic profiles ($\Delta E = \Delta H$) for relevant transition states in the hydroamination/cyclization of **I** and **III** catalyzed by **17**. Imido mechanism (**Scheme 4.4**) is assumed as the most realistic for the catalytic systems employed in the present study. Labeling refers to **Scheme 4.4**.[35]

Finally, negligible differences are observed in the optimized geometries of all intermediates and transition states associated with both profiles. All these data taken together lead us to conclude that any preferential substrate-complex interaction can be reasonably ruled out. It seems therefore apparent that the remarkable acceleration measured in the hydroamination of substrate **I** is exclusively ascribable to a *gem*-effect originated by the dangling phenyl groups.[15o]

Kinetic investigations on **17** and **18** confirmed the first order kinetics in substrate conversion, consistent with the protonolysis event being the rate limiting step of the process.[15a] **Figure 4.11** presents kinetic profiles as measured at room temperature (only for **17** - left) and at 80 °C (**17** and **18** - right), respectively. A comparison of catalyst's half-lives [t½] is provided for both systems under optimized reaction conditions (80 °C

– **Table 4.4**, entries 4 and 19). Measured [t½] values are found to be 4.76 and 21.5 min, respectively (**Figure 4.11** – right).[36]

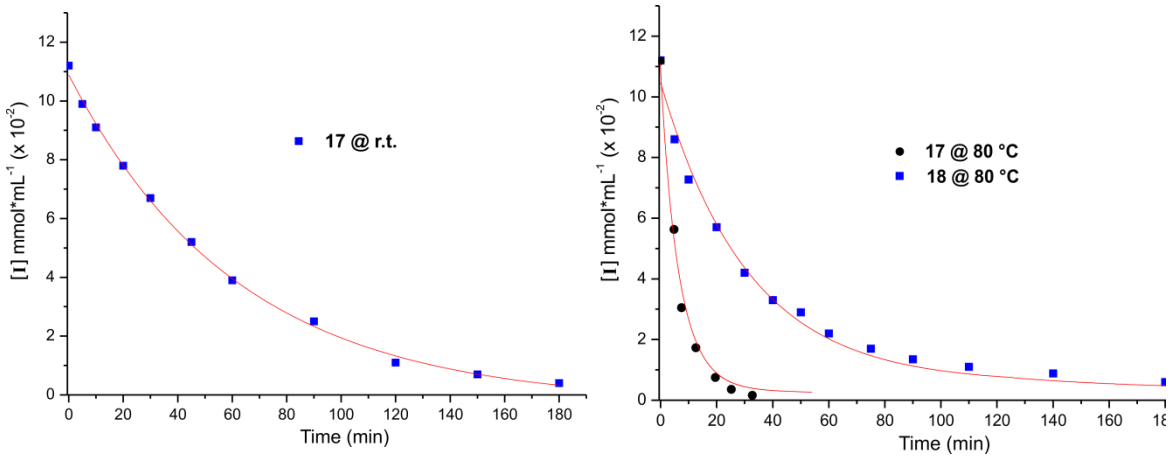

Figure 4.11. Plot of first-order substrate (**I**) conversion using 5 mol% of **17** at r.t. (left) and 5 mol% of **17** and **18** at 80°C (right). Catalysts half-lives have been determined for runs at 80 °C (right).

In addition, **Figure 4.12** shows the normalized Ln[substrate] *vs*. time plots measured for three different concentrations of the most active system **17**, while figure's inset accounts for the linearity of the observed K_{obs} values *vs*. catalyst concentration. All these data taken together are in line with first order in catalyst and substrate concentration as previously reported for other neutral zirconium systems.[15]

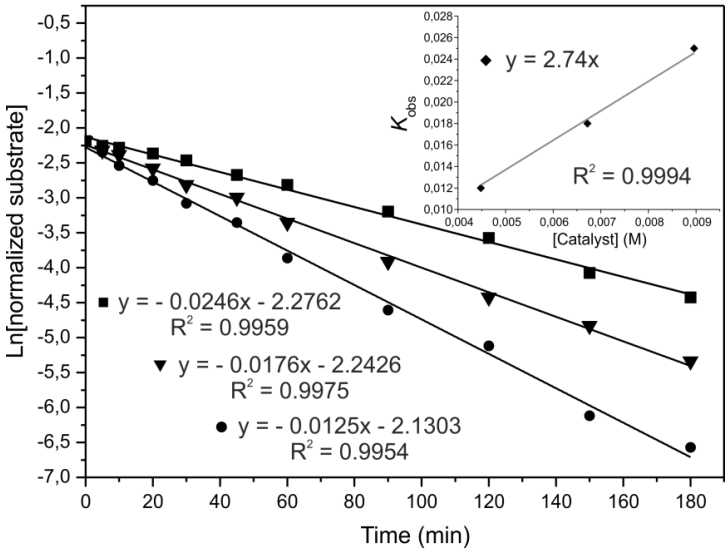

Figure 4.12. Plot of first-order catalyst dependence for intramolecular hydroamination of **I** at different concentrations of **17** (■ = 4 mol%; ▼ = 6 mol%; ● = 8 mol%). Inset refers to the linearity of the observed K values *vs*. catalyst concentration.

4.4 Conclusions

Overall, this study provides a convenient way to the preparation of unsymmetrical dianionic *N,C,N'* Group IV pincer complexes and proves their successful application in the intramolecular hydroamination reaction of primary aminoalkenes. A proper choice of both ligand donor atom set and substituents led to an easier aryl C-H bond activation (*via* intramolecular σ-bond metathesis), where other recent and related synthetic approaches failed.[3d] A non-innocent role of the N-coordinating pyrazolyl moiety was finally invoked to rationalize the cyclometallation kintetic gap measured in the presence of H_2L and H_2L^{Me} ligands, respectively. To the best of our knowledge, this class of compounds represents the first example of thermally stable, unsymmetrical Group-IV metal complexes stabilized by dianionic *N,C,N'* pincer ligands reported in the literature up to date. In addition, only a few classes of Group IV pincer-type complexes are reported as active systems in hydroamination reactions, all of them typically requiring severe reaction conditions.[37] The ability of our neutral amido systems to promote the intramolecular hydroamination reaction of model primary aminoalkenes (providing, for selected substrates, fast and complete conversions already at room temperature) constitutes a remarkable step forward towards catalytic systems capable of operating at relatively low catalyst's loadings (5 mol%) and under milder (time and temperature) reaction conditions. Preliminary kinetic investigations and substrate scope studies, in conjunction with DFT calculations on the real systems, have been used to elucidate the effects of the substrate substitution on the catalyst performance, as well as to support the most reliable mechanistic path operative in the hydroamination reaction.

All these findings taken together pave the way to the future development of original *N,C,N'* pincer-type early-transition metal complexes based on C_1 symmetric ligands for the investigation of stereoselective hydroamination processes.

4.5 Experimental Section

General Considerations and materials characterization. All air- and/or moisture-sensitive reactions were performed under inert atmosphere in flame-dried flasks using standard Schlenk-type techniques or in a dry-box filled with nitrogen. Anhydrous toluene, THF and Et_2O were obtained by means of an MBraun Solvent Purification Systems, while CH_2Cl_2 and MeOH were distilled over CaH_2 and Mg, respectively. Unless otherwise stated, all the other reagents and solvents were used as purchased from commercial suppliers. (3-bromophenyl)hydrazine (**5**) was straightforwardly obtained from crystalline (3-bromophenyl)hydrazine·hydrochloride upon washing it with a NaOH water solution (30 % w/w) and successive extraction in benzene.[38] Ethyl 2-((dimethylamino)methylene)-3-oxobutanoate (**6**) was prepared in a multigram scale according to literature procedures.[20] Benzene-d_6 and toluene-d_8 were dried over sodium/benzophenone ketyl and condensed *in vacuo* over activated 4Å molecular sieves prior to use. 1D (^{1}H and ^{13}C{^{1}H}) and 2D (COSY H,H, HETCOR H,C) NMR spectra of all organometallic species were obtained on either a Bruker Avance DRX-400 spectrometer (400.13 and 100.61 MHz for ^{1}H and ^{13}C, respectively) or a Bruker Avance 300 MHz instrument (300.13 and 75.47 MHz for ^{1}H and ^{13}C, respectively). Chemical shifts are reported in ppm (δ) relative to TMS, referenced to the chemical shifts of residual solvent resonances (^{1}H and ^{13}C). The multiplicities of the ^{13}C{^{1}H} NMR spectra were determined on the basis of the ^{13}C{^{1}H} JMOD sequence and quoted as: CH_3, CH_2, CH and C for primary, secondary, tertiary and quaternary carbon atoms, respectively. The C, H, N, S elemental analyses were made at ICCOM-CNR using a Thermo FlashEA 1112 Series CHNS-O elemental analyzer with an accepted tolerance of ± 0.4 units on carbon (C), hydrogen (H) and nitrogen (N).

X-ray data measurements. Single crystal X-Ray data were collected at low temperature (100 or 120 K) on an Oxford Diffraction XCALIBUR 3 diffractometer equipped with a CCD area detector using Mo Kα radiation (λ = 0.7107 Å). The program used for the data collection was CrysAlis CCD 1.171.[39] Data reduction was carried out with the program CrysAlis RED 1.171[40] and the absorption correction was applied with the program ABSPACK 1.17. Direct methods implemented in Sir97[41] were used to solve the structures and the refinements were performed by full-matrix least-squares against F^2 implemented in SHELX97.[42] All the non-hydrogen atoms were refined anisotropically while the hydrogen atoms were fixed in calculated positions and refined isotropically with the thermal factor depending on the one of the atom to which they are bound (riding model). Disorder on the $-NMe_2$ substituents in **19** and **20** was not explicitely treated, since this did not lead to a significant improvement of the structural final R factors. Molecular plots were produced by the program ORTEP3.[43] GC analyses of the reaction products were performed on a Shimadzu GC-17 gas chromatograph equipped with a flame ionization detector and a Supelco SPB-1 fused silica capillary column (30 m length, 0.25 mm i.d., 0.25 μm film thickness) or a HP-PLOT Al_2O_3 KCl column (50 m length, 0.53 mm i.d., 15 μm film thickness). The GC/MS analyses were performed on a Shimadzu QP2010S apparatus equipped with a column identical with that used for GC analysis.

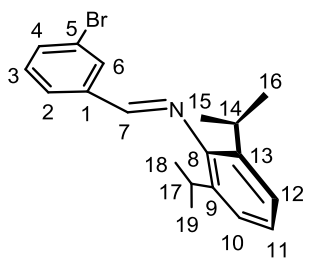

Synthesis of N-(3-bromobenzylidene)-2,6-diisopropylaniline (2) A solution of 3-bromobenzaldehyde (0.945 mL, 8.1 mmol), 2.29 mL (12.15 mmol) of 2,6-diisopropylaniline, and 0.230 g (1.21 mmol) of 4-toluensulfonic acid in 40 mL of distilled toluene was maintained at reflux of the solvent for 12 h in a Dean-Stark apparatus. The mixture was allowed to cool to room

temperature and then treated with 15 mL of 0.5 M aqueous NaOH solution. The formed layers were separated and the aqueous phase was extracted with AcOEt (3 x 15 mL). The combined organic extracts were dried over Na_2SO_4. After removal of the solvent under reduced pressure, crude yellow oil was obtained. The pure N-(3-bromobenzylidene)-2,6-diisopropylaniline was finally precipitated by cold hexane (-20 °C) and the yellow crystals were separated off by filtration. The collected crystals were washed with cold hexane and dried in vacuum to constant weight. Yield: 2.200 g, 78.8 %. ^{1}H NMR (300 MHz, CD_2Cl_2, 293K): δ 1.19 (d, $^3J_{HH}$ = 6.9 Hz, 12H, CH(CH_3), $H^{15,16,18,19}$), 2.97 (sept, $^3J_{HH}$ = 6.9 Hz, 2H, CH(CH_3), $H^{14,17}$), 7.11-7.21 (3H, CH Ar, $H^{10,11,12}$), 7.43 (m, 1H, CH Ar, H^3), 7.70 (m, 1H, CH , H^4), 7.86 (m, 1H, CH Ar, H^2), 8.16-8.18 (2H, $H^{6,7}$). ^{13}C{^{1}H} NMR (75 MHz, CD_2Cl_2, 293 K): δ 23.2 (CH(CH_3)$_2$, $C^{15,16,18,19}$), 27.9 ($CH(CH_3)_2$, $C^{14,17}$), 122.9 (C^5), 123.0 ($C^{10,12}$), 124.2 (C^{11}), 127.4 (C^2), 130.4 (C^3), 130.9 (C^6), 134.2 (C^4), 137.4 ($C^{9,13}$), 138.0 (C^8), 148.8 (C^1), 160.5 (C^7). Anal. Calcd (%) for $C_{19}H_{22}BrN$ (344.29): C 66.28, H 6.44, N 4.07; found C 66.15, H 6.38, N 4.33

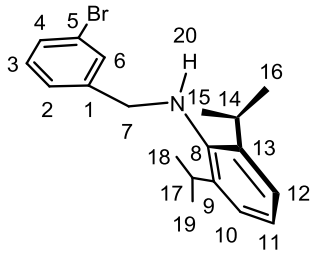

Synthesis of N-(3-bromobenzyl)-2,6-diisopropylaniline (3). To a cooled (0 °C) solution of **2** (2.00 g, 5.80 mmol), in a 1:1 mixture of dry and degassed MeOH (18 mL) and THF (18 mL), $NaBH_3CN$ (0.54 g, 8.71 mmol) and acetic acid (0.54 mL, 8.71 mmol) were added in sequence under nitrogen atmosphere. The reaction temperature was raised to 50 °C and the resulting mixture was stirred at the same temperature for 2h. Afterwards, the reaction was allowed to cool to room temperature and a 1:1 mixture of saturated Na_2CO_3 and water (40 mL) was added in one portion. The organic phase was separated and the aqueous layer was extracted with AcOEt (3 x 20 mL). The collected organic layers were dried over Na_2SO_4 and the residue was

purified by flash chromatography (silica gel; petroleum ether : AcOEt = 95 : 5) to give the pure product **3** as white crystals. Yield: 1.95 g, 97 %. ^{1}H NMR (300 MHz, CD_2Cl_2, 293K): δ 1.26 (d, $^{3}J_{HH}$ = 6.8 Hz, 12H, CH(C*H*$_3$), H^{15,16,18,19}), 3.21 (bs, 1H, N*H*, H^{20}), 3.32 (sept, $^{3}J_{HH}$ = 6.8 Hz, 2H, C*H*(CH$_3$), H^{14,17}), 4.05 (s, 1H, C*H*$_2$NH, H^{7}), 7.09-7.18 (3H, C*H* Ar, H^{10,11,12}), 7.29 (m, 1H, C*H* Ar, H^{3}), 7.41 (m, 1H, C*H* , H^{2}), 7.48 (m, 1H, C*H* Ar, H^{4}), 7.65 (m, 1H, C*H* Ar, H^{6}). ^{13}C{^{1}H} NMR (75 MHz, CD_2Cl_2, 293 K): δ 24.0 (CH(*C*H$_3$)$_2$, C^{15,16,18,19}), 27.6 (*C*H(CH$_3$)$_2$, C^{14,17}), 55.3 (C^{7}), 122.4 (C^{5}), 123.5 (C^{10,12}), 124.2 (C^{11}), 126.5 (C^{2}), 130.1 (C^{3}), 130.2 (C^{4}), 130.7 (C^{6}), 142.5 (C^{1}), 142.7 (C^{8}), 143.0 (C^{9,13}). Anal. Calcd (%) for $C_{19}H_{24}BrN$ (346.30): C 65.90, H 6.99, N 4.04; found C 65.85, H 6.94, N 4.16.

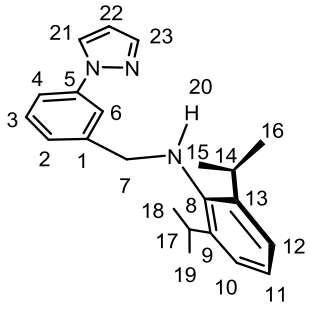

Synthesis of N-(3-(1H-pyrazol-1-yl)benzyl)-2,6-diisopropylaniline {H_2L} (4). To a solution of **3** (0.400 mL, 1.15 mmol) in N-methylpyrrolidinone (7 mL) were added potassium carbonate (0.32 g, 2.30 mmol), Cu^{I}I (0.022 g, 0.11 mmol) and pyrazole (0.082 g, 1.21 mmol). The mixture was heated under N_2 atmosphere at 210 °C for 5 h using microwaves on a CEM Discover apparatus operating at 250 W. Afterwards, the reaction mixture was cooled to room temperature and filtered over a celite® pad using AcOEt as washing solvent. The filtrate was evaporated under vacuum and the residue was purified by flash chromatography (silica gel; petroleum ether : AcOEt = 92 : 8) to give the final product **4** as white-off crystals. Yield: 0.340 g, 88.5 %. ^{1}H NMR (300 MHz, CD_2Cl_2, 293K): δ 1.37 (d, $^{3}J_{HH}$ = 6.8 Hz, 12H, CH(C*H*$_3$), H^{15,16,18,19}), 3.44-3.53 (2H, H^{14,17,20}), 4.25 (s, 1H, C*H*$_2$NH, H^{7}), 6.57 (m, 1H, C*H* Ar, H^{22}), 7.19-7.29 (3H, C*H* Ar, H^{10,11,12}), 7.48-7.57 (2H, C*H* Ar, H^{3,2}), 7.76 (m, 1H, C*H* Ar, H^{4}), 7.83 (m, 1H, C*H* Ar, H^{23}), 7.97 (m, 1H, C*H* Ar, H^{6}), 8.08 (d, $^{3}J_{HH}$ = 2.4 Hz, 1H, C*H* Ar, H^{21}) . ^{13}C{^{1}H} NMR (75 MHz, CD_2Cl_2, 293 K): δ 24.2

($CH(CH_3)_2$, $C^{15,16,18,19}$), 27.8 ($CH(CH_3)_2$, $C^{14,17}$), 55.8 (C^7), 117.8 (C^4), 118.3 (C^6), 123.7 ($C^{10,12}$), 124.3 (C^{11}), 125.7 (C^2), 126.8 (C^{21}), 129.5 (C^3), 140.4 (C^5), 141.0 (C^{23}), 142.1 (C^8), 142.9 (C^1), 143.1 ($C^{9,13}$). Anal. Calcd (%) for $C_{22}H_{27}N_3$ (333.47): C 79.24, H 8.16, N 12.60; found C 79.19, H 8.14, N 12.67.

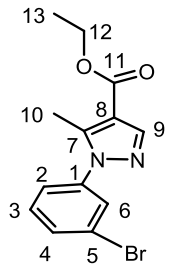

Synthesis of ethyl 1-(3-bromophenyl)-5-methyl-1H-pyrazole-4-carboxylate (7). To a solution of ethyl 2-((dimethylamino)methylene)-3-oxobutanoate (0.660 g, 3.56 mmol) in ethanol (7.5 mL), a solution of (3-bromophenyl)hydrazine (0.700 g, 3.74 mmol) in ethanol (7.5 mL) was added drop wise. The resulting solution was refluxed for 2 hours and evaporated under reduced pressure. The crude residue was diluted with water (15 mL) and extracted twice with chloroform (15 mL). The chloroform extracts were washed three times with a saturated solution of sodium hydrogen carbonate and with water, dried over Na_2SO_4 and evaporated under reduced pressure to give a crude yellow oil that was purified by flash chromatography (silica gel, petroleum ether : AcOEt = 90 : 10) to give the pure **7** as orange crystals. Yield: 0.960 g, 87.2 %. ^{1}H NMR (300 MHz, CD_2Cl_2, 293K): δ 1.35 (t, $^3J_{HH}$ = 7.1 Hz, 3H, CH_2CH_3), H^{13}), 2.56 (s, 3H, CH_3, H^{10}), 4.29 (q, $^3J_{HH}$ = 7.1 Hz, 2H, CH_2CH_3, H^{12}), 7.38-7.40 (2H, $H^{2,3}$), 7.58-7.63 (2H, $H^{4,6}$), 7.98 (s, 1H, C*H* Ar, H^9). $^{13}C\{^1H\}$ NMR (75 MHz, CD_2Cl_2, 293 K): δ 11.7 (C^{10}), 14.1 (CH_2CH_3, C^{13}), 59.9 (CH_2CH_3, C^{12}), 113.3 (C^8), 122.4 (C^5), 123.9 (C^2), 128.4 (C^6), 130.4 (C^3), 131.4 (C^4), 140.1 (C^1), 141.9 (C^9), 143.5 (C^7), 163.4 (C^{11}). Anal. Calcd (%) for $C_{13}H_{13}BrN_2O_2$ (309.16): C 50.50, H 4.24, N 9.06; found C 50.47, H 4.22, N 9.14.

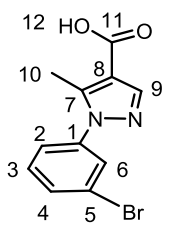

Synthesis of 1-(3-bromophenyl)-5-methyl-1H-pyrazole-4-carboxylic acid (8). To a solution of **7** (0.900 g, 2.91 mmol) in ethanol/water (40 mL, mixture 8:2), LiOH (0.976 g, 23.28 mmol) was added in one portion.

The resulting solution was stirred at 80 °C for 16 hours and then cooled to room temperature. Ethanol was evaporated under reduced pressure and the resulting mixture was diluted with water (10 mL). Afterwards, the solution pH was adjusted to pH 4 using a few drops of AcOH and the resulting mixture was extracted with CH_2Cl_2 (2 x 10 mL). The organic layers were combined, dried over Na_2SO_4 and evaporated under reduced pressure to give the crude **8** as a white solid. The as prepared material was no further purified and it was used in the subsequent step as it is. Yield: 0.783 g, 95.7 %. ^{1}H NMR (300 MHz, $CDCl_3$, 293K): δ 2.59 (s, 3H, C*H*$_3$, H^{10}), 7.36-7.38 (2H, H^{2,3}), 7.57-7.62 (2H, H^{4,6}), 8.09 (s, 1H, C*H* Ar, H^9). ^{13}C{^{1}H} NMR (75 MHz, $CDCl_3$, 293 K): δ 12.0 (C^{10}), 112.5 (C^8), 122.7 (C^5), 124.0 (C^2), 128.7 (C^6), 130.5 (C^3), 131.9 (C^4), 139.7 (C^1), 142.9 (C^9), 144.7 (C^7), 169.0 (C^{11}).

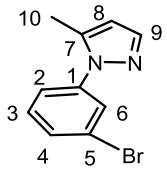

Synthesis of 1-(3-bromophenyl)-5-methyl-1H-pyrazole (9). The carboxylic acid **9** (0.300 g, 1.06 mmol) was collected in a sealed glass vial under inert atmosphere and heated at 215°C for 60 hours. The resulting brown oil was purified by flash chromatography (silica gel; petroleum ether : AcOEt = 80 : 20) to give the pure product **9** as a pure colorless oil. Yield: 0.234 g, 93 %. ^{1}H NMR (300 MHz, CD_2Cl_2, 293K): δ 2.39 (s, 3H, C*H*$_3$, H^{10}), 6.23 (m, 1H, C*H* Ar, H^8), 7.36-7.47 (2H, H^{2,3}), 7.53-7.56 (2H, H^{4,9}), 7.70 (m, 1H, C*H* Ar, H^6). ^{13}C{^{1}H} NMR (75 MHz, CD_2Cl_2, 293 K): δ 12.3 (C^{10}), 107.3 (C^8), 122.3 (C^5), 123.0 (C^2), 127.6 (C^6), 130.2 (C^{3,4}), 138.8 (C^1), 140.1 (C^9), 141.2 (C^7). Anal. Calcd (%) for $C_{10}H_9BrN_2$ (237.10): C 50.66, H, 3.83, N 11.82; found C 50.70, H, 3.85, N 11.84.

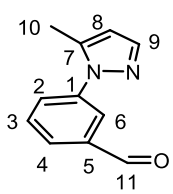

Synthesis of 3-(5-methyl-1H-pyrazol-1-yl)benzaldehyde (10). A suspension of **9** (0.360 g, 1.52 mmol) and sodium formate (0.133 g, 2.28 mmol) in dry DMF (4 mL) was treated with bis(triphenylphosphine)palladium(II) chloride (0.045 g, 0.07 mmol). CO was gently

bubbled through the suspension using a Teflon® cannula and the mixture was stirred at 110 °C for 1 hour. After cooling, the mixture was treated with an aqueous Na_2CO_3 solution and extracted with AcOEt (3 x 30 mL). The collected organic layers were then dried over Na_2SO_4 and evaporated under reduced pressure to give a crude semisolid material. Purification by flash chromatography (silica gel; petroleum ether : AcOEt = 80 : 20) gave the pure **10** as a pale yellow oil. Yield: 0.235 g, 83 %. ^{1}H NMR (300 MHz, CD_2Cl_2, 293K): δ 2.34 (s, 3H, C*H*$_3$, H^{10}), 6.18 (m, 1H, C*H* Ar, H^8), 7.51 (m, 1H, C*H* Ar, H^9), 7.69 (m, 1H, C*H* Ar, H^3), 7.71 (m, 1H, C*H* Ar, H^4), 7.81 (m, 1H, C*H* Ar, H^2), 7.91 (m, 1H, C*H* Ar, H^6), 10.00 (s, 1H, C*H*O, H^{11}). ^{13}C{^{1}H} NMR (75 MHz, CD_2Cl_2, 293 K): δ 12.3 (C^{10}), 107.4 (C^8), 124.8 (C^6), 128.1 (C^2), 129.9 (C^{3,4}), 137.3 (C^5), 138.9 (C^7), 140.2 (C^9), 140.8 (C^1), 191.2 (C^{11}). Anal. Calcd (%) for $C_{11}H_{10}N_2O$ (186.21): C 70.95, H, 5.41, N 15.04; found C, 70.92; H, 5.43; N, 15.09.

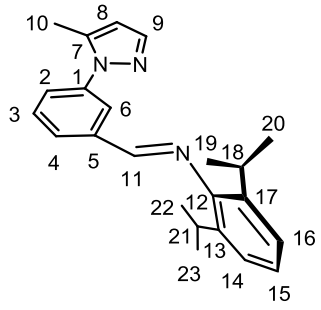

Synthesis of 2,6-diisopropyl-N-(3-(5-methyl-1H-pyrazol-1-yl)benzylidene)aniline (11). A solution of the benzaldehyde **10** (0.170 g, 0.9 mmol) in 10 mL of distilled toluene was treated with 0.26 mL (1.37 mmol) of 2,6-diisopropylaniline and 0.02 g (0.13 mmol) of 4-toluensulfonic acid. The resulting solution was then heated to reflux of solvent for 12 h in a Dean-Stark apparatus. Afterwards, the mixture was cooled to room temperature and then treated with 5 mL of 0.5 M aqueous NaOH solution. The formed layers were separated and the aqueous phase was washed with AcOEt (3 x 10 mL). The collected organic extracts were dried over Na_2SO_4 and the solvent was evaporated under reduced pressure to give crude yellow oil. The pure product was finally precipitated from cold hexane (-20 °C) in the form of pure yellow crystals. The latter were then separated by filtration and washed with cold hexane. Yield: 0.295 g, 93.6 %. ^{1}H NMR (300 MHz,

CD_2Cl_2, 293K): δ 1.20 (d, $^3J_{HH}$ = 6.8 Hz, 12H, CH(C*H*$_3$), H^{19,20,22,23}), 2.46 (s, 3H, C*H*$_3$, H^{10}), 3.00 (sept, $^3J_{HH}$ = 6.8 Hz, 2H, C*H*(CH$_3$), H^{18,21}), 6.28 (m, 1H, C*H*, H^8), 7.11-7.15 (m, 1H, C*H* Ar, H^{15}), 7.19-7.21 (2H, C*H* Ar, H^{14,16}), 7.61 (m, 1H, C*H* Ar, H^9), 7.65-7.66 (2H, C*H* Ar, H^{2,3}), 7.94-7.96 (m, 1H, C*H* Ar, H^4), 8.06 (m, 1H, H^6), 8.26, (s, 1H, C*H*N , H^{11}). ^{13}C{^{1}H} NMR (75 MHz, CD_2Cl_2, 293 K): δ 12.3 (C^{10}), 23.1 (CH(*C*H$_3$)$_2$, C^{19,20,22,23}), 27.9 (*C*H(CH$_3$)$_2$, C^{18,21}), 107.2 (C^8), 122.9 (C^{14,16}), 124.1 (C^{6,15}), 127.1 (C^2), 127.4 (C^4), 129.4 (C^3), 137.1 (C^5), 137.4 (C^{13,17}), 138.8 (C^7), 140.0 (C^9), 140.6 (C^1), 149.0 (C^{12}), 161.1 (C^{11}). Anal. Calcd (%) for $C_{23}H_{27}N_3$ (345.48): C 79.96, H 7.88, N 12.16; found C 80.00, H 7.93, N 12.07.

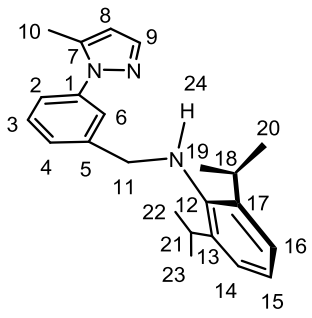

Synthesis of 2,6-diisopropyl-N-(3-(5-methyl-1H-pyrazol-1-yl)benzyl)aniline {H_2L^{Me}} (12). To a cooled solution (0 °C) of **11** (0.295 g, 0.85 mmol), in a 1:1 mixture of dry and degassed MeOH (2.5 mL) and THF (2.5 mL), $NaBH_3CN$ (0.06 g, 1.02 mmol) and acetic acid (0.06 mL, 1.02 mmol) were added in sequence and the resulting mixture was maintained under stirring and inert atmosphere at r.t for 1 h. Afterwards, a 1:1 mixture of saturated Na_2CO_3 and water were added. The organic phase was separated and the aqueous layer was extracted with AcOEt (3 x 10 mL). The collected organic layers were dried over Na_2SO_4 and the solvent was evaporated under reduced pressure. The crude residue was purified by flash chromatography (silica gel; petroleum ether : AcOEt = 83 : 17) to give the pure product **12** as a colourless oil. Yield: 0.272 g, 92.0 %. ^{1}H NMR (300 MHz, CD_2Cl_2, 293K): δ 1.30 (d, $^3J_{HH}$ = 6.8 Hz, 12H, CH(C*H*$_3$), H^{19,20,22,23}), 2.41 (s, 3H, C*H*$_3$, H^{10}), 3.33-3.45 (3H, C*H*(CH$_3$), N*H*, H^{18,21,24}), 4.18 (s, 1H, C*H*$_2$NH, H^{11}), 6.28 (m, 1H, C*H*, H^8), 7.12-7.21 (3H, C*H* Ar, H^{14,15,16}), 7.43-7.54 (3H, C*H* Ar, H^{2,3,4}), 7.61-7.63 (2H, C*H* Ar, H^{9,6}). ^{13}C{^{1}H} NMR (75 MHz, CD_2Cl_2, 293 K): δ 12.3 (C^{10}), 24.1 (CH(*C*H$_3$)$_2$, C^{19,20,22,23}),

27.7 (*C*H(CH$_3$)$_2$, C^{18,21}), 55.6 (C^{11}), 106.9 (C^8), 123.4 (C^2), 123.6 (C^{14,16}), 124.0 (C^6), 124.2 (C^{15}), 126.8 (C^4), 129.0 (C^3), 138.7 (C^7), 139.6 (C^9), 140.2 (C^1), 141.6 (C^{12}), 142.7 (C^5), 143.0 (C^{13,17}). Anal. Calcd (%) for $C_{23}H_{29}N_3$ (347.50): C 79.50, H 8.41, N 12.09; found C 79.55, H 8.43, N 12.02.

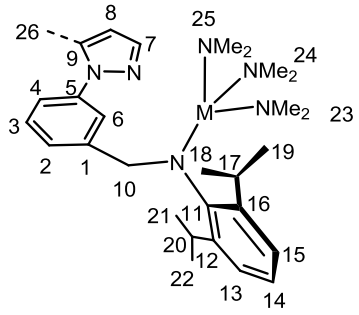

General procedure for the synthesis of complexes Zr^{IV}{*κ-N*-HL}(NMe$_2$)$_3$ (13), Hf^{IV}{*κ-N*-HL}(NMe$_2$)$_3$ (14), Zr^{IV}{*κ-N*-HL^{Me}}(NMe$_2$)$_3$ (15) and Hf^{IV}{*κ-N*-HL^{Me}}(NMe$_2$)$_3$ (16). A solution of the selected ligand {H$_2$L; **4** or H$_2$L^{Me}; **12**} (1 mmol) in dry and degassed benzene (4 mL) was treated drop wise with a benzene solution (3 mL) of the proper metal precursor [M^{IV}(NMe$_2$)$_4$, 99 % ; M = Zr, Hf] (1.05 equiv.). The reaction mixture was maintained under stirring at r.t for 20 h and then concentrated *in vacuum* to afford semisolid yellow pale crude materials. Complex purification for compounds **13** and **14** was conveniently achieved by crystallization from concentrated pentane solutions cooled at -30° C. **13** and **14** (94 % isolated yield) were obtained as yellow pale and white crystals, respectively, suitable for X-ray diffraction analyses. As for complexes **15** and **16** they were obtained as pale yellow oils and all attempts to isolate crystals, failed. In spite of that both complexes resulted analytically pure with no traces of residual reagents/solvents. Both oils were dried under vacuum to constant weight and spectroscopically characterized. **13**: (96 % isolated yield); ^{1}H NMR (300 MHz, CD_2Cl_2, 293K): δ 1.06 (d, $^3J_{HH}$ = 6.9 Hz, 6H, CH(CH$_3^A$C*H*$_3^B$, H^{19,22}), 1.16 (d, $^3J_{HH}$ = 6.9 Hz, 6H, CH(C*H*$_3^A$CH$_3^B$, H^{18,21}), 2.75 (br s, 18H, N(C*H*$_3$)$_2$, H^{23,24,25}), 3.50 (sept, $^3J_{HH}$ = 6.9 Hz, 2H, C*H*(CH$_3$)$_2$, H^{17,20}), 4.44 (s, 2H, *CH*$_2$N, H^{10}), 6.48 (m, 1H, C*H* Ar, H^8), 7.12-7.15 (4H, C*H* Ar, H^{2,13,14,15}), 7.38 (t, $^3J_{HH}$ = 7.8 Hz, 1H, C*H* Ar, H^3), 7.47 (m, 1H, C*H* Ar, H^6), 7.60 (m, 1H, C*H* Ar, H^4), 7.70 (m, 1H, C*H* Ar, H^7), 7.85 (m, 1H, C*H* Ar, H^9) .

$^{13}C\{^{1}H\}$ NMR (75 MHz, CD_2Cl_2, 293 K): δ 24.0 ($CH(CH_3^ACH_3^B)$, $C^{18,21}$), 25.0 ($CH(CH_3^ACH_3^B)$, $C^{19,22}$), 27.7 ($CH(CH_3)_2$, $C^{17,20}$), 41.0 ($N(CH_3)$, $C^{23,24,25}$), 60.4 (C^{10}), 107.3 (C^8), 117.7 (C^4), 120.1 (C^6), 123.7 ($C^{13,15}$), 124.9 (C^{14}), 126.5 (C^9), 127.6 (C^2), 129.1 (C^3), 140.7 (C^7), 142.7 (C), 143.0 (C), 144.0 (C), 147.8 ($C^{12,16}$). Anal. Calcd (%) for $C_{28}H_{44}N_6Zr$ (555.91): C 60.49, H 7.98, N 15.12; found C 60.52, H 8.03, N 15.10. **14**: (94 % isolated yield) ^1H NMR (300 MHz, CD_2Cl_2, 293K): δ 1.05 (d, $^3J_{HH}$ = 6.9 Hz, 6H, $CH(CH_3^ACH_3^B$, $H^{19,22}$), 1.17 (d, $^3J_{HH}$ = 6.9 Hz, 6H, $CH(CH_3^ACH_3^B$, $H^{18,21}$), 2.78 (br s, 18H, $N(CH_3)_2$, $H^{23,24,25}$), 3.52 (sept, $^3J_{HH}$ = 6.9 Hz, 2H, $CH(CH_3)_2$, $H^{17,20}$), 4.50 (s, 2H, CH_2N, H^{10}), 6.48 (m, 1H, C*H* Ar, H^8), 7.10-7.14 (4H, C*H* Ar, $H^{2,13,14,15}$), 7.38 (t, $^3J_{HH}$ = 7.8 Hz, 1H, C*H* Ar, H^3), 7.44 (m, 1H, C*H* Ar, H^6), 7.70 (m, 1H, C*H* Ar, H^4), 7.70 (m, 1H, C*H* Ar, H^7), 7.84 (m, 1H, C*H* Ar, H^9) . $^{13}C\{^{1}H\}$ NMR (75 MHz, CD_2Cl_2, 293 K): δ 24.0 ($CH(CH_3^ACH_3^B)$, $C^{18,21}$), 25.0 ($CH(CH_3^ACH_3^B)$, $C^{19,22}$), 27.7 ($CH(CH_3)_2$, $C^{17,20}$), 40.6 ($N(CH_3)$, $C^{23,24,25}$), 60.0 (C^{10}), 107.3 (C^8), 117.7 (C^4), 120.2 (C^6), 123.7 ($C^{13,15}$), 125.0 (C^{14}), 126.5 (C^9), 127.6 (C^2), 129.1 (C^3), 140.0 (C), 140.7 (C^7), 142.6 (C), 143.9 (C), 147.9 ($C^{12,16}$). Anal. Calcd (%) for $C_{28}H_{44}N_6Hf$ (643.18): C 52.29, H 6.90, N 13.07; found C 52.34, H 6.95, N, 13.00. **15**: (95 % yield) ^1H NMR (400 MHz, CD_2Cl_2, 293K): δ 1.02 (d, $^3J_{HH}$ = 6.9 Hz, 6H, $CH(CH_3^ACH_3^B$, $H^{19,22}$), 1.17 (d, $^3J_{HH}$ = 6.9 Hz, 6H, $CH(CH_3^ACH_3^B$, $H^{18,21}$), 2.19 (s, 3H, CH_3, H^{26}), 2.79 (br s, 18H, $N(CH_3)_2$, $H^{23,24,25}$), 3.48 (sept, $^3J_{HH}$ = 6.9 Hz, 2H, $CH(CH_3)_2$, $H^{17,20}$), 4.51 (s, 2H, CH_2N, H^{10}), 6.18 (m, 1H, C*H* Ar, H^8), 7.11 (br s, 3H, C*H* Ar, $H^{13,14,15}$), 7.18 (br s, 1H, C*H* Ar, H^6), 7.26 (m, 1H, C*H* Ar, H^2), 7.33 (m, 1H, C*H* Ar, H^4), 7.39-7.44 (1H, C*H* Ar, H^3), 7.52 (m, 1H, C*H* Ar, H^7). $^{13}C\{^{1}H\}$ NMR (100 MHz, CD_2Cl_2, 293 K): δ 12.0 (CH_3, C^{26}), 24.0 ($CH(CH_3^ACH_3^B)$, $C^{18,21}$), 24.9 ($CH(CH_3^ACH_3^B)$, $C^{19,22}$), 27.7 ($CH(CH_3)_2$, $C^{17,20}$), 41,1 ($N(CH_3)$, $C^{23,24,25}$), 60.0 (C^{10}), 106.6 (C^8), 123.0 (C^4), 123.7 ($C^{13,15}$), 125.0 (C^{14}), 125.7 (C^6), 128.2 (C^2), 128.7 (C^3), 138.5 (C^9), 139.4 (C^7), 139.8 (C), 142.2 (C), 143.5 (C), 147.8 ($C^{12,16}$). Anal.

Calcd (%) for $C_{29}H_{46}N_6Zr$ (569.94): C 61.11, H 8.14, N 14.75; found C 61.15, H 8.17, N 14.71. **16**: (91 % yield) ^{1}H NMR (400 MHz, CD_2Cl_2, 293K): δ 0.97 (d, $^3J_{HH}$ = 6.9 Hz, 6H, CH($CH_3^ACH_3^B$, $H^{19,22}$), 1.13 (d, $^3J_{HH}$ = 6.9 Hz, 6H, CH($CH_3^ACH_3^B$, $H^{18,21}$), 2.13 (s, 3H, *C*H_3, H^{26}), 2.77 (br s, 18H, N(CH_3)$_2$, $H^{23,24,25}$), 3.45 (sept, $^3J_{HH}$ = 6.9 Hz, 2H, C*H*(CH_3)$_2$, $H^{17,20}$), 4.50 (s, 2H, *C*H_2N, H^{10}), 6.14 (m, 1H, C*H* Ar, H^8), 7.07 (br s, 3H, C*H* Ar, $H^{13,14,15}$), 7.11 (br s, 1H, C*H* Ar, H^6), 7.19 (m, 1H, C*H* Ar, H^2), 7.29 (m, 1H, C*H* Ar, H^4), 7.35-7.39 (1H, C*H* Ar, H^3), 7.48 (m, 1H, C*H* Ar, H^7). $^{13}C\{^1H\}$ NMR (100 MHz, CD_2Cl_2, 293 K): δ 12.0 (*C*H_3, C^{26}), 24.0 (CH($CH_3^AC H_3^B$), $C^{18,21}$), 24.9 (*C*H(*C*$H_3^ACH_3^B$), $C^{19,22}$), 27.7 (*C*H(CH_3)$_2$, $C^{17,20}$), 40.6 (N(*C*H_3), $C^{23,24,25}$), 59.5 (C^{10}), 106.6 (C^8), 123.1 (C^4), 123.7 ($C^{13,15}$), 125.0 (C^{14}), 125.7 (C^6), 128.7 (C^2), 128.8 (C^3), 138.5 (C^9), 139.4 (C^7), 139.8 (C), 142.1 (C), 143.5 (C), 147.9 ($C^{12,16}$). Anal. Calcd (%) for $C_{29}H_{46}N_6Hf$ (657.21): C 53.00, H 7.05, N 12.79; C, 53.07; H, 7.11, N 12.82.

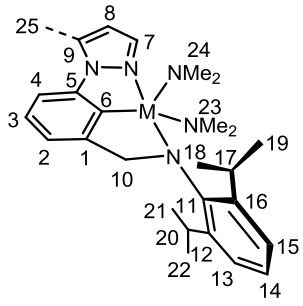

General procedure for the synthesis of complexes $Zr^{IV}\{\kappa^3$-*N*,*C*,*N*-L$\}(NMe_2)_2$ (17), $Hf^{IV}\{\kappa^3$-*N*,*C*,*N*-L$\}(NMe_2)_2$ (18), $Zr^{IV}\{\kappa$-*N*,*C*,*N*-$L^{Me}\}(NMe_2)_2$ (19) and $Hf^{IV}\{\kappa$-*N*,*C*,*N*-$L^{Me}\}(NMe_2)_2$ (20). A solution of the selected ligand {H_2L; **4** or H_2L^{Me}; **12**} (1 mmol) in dry and degassed xylene (4 mL) was treated drop wise with a xylene solution (4 mL) of the proper metal precursor [$M^{IV}(NMe_2)_4$, 99 % ; M = Zr, Hf] (1.05 equiv.). The reaction mixture was maintained under stirring at reflux of the solvent for the appropriate reaction time (see **Table 4.3**) till completeness. Solvent evaporation under vacuum afforded the crude cyclometallated species as either dark yellow (Zr^{IV} derivatives) or yellow pale (Hf^{IV} derivatives) microcrystals. Complex purification was achieved by crystallization from concentrated toluene/pentane (1:1 v/v) solutions cooled at -30 °C. Crystals suitable for X-ray diffraction analyses were obtained from each sample. **17**: (87 % isolated yield) ^{1}H NMR

(400 MHz, CD_2Cl_2, 293K): δ 1.15 (d, $^3J_{HH}$ = 6.9 Hz, 6H, CH($CH_3^ACH_3^B$, $H^{19,22}$), 1.21 (d, $^3J_{HH}$ = 6.9 Hz, 6H, CH($CH_3^ACH_3^B$, $H^{18,21}$), 2.73 (s, 12H, N(CH_3)$_2$, $H^{23,24}$), 3.66 (sept, $^3J_{HH}$ = 6.9 Hz, 2H, C*H*(CH_3)$_2$, $H^{17,20}$), 4.71 (s, 2H, *C*H_2N, H^{10}), 6.61 (m, 1H, C*H* Ar, H^8), 7.06-7.18 (5H, C*H* Ar, $H^{2,4,13,14,15}$), 7.24 (t, $^3J_{HH}$ = 7.8 Hz, 1H, C*H* Ar, H^3), 7.78 (d, $^3J_{HH}$ = 2.1 Hz, 1H, C*H* Ar, H^7), 8.13 (d, $^3J_{HH}$ = 2.5 Hz, 1H, C*H* Ar, H^9). $^{13}C\{^1H\}$ NMR (100 MHz, CD_2Cl_2, 293 K): δ 24.0 (CH($CH_3^AC H_3^B$), $C^{18,21}$), 26.0 (*C*H(*C*$H_3^ACH_3^B$), $C^{19,22}$), 27.3 (*C*H(CH_3)$_2$, $C^{17,20}$), 39.9 (N(*C*H_3), $C^{23,24}$), 68.8 (C^{10}), 107.0 (C^4), 108.0 (C^8), 121.2 (C^2), 123.0 ($C^{13,15}$), 123.5 (C^{14}), 125.7 (C^9), 127.8 (C^3), 140.5 (C^7), 144.3 (C), 147.4 ($C^{12,16}$), 148.4 (C), 157.3 (C), 174.0 (C^6). Anal. Calcd (%) for $C_{26}H_{37}N_5Zr$ (510.83): C 61.13, H 7.30, N 13.71: found C 61.17, H 7.34, N 13.64. **18**: (79 % isolated yield) ^{1}H NMR (400 MHz, CD_2Cl_2, 293K): δ 1.16 (d, $^3J_{HH}$ = 6.9 Hz, 6H, CH($CH_3^ACH_3^B$, $H^{19,22}$), 1.21 (d, $^3J_{HH}$ = 6.9 Hz, 6H, CH($CH_3^ACH_3^B$, $H^{18,21}$), 2.75 (s, 12H, N(CH_3)$_2$, $H^{23,24}$), 3.68 (sept, $^3J_{HH}$ = 6.9 Hz, 2H, C*H*(CH_3)$_2$, $H^{17,20}$), 4.11 (s, 2H, *C*H_2N, H^{10}), 6.60 (m, 1H, C*H* Ar, H^8), 7.08 (m, 1H, CH Ar, H^{14}), 7.10-7.17 (3H, C*H* Ar, $H^{2,13,15}$), 7.23-7.26 (2H, CH Ar, $H^{3,4}$), 7.24 (t, $^3J_{HH}$ = 7.8 Hz, 1H, C*H* Ar, H^3), 7.81 (d, $^3J_{HH}$ = 1.9 Hz, 1H, C*H* Ar, H^7), 8.13 (d, $^3J_{HH}$ = 2.5 Hz, 1H, C*H* Ar, H^9). $^{13}C\{^1H\}$ NMR (100 MHz, CD_2Cl_2, 293 K): δ 24.0 (CH($CH_3^AC H_3^B$), $C^{18,21}$), 26.0 (*C*H(*C*$H_3^ACH_3^B$), $C^{19,22}$), 27.2 (*C*H(CH_3)$_2$, $C^{17,20}$), 39.7 (N(*C*H_3), $C^{23,24}$), 67.9 (C^{10}), 107.2 (C^4), 108.1 (C^8), 121.6 (C^2), 123.0 ($C^{13,15}$), 123.6 (C^{14}), 126.1 (C^9), 127.9 (C^3), 140.7 (C^7), 145.0 (C), 147.5 ($C^{12,16}$), 148.8 (C), 157.3 (C), 181.8 (C^6). Anal. Calcd (%) for $C_{26}H_{37}N_5Hf$ (598.10): C 52.21, H 6.24, N 11.71; found C 52.26, H 6.24, N 11.67. **19**: (86 % isolated yield) ^{1}H NMR (400 MHz, CD_2Cl_2, 293K): δ 1.19 (d, $^3J_{HH}$ = 6.9 Hz, 6H, CH($CH_3^ACH_3^B$, $H^{19,22}$), 1.24 (d, $^3J_{HH}$ = 6.9 Hz, 6H, CH($CH_3^ACH_3^B$, $H^{18,21}$), 2.75 (s, 12H, N(CH_3)$_2$, $H^{23,24}$), 2.79 (s, 3H, *C*H_3, H^{25}) 3.70 (sept, $^3J_{HH}$ = 6.9 Hz, 2H, C*H*(CH_3)$_2$, $H^{17,20}$), 4.74 (s, 2H, *C*H_2N, H^{10}), 6.35 (m, 1H, C*H* Ar, H^8), 7.10-7.18 (4H, C*H* Ar,

$H^{2,13,14,15}$), 7.25 (t, $^{3}J_{HH}$ = 7.8 Hz, 1H, C*H* Ar, H^{3}), 7.33 (d, $^{3}J_{HH}$ = 7.8 Hz, 1H, C*H* Ar, H^{4}), 7.68 (m, 1H, C*H* Ar, H^{7}). $^{13}C\{^{1}H\}$ NMR (100 MHz, CD_2Cl_2, 293 K): δ 14.1 (CH_3, C^{25}), 24.0 ($CH(CH_3{}^{A}CH_3{}^{B})$, $C^{18,21}$), 26.1 ($CH(CH_3{}^{A}CH_3{}^{B})$, $C^{19,22}$), 27.3 ($CH(CH_3)_2$, $C^{17,20}$), 40.0 ($N(CH_3)$, $C^{23,24}$), 68.7 (C^{10}), 109.1 (C^{4}), 109.5 (C^{8}), 120.9 (C^{2}), 123.0 ($C^{13,15}$), 123.5 (C^{14}), 127.7 (C^{3}), 140.0 (C^{7}), 140.3 (C^{9}), 146.3 (C), 147.4 ($C^{12,16}$), 148.6 (C), 157.1 (C), 175.5 (C^{6}). Anal. Calcd (%) for $C_{27}H_{39}N_5Zr$ (524.86): C 61.79, H 7.49, N 13.34; found C 61.83, H 7.52, N 13.28. **20**: (83 % isolated yield) ^{1}H NMR (400 MHz, CD_2Cl_2, 293K): δ 1.17 (d, $^{3}J_{HH}$ = 6.9 Hz, 6H, $CH(CH_3{}^{A}CH_3{}^{B}$, $H^{19,22}$), 1.21 (d, $^{3}J_{HH}$ = 6.9 Hz, 6H, $CH(CH_3{}^{A}CH_3{}^{B}$, $H^{18,21}$), 2.74 (s, 12H, $N(CH_3)_2$, $H^{23,24}$), 2.79 (s, 3H, CH_3, H^{25}) 3.68 (sept, $^{3}J_{HH}$ = 6.9 Hz, 2H, $CH(CH_3)_2$, $H^{17,20}$), 4.81 (s, 2H, CH_2N, H^{10}), 6.32 (m, 1H, C*H* Ar, H^{8}), 7.08 (m, 1H, C*H* Ar, H^{14}), 7.14-7.16 (3H, C*H* Ar, $H^{2,13,15}$), 7.24 (t, $^{3}J_{HH}$ = 7.8 Hz, 1H, C*H* Ar, H^{3}), 7.37 (d, $^{3}J_{HH}$ = 7.8 Hz, 1H, C*H* Ar, H^{4}), 7.69 (m, 1H, C*H* Ar, H^{7}). $^{13}C\{^{1}H\}$ NMR (100 MHz, CD_2Cl_2, 293 K): δ 14.0 (CH_3, C^{25}), 24.0 ($CH(CH_3{}^{A}CH_3{}^{B})$, $C^{18,21}$), 26.0 ($CH(CH_3{}^{A}CH_3{}^{B})$, $C^{19,22}$), 27.2 ($CH(CH_3)_2$, $C^{17,20}$), 39.7 ($N(CH_3)$, $C^{23,24}$), 67.8 (C^{10}), 109.3 (C^{4}), 109.5 (C^{8}), 121.2 (C^{2}), 122.9 ($C^{13,15}$), 123.5 (C^{14}), 127.8 (C^{3}), 140.3 (C^{7}), 140.7 (C^{9}), 146.8 (C), 147.4 ($C^{12,16}$), 149.1 (C), 157.1 (C), 183.1 (C^{6}). Anal. Calcd (%) for $C_{27}H_{39}N_5Hf$ (612.12): C 52.98, H 6.42, N 11.44; found C 53.02, H 6.43, N 11.39.

General Procedure for Intramolecular Hydroamination of Aminoalkenes I-V. All catalytic tests were set-up under inert atmosphere in a N_2-filled dry-box. Amido precursors **13**, **14** and **17-20** were tested as neutral catalysts in the intramolecular hydroamination reaction using a two-necked 10 mL round bottom flask equipped with a magnetic stir bar, a glass stopper and a septum. In a typical procedure, a solution of the catalyst (5 mol%) in dry and degassed benzene (1.5 mL) [toluene was used for selected issues, see **Table 4.4**] was treated in one portion with a solution of the aminoalkene

(0.632 mmol) in dry and degassed benzene (0.5 mL) and ferrocene as internal standard (0.2 mL of a stock 0.17 M ferrocene solution in benzene). Afterwards, the system was heated at the final temperature and the reaction course was periodically monitored by sampling the mixture and analyzing it *via* GC/MS, till completeness or at fixed times. The reaction's conversion was calculated by comparative integration of the product and substrate peak signals (on the ^{1}H NMR spectrum) with the internal standard peak (ferrocene). For selected issues, the reaction mixture was finally concentrated under reduced pressure and the crude material was purified by flash-chromatography (typically: CH_2Cl_2 + 5% MeOH) to give the pure pyrrolidine product.

Kinetic measurements on 17 and 18. Kinetic studies were performed for the conversion of **I**, at room temperature and under optimized reaction conditions (**Table 4.4**, entries 4 and 19). Variable catalyst's concentration (4, 6 or 8 mol%) were also used for the best performing catalysts **17** at room temperature. All measurements were carried out in a sealed J-Young NMR tube and the reaction course was monitored *via* ^{1}H NMR spectra recorded at constant times using ferrocene as internal standard for the relative integration of the ^{1}H NMR signals. Comparison of the integration of product and substrate peaks with internal standard peaks was used to calculate the relative percentage of substrate and product at any given time. Both catalyst precursors **17** and **18** showed a first order dependence in substrate consumption/cyclization. In a typical procedure, stock solutions of catalyst precursors **17** and **18** were prepared by dissolving 20 mg of each complex in 0.5 mL of benzene-d_6. 20 mg of **I** and 5 mg (26.87 μmol) of ferrocene 98% (internal standard)[15h] were weighted into a 1 mL volumetric flask and dissolved in approximately 0.2 mL of benzene-d_6. Afterwards, a proper amount of the stock solution of the catalyst precursor [0.05 mL of **17**; 0.06 mL of **18**] was added to the 1 mL volumetric flask and the volume was topped to 1 mL with benzene-d_6. The as

prepared solution was shaken and 0.8 mL rapidly transferred into the J-Young NMR tube. The tube was placed into a 300 MHz NMR probe and acquisitions started immediately. For kinetic measurements carried out at 80 °C, a pre-heated 300 MHz NMR probe was used and the sample was allowed to thermally equilibrate for 2 minutes prior starting to collect the first ^{1}H NMR spectrum at t = t_0. The ^{1}H NMR spectra (8 scans) were collected every 5/10 minutes till the almost complete substrate conversion (at least 90 %).

Computational Details. Density Functional Theory (DFT) geometry optimizations in the gas phase of the real systems **13** and **15** were performed using the *Gaussian09* program (revision *A.02*).[44] The starting geometry for **13** was obtained from its XRD structure by rotating the phenyl-pyrazole fragment around the N(1)-C(7) bond of about 180° (see main text for atom numbering), in order to get a more suitable conformer for cyclometallation to occur. The starting geometry for **15** was then obtained from the optimized structure of **13** by replacing the proton on C(22) of the pyrazole ring with a methyl group. Both initial guesses were optimized with a M06 functional[45] using the LANL2DZ pseudopotential[46] and related basis set[47] on the Zirconium atom and a 6-31G* basis set on all the other atoms. An extra *f*-type polarization function for Zr was added to the standard set.[47] Energetic profiles for the reaction pathways related to the hydroamination/cyclization of **I** and **III** catalyzed by **17** were simulated with the CP2K/Quickstep package, using a hybrid Gaussian and plane wave method[48] within a DFT framework. A double quality Gaussian basis set plus polarization function (DZVP) was employed for all atoms. The Goedecker-Teter-Hutter pseudopotentials[49] together with a 320 Ry plane wave cutoff were used to expand the densities obtained with the Perdew-Burke-Ernzerhof (PBE)[50] exchange-correlation density functional. VdW forces are taken in account with the Grimme D3 Method.[51] Molecular geometry optimization

of stationary points used the Broyden–Fletcher–Goldfarb–Shanno (BFGS) method. The transition states were searched with the "distinguished reaction coordinate procedure" along the emerging bonds. Entropic and solvents effects for the cyclization process catalyzed by **17** and involving precursors **I** and **III** can be reasonably considered comparable and their contribution have been omitted. Finally, incoming substrates involved in the protonolysis steps (**Figure 9.9**, TS3 and TS4) are modelled by adopting the simpler 1-aminopent-4-ene since only the amino termination is interested in the proton transfer processes investigated.

4.6 References

1 For comprehensive review papers and books on pincer-type complexes and their application in catalysis see: a) M. H. P. Rietveld, D. M. Grove, G. van Koten, *New. J. Chem.*, **1997**, *21*, 751. b) M. Albrecht, G. van Koten, *Angew. Chem. Int. Ed.*, **2001**, *40*, 3750. c) M. E. Van Der Boom, D. Milstein, *Chem. Rev.*, **2003**, *103*, 1759. d) J. T. Singleton, *Tetrahedron*, **2003**, *59*, 1837. e) D. Morales-Morales, *Rev. Quim. Méx.*, **2004**, *48*, 338. f) M. Q. Slagt, D. A. P. Zwieten, A. J. C. M. Moerkerk, R. J. M. K. Gebbink, G. van Koten, *Coord. Chem. Rev.*, **2004**, *248*, 2275. g) D. Pugh, A. A. Danopoulos, *Coord. Chem. Rev.*, **2007**, *251*, 610. h) D. Morales-Morales, C. M. Jensen in *The Chemistry of Pincer Compounds*, Elsevier Science, **2007**, pp. 450, ISBN: 978-0-444-53138-4. i) J-L. Niu, X-Q. Hao, J-F. Gong, M-P. Song, *Dalton Trans*., **2011**, *40*, 5135. j) N. Selander, K. J. Szabó, *Chem. Rev*, **2011**, *111*, 2048.

2 G. van Koten, J. T. B. H. Jastrzebski, J. G. Noltes, A. L. Spek, J. C. Schoone, *J. Organomet. Chem.*, **1978**, *148*, 233.

3 For selected examples of mono- and trianionic {N,C,N}-pincer complexes with early transition metals see: a) J. G. Donkervoort, J. T. B. H. Jastrzebski, B-J. Deelman, H. Kooijman, N. Veldman, A. L. Spek, G. van Koten, *Organometallics*, **1997**, *16*, 4174. b) M. Contel, M. Stol, M. A. Casado, G. P. M. van Klink, D. D. Ellis, A. L. Spek, G. van Koten, *Organometallics*, **2002**, *21*, 4556. c) J. Koller, S. Sarkar, K. A. Abboud, A. S. Veige, *Organometallics*, **2007**, *26*, 5438. d) S. Sarkar, K. P. McGowan, J. A. Culver, A. R. Carloson, J. Koller, A. J. Peloquin, M. K. Veige, K. A. Abboud, A. S. Veige, *Inorg. Chem.*, **2010**, *49*, 5143. e) A. V. Chuchuryukin, R. Huang, M. Lutz, J. C. Chadwick, A. L. Spek, G. van Koten, *Organometallics*, **2011**, *30*, 2819. f) A. V. Chuchuryukin, R. Huang, E. E. van Faassen, G. P. M. van Klink, M. Lutz, J. C. Chadwick, A. L. Spek, G. van Koten, *Dalton Trans.*, **2011**, *40*, 8887. g) K. P. McGowan, K. A. Abboud, A. S. Veige, *Organometallics*, **2011**, *30*, 4949.

4 For representative symmetrical N donors NCN-pincer complexes see: [N = amines] a) O. A. Wallner, K.J. Szabó, *Org. Lett*. **2004**, *6*, 1829. b) J. Kjellgren, H. Sundén, K. J. Szabó, *J. Am. Chem. Soc.*, **2004**, *126*, 474. c) M. Q. Slagt, G. Rodrìguez, M. M. P. Grutters, R. J. M. K. Gebbink, W. Klopper, L. W. Jenneskens, M. Lutz, A. L. Spek, G. van Koten, *Chem. Eur. J*., **2004**, *10*, 1331. [N = imines] d) K. Takenaka, M. Minakawa, Y. Uozumi, *J. Am. Chem. Soc*., **2005**, *127*, 12273. e) J. S. Fossey, M. L. Russell, K. M. A. Malik, C. J. Richards, *J. Organomet. Chem*., **2007**, *692*, 4843. [N = pyridines] f) B. Soro, S. Stoccoro, G. Minghetti, A. Zucca, M. A. Cinellu, S. Gladiali, M. Manassero, M. Sansoni, *Organometallics*, **2005**, *24*, 53. g) B. Soro, S. Stoccoro, G. Minghetti, A. Zucca, M. A. Cinellu, M. Manassero, S. Gladiali, *Inorg. Chim. Acta*, **2006**, *359*, 1879. h) M. S. Yoon, R. Ramesh, J. Kim, D. Ryu, K. H. Ahn, *J. Organomet. Chem*., **2006**, *691*, 5927. [N = oxazolines] i) H. Nishiyama, *Chem. Soc. Rev*., **2007**, *36*, 1133. l) Y. Motoyama, N. Makihara, Y. Mikami, K. Aoki, H. Nishiyama, *Chem. Lett*., **1997**, 951. m) M. A. Stark, C. J. Richards, *Tetrahedron Lett*., **1997**, *38*, 5881. n) S. E. Denmark, R. A. Stavenger, A. M. Faucher, J. P. Edwards, *J. Org. Chem.*, **1997**, *62*, 3375. o) M. A. Stark, G. Jones, C. J. Richards, *Organometallics*, **2000**, *19*, 1282. p) T. Takemoto, S. Iwasa, H. Hamada, K. Shibatomi, M. Kameyama, Y. Motoyama, H. Nishiyama, *Tetrahedron Lett*., **2007**, *48*, 3397. q) A. Bugarin, B. T. Connell, *Organometallics*, **2008**, *27*, 4357. r) T. Kimura, Y. Uozumi, *Organometallics*, **2008**, *27*, 5159. [N = pyrazole] s) C. M. Hartshorn, P. J. Steel, *Organometallics*, **1998**, *17*, 3487. t) H. P. Dijkstra, M. D. Meijer, J. Patel, R. Kreiter, G. P. M. van Klink, M. Lutz, A. L. Spek, A. J. Canty, G. van Koten, *Organometallics*, **2001**, *20*, 3159.

5 a) X-Q. Hao, Y-N. Wang, J-R. Liu, K-L. Wang, J-F. Gong, M-P. Song, *J. Organomet. Chem.*, **2010**, *695*, 82.

6 For a general review on unsymmetrical *ECE'* and *ECZ* pincer Pd(II) complexes, see: I. Moreno, R. SanMartin, B. Inés, M. T. Herrero, E. Domínguez, *Curr. Org. Chem.*, **2009**, *13*, 878.

7 For a related example of unsymmetrical NCN'-pincer complex incorporating an N-heterocyclic carbene (NHC) functional group, see: N. Schneider, V. César, S. Bellemin-Laponnaz, L. H. Gade, *Organometallics*, **2005**, *24*, 4886.

8 G. Giambastiani, L. Luconi, R. L. Kuhlman, P. D. Hustad, in *Olefin Upgrading Catalysis by Nitrogen-based Metal Complexes I* (Eds. G. Giambastiani, J. Campora - ISBN 978-90-481-3814-2), Springer, London, **2011**, pp. 197-282 and refs cited therein.

9 L. Luconi, A. Rossin, G. Tuci, I. Tritto, L. Boggioni, J. J. Klosin, C. N. Theriault, G. Giambastiani, *Chem. Eur. J.*, **2012**, *18*, 671.

10 L. Luconi, A. Rossin, G. Tuci, S. Germain, E. Schulz, J. Hannedouche, G. Giambastiani, *ChemCatChem*, **2012**, DOI: 10.1002/cctc.201200389.

11 L. Luconi, G. Giambastiani, A. Rossin, C. Bianchini, A. Lledós, *Inorg. Chem.*, **2010**, *49*, 6811.

12 a) R. Mukherjee, *Coord. Chem. Rev*., **2000**, *203*, 151. b) S. Radia, A. Ramdania, Y. Lekchirib, M. Morcelletc, G. Crinic, J. Morcelletc, L. Janus, *Eur. Polym. J*., **2000**, *36*, 1885.

13 An unique example of pirydylamido N,C,N' dianionic systems in combination with Group-IV metal complexes as polymerization precatalysts is mentioned in the following US patent application: G. R. Giesbrecht, T. M. Boller, A. Z. Voskoboynikov, A. F. Asachenko, M. V. Nikulin, A. A. Tsarev, US patent Applic, 2011/0098429 Al.

14 For general reviews on metal-mediated hydroamination reaction see a) K. D. Hesp, M. Stradiotto, *Chem.Cat.Chem.* **2010**, *2*, 1192; b) G. Zi, *Dalton Trans.* **2009**, 9101; c) S. C. Chemler, *Org. Biomol. Chem.* **2009**, 3009; d) T. E. Müller, K. C. Hultzsch, M. Yus, F. Foubelo, M. Tada, *Chem. Rev.* **2008**, *108*, 3795; e) I. Aillaud, J. Collin, J. Hannedouche, E. Schulz, *Dalton Trans.* **2007**, 5105; f) R. Severin, S. Doye, *Chem. Soc. Rev*. **2007**, *36*, 1407; g) K. C. Hultzsch, *Adv. Synth. Catal.* **2005**, *347*, 367; h) K. C. Hultzsch, *Org. Biomol. Chem.* **2005**, *3*, 1819; i) S. Hong, T. J. Marks, *Acc. Chem. Res.* **2004**, *37*, 673; j) P. W. Roesky, T. E. Müller, *Angew. Chem.* **2003**, *115*, 2812; *Angew. Chem., Int. Ed.* **2003**, *42*, 2708; k) T. E. Müller, M. Beller, *Chem. Rev.* **1998**, *98*, 675.

15 For neutral Group 4 metal-catalyzed hydroamination of aminoalkenes, see: a) R. K. Thomson, J. A. Bexrud, L. L. Schafer, *Organometallics* **2006**, *25*, 4069; b) M. C. Wood, D. C. Leitch, C. S. Yeung, J. A. Kozak, L. L. Schafer, *Angew. Chem., Int. Ed*. **2007**, *46*, 354; c) S. Majumder, A. L. Odom, *Organometallics* **2008**, *27*, 1174; d) A. L. Gott, A. J. Clarke, G. J. Clarkson, P. Scott, *Chem. Commun.*, **2008**, 1422; e) C. Müller, W. Saak, S. Doye, *Eur. J. Org. Chem*. **2008**, 2731; f) J. Cho, T. K. Hollis, T. R. Helgert, E. J. Valente, *Chem. Commun*. **2008**, 5001; g) D. C. Leitch, P. R. Payne, C. R. Dunbar, L. L. Schafer, *J. Am. Chem. Soc*. **2009**, *131*, 18246; h) A. L. Reznichenko, K. C. Hultzsch, *Organometallics* **2010**, *29*, 24; i) J. A. Bexrud, L. L. Schafer, *Dalton Trans*. **2010**, *39*, 361; j) Y.-C. Hu, C.-F. Liang, J.-H. Tsai, G. P. A. Yap, Y.-T. Chang, T.-G. Ong, *Organometallics* **2010**, *29*, 3357; k) K. Manna, A. Ellern, A. D. Sadow, *Chem. Commun*. **2010**, *46*, 339; l) K. Manna, S. Xu, A. D. Sadow, *Angew. Chem., Int. Ed*. **2011**, *50*, 1865-1868. m) J. Cho, T. K. Hollis, E. J. Valente, J. M. Trate, *J. Organomet. Chem.* **2011**, *696*, 373; n) H. Kim, P. H. Lee, T. Livinghouse, *Chem. Commun*. **2005**, 5205; o) J. A. Bexrud, J. D. Beard, D. C. Leitch, L. L. Schafer, *Org. Lett.* **2005**, *7*, 1959; p) H. Kim, Y. K. Kim, J. H. Shim, M. Kim, M. Han, T. Livinghouse, P. H. Lee, *Adv. Synth. Catal.* **2006**, *348*, 2609; q) D. A. Watson, M. Chiu, R. G. Bergman, *Organometallics* **2006**, *25*, 4731; r) A. L. Gott, A. J. Clarke, G. J. Clarkson, P. Scott, *Organometallics* **2007**, *26*, 1729; s) X. Li, S. Haibin, G. Zi, *Eur. J. Inorg. Chem.* **2008**, 1135. t) G. Zi, Q. Wang, L. Xiang, H. Song, *Dalton Trans*. **2008**, 5930; u) G. Zi, X. Liu, L. Xiang, H. Song *Organometallics* **2009**, *28*, 1127; v) G. Zi, F. Zhang, L. Xue, L. Ai, H. Song, *J. Organomet. Chem.* **2010**, *695*, 730; w) G. Zi, F. Zhang, L. Xiang, Y. Chen, W. Fang, H. Song, *Dalton Trans*. **2010**, *39*, 4048; x) A. Mukherjee, S. Nembenna, T. K. Sen,

S. Pillai Sarish, P. Kr. Ghorai, H. Ott, D. Stalke, S. K. Mandal, H. W. Roesky, *Angew. Chem., Int. Ed.* **2011**, *50*, 3968. z) T. R. Helgert, T. K. Hollis, E. J. Valente, *Organometallics* **2012**, *31*, 3002.

16 a) Bianchini, C.; Giambastiani, G.; Mantovani, G.; Meli, A.; Mimeau, D. *J. Organomet. Chem.*, **2004**, *689*, 1356. b) Barbaro, P.; Bianchini, C.; Giambastiani, G.; Guerrero Rios, I.; Meli, A.; Oberhauser, W.; Segarra, A. M.; Sorace, L.; Toti, A. *Organometallics*, **2007**, *26*, 4639. c) Bianchini, C.; Giambastiani, G.; Guerrero Rios, I.; Meli, A.; Oberhauser, W.; Sorace, L.; Toti, A. *Organometallics*, **2007**, *26*, 5066.

17 Salter, M. M.; Kobayashi, J.; Shimizu, Y.; Kobayashi, S. *Org. Lett.* **2006**, *8*, 3533.

18 Wu, Y.-J.; He, H.; L'Heureux, A. *Tetrahedron Lett.* **2003**, *44*, 4217.

19 Other "ligand-free" and/or microwave-free Cu-mediated conditions applied to this specific Ullmann coupling gave (in our hands) from 25 to 35 % reduced yields. See also ref. a) Correa, A.; Bolm, C. *Adv. Synth. Catal.* **2007**, *349*, 2673. b) Cristau, H.-J.; Cellier, P. P.; Spindler, J.-F.; Taillefer, M. *Eur J. Org. Chem.* **2004**, 695.

20 Menozzi, G.; Mosti, L.; Schenone, P. *J. Heterocyclic Chem.* **1987**, *24*, 1669.

21 Cho, C. S.; Lim, D. K.; Heo, N. H.; Kim, T.-J-; Shim, S. C. *Chem. Commun.* **2004**, 104.

22 Kelly, M. G.; Kincaid, J.; Duncton, M.; Sahasrabudhe, K.; Janagani, S.; Upasani, R. B.; Wu, G.; Fang, Y.; Wei, Z.-L. US patent 2006/0194801 Al, pag 39.

23 Joule, J. A. and Mills K. in *Heterocyclic Chemistry (5th Edition)*, Wiley Ed. **2010**, pp.718. ISBN: 978-1-4051-9365-8

24 This co-existence is reasonably caused by the combination of three factors: (a) disorder present on the dimethylamido ligands; (b) the (very) low temperature data collection and (c) the employ of two-dimensional CCD X-ray detectors.

25 Similarly to compounds **13** and **14**, two almost identical molecules are present in the asymmetric unit; they are related to each other through a C_2 pseudo-symmetry axis along the *b* direction. Consequently, the same chemical species is "seen" as two structurally different molecules. See also ref. 9. Half of a pentane molecule was found as part of the asymmetric unit of **18** as crystallization solvent.

26 The calculated index of trigonality for each structure is 0.16, 0.22, 0.21 and 0.22 for **17**, **18**, **19** and **20**, respectively. See also ref. Addison, A. W.; Rao, T. N.; Reedijk, J.; van Rijn, J.; Verschoor, G. C. *J. Chem. Soc. Dalton Trans.* **1984**, 1349.

27 For related structures containing M-amido bonds see also: [Zr] a) see refs. 10 and 15u b) Panda, T. K.; Tsurugi, H.; Pal, K.; Kaneko, H.; Mashima, K. *Organometallics*, **2010**, *29*, 34. c) See also ref. 3d. [Hf] e) Nienkemper, K.; Kehr, G.; Kehr, S.; Frohlich, R.; Erker, G. *J. Organomet. Chem.*, **2008**, 693, 1572. f) See also refs. 3d,10, 27b

28 For related structures containing M-$N_{pyrazolyl}$ bonds see also: [Zr] a) Otero, A.; Fernandez-Baeza, J.; Tejeda, J.; Lara-Sanchez, A.; Franco, S.; Martinez-Ferrer, J.; Carrion, M. P.; Lopez-Solera, I.; Rodriguez, A. M.; Sanchez-Barba, L. F. *Inorg.Chem.*, **2011**, *50*, 1826. [Hf] b) Otero, A.; Fernandez-Baeza, J.; Antinolo, A.; Tejeda, J.; Lara-Sanchez, A.; Sanchez-Barba, L.; Fernandez-Lopez, M.; Lopez-Solera, I. *Inorg.Chem.*, **2004**, *43*, 1350.

29 For related structures containing M-Ar bonds see also: [Zr] a) Bouwkamp, M.; van Leusen, D.; Meetsma, A.; Hessen, B. *Organometallics*, **1998**, *17*, 3645. b) Rubio, R. J.; Andavan, G. T. S.; Bauer, E. B.; Hollis, T. K.; Cho, J.; Tham, F. S.; Donnadieu, B. *J. Organomet. Chem*. **2005**, *690*, 5353. [Hf] c) see also ref. 3c,d. d) Tsurugi, H.; Yamamoto, K.; Mashima, K. *J. Am. Chem. Soc.*,**2011**, *133*, 732.

30 The theoretical Mulliken electronic charge on the pyrazolyl moieties of **13** and **15** did not show any relevant difference of the nucleophilic character of the pyridinic nitrogen on both systems. N_{py}: **13** = –0.344 e; **15** = –0.323 e.

31 For a selected example of cationic Zr complexes operating under mild reaction conditions see: X. Wang, Z. Chen, X.-L. Sun, Y. Tang, Z. Xie, *Org. Lett*., **2011**, *13*, 4758.

32 For rare examples of neutral Group-IV complexes catalyzing hydroamination of secondary aminoalkenes, see refs: 15h,m,x, 31.

33 C. Müller, R. Koch, S. Doye, *Chem. Eur. J.*, **2008**, *14*, 10430.

34 Calculated relative internal energies E have been reported for both systems. The relative Gibbs energy values G are not provided, being not relevant to the work's conclusions and beyond the scope of the present work

35 Although the authors are aware of the relatively high energy values calculated for TS4 (with both substrates) and associated to reactions occurring at room temperature, the present study is aimed at addressing, at molecular level, the existence of cooperative and favorable interactions between substrate(s) and complex. The supposed operative mechanism is assumed on the basis of several literature precedents and it well fits with all other experimental outcomes. Accordingly, very similar behaviors have been computationally ascertained for both substrates, at least on monitoring them by the most classic pathway assumed for this chemistry. Apart of this, the authors are convinced that an in-depth theoretical study will be needed to definitively clarify, *in silico*, the truly operative mechanistic path.

36 Slightly reduced conversions of **I** measured throughout the kinetic tests (compared to values reported on Table 4) are likely due to diffusive limiting factors for runs accomplished in a J-Young NMR tube (see Experimental Section)

37 To the best of our knowledge, C,C,C-*N*-heterocyclic carbene pincer complexes based on Group-IV transition metals represent the only pincer-type systems to date to be active catalysts in the hydroamination reaction of unactivated alkenes. All these complexes typically require extremely severe reaction conditions to promote the cyclization of variably substituted primary aminoalkenes. See refs. 15f,m,z

38 Zhukova, O. S.; Lazareva, L. P.; Artem'yanov, A. P. *Russian J. Electrochem.* **2001**, *37*, 738.

39 CrysAlisCCD 1.171.31.2 (release 07-07-2006), CrysAlis171 .NET, Oxford Diffraction Ltd.

40 CrysAlis RED 1.171.31.2 (release 07-07-2006), CrysAlis171 .NET, Oxford Diffraction Ltd.

41 A. Altomare, M. C. Burla, M. Camalli, G. L. Cascarano, C. Giacovazzo, A. Guagliardi, A. G. Moliterni, G. Polidori, R. Spagna, *J. Appl. Crystallogr.* **1999**, *32*, 115.

42 Sheldrick, G. M. SHELXL (**1997**).

43 L. J. Farrugia, *J. Appl. Crystallogr.* **1997**, *30*, 565.

44 Frisch M. J. *et al.*, *Gaussian09*, Revision A.02, Gaussian Inc., Wallingford CT, **2009**.

45 Zhao, Y.; Truhlar, D. G. *Theor. Chem. Account* **2008**, *120*, 215.

46 (a) Hay, P. J. Wadt, W. R. *J. Chem. Phys.* **1985**, *82*, 270. (b) Wadt, W. R.; Hay, P. J. *J. Chem. Phys.* **1985**, *82*, 284.

47 (a) Höllwarth, A.; Böhme, M.; Dapprich, S.; Ehlers, A. W.; Gobbi, A.; Jonas, V.; Köhler, K. F.; Stegmann, R.; Veldkamp, A.; Frenking, G. *Chem. Phys. Lett.* **1993**, *208*, 237. (b) Ehlers, A. W.; Böhme, M.; Dapprich, S.; Gobbi, A.; Höllwarth, A.; Jonas, V.; Köhler, K. F.; Stegmann, R.; Veldkamp, A.; Frenking, G. *Chem. Phys. Lett.* **1993**, *208*, 111.

48 The CP2K developers group. http://www.cp2k.org.

49 Goedecker, S.; Teter, M.; Hutter, J. *J. Phys. Rev. B* **1996**, *54*, 1703.

50 Perdew, J. P. Burke, K.; Ernzerhof, M. *Phys. Rev. Lett.* **1997**, *78*, 1396 (E).

51 Grimme, S. J.; Antony J.; Ehrlich, S; Krieg H. *Comput. Chem.* **2010**, *132*, 154104.

5

Cationic Group IV Pincer-type Complexes for Polymerization and Hydroamination Catalysis

5.1 Abstract

Neutral Zr^{IV} and Hf^{IV} dimethyl complexes stabilized by unsymmetrical dianionic {*N*,*C*,*N'*} pincer ligands have been prepared from their corresponding bis-amido complexes upon treatment with $AlMe_3$. Their structure consists of a central σ-bonded aryl donor group (*C*) capable of forming robust M-C bonds with the metal center, enforced by the synergic effect of both the coordination of peripheral donor groups (*N*) and the chelating rigid structure of the {*N*,*C*,*N*} ligand framework. Such a combination translates into systems having a unique balance between stability and reactivity. These Zr^{IV} and Hf^{IV} dimethyl complexes were converted *in situ* into cationic species $[M^{IV}\{N,C^-,N^-\}Me][B(C_6F_5)_4]$ which are active catalysts for the room temperature (r.t.) intramolecular hydroamination/cyclization of primary and secondary aminoalkenes as well as for the high temperature ethylene/1-octene copolymerizations.

5.2 Introduction

Tuning the performance of single site catalysts by designing novel ligand structures still remains one of the most challenging issues for many inorganic and organometallic chemists. Varying the steric and electronic properties of a given ligand's family, while maintaining its donor atom set unchanged, constitutes a key tool for controlling and investigating the reactivity, stability and catalytic performance at the coordinated metal center. Our recent studies on Group IV organometallics for C-C (polymerization and copolymerization)[1] and C-N (intramolecular hydroamination)[2] bond-forming reactions have provided original insights on the organometallic reactivity and catalysis of pyridylamido early transition metal compounds.[3] Redrawing their molecular framework (**Figure 5.1**, left *vs.* right) has resulted in the preparation of unsymmetrical dianionic $\{N,C,N'\}$ pincer-type systems characterized by remarkable thermal stability and catalytic activity.[4]

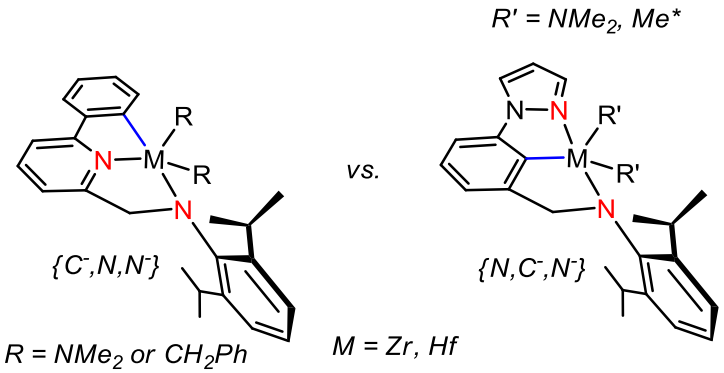

Figure 5.1. Left: Group-IV Pyridylamido Complexes.[1,2,3] Right: Group IV $\{N,C,N'\}$-pincer complexes;[4] (*) this work.

The basic structure of the newly synthesized complexes consists of a central σ-bonded aryl donor group (*C*) capable of forming robust M-C bonds with a given metal center which is enforced by the coordination of peripheral donor groups (*N*) and the chelating rigid structure of the $\{N,C,N\}$ framework. Such structural features translate into systems having a unique balance between stability and reactivity. While a relatively

large number of late transition metal complexes stabilized by symmetrical {*N*,*C*,*N*}-pincer-type ligands have been reported to date,[5] much less work has been devoted to the synthesis and characterization of their early transition metal counterparts.[6,5a] Indeed, prior to our recent study,[4] unsymmetrical {*N*,*C*,*N'*}-systems were rather uncommon and limited to complexes based on either palladium[7,8,9] or rhodium.[9] Unlike pyridylamido systems (**Figure 5.1**, left), pincer-type bis-amido Group-IV complexes (**Figure 5.1**, right) have shown only negligible activity in olefin polymerization while being good to excellent candidates for the intramolecular hydroamination/cyclization of primary aminoalkenes under mild reaction conditions (low reaction temperature and catalyst loading).[4]

In this work we describe the synthesis and characterization of the dimethyl Zr^{IV} and Hf^{IV} pincer complexes (starting from the bis-amido precursors) as well as their activation upon treatment with organoboron compounds. The resulting cationic species have been investigated with respect to their performance in high-temperature ethylene-1-octene copolymerization as well as in intramolecular hydroamination of primary and secondary aminoalkenes. This study also gives useful insights on specific organometallic activities of these Group-IV pincer complexes. In particular, the variety of their activation modes, resulting from the treatment of the dimethyl species with different organoboron compounds as well as the ability of the M^{IV}-C_{Ar} (M = Zr, Hf) bonds to undergo olefin insertion, compared to state-of-the-art Group-IV pyridylamido complexes, will be discussed.[1b,10]

5.3 Results and Discussions

5.3.1 Synthesis and characterization of [Zr^{IV}(κ^3-N,C,N')Me$_2$] (3) and [Hf^{IV}(κ^3-N,C,N')Me$_2$] (4) from the bis-amido derivatives[4] (1 and 2).

Conversion of **1** and **2** into their dimethyl analogues is carried out by following literature procedures already used for pyridylamido complexes.[11] Treatment of the bis-amido precursors in a cooled toluene solution with 5 equiv. of $AlMe_3$ results in a clean alkylation to give the dimethyl-derivatives **3** and **4** as light-brown and off-white microcrystals, respectively (**Scheme 5.1**). Purification by crystallization from concentrated pentane solutions at -30 °C is used to remove aluminium by-products providing **3** and **4** in excellent isolated yields (86 and 93 %, respectively).

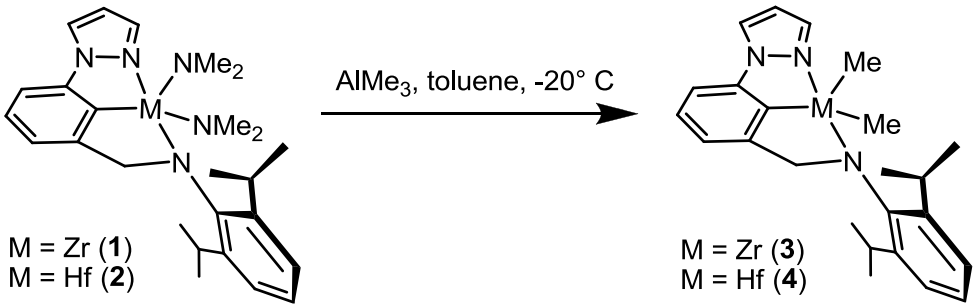

Scheme 5.1. Synthesis of [Zr^{IV}(κ^3-*N,C,N'*)Me$_2$] (**3**) and [Hf^{IV}(κ^3-*N,C,N'*)Me$_2$] (**4**).

Complexes **3** and **4** are isolated as air and moisture-sensitive microcrystals and are characterized by spectroscopic data and, in the case of **4**, X-ray diffraction studies. The ^{1}H and ^{13}C{^{1}H} NMR spectra indicate that both dimethyl complexes possess C_s symmetry in solution. Both complexes are highly soluble in aromatic hydrocarbons, but only sparingly soluble in aliphatic hydrocarbons (*n*-pentane, *n*-hexane). While colorless plate-like specimens of **4** are successfully grown by slow evaporation of a benzene-d_6-hexane solution at r.t., all attempts to isolate crystals of **3** suitable for X-ray analysis failed. An ORTEP representation of the crystal structure of **4** is given in **Figure 5.2**.

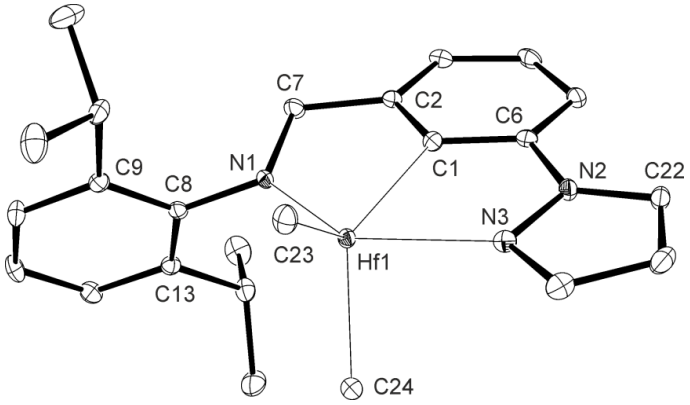

Figure 5.2. Crystal structure of [Hf^{IV}(κ^3-*N*,*C*,*N'*)Me_2] (**4**). Thermal ellipsoids are drawn at the 40% probability level. Hydrogen atoms are omitted for clarity.

Table 5.1 lists the main crystal and structural-refinement data, while selected bond lengths and angles are summarized in **Table 5.2**.

Table 5.1. Crystal data and structure refinement for complex **4.**

	4
CCDC number	942401
Empirical formula	$C_{24}H_{31}N_3Hf$
Formula weight	540.01
Temperature [K]	100(2)
Wavelength [Å]	0.71073
Crystal system, space group	Orthorhombic, *Pbca*
a [Å]	10.5097(2)
b [Å]	12.3812(2)
c [Å]	33.8422(5) Å
α [°]	90
β [°]	90
γ [°]	90
V [$Å^3$]	4403.64(13)
Z, D_c [g m^{-3}]	8, 1.629
Absorption coefficient [mm^{-1}]	4.751
F(000)	2144
Crystal size [mm]	0.22 × 0.22 × 0.04
Θ Range for data collection [°]	1.20 ÷ 27.50
Limiting indices	$-12 \le h \le 13$ $-16 \le k \le 16$ $-43 \le l \le 43$
Reflections collected/unique	51747/4968
GOF on F^2	1.198
Data/restraints/parameters	4968 / 0 / 259
Final *R* indices [I>2σ(*I*)]	*R*1=0.0207, w*R*2= 0.0374
R indices (all data)	*R*1=0.0258 w*R*2= 0.0387
Largest diff. peak and hole [e $Å^{-3}$]	0.643 and –1.670

Table 5.2. Selected bond distances (Å) and angles (°) for complex **4.**

	4
Hf(1)-N(1)	2.062(2)
Hf(1)-N(3)	2.313(2)
Hf(1)-C(1)	2.223(3)
Hf(1)-C(23)	2.245(3)
Hf(1)-C(24)	2.229(3)
N(2)-N(3)	1.368(3)
N(1)-C(7)	1.477(3)
N(1)-Hf(1)-N(3)	142.58(8)
N(1)- Hf(1)-C(1)	73.75(9)
N(3)- Hf(1)-C(1)	68.84(8)
C(1)-C(2)-C(7)-N(1)	-13.6(3)
C(1)-C(6)-N(2)-N(3)	5.0(3)
C(7)-N(1)-C(8)-C(9)	-100.3(3)
C(7)-N(1)-C(8)-C(13)	78.6(3)

The coordination environment at the metal center consists of two nitrogen atoms and one carbon atom from the dianionic tridentate $\{N,C^-,N^-\}$ ligand (κ^3-coordination) and two methyl groups. Similarly to parent bis-amido precursors, **4** shows a distorted square-pyramidal coordination geometry, with the ligand donor atoms and one methyl group lying equatorially and the other Me fragment occupying the axial position.[12] The κ^3-coordinated fragment is almost planar, with the pyrazolyl moieties slightly tilted away from the phenyl central core [θ(C1-C6-N2-N3) = 5.02]. Finally, the Hf(1)-N(1), Hf(1)-N(3) and Hf(1)-C(1) distances fall in a similar range to those measured for related structures.[13,14,15] Complexes **3** and **4** are indefinitely stable when stored under inert atmosphere, in the dark, at r.t.

5.3.2 In situ catalyst activation upon treatment with either trityl tetrakis(pentafluorophenyl)borate [Ph_3C][$B(C_6F_5)_4$] or tris(pentafluorophenyl)boron $B(C_6F_5)_3$: synthesis and characterization of cationic (3a, 4a) and neutral (3b, 4b) derivatives.

The cationic Zr^{IV} and Hf^{IV} complexes **3a** and **4a** are obtained upon treatment of **3** and **4** with 1 equiv. of [Ph_3C][$B(C_6F_5)_4$]. The reactions are performed at r.t. in benzene-d_6 and proceed rapidly through the clean abstraction of one methyl group from the metal center giving red-orange cationic species **3a** and **4a** (**Scheme 5.2**). Both compounds are barely soluble in apolar hydrocarbons (benzene and toluene) where they rapidly separate out as either dark-red (**3a**) or orange (**4a**) semi-solid compounds.

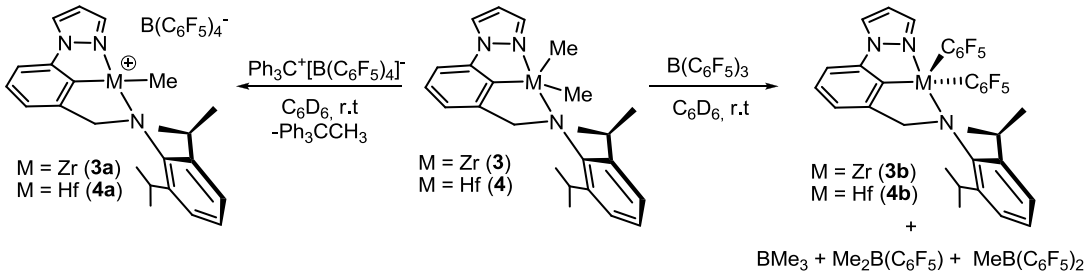

Scheme 5.2. Catalyst activation upon treatment with $[Ph_3C][B(C_6F_5)_4]$ and $B(C_6F_5)_3$.

Besides limiting their spectroscopic characterization, the scarce solubility of both ion pairs in apolar aromatic solvents is suggestive of weak ion pairing.[16] On the other hand, both ion pairs are highly soluble in polar aromatics such as mono- or dihalobenzene (halo = Cl, Br) where they form orange-red solutions. However, these solvents cause their rapid (within a few minutes) decomposition with the formation of further untreatable brown semi-solid compounds. **3a** forms a relatively stable solution in THF-d_8 which allows its complete spectroscopic characterization. As can be inferred from the ^{1}H NMR spectrum of **3a** (**Figure 5.3**), the weak coordinating character of the $B(C_6F_5)_4^-$ counterion translates into a C_s-symmetric system characterized by only two non-equivalent Me groups from the ^{i}Pr fragments and by two well-defined singlets at δ = 0.54 and 5.11 ppm, assigned to Zr-CH_3 and to ArCH_2N, respectively. Finally, the presence of the 1,1,1-triphenylethane side-product is confirmed by a residual singlet at δ = 2.16 ppm. Chemical conversion of **3** into the cationic system **3a** was spectroscopically estimated (^{1}H NMR) over 97 %.

All attempts to characterize **4a** in the same way (from a THF-d_8 solution) were frustrated by its ability to polymerize the solvent. Although highly soluble in THF, the resulting yellow-orange solution rapidly turns into a gel, thus hampering the full complex characterization.

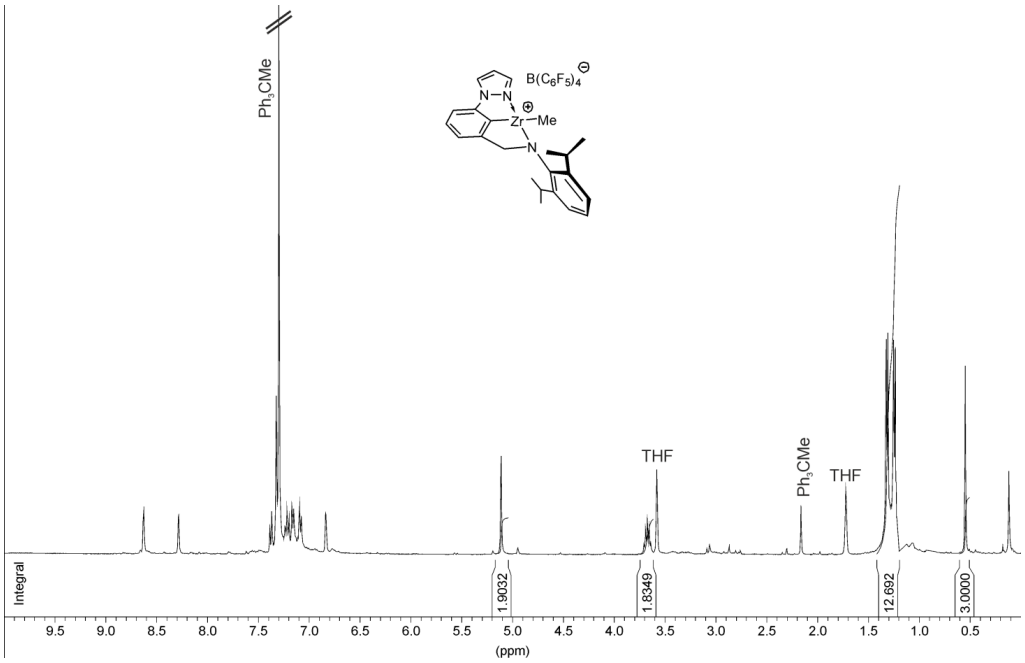

Fig. 5.3. ^{1}H-NMR spectrum (400 MHz, THF-d_8, 298K) of **3a**.

Similarly to the procedure outlined above, we have also studied the reactivity of **3** and **4** in the presence of 1 equiv. of the Lewis acid $B(C_6F_5)_3$ as an alkyl abstractor. The reaction is performed at r.t. in benzene-d_6 as solvent and its course is monitored by ^{1}H NMR spectroscopy. Both complexes react smoothly with borane, resulting in the clean and quantitative formation of new C_s-symmetric species although no resonance can be assigned to a residual methyl group. In this case, the reaction does not yield the expected cationic complexes $[M^{IV}(\kappa^3\text{-}N,C,N')Me][MeB(C_6F_5)_3]$ (M = Zr, Hf) but rather produces neutral compounds (**3b** and **4b**, **Scheme 5.2**) which arise from the C_6F_5 group transfer.[17] Benzene-d_6 solutions of **3b** and **4b** proved to be stable over a prolonged period of time at r.t. (and even at higher temperatures) without any apparent alteration. Multinuclear NMR spectra (^{1}H, ^{13}C{^{1}H}, ^{19}F{^{1}H} and ^{11}B{^{1}H}) of the reaction mixtures showed the progressive disappearance (within few minutes) of the distinctive signals attributed to the dimethyl precursors and the appearance of new peaks from **3b** and **4b** together with signals ascribed to the side-products BMe_3, $Me_2B(C_6F_5)$, and $MeB(C_6F_5)_2$.

Such a fast "groups exchange" is supposed to be responsible for the catalyst deactivation in the hydroamination experiments (*vide infra*).

5.3.3 Olefin polymerization and copolymerization studies.

Following our recent results in the field of polymerization catalysis using pyridylamido systems as polymerization catalysts,[1] cationic pincers **3a** and **4a** have been preliminarily evaluated with respect to their catalytic performance in room-temperature 1-hexene homo-polymerization.

Unlike cationic pyridylamido catalysts (**Figure 5.1**, left),[1b] **3a** and **4a** do not show any appreciable catalytic activity for 1-hexene polymerization under mild reaction conditions. It is noteworthy that, while cyclometallated pyridylamido catalysts typically undergo permanent complex modification *via* monomer insertion into the *lateral* reactive M^{IV}-Ar (M = Zr, Hf) bond,[18] **3a** and **4a** do not follow the same reactivity path at their *central* M-Ar bond. GC-MS analysis of the hydrolyzed reaction mixtures from the stoichiometric reactions of **3a** and **4a** with 1-hexene at r.t., reveal the presence of a unique peak (m/z = 333; retention time: 21.7 min) attributed to the unmodified ligand (**Figure 5.4**).[19] Looking beyond the simple re-distribution of the donor atom set around the metal center [{*C,N,N'*} *vs.* {*N,C,N'*}, **Figure 5.1**], one may argue that *in situ* monomer insertion into the M-Ar bond (occurring on the pyridylamido systems exclusively), constitutes a key element for the generation of kinetically active species in low temperature polymerization runs.[10]

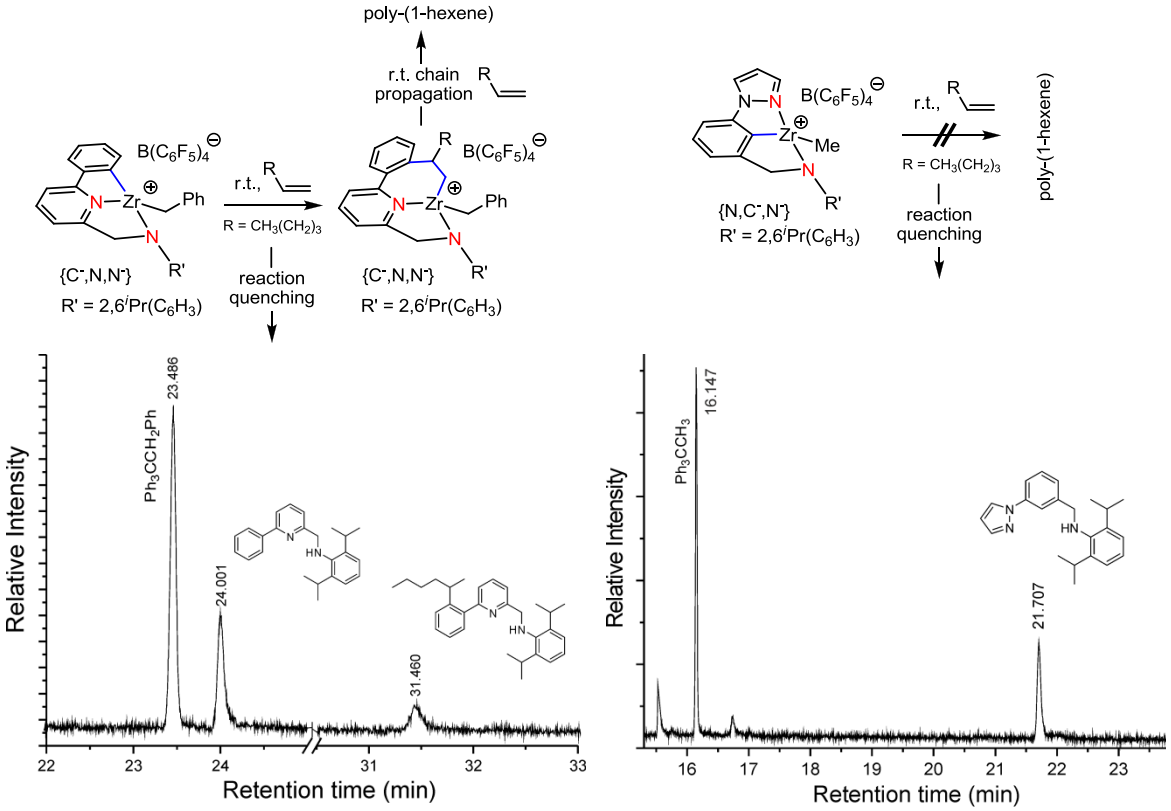

Figure 5.4. Left: α-olefin insertion into the *lateral* M-Ar bond of a state-of-the-art Group IV amidopyridinate complex[18] and GC trace[19] (reproduced with permission from Wiley)[1b] of the reaction solution (catalyst:monomer 1:1) after quenching with MeOH. Right: GC trace[19] of the reaction solution (catalyst **3a**:monomer 1:1) after quenching with MeOH.

5.3.4 High-temperature ethylene/1-octene copolymerization study.

Ethylene/1-octene copolymerization tests have been carried out at 120 °C in a 2 L batch reactor filled with ethylene and 1-octene. Both pre-catalysts **3** and **4** are activated *in situ* using $[HNMe(C_{18}H_{37})_2][B(C_6F_5)_4]$ (1.2 equiv., relative to pre-catalyst) as activator. For the sake of completeness of the copolymerization study, the C_s-[1b] (**5**) and C_1-symmetric[20] (**6**) pyridylamido polymerization catalysts of state-of-the-art (**Figure 5.5**), having identical denticity but different distribution of the donor atom set around the metal center [{*C,N,N'*} *vs.* {*N,C,N'*}], have been evaluated, under identical conditions, for comparison.

Ethylene/1-octene copolymerization data are summarized in **Table 5.3**. Both pincer systems are moderately active in copolymerization catalysis giving ethylene/1-octene

copolymers (linear low-density polyethylenes - LLDPEs) with molecular weights ranging from 143 kDa for **3** to 265 kDa for **4**.

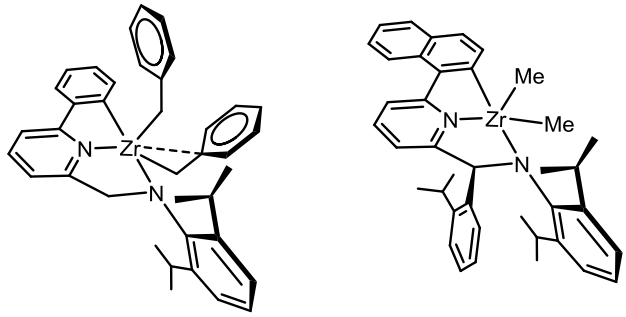

5 **6**

Figure 5.5. State-of-the-art pyridylamido polymerization catalysts.

In spite of moderate productivities compared to the pyridylamido systems **5** and **6** (**Table 5.3**, entries 1-3 *vs*. 4-5), **3** and **4** provide copolymers with a relatively high degree of 1-octene incorporation in the polymer microstructure. Notably, **4** gives copolymers with the highest 1-octene incorporation degree, even better than the best performing pyridylamido catalyst **6** (up to 12.7 mol%, **Table 5.3**, entries 2 *vs*. 5). Such a level of incorporation is close to that found in ethylene-1-octene copolymers prepared by Ti-CGC {[(η^5-C_5Me_4)$SiMe_2$(^{t}BuN)$TiMe_2$)]}. The latter, which represents a real milestone in the ethylene/α-olefins copolymerization catalysis,[21,22] provides ethylene/1-octene copolymers with a co-monomer content of 13.8 mol% under identical conditions.20

Table 5.3. Ethylene/1-octene copolymerization data.[a]

Entry	pre-catalyst [μmol]	Yield [g]	Catalyst productivity [b]	M_w [kDa]	M_w/M_n	Octene content [mol%][c]
1	**3** [20]	8.6	430	143	48.78	5.3
2	**4** [6]	3.6	600	134	2.7	12.7
3	**4** [20]	9.9	495	265	4.9	11.2
4	**5** [10]	16.7	1670	542	2.4	4.2
5	**6** [0.7]	12.3	17572	2010	1.6	8.4

[a] Polymerization conditions: temp = 120 °C; 533 mL of Isopar-E; 250 g of 1-octene; ethylene pressure = 460 psi (~ 31.7 bar); precatalyst : activator : MMAO = 1 : 1.2 : 10; activator: [$HNMe(C_{18}H_{37})_2$][$B(C_6F_5)_4$]; polymerization time: 10 min. [b] Expressed as g of polymer x (mmol of catalyst)$^{-1}$. [c] Measured by IR spectroscopy.

Finally, both *pincer* complexes form copolymers with higher polydispersities than those resulting from polyolefins produced by state-of-the-art pyridylamido systems (**Table 5.3**, entries 1-3 vs. 4-5). Overall, while copolymers produced by pre-catalyst **4** show the higher co-monomer content together with moderate polydispersities and monomodal distribution of the polymer molecular weights, the Zr-analogue **3** generates polyolefins with relatively low co-monomer contents, significantly higher M_w/M_n values and polymodal distribution of the polymer molecular weights.

5.3.5 Catalytic activity of cationic pincer complexes in the intramolecular hydroamination of primary and secondary aminoalkenes.[23]

Our interest in the hydroamination reaction stems from previous studies involving the neutral bis-amido complexes **1** and **2** (**Scheme 5.1**), which readily and efficiently promote the intramolecular hydroamination of primary aminoalkenes under mild reaction conditions (*i.e.*, reaction temperature and catalyst loading).[4,24,25] It was of interest for us to determine whether the activated **3a,b** and **4a,b** species could promote the hydroamination reaction as efficiently as neutral bis-amido parent **1** and **2**.[4] All catalytic runs (**Scheme 5.3**) are performed under inert atmosphere in a J-Young NMR tube and the reaction process is monitored by ^{1}H NMR with spectra recorded at constant reaction times. Under the adopted experimental conditions, all hydroamination runs are extremely selective towards the cyclization product, with no evidence for any side-product.

Substrate conversions are determined by ^{1}H NMR spectroscopy using ferrocene as internal standard (spectra acquired at different reaction times) and are confirmed by gas-chromatography of the final crude reaction mixture. All catalytic details and optimized cyclization conditions are listed in **Table 5.4**.

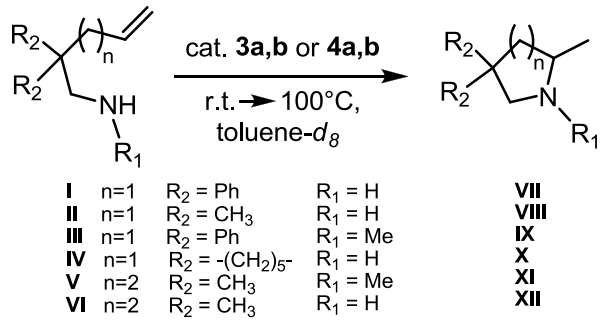

Scheme 5.3. Intramolecular hydroamination of primary and secondary aminoalkenes with pre-catalysts **3** and **4**.

As **Table 5.4** shows, both cationic systems **3a** and **4a** are active catalysts for the intramolecular hydroamination reaction of a number of model primary and secondary aminoalkenes providing, for selected issues, relatively fast and complete substrate conversions already at r.t. (**Table 5.4**, entries 2 and 5). Only one other cationic Group-IV complex is known leading to the complete cyclization of **I** under the above-mentioned reaction conditions (i.e., reaction temperature and catalyst loading).[25c,26] Notably, structurally related $\{C^-,N,N^-\}$ cationic Group IV pyridylamido complexes, recently reported by some of us,[2] typically require more severe reaction conditions and high catalyst loadings to promote the cyclization of **I**, efficiently (100 °C, 10 mol% of the catalyst). Comparing different cyclization precursors under similar reaction conditions (**Table 5.4**, entries 2 and 5 *vs*. 7 and 9, 12 and 15, 22 and 24), makes clear the existence of a significant substrate dependence on the cyclization rate. In particular, the diphenyl-substituted precursor **I** provides the cyclization product **VII** quantitatively (entries 1-2) either at r.t. within 20 min or more rapidly upon heating at 100 °C (entry 3). For all other cyclization precursors (**II, IV-VI**), only more severe reaction conditions (from 50 to 100 °C) result in appreciable substrate conversions.

Analysis of the cyclization results shows the higher the reaction temperature, the higher the substrate conversion and the shorter the reaction time (entries 12 *vs*. 13-14, 15 *vs*. 16-17).

Table 5.4. Intramolecular hydroamination of primary and secondary aminoalkenes catalyzed by complexes **3a,b** – **4a,b**.[a]

Entry	Catalyst[b]	Substrate	Product	T [° C]	*t* [h]	Conver.[%][c]
1	**3a**	**I**	**VII**	r.t	0.16	75
2	**3a**	**I**	**VII**	r.t	0.33	> 99
3	**3a**	**I**	**VII**	100	0.16	> 99
4	**4a**	**I**	**VII**	r.t	0.16	70
5	**4a**	**I**	**VII**	r.t	0.33	> 99
6	**4a**	**I**	**VII**	100	0.16	94
7	**3a**	**II**	**VIII**	100	5	68
8	**3a**	**II**	**VIII**	100	10	97
9	**4a**	**II**	**VIII**	100	24	78
10	**4a**	**II**	**VIII**	100	48	95
11	**3a**	**III**	**IX**	r.t.	2	31
12	**3a**	**III**	**IX**	50	6	80
13	**3a**	**III**	**IX**	100	0.5	96
14	**3a**	**III**	**IX**	100	1	> 99
15	**4a**	**III**	**IX**	50	8	78
16	**4a**	**III**	**IX**	100	0.66	90
17	**4a**	**III**	**IX**	100	1	> 99
18	**3a**	**IV**	**X**	100	0.16	92
19	**3a**	**IV**	**X**	100	0.33	> 99
20	**4a**	**IV**	**X**	100	0.16	92
21	**4a**	**IV**	**X**	100	0.33	> 99
22	**3a**	**V**	**XI**	100	10	87
23	**3a**	**V**	**XI**	100	17	> 99
24	**4a**	**V**	**XI**	100	40	51
25	**3a**	**VI**	**XII**	100	17	94
26	**4a**	**VI**	**XII**	100	17	92
27	**3b**	**I**	**VII**	100	24	-[d]
28	**3b**	**III**	**IX**	100	24	-[d]
29	**4b**	**I**	**VII**	100	12	-[d]

[a]Reaction conditions: substrate: 0.16 mmol, catalyst: 5 mol% (8 μmol), solvent: Toluene-d_8 (0.6 mL). [b] Complexes 3a-b and 4a-b are generated *in situ* from 3 and 4 as described in the experimental section [c] Determined by *in-situ* ^{1}H NMR spectroscopy using ferrocene as internal standard. [d] appreciable amounts of cyclization product were not observed. r.t.: 21-22°C.

Furthermore, cyclization of primary aminoalkenes (generally) proceeds more efficiently compared to the cyclization of secondary ones (entries 1 *vs*. 11, 3 *vs*. 13, 6 *vs*. 16 and 26 *vs*. 24). Although this latter trend cannot be considered as a real distinctive feature of the catalytic systems used, the relevant reactivity gap observed between **I** and **II**, **IV**-**VI**, suggests the occurrence of cooperative and positive substrate-complex interactions beyond the simple kinetic Thorpe-Ingold effect. DFT calculations are currently ongoing to address both the existence and the nature of the above mentioned substrate-complex interactions and will be reported elsewhere.

Similarly to several literature precedents[24,25] with Group IV catalysts employed in hydroamination reactions, **3a** displays (under similar reaction conditions) higher catalytic performances compared to the **4a** analogue. Unlike neutral bis-amido parent precursors, hydroaminations with cationic **3a** and **4a** proceed efficiently on both primary and secondary aminoalkenes (entries 1 *vs*. 3, 3 *vs*. 13, 6 *vs*. 17, 23 *vs*. 25). All these evidences taken together support the hypothesis of $8e^-$ amido species as intermediates in the catalytic cycle.[25c] Finally, only catalyst activation with $[Ph_3C][B(C_6F_5)_4]$ gives catalytically (cationic) active forms (**3a** and **4a**) whereas complexes obtained upon catalyst activation with $B(C_6F_5)_3$ (**3b** and **4b**) do not show any apparent catalytic performance, even after prolonged reaction times (**Table 5.4**, entries 27-29). Such a reactivity trend is in line with the different activation paths of the dimethyl complexes **3** and **4** as outlined above {$[Ph_3C][B(C_6F_5)_4]$ *vs*. $B(C_6F_5)_3$}.

5.4 Conclusions

The study describes the preparation of cationic unsymmetrical {*N*,*C*,*N*'} Group IV pincer complexes and demonstrates their ability to promote efficiently intramolecular hydroamination reactions as well as ethylene/1-octene copolymerizations in high temperature solution processes. Unlike neutral bis-amido precursors, cationic Zr^{IV} and Hf^{IV} species are active forms in the hydroamination reaction of primary and secondary aminonoalkenes revealing a remarkable substrate dependence on the cyclization rate. As a result, only selected substrates undergo quantitative and rapid hydroamination/cyclization already at r.t. Aimed at widening the catalysts application range, cationic Zr^{IV} and Hf^{IV} species have also been investigated in ethylene/1-octene copolymerizations. In spite of moderate productivities both systems provide copolymers with a relatively high degree of 1-octene incorporation (up to 12.7 mol%) similar to that

obtained with the best performing state-of-the-art half-sandwich Ti-CGC. Specifics of the activation modes (generation of cationic species from dimethyl precursors) for these Group-IV pincer complexes are given in detail. Overall the study highlights the ability of robust and thermally stable cationic Group IV systems to operate efficiently within *ad-hoc* catalytic processes under increasing temperature conditions.

5.5 Experimental Section

General considerations and materials characterization. All air- and/or moisture-sensitive reactions were performed under inert atmosphere in flame-dried flasks by using standard Schlenk-type techniques or in a drybox filled with nitrogen. Benzene and toluene were purified by distillation from sodium/triglyme benzophenone ketyl and stored over 4 Å molecular sieves or were obtained by means of a MBraun solvent purification system. Benzene-d_6 and toluene-d_8 were dried over sodium/benzophenone ketyl and condensed *in vacuo* over activated 4 Å molecular sieves prior to use. Amino alkenes **I**,[27] **II**,[28] **III**,[29] **IV**,[30] **V**[25a] and **VI**[28] were prepared according to literature procedures. All other reagents and solvents were used (unless otherwise stated) as purchased from commercial suppliers without further purification. The bis(amido) pincer-complexes [Zr^{IV}(κ_3-*N,C,N'*)$(NMe_2)_2$] (**1**), [Hf^{IV}(κ_3-*N,C,N'*)$(NMe_2)_2$] (**2**) were obtained on a gram scale according to standard procedures described in the literature.4 1D (^{1}H and ^{13}C{^{1}H}) and 2D (COSY H–H, HETCOR H–C) NMR spectra of all organometallic species were obtained on either a Bruker Avance DRX-400 spectrometer (400.13 and 100.61 MHz for ^{1}H and ^{13}C, respectively) or a Bruker Avance 300 MHz instrument (300.13 and 75.47 MHz for ^{1}H and ^{13}C, respectively). Chemical shifts (δ) are reported in ppm relative to trimethylsilane (TMS), referenced to the chemical shifts of residual solvent resonances (^{1}H and ^{13}C). The multiplicities of the ^{13}C{^{1}H} NMR

spectra were determined on the basis of the $^{13}C\{^{1}H\}$ JMOD sequence and quoted as: CH_3, CH_2, CH, and C for primary, secondary, tertiary, and quaternary carbon atoms, respectively. The C, H, N elemental analyses were made at ICCOM-CNR using a Thermo FlashEA 1112 Series CHNS-O elemental analyzer with an accepted tolerance of ±0.4 units on carbon (C), hydrogen (H), and nitrogen (N). Molecular weight distribution (Mw, Mn) was determined by analysis on a custom Dow-built Robotic-Assisted Dilution High-Temperature Gel Permeation Chromatographer (RAD-GPC). Polymer samples were dissolved for 90 minutes at 160°C at a concentration of 30 mg/mL in 1,2,4-trichlorobenzene (TCB) and stabilized by 300 ppm BHT. They were then diluted to 1 mg/mL immediately before a 400µL aliquot of the sample was injected. The GPC utilized two Polymer Labs PLgel 10µm MIXED-B columns (300x10mm) at a flow rate of 2.0 mL/minute at 150 °C. Sample detection was performed using a PolyChar IR4 detector in concentration mode. A conventional calibration of narrow Polystyrene (PS) standards was utilized, with apparent units adjusted to homo-polyethylene (PE) using known Mark-Houwink coefficients for PS and PE in TCB at this temperature. Thermal characterization was performed on a TA Instruments Q2000 DSC. 5 mg of each sample was weighed into a TZero aluminum DSC pan with lid. A heat:cool:heat profile from -90 °C to 200 °C at 10 °C/min was used, under nitrogen purge. Data analysis was performed using TA Universal Analysis software. T_g (where appropriate) was calculated using an onset-at-inflection methodology. T_m was determined by calculating $T_{m(peak)}$ after linear integration of extrapolation from post-melt plateau. Both T_g and T_m were calculated from the second heat cycle.

X-ray data measurement. X-ray intensity data were collected on a Bruker SMART diffractometer using MoKα radiation (λ = 0.71073 Å) and an APEXII CCD area

detector. Raw data frames were read by program SAINT[31] and integrated using 3D profiling algorithms. The resulting data were reduced to produce hkl reflections and their intensities and estimated standard deviations. The data were corrected for Lorentz and polarization effects and multiscan absorption corrections were applied. The structure was solved (SHELXS-97) and refined (SHELXL-2013) using full-matrix least-squares refinement. The non-H atoms were refined with anisotropic thermal parameters and H atoms were calculated in idealized positions and refined riding on their parent atoms. The refinement was carried out using F^2 rather than F values. R_1 is calculated to provide a reference to the conventional R value, but its function is not minimized. Crystals were grown by slow evaporation of a benzene-d_6/hexane solvent mixture at r.t. A clear colorless plate-like specimen of **4** was used for the X-ray crystallographic analysis.

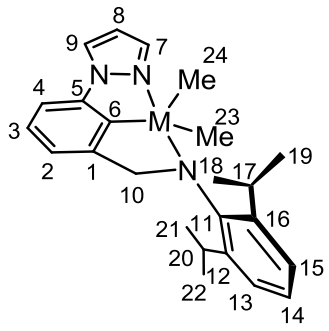

General procedure for the synthesis of complexes $Zr^{IV}\{\kappa^3$-*N,C,N'*$\}Me_2$ (3) and $Hf^{IV}\{\kappa^3$-*N,C,N'*$\}Me_2$ (4). A toluene (7 mL) solution of the selected complex $M^{IV}\{\kappa^3$-*N,C,N'*$\}(NMe_2)_2$ (M^{IV} = Zr, Hf) (0.5 mmol) was cooled down to -20 °C for 3 h, and a 2 M hexane solution of $AlMe_3$ (2.5 mmol, 5 equiv.) was added dropwise. The solution was then allowed to warm at r.t. within 2 h under stirring. Afterwards, the solvent was removed under reduced pressure and the semi-solid crude material was dried under reduced pressure. Crude complexes **3** and **4** were purified by crystallization at -30 °C from concentrated pentane solutions. Brown and off-white microcrystals were collected for **3** and **4**, respectively. Suitable crystals of **4** were grown at r.t. as colorless plate-like specimens from a benzene-d_6/hexane mixture. **3**: (86 % isolated yield); ^{1}H NMR (300 MHz, C_6D_6, 293K): δ 0.50 (s, 6H, Me, $H^{23,24}$), 1.26 (d, $^3J_{HH}$ = 6.8 Hz, 6H, $CH(CH_3{}^ACH_3{}^B)$, $H^{19,22}$), 1.44 (d, $^3J_{HH}$ =

6.8 Hz, 6H, CH(C$H_3{}^A$C$H_3{}^B$, $H^{18,21}$), 4.07 (sept, $^3J_{HH}$ = 6.8 Hz, 2H, CH(CH_3)$_2$, $H^{17,20}$), 5.11 (s, 2H, CH_2N, H^{10}), 5.65 (m, 1H, CH Ar, H^8), 6.47 (m, 1H, CH Ar, H^3), 6.82 (m, 1H, CH Ar, H^9), 7.03 (m, 2H, CH Ar, $H^{2,4}$), 7.27-7.30 (4H, CH Ar, $H^{7,13,14,15}$). $^{13}C\{^1H\}$ NMR (75 MHz, C_6D_6, 293 K): δ 23.9 (CH(CH$_3$)$_2$, $C^{17,20}$), 28.0 (CH(CH$_3{}^A$$CH_3{}^B$), $C^{18,21}$), 28.1 (CH(CH$_3{}^A$CH$_3{}^B$), $C^{19,22}$), 45.2 (CH$_3$, Me, $C^{23,24}$), 70.0 (C^{10}), 107.3 (C^3), 107.9 (C^8), 122.0 (C^2), 124.2 ($C^{13,15}$), 125.3 (C^9), 126.7 (C^{14}), 128.9 (C^4), 141.1 (C^7), 142.1 (C), 143.4 (C), 148.5 (C), 156.2 (C), 177.7 (C^6). Anal. Calcd (%) for $C_{24}H_{31}N_3Zr$ (452.75): C 63.67, H 6.90, N 9.28; found C 63.75, H 6.95, N 9.32. **4**: (93 % isolated yield); ^1H NMR (300 MHz, C_6D_6, 293K): δ 0.33 (s, 6H, Me, $H^{23,24}$), 1.27 (d, $^3J_{HH}$ = 6.8 Hz, 6H, CH(CH$_3{}^A$C$H_3{}^B$), $H^{19,22}$), 1.46 (d, $^3J_{HH}$ = 6.8 Hz, 6H, CH(C$H_3{}^A$CH$_3{}^B$, $H^{18,21}$), 4.08 (sept, $^3J_{HH}$ = 6.8 Hz, 2H, CH(CH$_3$)$_2$, $H^{17,20}$), 5.24 (s, 2H, CH_2N, H^{10}), 5.61 (m, 1H, CH Ar, H^8), 6.53 (m, 1H, CH Ar, H^2), 6.81 (m, 1H, CH Ar, H^9), 7.01-7.11 (2H, CH Ar, $H^{3,4}$), 7.24 (m, 1H, CH Ar, H^7), 7.31 (3H, CH Ar, $H^{13,14,15}$). $^{13}C\{^1H\}$ NMR (75 MHz, C_6D_6, 293 K): δ 24.0 (CH(CH$_3{}^A$$CH_3{}^B$), $C^{18,21}$), 27.8 (CH(CH$_3$)$_2$, $C^{17,20}$), 28.1 (CH(CH$_3{}^A$CH$_3{}^B$), $C^{19,22}$), 59.5 (CH$_3$, Me, $C^{23,24}$), 69.2 (C^{10}), 107.4 (C^2), 108.0 (C^8), 122.5 (C^4), 124.2 ($C^{13,15}$), 125.8 (C^9), 126.3 (C^{14}), 129.0 (C^3), 141.3 (C^7), 143.3 (C), 144.0 (C), 148.3 (C), 156.2 (C), 187.9 (C^6). Anal. Calcd (%) for $C_{24}H_{31}HfN_3$ (540.01): C 53.38, H 5.79, N 7.78; found C 53.42, H 5.83, N 7.82.

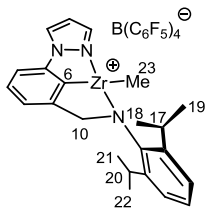

General procedure for the activation of the dimethyl precursors 3 and 4 with $Ph_3C^+[B(C_6F_5)_4]^-$. A solution of $Ph_3C^+[B(C_6F_5)_4]^-$ (1 equiv.) in C_6H_6 (1 mL) was added in one portion to a dry and degassed solution of the complex **3** (0.025 g, 55 μmol) in C_6H_6 (1 mL) at r.t. The mixture was stirred at r.t. for 20 min while a dark-red semi-solid material precipitates out. The semi-solid compound was decanted from the supernatant and washed with C_6H_6 (2 x 1.5 mL) and pentane (2 x 1.5 mL). The recovered material was

dried under vacuum to constant weight before being characterized spectroscopically in THF-d_8. **3a**: (estimated yield > 97% - conversion of **3** based on ^{1}H-NMR spectroscopy). ^{1}H NMR (400 MHz, THF-d_8, 293K, select data): δ 0.54 (s, 3H, Me, H^{23}), 1.24 (d, $^3J_{HH}$ = 6.8 Hz, 6H, CH(CH$_3^A$CH$_3^B$), H^{19,22}), 1.31 (d, $^3J_{HH}$ = 6.8 Hz, 6H, CH(CH$_3^A$CH$_3^B$, H^{18,21}), 3.65 (sept, $^3J_{HH}$ = 6.8 Hz, 2H, CH(CH$_3$)$_2$, H^{17,20}), 5.11 (s, 2H, CH$_2$N, H^{10}). ^{13}C{^{1}H} NMR (100 MHz, THF-d_8, 293 K, select data): δ 24.1(CH(CH$_3$)$_2$, C^{17,20}), 27.9 (CH(CH$_3^A$CH$_3^B$), C^{18,21}), 28.6 (CH(CH$_3^A$CH$_3^B$), C^{19,22}), 51.7 (CH$_3$, Me, C^{23,24}), 73.4 (C^{10}), 178.7 (C^6). ^{19}F{^{1}H} NMR (376.3 MHz, THF-d_8, 293 K): δ -131.4 (s, *o*-C$_6$F$_5$), -161.6 (t, *p*-C$_6$F$_5$, J_{F-F} = 21.3 Hz), -165.5 (m, *m*-C$_6$F$_5$).

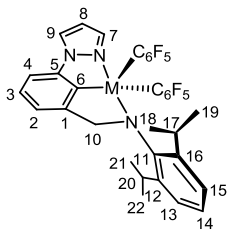

Reaction of 3 and 4 with B(C$_6$F$_5$)$_3$ in C$_6$D$_6$: A solution of B(C$_6$F$_5$)$_3$ (1 equiv.) in benzene-d_6 (0.5 mL) was added in one portion to a dry and degassed solution of the dimethyl complex (**3** or **4**) (0.025 g) in benzene-d_6 (0.5 mL). The reaction was periodically monitored via ^{1}H-NMR spectroscopy until complete conversion of the starting materials into **3b** or **4b** (10 min) together with boranes of formula MeB(C$_6$F$_5$)$_2$, Me$_2$B(C$_6$F$_5$) and BMe$_3$. **3b**: (estimated yield > 98% - conversion of **3** based on multinuclear NMR spectroscopy) ^{1}H NMR (400 MHz, C$_6$D$_6$, 293K): δ 0.67 (d, $^3J_{HH}$ = 6.8 Hz, 6H, CH(CH$_3^A$CH$_3^B$), H^{19,22}), 0.73 (br s, B(CH$_3$)$_3$), 0.96 (br s, B(CH$_3$)$_2$(C$_6$F$_5$)), 1.07 (d, $^3J_{HH}$ = 6.8 Hz, 6H, CH(CH$_3^A$CH$_3^B$, H^{18,21}), 1.33 (br s, BCH$_3$(C$_6$F$_5$)$_2$), 3.67 (sept, $^3J_{HH}$ = 6.8 Hz, 2H, CH(CH$_3$)$_2$, H^{17,20}), 5.28 (s, 2H, CH$_2$N, H^{10}), 5.63 (m, 1H, CH Ar, H^8), 6.37 (m, 1H, CH Ar, H^2), 6.73 (m, 1H, CH Ar, H^9), 6.98-6.93 (2H, CH Ar, H^{3,4}), 7.05-7.03 (2H, CH Ar, H^{13,15}), 7.16 (1H, CH Ar, H^{14}), 7.26 (m, 1H, CH Ar, H^7). ^{13}C{^{1}H} NMR (100 MHz, C$_6$D$_6$, 293 K): δ 22.4 (CH(CH$_3$)$_2$, C^{17,20}), 27.04 (CH(CH$_3^A$CH$_3^B$), C^{18,21}), 28.1 (CH(CH$_3^A$CH$_3^B$), C^{19,22}), 71.2 (C^{10}), 107.9 (C^2), 108.8 (C^8), 122.5 (C^4), 124.4 (C^{13,15}), 126.3 (C^9), 128.8 (C^{14}), 130.8 (C^3), 135.8 (C), 141.2 (C^7), 142.4 (C), 148.7 (C), 155.9

(C), 177.7 (C^6). $^{11}B\{^1H\}$ NMR (96.2 MHz, C_6D_6, 293 K): δ 52.5 $BCH_3(C_6F_5)_2$ (61.8 %), 62.2 $B(CH_3)_2(C_6F_5)$ (30.1 %), 67.9 $B(CH_3)_3$ (8.1 %). $^{19}F\{^1H\}$ NMR (376.3 MHz, C_6D_6, 293 K): $[LZr(C_6F_5)_2]$ δ -122.3 (brs, 4 F, F_o C_6F_5), -150.0 (t, 2 F, ^3J = 19.2 Hz, F_p C_6F_5), -158.8 (m, 4 F, F_m C_6F_5); $[B(CH_3)(C_6F_5)_2]$ -128.4 (m, 4 F, F_o C_6F_5), -145.5 (t, 2 F, ^3J = 21.0 Hz, F_p C_6F_5), -159.8 (m, 4, F_m C_6F_5); $[B(CH_3)_2(C_6F_5)]$ -129.4 (m, 2 F, F_o C_6F_5), -149.9 (t, 1 F, ^3J = 24.4 Hz, F_p C_6F_5), - 161.0 (m, 2, F_m C_6F_5). **4b**: (estimated yield > 98% - conversion of **4** based on multinuclear NMR spectroscopy) ^1H NMR (400 MHz, C_6D_6, 293K): δ 0.68 (d, $^3J_{HH}$ = 6.8 Hz, 6H, $CH(CH_3{}^ACH_3{}^B)$, $H^{19,22}$), 0.73 (br s, $B(CH_3)_3$), 0.97 (br s, $B(CH_3)_2(C_6F_5)$), 1.11 (d, $^3J_{HH}$ = 6.8 Hz, 6H, $CH(CH_3{}^ACH_3{}^B$, $H^{18,21}$), 1.34 (br s, $BCH_3(C_6F_5)_2$), 3.72 (sept, $^3J_{HH}$ = 6.8 Hz, 2H, $CH(CH_3)_2$, $H^{17,20}$), 5.48 (s, 2H, CH_2N, H^{10}), 5.61 (m, 1H, C*H* Ar, H^8), 6.46 (m, 1H, C*H* Ar, H^2), 6.75 (m, 1H, C*H* Ar, H^9), 7.07-6.97 (5H, C*H* Ar, $H^{3,4,13,14,15}$), 7.24 (m, 1H, C*H* Ar, H^7). $^{13}C\{^1H\}$ NMR (100 MHz, C_6D_6, 293 K): δ 22.7 ($CH(CH_3)_2$, $C^{17,20}$), 27.1 ($CH(CH_3{}^ACH_3{}^B$), $C^{18,21}$), 27.9 ($CH(CH_3{}^ACH_3{}^B$), $C^{19,22}$), 69.0 (C^{10}), 108.1 (C^2), 108.9 (C^8), 123.2 (C^4), 124.3 ($C^{13,15}$), 126.9 (C^9), 130.8 (C^3), 138.6 (C), 141.4 (C^7), 143.2 (C), 147.7 (C), 156.3 (C), 192.5 (C^6). $^{11}B\{^1H\}$ NMR (96.2 MHz, C_6D_6, 293 K): δ 52.5 $BCH_3(C_6F_5)_2$ (48 %), 62.2 $B(CH_3)_2(C_6F_5)$ (48 %), 67.9 $B(CH_3)_3$ (4 %). $^{19}F\{^1H\}$ NMR (376.3 MHz, C_6D_6, 293 K): $[LHf(C_6F_5)_2]$ δ -122.1 (brs, 4 F, F_o C_6F_5), -149.5 (t, 2 F, ^3J = 19.6 Hz, F_p C_6F_5), -158.8 (m, 4 F, F_m C_6F_5); $[B(CH_3)(C_6F_5)_2]$ -128.4 (m, 4 F, F_o C_6F_5), -145.4 (t, 2 F, ^3J = 21.4 Hz, F_p C_6F_5), -159.8 (m, 4, F_m C_6F_5); $[B(CH_3)_2(C_6F_5)]$ -129.4 (m, 2 F, F_o C_6F_5), -149.8 (t, 1 F, ^3J = 24.4 Hz, F_p C_6F_5), -161.0 (m, 2, F_m C_6F_5).

General procedure for intramolecular hydroamination of aminoalkenes. All catalytic tests were carried out under inert atmosphere and samples were prepared and handled in an N_2-filled dry box. In a general procedure, a solution of **3a** or **4a** (8 μmol) in toluene-d_8 (0.6 mL) at r.t. was activated upon treatment with $Ph_3C^+[B(C_6F_5)_4]^-$ (1

equiv.). The resulting solution was allowed to stir for a few minutes and then transferred into a vial containing the corresponding aminoalkene (0.16 mmol). The reaction mixture was then introduced into a J. Young-tap NMR tube and placed in an oil bath heated at 100 °C. The conversion of each reaction was monitored spectroscopically (by a comparative integration of selected proton signals on the substrate and their corresponding protons on the cyclization product) and gas-chromatographically (by integration of the reagent and the product signals). Selected experiments were additionally monitored by ^{1}H NMR spectroscopy using ferrocene as internal standard (0.2 mL of a stock 0.17 M ferrocene solution in toluene-d_8). The internal standard was used to measure the substrate conversion and confirm the appropriate reaction mass balance. For all the scrutinized issues, the reaction mass balance was confirmed in the limit of the NMR spectrometer experimental error (^{1}H NMR acquisition parameters: acquisition time (aq.): 5 sec.; d1: 8 sec.; scan number (ns): 32).

Polymerization Procedure. *Ethylene-1-octene copolymerization*. A stirred 2-liter Parr reactor was used in the polymerizations. All feeds were passed through columns of alumina and Q-5™ catalyst (available from Engelhard Chemicals Inc.) prior to introduction into the reactor. Pre-catalyst and cocatalyst (activator) solutions were handled in the glove box. The reactor was charged with about 533 g of mixed alkanes solvent and 250 g of 1-octene comonomer. The reactor contents were heated to the polymerization temperature of 120 °C while 10 μmol of MMAO were added to the reactor as a scavenger for trace O_2 and water. Once at temperature, the reactor was saturated with ethylene at 460 psig (3.4 MPa). Catalysts and cocatalysts, as dilute solutions in toluene, were mixed and transferred to a catalyst addition tank and injected into the reactor. The polymerization conditions were maintained for 10 minutes with ethylene added on demand. Heat was continuously removed from the reaction vessel

through an internal cooling coil. The resulting solution was removed from the reactor and added to 5 mL of a toluene solution containing approximately 67 mg of a hindered phenol antioxidant (Irganox™ 1010 from Ciba Geigy Corporation) and 133 mg of a phosphorus stabilizer (Irgafos™ 168 from Ciba Geigy Corporation). Between polymerization runs, a wash cycle was conducted in which 850 g of mixed alkanes were added to the reactor and the reactor was heated to 150 °C. The reactor was then emptied of the heated solvent immediately before beginning a new polymerization run. Polymers were recovered by drying for about 12 h in a temperature-ramped vacuum oven with a final set point of 140 °C.

5.6 References

1 (a) L. Luconi, G. Giambastiani, A. Rossin, C. Bianchini, A. Lledós, *Inorg. Chem*., **2010**, *49*, 6811. (b) L. Luconi, A. Rossin, G. Tuci, I. Tritto, L. Boggioni, J. J. Klosin, C. N. Theriault, G. Giambastiani, *Chem. Eur. J*., **2012**, *18*, 671.

2 L. Luconi, A. Rossin, G. Tuci, S. Germain, E. Schulz, J. Hannedouche, G. Giambastiani, *ChemCatChem*, **2013**, *5*, 1142.

3 For a comprehensive review contribution see: G. Giambastiani, L. Luconi, R. L. Kuhlman, P. D. Hustad, in *Olefin Upgrading Catalysis by Nitrogen-based Metal Complexes I* (Eds. G. Giambastiani, J. Campora - ISBN 978-90-481-3814-2), Springer, London, **2011**, pp. 197-282 and references cited therein.

4 L. Luconi, A. Rossin, A. Motta, G. Tuci, G. Giambastiani, *Chem. Eur. J*., **2013**, *19*, 4906.

5 For comprehensive review papers and books on pincer-type complexes and their application in catalysis see: (a) M. H. P. Rietveld, D. M. Grove, G. van Koten, *New. J. Chem.*, **1997**, *21*, 751. (b) M. Albrecht, G. van Koten, *Angew. Chem. Int. Ed.*, **2001**, *40*, 3750. (c) M. E. Van Der Boom, D. Milstein, *Chem. Rev.*, **2003**, *103*, 1759. (d) J. T. Singleton, *Tetrahedron*, **2003**, *59*, 1837. (e) D. Morales-Morales, *Rev. Quim. Méx*., **2004**, *48*, 338. (f) M. Q. Slagt, D. A. P. Zwieten, A. J. C. M. Moerkerk, R. J. M. K. Gebbink, G. van Koten, *Coord. Chem. Rev.*, **2004**, *248*, 2275. (g) D. Pugh, A. A. Danopoulos, *Coord. Chem. Rev.*, **2007**, *251*, 610. (h) D. Morales-Morales, C. M. Jensen in *The Chemistry of Pincer Compounds*, Elsevier Science, **2007**, pp. 450, ISBN: 978-0-444-53138-4. (i) J-L. Niu, X-Q. Hao, J-F. Gong, M-P. Song, *Dalton Trans*., **2011**, *40*, 5135. (j) N. Selander, K. J. Szabó, *Chem. Rev*, **2011**, *111*, 2048.

6 For selected examples of mono- and trianionic {*N,C,N*}-pincer complexes with early transition metals see: (a) J. G. Donkervoort, J. T. B. H. Jastrzebski, B-J. Deelman, H. Kooijman, N. Veldman, A. L. Spek, G. van Koten, *Organometallics*, 1997, **16**, 4174. (b) M. Contel, M. Stol, M. A. Casado, G. P. M. van Klink, D. D. Ellis, A. L. Spek, G. van Koten, *Organometallics*, **2002**, *21*, 4556. (c) J. Koller, S. Sarkar, K. A. Abboud, A. S. Veige, *Organometallics*, **2007**, *26*, 5438. (d) S. Sarkar, K. P. McGowan, J. A. Culver, A. R. Carloson, J. Koller, A. J. Peloquin, M. K. Veige, K. A. Abboud, A. S. Veige, *Inorg. Chem.*, **2010**, *49*, 5143. (e) A. V. Chuchuryukin, R. Huang, M. Lutz, J. C. Chadwick, A. L. Spek, G. van Koten, *Organometallics*, **2011**, *30*, 2819. (f) A. V. Chuchuryukin, R. Huang, E. E. van Faassen, G. P. M. van Klink, M. Lutz, J. C. Chadwick, A. L. Spek, G. van Koten, *Dalton Trans.*, **2011**, *40*, 8887. (g) K. P. McGowan, K. A. Abboud, A. S. Veige, *Organometallics*, **2011**, *30*, 4949.

7 X.-Q. Hao, Y.-N. Wang, J.-R. Liu, K-L. Wang, J.-F. Gong, M.-P. Song, *J. Organomet. Chem.*, **2010**, *695*, 82.

8 For a general review on unsymmetrical {*E,C,E*'} and {*E,C,Z*}-pincer Pd^{II} complexes, see: I. Moreno, R. SanMartin, B. Inés, M. T. Herrero, E. Domínguez, *Curr. Org. Chem*., **2009**, *13*, 878.

9 For a related example of unsymmetrical {*N,C,N*'}-pincer complex incorporating an N-heterocyclic carbene functional group, see: N. Schneider, V. César, S. Bellemin-Laponnaz, L. H. Gade, *Organometallics*, **2005**, *24*, 4886.

10 R. D. J. Froese, P. D. Hustad, R. L. Kuhlman, T. T. Wenzel, *J. Am. Chem. Soc*. **2007**, *129*, 7831.

11 (a) G. M. Diamond, R. F. Jordan, J. L. Petersen, *J. Am. Chem. Soc.*, **1996**, *118*, 8024. (b) R. T. Boussie, G. M. Diamond, C. Goh, K. A. Hall, A. M. La-Pointe, M. K. Leclerc, V. Murphy, J. A. W. Shoemaker, H. Turner, R. K. Rosen, J. C. Stevens, F. Alfano, V. Busico, R. Cipullo, G. Talarico, *Angew. Chem*. **2006**, *45*, 3278.

12 The calculated index of trigonality "τ" for this structure is 0.26; see also A. W. Addison, T. N. Rao, J. Reedijk, J. van Rijn, G. C. Verschoor, *J. Chem. Soc. Dalton Trans*. **1984**, 1349.

13 For related structures containing Hf–amido bonds, see: (a) K. Nienkemper, G. Kehr, S. Kehr, R. Frohlich, G. Erker, *J. Organomet. Chem*. **2008**, *693*, 1572; see also refs [1b, 2 and 4].

14 For related structures containing Hf-Npyrazolyl bonds, see: (a) A. Otero, J. Fernandez-Baeza, A. Antinolo, J. Tejeda, A. Lara-Sanchez, L. Sanchez-Barba, M. Fernandez-Lopez, I. Lopez-Solera, *Inorg. Chem.* **2004**, *43*, 1350. b) see also ref. 4.

15 For related structures containing Hf-Ar bonds, see: (a) H. Tsurugi, K. Yamamoto, K. Mashima, *J. Am. Chem. Soc*. **2011**, *133*, 732. (b) see also refs: [1b, 2, 4 and 6c].

16 C. L. Beswick, T. J. Marks, *Organometallics* **1999**, *18*, 2410.

17 (a) R. F. Munhá, M. A. Antunes, L. G. Alves, L. F. Veiros, M. D. Fryzuk, A. M. Martins, *Organometallics* **2010**, *29*, 3753; (b) C. Krempner, M. Köckerling, H. Reinke, K. Weichert, *Inorg. Chem*. **2006**, *45*, 3203. (c) Z. J. Tonzetich, R. R. Schrock, *Polyhedron* **2006**, *25*, 469; (d) R. M. Gauvin, C. Mazet, J. Kress, *J. Organomet. Chem.* **2002**, *658*, 1. (e) S. J. Lancaster, M. Bochmann, *Organometallics* **2001**, ***20***, 2093.

18 Such a reactivity translates into a lowering of the symmetry of the active species. For literature precedents see: (a) G. J. Domski, E. B. Lobkovsky, G. W. Coates, *Macromolecules*, **2007**, *40*, 3510. (b) C. Zuccaccia, A. Macchioni, V. Busico, R. Cipullo, G. Talarico, F. Alfano, H. W. Boone, K. A. Frazier, P. D. Hustad, J. C. Stevens, P. C. Vosejpka, K. A. Abboud, *J. Am. Chem. Soc*. **2008**, *130*, 10354. c) C. Zuccaccia, V. Busico, R. Cipullo, G. Talarico, R. D. J. Froese, P. C. Vosejpka, P. D. Hustad, A. Macchioni, *Organometallics* **2009**, *28*, 5445. See also references. 10, 1b.

19 GC program: 40°C for 1 min, 15 °C/min, 250 °C for 20 min.

20 K. A. Frazier, R. D. Froese, Y. He, J. Klosin, C. N. Theriault, P. C. Vosejpka, Z. Zhou, K. A. Abboud, *Organometallics* **2011**, *30*, 3318.

21 A. L. McKnight, R. M. Waymouth, *Chem. Rev*. **1998**, *98*, 2587.

22 (a) T. R. Boussie, G. M. Diamond, C. Goh, K. A. Hall, A. M. LaPointe, M. Leclerc, C. Lund, V. Murphy, J. A. W. Shoemaker, U. Tracht, H. Turner, J. Zhang, T. Uno, R. K. Rosen, J. C. Stevens, *J. Am. Chem. Soc*. **2003**, *125*, 4306. (b) Eur. Patent Appl. EP 416 815-A2 (**1991**), Dow Chemical Co., invs.: J. C. Stevens, F. J. Timmers, D. R. Wilson, G. F. Schmidt, P. N. Nickias, R. K. Rosen, T. R. Boussie, G. M. Diamond, C. Goh, K. A. Hall, A. M. LaPointe, M. Leclerc, C. Lund, V. Murphy, J. A. W. Shoemaker, U. Tracht, H. Turner, J. Zhang, T. Uno, G. W. Knight, S. Lai; Chem. Abstr. **1991**, *115*, 93163. (c) J. Klosin, W. J. Jr. Kruper, P. N. Nickias, G. R. Roof, P. De Waele, K. A. Abboud, *Organometallics* **2001**, *20*, 2663.

23 For recent general reviews on hydroamination catalysis see: a) T. E. Müller, K. C. Hultzsch, M. Yus, F. Foubelo and M. Tada, *Chem. Rev*., **2008**, *108*, 3795. b) J. Hannedouche, E. Schulz, *Chem. Eur. J*. **2013**, *19*, 4972.

24 For a selection of neutral group IV metal-catalyzed hydroamination of aminoalkenes see: (a) R. K. Thomson, J. A. Bexrud, L. L. Schafer, *Organometallics* **2006**, *25*, 4069; (b) M. C. Wood, D. C. Leitch, C. S. Yeung, J. A. Kozak, L. L. Schafer, *Angew. Chem., Int. Ed*. **2007**, *46*, 354; (c) S. Majumder, A. L. Odom, *Organometallics* **2008**, *27*, 1174; (d) A. L. Gott, A. J. Clarke, G. J. Clarkson, P. Scott, *Chem. Commun.*, **2008**, 1422; (e) C. Müller, W. Saak, S. Doye, *Eur. J. Org. Chem*. **2008**, 2731; (f) J. Cho, T. K. Hollis, T. R. Helgert, E. J. Valente, *Chem. Commun*. **2008**, 5001; (g) D. C. Leitch, P. R. Payne, C. R. Dunbar, L. L. Schafer, *J. Am. Chem. Soc*. **2009**, *131*, 18246; (h) A. L. Reznichenko, K. C. Hultzsch, *Organometallics* **2010**, *29*, 24; (i) J. A. Bexrud, L. L. Schafer, *Dalton Trans*. **2010**, *39*, 361; (j) Y.-C. Hu, C.-F. Liang, J.-H. Tsai, G. P. A. Yap, Y.-T. Chang, T.-G. Ong, *Organometallics* **2010**, *29*, 3357; (k) K. Manna, A. Ellern, A. D. Sadow, *Chem. Commun*. **2010**, *46*, 339; (l) K. Manna, S. Xu, A. D. Sadow, *Angew. Chem., Int. Ed*. **2011**, *50*, 1865; (m) J. Cho, T. K. Hollis, E. J. Valente, J. M. Trate, *J. Organomet. Chem.* **2011**, *696*, 373; (n) H. Kim, P. H. Lee, T. Livinghouse, *Chem. Commun*. **2005**, 5205; (o) J. A. Bexrud, J. D. Beard, D. C. Leitch, L. L. Schafer, *Org. Lett.* **2005**, *7*, 1959; (p) H. Kim, Y. K. Kim, J. H.

Shim, M. Kim, M. Han, T. Livinghouse, P. H. Lee, *Adv. Synth. Catal*. **2006**, *348*, 2609; (q) D. A. Watson, M. Chiu, R. G. Bergman, *Organometallics* **2006**, *25*, 4731; (r) A. L. Gott, A. J. Clarke, G. J. Clarkson, P. Scott, *Organometallics* **2007**, *26*, 1729; (s) X. Li, S. Haibin, G. Zi, *Eur. J. Inorg. Chem.* **2008**, 1135. (t) G. Zi, Q. Wang, L. Xiang, H. Song, *Dalton Trans*. 2008, 5930; (u) G. Zi, X. Liu, L. Xiang, H. Song *Organometallics* **2009**, *28*, 1127; (v) G. Zi, F. Zhang, L. Xue, L. Ai, H. Song, *J. Organomet. Chem.* **2010**, *695*, 730; (w) G. Zi, F. Zhang, L. Xiang, Y. Chen, W. Fang, H. Song, *Dalton Trans*. **2010**, *39*, 4048; (x) T. R. Helgert, T. K. Hollis, E. J. Valente, *Organometallics* **2012**, *31*, 3002. (z) K. Manna, W. C. Everett, G. Schoendorff, A. Ellern, T. L. Windus, A. D. Sadow, *J. Am. Chem. Soc*. **2013**, *135*, 7235.

25 For cationic group IV metal-catalyzed hydroamination of aminoalkenes see: (a) P. D. Knight, I. Munslow, P. N. O'Shaughnessy, P. Scott, *Chem. Commun*. **2004**, 894; (b) D. V. Gribkov, K. C. Hultzsch, *Angew. Chem*. **2004**, *116*, 5659; *Angew. Chem. Int. Ed*. **2004**, *43*, 5542; (c) X. Wang, Z. Chen, X.-L. Sun, Y. Tang, Z. Xie, *Org. Lett*. **2011**, *13*, 4758; (d) A. Mukherjee, S. Nembenna, T. K. Sen, S. Pillai Sarish, P. Kr. Ghorai, H. Ott, D. Stalke, S. K. Mandal, H. W. Roesky, *Angew. Chem*. **2011**, *123*, 4054; *Angew. Chem. Int. Ed*. **2011**, *50*, 3968.

26 For a selection of seminal papers dealing with hydroamination catalysis by neutral Group-IV complexes under mild reaction conditions see also: references 24k,l,z

27 S. Hong, S. Tian, M. V. Metz and T. J. Marks, *J. Am. Chem. Soc*., **2003**, *125*, 14768.

28 J. Y. Kim, T. Livinghouse, *Org. Lett*. **2005**, *7*, 1737.

29 B.-D. Stubbert, T. J. Marks *J. Am. Chem. Soc.* **2007**, *129*, 4253.

30 I. Aillaud, J. Collin, C. Duhayon, R. Guillot, D. Lyubov, E. Schulz and A. Trifonov, *Chem.–Eur. J*., **2008**, *14*, 2189.

31 Sheldrick, G. M. (**2008**). SHELXTL 6.1. Crystallographic software package. Bruker AXS, Inc. Madison, Wisconsin, USA.

Satellite Papers

Selective σ-Bond Metathesis in Alkyl−Aryl and Alkyl−Benzyl Yttrium Complexes. New Aryl− and Benzyl−Hydrido Yttrium Derivatives Supported by Amidopyridinate Ligands

D. M. Lyubov,[†] G. K. Fukin,[†] A. V. Cherkasov,[†] Andrei S. Shavyrin,[†] A. A. Trifonov,*[,†] L. Luconi,[‡] C. Bianchini,[‡] A. Meli,[‡] and G. Giambastiani*[,‡]

G. A. Razuvaev Institute of Organometallic Chemistry of Russian Academy of Sciences, Tropinina 49, GSP-445, 603950 Nizhny Novgorod, Russia, and Istituto di Chimica dei Composti Organometallici (ICCOM - CNR), Via Madonna del Piano 10, 50019, Sesto Fiorentino, Italy

Received October 30, 2008

Yttrium dialkyl complexes coordinated by 6-aryl-substituted amidopyridinate ligands undergo selective intramolecular sp^2 or sp^3 C−H bond activation. Upon treatment with $PhSiH_3$ of the resulting Y−C(alkyl, aryl) or Y−C(alkyl,benzyl) systems, a σ-bond metathesis reaction takes place selectively at the Y−C(alkyl) bond, generating rare dimeric aryl−hydrido or benzyl−hydrido yttrium complexes, respectively.

Rare-earth-metal hydrides currently attract a great deal of attention due to the variety of their unique structural and chemical properties.[1] These compounds have proved to be promising catalysts in several olefin transformations[2] and have demonstrated extremely high reactivity in stoichiometric reactions, including C−F bond activation.[3] Rare-earth-metal hydrides are generally constituted by sandwich-[1] and half-sandwich-type ("constrained geometry")[4] complexes, and very few classes of cyclopentadienyl-free analogues have been systematically explored up to now.[5]

The reactivity of rare-earth-metal compounds is known to be defined by both the metal electrophilicity and the free coordination sites at the metal center and can be substantially modulated by tuning the electronic and steric properties of the ligand framework. This issue makes the design of new coordination environments crucial for generating a rational balance between the kinetic stability and the high reactivity of the resulting complexes. Recently the use of bulky amidopyridinate ligands has allowed us to synthesize and characterized a novel class of rare-earth alkyl−hydrido clusters containing highly reactive Ln−C and Ln−H bonds, that demonstrate an intriguing reactivity.[6]

In order to explore the potential of such a class of nitrogen-containing ligands for the synthesis of new alkyl and/or hydrido rare-earth complexes, we focused our attention on 6-aryl-substituted aminopyridinate systems which were straightforwardly prepared by reductive alkylation[7] of related iminopyridines (Schemes 1 and 2). The iminopyridine **1** was prepared according to a procedure reported in the literature,[8] while the new xylyl -substituted iminopyridyl ligand **2** was synthesized on a multigram scale through the five-step synthesis shown in Scheme 1.

All our attempts to synthesize yttrium bis(alkyl) species via monoalkane elimination by reacting $Y(CH_2SiMe_3)_3(THF)_2$[9] with the aminopyridine N_2H^{Ph} (**3**) in *n*-hexane at 0 °C resulted in

* To whom correspondence should be addressed. Fax: (+7)8314621497 (A.A.T.). E-mail: trif@iomc.ras.ru (A.A.T.); giuliano.giambastiani@iccom.cnr.it (G.G.).

[†] G. A. Razuvaev Institute of Organometallic Chemistry of Russian Academy of Sciences.

[‡] Istituto di Chimica dei Composti Organometallici (ICCOM - CNR).

(1) (a) Ephritikhine, M. *Chem. Rev.* **1997**, *97*, 2193–2242. (b) Hou, Z.; Nishiura, M.; Shima, T. *Eur. J. Inorg. Chem.* **2007**, 2535–2545, and references therein.

(2) (a) Edelmann, F. T. *Top. Curr. Chem.* **1996**, *179*, 247–262. (b) Anwander, R. In *Applied Homogeneous Catalysis with Organometallic Compounds*; Cornils, B., Hermann, W. A., Eds.; Wiley-VCH: Weinheim, Germany, 2002; p 974. (c) Jeske, G.; Lauke, H.; Mauermann, H.; Swepston, P. N.; Schumann, H.; Marks, T. J. *J. Am. Chem. Soc.* **1985**, *107*, 8091–8103. (d) Jeske, G.; Schock, L. E.; Swepston, P. N.; Schumann, H.; Marks, T. J. *J. Am. Chem. Soc.* **1985**, *107*, 8103–8110. (e) Desurmont, G.; Li, Y.; Yasuda, H.; Maruo, T.; Kanehisa, N.; Kai, Y. *Organometallics* **2000**, *19*, 1811–1813. (f) Desurmont, G.; Tokomitsu, T.; Yasuda, H. *Macromolecules* **2000**, *33*, 7679–7681. (g) Giardello, M. A.; Conticello, V. P.; Brard, L.; Gagne, M. R.; Marks, T. J. *J. Am. Chem. Soc.* **1994**, *116*, 10241–10254. (h) Fu, P.-F.; Brard, L.; Marks, T. J. *J. Am. Chem. Soc.* **1995**, *117*, 7157–7168.

(3) (a) Werkema, E. L.; Messines, E.; Perrin, L.; Maron, L.; Eisenstein, O.; Andersen, R. A. *J. Am. Chem. Soc.* **2005**, *127*, 7781–7795. (b) Maron, L.; Werkema, E. L.; Perrin, L.; Eisenstein, O.; Andersen, R. A. *J. Am. Chem. Soc.* **2005**, *127*, 279–292.

(4) (a) Arndt, S.; Okuda, J. *Chem. Rev.* **2002**, *102*, 1593–1976. (b) Okuda, J. *Dalton Trans.* **2003**, 2367–2378.

(5) (a) Trifonov, A. A. *Russ. Chem. Rev.* **2007**, *76*, 1051–1072. (b) Trifonov, A. A.; Skvortsov, G. G.; Lyubov, D. M.; Skorodumova, N. A.; Fukin, G. K.; Baranov, E. V.; Glushakova, V. N. *Chem. Eur. J.* **2006**, *12*, 5320–5327, and references cited therein. (c) Ruspiv, C.; Spielman, J.; Harder, S. *Inorg. Chem.* **2007**, *46*, 5320–5326. (d) Concol, M.; Spaniol, T. P.; Okuda, J. *Dalton. Trans.* **2007**, 4095–4102. (e) Konkol, M.; Okuda, J. *Coord. Chem. Rev.* **2008**, *252*, 1577–1591.

(6) Lyubov, D. M.; Döring, C.; Fukin, G. K.; Cherkasov, A. V.; Shavyrin, A. S.; Kempe, R.; Trifonov, A. A. *Organometallics* **2008**, *27*, 2905–2907.

(7) (a) Gibson, V. C.; Redshaw, C.; White, A. J. P.; Williams, D. J. *J. Organomet. Chem.* **1998**, *550*, 453–456. (b) Bruce, M.; Gibson, V. C.; Redshaw, C.; Solan, G. A.; White, A. J. P.; Williams, D. J. *Chem. Commun.* **1998**, 2523–2524. (c) Britovsek, G. J. P.; Gibson, V. C.; Mastroianni, S.; Oakes, D. C. H.; Redshaw, C.; Solan, G. A.; White, A. J. P.; Williams, D. J. *Eur. J. Inorg. Chem.* **2001**, 431–437.

(8) (a) Bianchini, C.; Sommazzi, A.; Mantovani, G.; Santi, R.; Masi, F. U.S. Patent 6,916,931 B2. (b) Bianchini, C.; Giambastiani, G.; Mantovani, G.; Meli, A.; Mimeau, D. *J. Organomet. Chem.* **2004**, *689*, 1356. (c) Bianchini, C.; Giambastiani, G.; Guerrero Rios, I.; Mantovani, G.; Meli, A.; Segarra, A. M. *Coord. Chem. Rev.* **2006**, *250*, 1391–1418, and references cited therein. (d) Bianchini, C.; Gatteschi, D.; Giambastiani, G.; Guerrero Rios, I.; Ienco, A.; Laschi, F.; Mealli, C.; Meli, A.; Sorace, L.; Toti, A.; Vizza, F. *Organometallics* **2007**, *26*, 726. (e) Barbaro, P.; Bianchini, C.; Giambastiani, G.; Guerrero, I. R.; Meli, A.; Oberhauser, W.; Segarra, A. M.; Sorace, L.; Toti, A. *Organometallics* **2007**, *26*, 4639–4651. (f) Bianchini, C.; Giambastiani, G.; Guerrero, I. R.; Meli, A.; Oberhauser, W.; Sorace, L.; Toti, A. *Organometallics* **2007**, *26*, 5066–5078.

(9) Lappert, M. F.; Pearce, R. J. *J. Chem. Soc., Chem. Commun.* **1973**, 126–127.

10.1021/om801044h CCC: $40.75
Publication on Web 01/21/2009

Scheme 1[a]

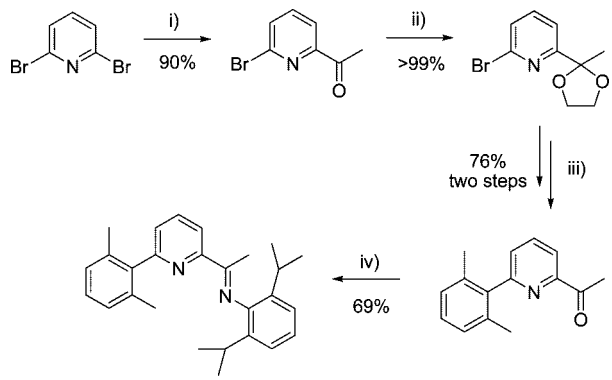

[a] Legend: (i) *t*-BuLi, *N*,*N*-dimethylacetamide, Et_2O, −78 °C; (ii) ethylene glycol, *p*-toluenesulfonic acid, benzene, reflux 12 h, Dean−Stark apparatus; (iii) Kumada coupling conditions, $Me_2(C_6H_3)MgBr$, $NiCl_2(PCy_3)_2$ cat., THF, 50 °C, 72 h and then HCl 2 M, 85 °C, 2 h; (iv) $iPr_2(C_6H_3)NH_2$, HCOOH cat., MeOH, reflux 62 h.

Scheme 2

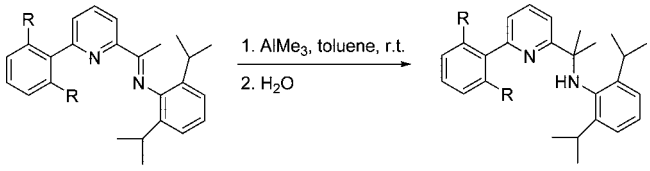

the quantitative generation of the metallacyclic compound **5** as a result of an intramolecular sp^2-CH bond activation at one of the ortho positions of the phenyl substituent (Scheme 3). The ^1H and $^{13}C\{^1H\}$ NMR spectra for complex **5** were consistent with the expected yttrium coordination sphere. The ^1H NMR spectrum of **5**, which contains both Y−C(alkyl) and Y−C(aryl) bonds, shows one clear doublet centered at −0.54 ppm ($^2J_{YH}$ = 3.0 Hz), attributed to the hydrogen atoms of the methylene group attached to the yttrium. The $^{13}C\{^1H\}$ NMR spectrum contains a doublet for the sp^3 carbon atom centered at 30.3 ppm ($^1J_{YC}$ = 39.5 Hz), while a further doublet at 190.6 ppm ($^1J_{YC}$ = 41.2 Hz) is readily assigned to the sp^2 carbon of the phenyl ring *σ*-bonded to the metal center.

Unexpectedly, the xylyl-substituted aminopyridine system N_2H^{Xyl} (**4**) did not allow us to generate dialkyl species due to an intramolecular activation of the sp^3-hybridized C−H bond of one methyl group (Scheme 3). The reaction actually gave the mononuclear metallacyclic monoalkyl complex **6**, where the yttrium atom turned out to be five-coordinated by a tridentate aminopyridinate ligand, a residual (trimethylsilyl)methylene fragment, and a THF molecule.

Unlike the case for **5**, the ^1H NMR spectrum of **6** shows two sets of diastereotopic protons, one for the methylene group of the residual alkyl fragment attached to the yttrium atom (doublet of doublets at −0.92 and −0.76 ppm ($^2J_{HH}$ = 10.8 Hz, $^2J_{YH}$ = 3.0 Hz, respectively)) and one for the "benzylic" methylene $Me(C_6H_3)CH_2Y$ group (doublet of doublets at 1.81 and 2.00 ppm ($^2J_{HH}$ = 5.5 Hz, $^2J_{YH}$ = 2.0 Hz, respectively)). The corresponding $^{13}C\{^1H\}$ NMR spectrum contains a broad doublet centered at 27.3 ppm ($^1J_{YC}$ = 43.3 Hz) attributable to the Me_3SiCH_2Y group, while a doublet at 49.2 ppm ($^1J_{YC}$ = 22.8 Hz) is assigned to the "benzylic" sp^3 carbon. The two isopropyl fragments as well as the two methyl groups at the sp^3 carbon are not magnetically equivalent and show ^1H NMR and $^{13}C\{^1H\}$ NMR spectra distinguished by a set of eight distinct signals for the methyl groups and for the methyne protons, the latter providing two well-separated septets at 3.18 and 4.50 ppm, respectively. Such a situation reflects the existence of two possible conformations for **6** differing from each other in the location of the benzylic CH_2 group: above or below the amidopyridinate ligand plane, respectively.

Although inter- and intramolecular metalations of sp^2- and sp^3-hybridized C−H bonds have been previously documented for cyclopentadienyl[10] and cyclopentadienyl-free[11] lanthanide alkyl and hydride complexes, they still attract considerable interest for their ability to activate inert chemical bonds.

Crystallization by slow cooling of a concentrated *n*-hexane solution of **6** to −20 °C resulted in the formation of single crystals suitable for X-ray diffraction analysis. The molecular structure of the monomeric complex **6** is shown in Figure 1. The coordination environment of the yttrium atom is set up by two nitrogen atoms of the chelating aminopyridinate ligand, one sp^3 carbon atom from the residual alkyl group, one further sp^3 carbon atom from the "benzylic" group, and one oxygen atom from a THF molecule. Moreover, a close contact (2.9421(17) Å) between the yttrium and the ipso carbon on the "benzylic" group is finally observed, which increases the coordination number to 6. The $Y-C_{Alkyl}$ bond length (2.4139(17) Å) is comparable to the values reported for related yttrium systems (2.410(8)−2.439(3) Å),[12] while the $Y-C_{Bn}$ distance (2.4520(18) Å) is slightly longer than that measured for analogous C−H activation products ($Ap'(Ap_{-H}')Y(thf)$] (2.420(11) Å).[13] It is worth noting that the covalent Y−N bond (2.2015(14) Å) is evidently shorter than that measured in analogous six-coordinated yttrium complexes containing amidopyridinate ligands with a shorter backbone (2.273(3) Å).[14]

The most common synthetic route to rare-earth hydrido complexes is the reaction of alkyl derivatives with either dihydrogen[15] or phenylsilane.[16] We have found that, by treat-

(10) (a) Okuda, J. *Dalton Trans.* **2003**, 2367–2378. (b) Watson, P. L. *J. Chem. Soc., Chem. Commun.* **1983**, 276–277. (c) Watson, P. L.; Parshall, G. B. *Acc. Chem. Res.* **1985**, *18*, 51–56. (d) Thompson, M. E.; Baxter, S. M.; Bulls, A. R.; Burger, B. J.; Nolan, M. C.; Santarsiero, B. D.; Schaefer, W. P.; Bercaw, J. E. *J. Am. Chem. Soc.* **1987**, *109*, 203–219. (e) den Haan, K. H.; Wiestra, Y.; Teuben, J. H. *Organometallics* **1987**, *6*, 2053–2060. (f) Watson, P. L. *J. Am. Chem. Soc.* **1983**, *105*, 6491–6493. (g) Duchateau, R.; van Wee, C. T.; Teuben, J. H. *Organometallics* **1996**, *15*, 2291–2302. (h) Mu, Y.; Piers, W. E.; MacQuarrie, D. C.; Zaworotko, M. J.; Young, V. G. *Organometallcs* **1996**, *15*, 2720–2726. (i) Evans, W. J.; Champagne, T. M.; Ziller, J. W. *J. Am. Chem. Soc.* **2006**, *128*, 14270–14271. (j) Evans, W. J.; Perotti, J. M.; Ziller, J. W. *J. Am. Chem. Soc.* **2005**, *127*, 1068–1069. (k) Booij, M.; Kiers, N. H.; Meetsma, A.; Teuben, J. H.; Smeets, W. J. J.; Spek, A. L. *Organometallics* **1989**, *8*, 2454–2461.

(11) (a) Duchateau, R.; Van Wee, C. T.; Meetsma, A.; Teuben, J. H. *J. Am. Chem. Soc.* **1993**, *115*, 4931–4932. (b) Emslie, D. J. H.; Piers, W. E.; Parvez, M.; McDonald, R. *Organometallics* **2002**, *21*, 4226–4240. (c) Sigiyama, H.; Gambarotta, S.; Yap, G. P. A.; Wilson, D. R.; Thiele, S. K.-H. *Organometallics* **2004**, *23*, 5054–5061. (d) Duchateau, R.; Tuinstra, T.; Brussee, E. A. C.; Meetsma, A.; Van Duijnen, P. T.; Teuben, J. H. *Organometallics* **1997**, *16*, 3511–3522. (e) Fryzuk, M. D.; Haddad, T. S.; Rettig, S. J. *Organometallics* **1991**, *10*, 2026–2036. (f) Emslie, D. J. H.; Piers, W. E.; Parvez, M. *Dalton Trans.* **2003**, 2615–2620.

(12) (a) Wang, D.; Cui, D.; Miao, M.; Huang, B. *Dalton Trans.* **2007**, 4576–4581. (b) Liu, X.; Shang, X.; Tang, T.; Hu, N.; Pei, F.; Cui, D.; Chen, X.; Jing, X. *Organometallics* **2007**, *26*, 2747–2757. (c) Cai, C.-X.; Toupet, L.; Lehmann, C. W.; Carpentier, J.-F. *J. Organomet. Chem.* **2003**, *683*, 131–136. (d) Bambirra, S.; Meetsma, A.; Hessen, B.; Teuben, J. H. *Organometallics* **2001**, *20*, 782–785.

(13) Skvortsov, G. G.; Fukin, G. K.; Trifonov, A. A.; Noor, A.; Döring, C.; Kempe, R. *Organometallics* **2007**, *26*, 5770–5773.

(14) Kretschmer, W. P.; Meetsma, A.; Hessen, B.; Schmalz, T.; Qayyum, S.; Kempe, R. *Chem. Eur. J.* **2006**, *12*, 8969–8978.

(15) (a) Jeske, G.; Lauke, H.; Mauermann, H.; Swepston, P. N.; Schumann, H.; Marks, T. J. *J. Am. Chem. Soc.* **1985**, *107*, 8091–8103. (b) Jeske, G.; Schock, L. E.; Swepston, P. N.; Schumann, H.; Marks, T. J. *J. Am. Chem. Soc.* **1985**, *107*, 8103–8110.

Scheme 3

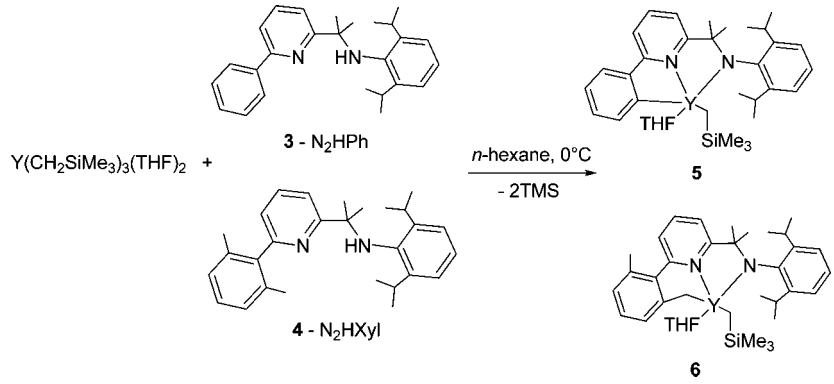

ment with an equimolar amount of $PhSiH_3$ in *n*-hexane at 0 °C, **5** and **6** undergo rapid σ-bond metathesis of the residual $Y-CH_2SiMe_3$ bonds to give selectively the novel aryl−hydrido and benzyl−hydrido complexes **7** and **8** (Scheme 4). Surprisingly, the Y−C(Aryl) and Y−C(Bn) bonds in **5** and **6** did not react with $PhSiH_3$, even after 24 h at room temperature and in the presence of a 2-fold excess of silane. In fact, complexes **7** and **8** were recovered in the same yield with no appreciable decomposition. Complexes **5** and **6** were finally reacted with H_2 (1 bar) in toluene with the aim of exploring whether **7** and **8** were obtainable through this alternative way. All our attempts to react **5** and **6** with H_2 resulted in their decomposition with formation of an off-white material that does not contain any amidopyridinate ligand and is insoluble in common organic solvents. This result proves the effectiveness of phenylsilane as a highly selective reagent for the synthesis of hydride species **7** and **8**.

The ^1H and $^{13}C\{^1H\}$ NMR spectra of **7** and **8** (20 °C, C_6D_6) are consistent with binuclear species distinguised by an internal mirror plane. The hydride signals in **7** and **8** appear, in the ^1H NMR spectrum, as sharp, well-resolved triplets at 7.76 ppm ($^1J_{YH}$ = 27.4 Hz) and at 7.37 ppm ($^1J_{YH}$ = 26.5 Hz),

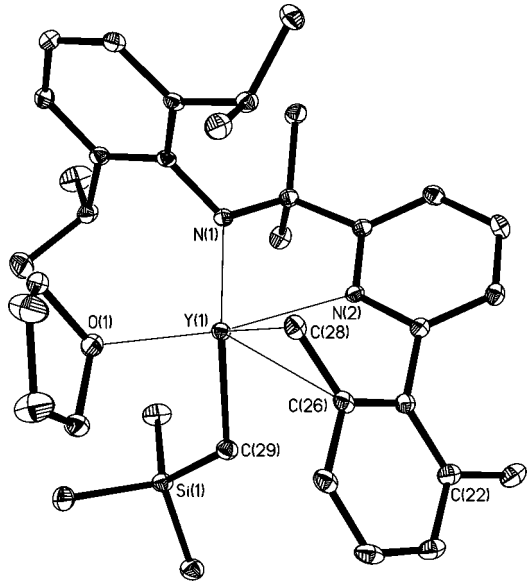

Figure 1. ORTEP diagram (30% probability thermal ellipsoids) of complex **6** showing the numbering scheme. Hydrogen atoms are omitted for clarity. Selected bond distances (Å) and angles (deg): Y(1)−N(1) = 2.2015(14), Y(1)−O(1) = 2.3422(13), Y(1)−C(29) = 2.4139(17), Y(1)−N(2) = 2.4200(14), Y(1)−C(28) = 2.4520(18), Y(1)−C(26) = 2.9421(17); C(29)−Y(1)−C(28) = 117.20(6), N(1)−Y(1)−N(2) = 70.00(5), C(28)−Y(1)−C(26) = 29.47(5).

Scheme 4

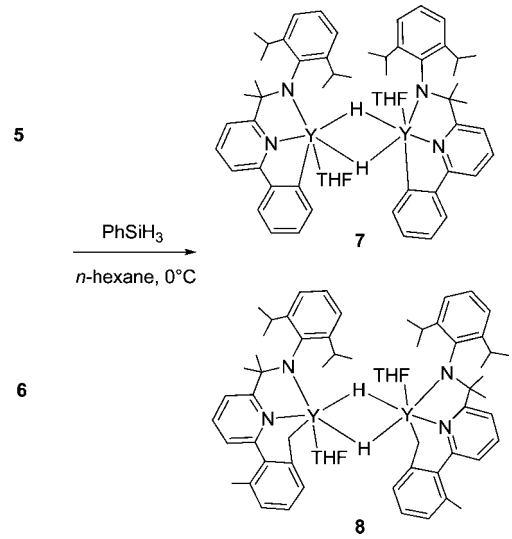

respectively, thus indicating the coupling of each hydride with two equivalent ^{89}Y nuclei. The $^{13}C\{^1H\}$ NMR signals of the carbon atoms bonded to yttrium appear as two doublets centered at 193.1 ppm ($^1J_{YC}$ = 46.2 Hz) and 51.3 ppm ($^1J_{YC}$ = 24.9 Hz) for complexes **7** and **8**, respectively.

Yellow single crystals of **7**, suitable for X-ray analysis, were prepared by slow cooling of an *n*-hexane solution of **7** down to −20 °C. The molecular structure of **7**is illustrated in Figure 2. The complex adopts a binuclear structure with two six-coordinate yttrium atoms. The metal coordination sphere is determined by the two nitrogen and one carbon atoms from the tridentate amidopyridinate ligand, two bridging hydrido ligands, and one oxygen atom from a residual THF molecule. The tetranuclear Y_2H_2 core is not planar; the dihedral angle between the Y(1)H(1)H(1A) and Y(1A)H(1)H(1A) planes is 20.1°. The Y−H bond lengths are 2.15(2) Å. It should be noted that N(1), N(2), and C(26) atoms lie in the same plane, though the entire chelating ligand is not planar.

The Y−C bond length in **7** (2.469(2) Å) is in good agreement with previously reported distances for similar six-coordinate yttrium aryl species,[17] while the Y−Y distance (3.5787(4) Å)

(16) Voskoboinikov, A. Z.; Parshina, I. N.; Shestakova, A. K.; Butin, K. P.; Beletskaya, I. P.; Kuz'mina, L. G.; Howard, J. A. K. *Organometallics* **1997**, *16*, 4041–4055.

(17) (a) Rabe, G. W.; Zhang-Presse, M.; Riederer, F. A.; Yap, G. P. A. *Inorg. Chem.* **2003**, *42*, 3527–3533. (b) Rabe, G. W.; Bérubé, C. D.; Yap, G. P. A.; Lam, K.-C.; Concolino, T. E.; Rheingold, A. L. *Inorg. Chem.* **2002**, *41*, 1446–1453. (c) Fryzuk, M. D.; Jafarpour, L.; Kerton, F. M.; Love, J. B.; Patrick, B. O.; Rettig, S. J. *Organometallics* **2001**, *20*, 1387–1396.

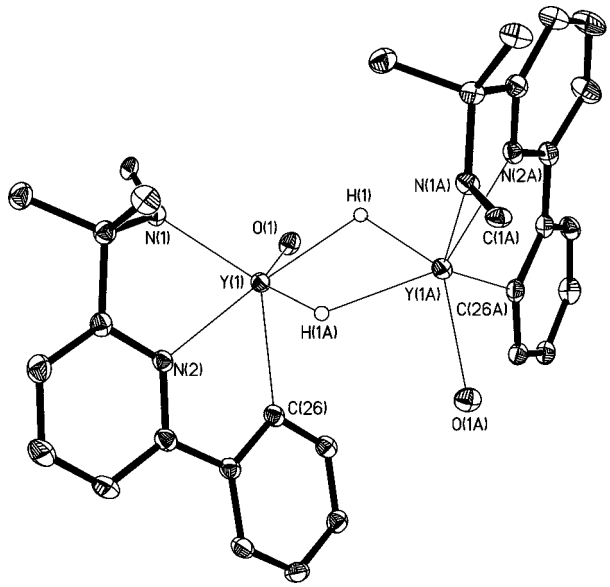

Figure 2. ORTEP diagram (30% probability thermal ellipsoids) of complex **7** showing the numbering scheme. Hydrogen atoms, 2,6-diisopropylphenyl fragments, and methylene groups of the THF molecules are omitted for clarity. Selected bond distances (Å) and angles (deg): Y−H = 2.15(2), Y(1)−N(1) = 2.2205(18), Y(1)−O(1) = 2.3609(15), Y(1)−N(2) = 2.4252(17), Y(1)−C(26) = 2.469(2), Y(1)−Y(1A) = 3.5780(4); N(1)−Y(1)−N(2) = 68.24(6), N(1)−Y(1)−C(26) = 130.34(7), N(2)−Y(1)−C(26) = 68.43(7).

is significantly shorter than those measured in related binuclear yttrium hydrides.[5a,18]

In conclusion, we have reported the synthesis of new yttrium dialkyl complexes stabilized by amidopyridinate ligands which rapidly undergo intramolecular sp^2 or sp^3 C−H bond activation with the formation of alkyl−aryl or alkyl−benzyl complexes. We have also found that the residual Y−C(alkyl) bonds undergo selective σ-bond metathesis upon treatment with $PhSiH_3$, while the Y−C(aryl) and Y−C(benzyl) bonds do not react with the silane under analogous conditions. As a result, rare[19] binuclear aryl−hydrido and benzyl−hydrido yttrium complexes have been synthesized and characterized. Polymerization tests with both Y−alkyl and Y−hydrido complexes using ethylene and propene as monomer feeds are currently under investigation in our laboratories. Preliminary results for ethylene polymerization under standard conditions (10 bar of C_2H_4, 25 mL of toluene, 30 °C) indicate that both precursors do not generate very active catalytic systems, as the highest turnover frequency observed was 870 mol of C_2H_4 converted (mol of metal)$^{-1}$ h^{-1}.

Experimental Section

General Considerations. All air- and/or water-sensitive reactions were performed under either nitrogen or argon in flame-dried flasks using standard Schlenk-type techniques. THF was purified by distillation from sodium/benzophenone ketyl, after drying over KOH. Et_2O, benzene, *n*-hexane, and toluene were purified by distillation from sodium/triglyme benzophenone ketyl or were obtained by means of a MBraun solvent purification system, while MeOH was distilled over Mg prior to use. C_6D_6 was dried over sodium/benzophenone ketyl and condensed in vacuo prior to use, while CD_2Cl_2 and $CDCl_3$ were dried over activated 4 Å molecular sieves. Literature methods were used to synthesize the iminopyridine ligand N_2^{Ph} (**1**).[8] $Y(CH_2SiMe_3)_3(THF)_2$ was prepared according to literature procedures.[2] All the other reagents and solvents were used as purchased from commercial suppliers. ^1H and $^{13}C\{^1H\}$ NMR spectra were obtained on either a Bruker ACP 200 (200.13 and 50.32 MHz, respectively) or a Bruker Avance DRX-400 (400.13 and 100.62 MHz, respectively). Chemical shifts are reported in ppm (δ) relative to TMS, referenced to the chemical shifts of residual solvent resonances (^1H and ^{13}C), and coupling constants are given in Hz. IR spectra were recorded as Nujol mulls or KBr plates on FSM 1201 and Bruker-Vertex 70 instruments. Lanthanide metal analyses were carried out by complexometric titration. The C, H elemental analyses were carried out in the microanalytical laboratory of the IOMC or at the ICCOM by means of a a Carlo Erba Model 1106 elemental analyzer with an accepted tolerance of ±0.4 unit on carbon (C), hydrogen (H), and nitrogen (N). Melting points were determined by using a Stuart Scientific SMP3 melting point apparatus.

Synthesis of 1-(6-Bromopyridin-2-yl)ethanone.[20] To a stirred solution of 2,6-dibromopyridine (7.11 g, 30.0 mmol) in Et_2O (130 mL) at −78 °C was added dropwise a 1.7 M solution of *t*BuLi (18.8 mL, 30.0 mmol) in *n*-pentane over 10 min. After 30 min of stirring at −78 °C, *N,N*-dimethylacetamide (3.1 mL, 33.0 mmol) was added and stirring maintained for 1.5 h. The resulting mixture was warmed to room temperature and treated with water (30 mL). The formed layers were separated, and the organic phase was washed with water (2 × 30 mL). The aqueous layer was extracted with Et_2O (3 × 30 mL). The combined organic layers were dried over Na_2SO_4. Removal of the solvent under reduced pressure gave a yellow oil that was dissolved in petroleum ether and cooled to −20 °C. After 6 h, small yellow pale crystals were separated by filtration (yield 90%). Mp: 44 °C. IR (KBr): ν 1695 cm^{-1} (C═O). ^1H NMR (200 MHz, $CDCl_3$, 293 K): δ 2.70 (s, 3H, C(O)Me), 7.68 (m, 2H, CH), 7.98 (dd, J = 6.5, 2.1, 1H, CH). $^{13}C\{^1H\}$ NMR (50 MHz, $CDCl_3$, 293 K): δ 26.4 (1C, C(O)*Me*), 121.1 (1C, CH), 132.4 (1C, CH), 139.8 (1C, CH), 142.0 (1C, C), 154.9 (1C, C), 198.5 (1C, *C*(O)Me). Anal. Calcd for C_7H_6BrNO (200.03): C, 42.03; H, 3.02; N, 7.00. Found: C, 42.09; H, 2.90; N, 7.02.

Synthesis of 6-Bromo-2-(2′-methyl-1′,3′-dioxolan-2′-yl)pyridine.[21] A solution of 1-(6-bromopyridin-2-yl)ethanone (1.0 g, 5 mmol), 1,2-ethanediol (0.34 mL, 6 mmol), and *p*-toluenesulfonic acid hydrate (PTSA, 0.1 g, 0.5 mmol) in 15 mL of distilled benzene was heated for 24 h under reflux in a Dean−Stark apparatus. The mixture was cooled to room temperature and then treated with 5 mL of 0.5 M aqueous NaOH solution. The layers that formed were separated. The aqueous phase was washed with Et_2O (2 × 5 mL), and the combined organic extracts were dried over $NaSO_4$. After removal of the solvent under reduced pressure a white solid was obtained in pure form (yield >99%). Mp: 40−42 °C. ^1H NMR (200 MHz, $CDCl_3$, 293 K): δ 1.80 (s, 3H, Me), 3.95−4.20 (m, 4H, CH_2), 7.49 (dd, J = 7.7, 1.3, 1H, CH Ar), 7.58−7.65 (2H, m, CH Ar). $^{13}C\{^1H\}$ NMR (50 MHz, $CDCl_3$, 298 K): δ 25.6 (1C, Me); 65.6 (2C, CH_2); 108.5 (1C, C Ar); 118.9 (1C, CH Ar); 128.1 (1C, CH Ar); 139.6 (1C, CH Ar); 142.5 (1C, CH Ar); 163.0 (1C, CH Ar). Anal. Calcd for $C_9H_{10}BrNO_2$ (244.09): C, 44.29; H, 4.13; N, 5.74. Found: C, 44.09; H, 4.22; N, 5.69.

(18) (a) Emslie, D. J. H.; Piers, W. E.; Parvez, M.; McDonald, R. *Organometallics* **2002**, *21*, 4226–4240. (b) Harder, S. *Organometallics* **2005**, *24*, 373–379. (c) Lyubov, D. M.; Bubnov, A. M.; Fukin, G. K.; Dolgushin, F. M.; Antipin, M. Yu.; Pelcé, O.; Schappacher, M.; Guillaume, S. M.; Trifonov, A. A. *Eur. J. Inorg. Chem.* **2008**, 2090–2098.

(19) For examples of alkyl−hydrido complexes see: (a) Tardif, O.; Nishiura, M.; Hou, Z. *Organometallics* **2003**, *22*, 1171–1173. (b) Voskoboinikov, A. Z.; Parshina, I. N.; Shestakova, A. K.; Butin, K. P.; Beletskaya, I. P.; Kuz'mina, L. G.; Howard, J. A. K. *Organometallics* **1997**, *16*, 4690–4700. (c) Voskoboinikov, A. Z.; Shestakova, A. K.; Beletskaya, I. P. *Organometallics* **2001**, *20*, 2794–2801. (d) Stern, D.; Sabat, M.; Marks, T. J. *J. Am. Chem. Soc.* **1990**, *112*, 9558–9575. (e) Evans, W. J.; Perotti, J. M.; Ziller, J. W. *Inorg. Chem.* **2005**, *44*, 5820–5825. (f) Evans, W. J.; Ulibarri, T. A.; Ziller, J. W. *Organometallics* **1991**, *10*, 134–142.

(20) Bolm, C.; Ewald, M.; Schilingloff, G. *Chem. Ber.* **1992**, *125*, 1169.

(21) Constable, E. C.; Heirtzler, F.; Neuburger, N.; Zehnder, M. *J. Am. Chem. Soc.* **1997**, *119*, 5606.

Synthesis of 1-(6-(2,6-Dimethylphenyl)pyridin-2-yl)ethanone.[22] To a solution of 6-bromo-2-(2′-methyl-1′,3′-dioxolan-2′-yl)pyridine (1.5 g, 6.14 mmol) in dry and degassed THF (40 mL) was added $NiCl_2(PCy_3)_2$ (0.29 g, 0.43 mmol) in one portion. A 1 M THF solution of $(2,6\text{-}Me_2C_6H_3)MgBr$ (7.4 mL, 7.4 mmol) was then added dropwise, and the resulting red solution was stirred at 50 °C for 72 h. Afterward, the mixture was cooled to room temperature and then treated with 30 mL of a saturated aqueous NH_4Cl solution. The layers that formed were separated, the aqueous phase was washed with Et_2O (3 × 25 mL), and the combined organic extracts were dried over $NaSO_4$. After removal of the solvent under reduced pressure a brown oil was obtained, and it was used in the next step without any further purification. The oil was then suspended in HCl 2 M (15 mL) and stirred at 80−85 °C for 2 h. The resulting mixture was then cooled in an ice bath, diluted with iced water (15 mL), and neutralized portionwise with solid $NaHCO_3$. A standard extractive workup with AcOEt (3 × 30 mL) gave, after removal of solvent, a crude slightly brown solid which was purified by filtration over a silica gel pad (AcOEt−petroleum ether, 10:90) to afford the expected compound as a pale yellow oil (yield 76%). ^{1}H NMR (200 MHz, CD_2Cl_2, 293 K): δ 1.98 (s, 6H, $(C_6H_3)(CH_3)_2$), 2.60 (s, 3H, $COCH_3$), 7.06−7.08 (2H, C*H* Ar), 7.16 (m, 1H, C_H Ar), 7.36 (dd, $^3J_{HH}$ = 7.8 Hz, 1H, C*H* Ar), 7.85 (t, $^3J_{HH}$ = 7.8 Hz, 1H, C*H* Ar), 7.92 (dd, $^3J_{HH}$ = 7.8 Hz, 1H, C*H* Ar).

Synthesis of [1-(6-(2,6-Dimethylphenyl)pyridin-2-yl)ethylidene]-(2,6-diisopropyphenyl)amine (2). A solution of 1-(6-(2,6-dimethylphenyl)pyridin-2-yl)ethanone (0.94 g, 4.17 mmol), 2,6-diisopropylaniline (2.4 mL, 12.5 mmol, 3 equiv) and a few drops of formic acid in MeOH (30 mL) was refluxed for 62 h. The reaction mixture was cooled to room temperature under stirring overnight and cooled for several hours to +4 °C to afford a yellow solid, which was filtered and washed several times with cold MeOH. Recrystallization from boiling MeOH gave a yellow solid in 69% yield. ^{1}H NMR (200 MHz, CD_2Cl_2, 293 K): δ 1.19 (d, $^3J_{HH}$ = 6.9 Hz, 12H, $CH(CH_3)_2$), 2.15 (s, 6H, $(C_6H_3)(CH_3)_2$), 2.19 (s, 3H, $CNCH_3$), 2.82 (sept, $^3J_{HH}$ = 6.9 Hz, 2H, $CH(CH_3)_2$), 6.09−7.14 (m, 1H, C*H* Ar), 7.16−7.22 (4H, C*H* Ar), 7.23−7.29 (m, 1H, C*H* Ar), 7.38 (dd, $^3J_{HH}$ = 7.7 Hz, 1H, C*H* Ar), 7.93 (t, $^3J_{HH}$ = 7.7 Hz, 1H, C*H* Ar), 8.32 (dd, $^3J_{HH}$ = 7.7 Hz, 1H, C*H* Ar). ^{13}C{^{1}H} NMR (50 MHz, CD_2Cl_2, 293 K): δ 17.1 (1C, $CNCH_3$), 20.1 (2C, CH_3 Ar), 22.5 (2C, $CH(CH_3)_2$), 23.0 (2C, $CH(CH_3)_2$), 28.1 (2C, $CH(CH_3)_2$), 119.0 (1C, CH Ar), 122.9 (2C, CH Ar), 123.4 (1C, CH Ar), 125.7 (1C, CH Ar), 127.6 (2C, CH Ar), 127.8 (1C, CH Ar), 135.8 (1C, CH Ar), 136.0 (2C, C Ar), 136.6 (2C, C Ar), 140.4 (1C, C Ar), 146.5 (1C, C Ar), 156.3 (1C, C Ar), 158.4 (1C, C Ar), 167.5 (1C, CN). Anal. Calcd for $C_{27}H_{32}N_2$ (384.56): C, 84.33; H, 8.39; N, 7.28. Found: C, 84.19; H, 8.42; N, 7.39.

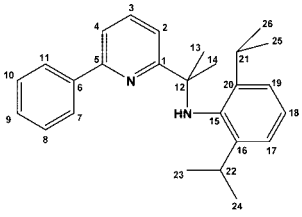

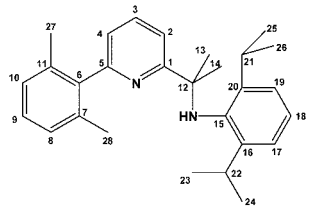

Synthesis of N_2H^{Ph} (3). A solution of the iminopyridine ligand N_2^{Ph} (**1**; 1.21 g, 3.4 mmol) in 35 mL of toluene was cooled to 0 °C in an ice bath and treated dropwise with a 2.0 M toluene solution of trimethylaluminum (TMA; 2.54 mL, 5.1 mmol). The reaction mixture was stirred at room temperature for 12 h and then was quenched with 30 mL of water. The aqueous phase was extracted with 3 × 25 mL of AcOEt, and the combined organic layers were dried over Na_2SO_4. Removal of the solvent under reduced pressure gave the amidopyridinate ligand as a crude dark white solid. The ligand was purified by crystallization from hot MeOH, by cooling the resulting solution to 4 °C overnight to afford white crystals in 93% yield (1.18 g). ^{1}H NMR (400 MHz, CD_2Cl_2, 293 K): δ 1.10 (d, $^3J_{HH}$ = 6.8 Hz, 12H, $CH(CH_3)$, $H^{23,24,25,26}$), 1.53 (s, 6H, $C(CH_3)_2$, $H^{13,14}$), 3.38 (sept, $^3J_{HH}$ = 6.8 Hz, 2H, $CH(CH_3)$, $H^{21,22}$), 4.56 (bs, 1H, N*H*), 7,10 (bs, 3H, C*H* Ar, $H^{17,18,19}$), 7.45−7.54 (m, 4H, C*H* Ar, $H^{2,8,9,10}$), 7.71 (d, 1H, $^3J_{HH}$ = 7.5 Hz, C*H* Ar, H^4), 7.81 (t, 1H, $^3J_{HH}$ = 7.5 Hz, C*H* Ar, H^3), 8.14−8.16 (m, 2H, C*H* Ar, $H^{7,11}$). ^{13}C{^{1}H} NMR (100 MHz, C_6D_6, 293 K): δ 23.7 ($CH(CH_3)_2$, $C^{23,24,25,26}$), 28.2 ($CH(CH_3)_2$, $C^{21,22}$), 28.9 ($C(CH_3)_2$, $C^{13,14}$), 59.4 ($C(CH_3)_2$; C^{12}), 117.7 ($C^{2,4}$), 122.9 ($C^{17,19}$), 124.4 (C^{18}), 126.8 ($C^{7,11}$), 128.6 ($C^{8,10}$), 128.8 (C^9), 137.2 (C^3), 139.5 (C^6), 140.5 ($C^{16,20}$), 146.8 (C^{15}), 155.4 (C^5), 167.8 (C^1). Mp: 107.8 °C. Anal. Calcd for $C_{26}H_{32}N_2$ (372.55): C, 83.82; H, 8.66; N, 7.52. Found: C, 83.91; H, 8.62; N, 7.37.

Synthesis of N_2H^{Xyl} (4). A solution of the iminopyridine ligand N_2^{Xyl} (**2**; 0.85 g, 2.2 mmol) in 20 mL of toluene was cooled to 0 °C in an ice bath and treated dropwise with a 2.0 M toluene solution of trimethylaluminum (TMA; 1.65 mL, 3.3 mmol). The reaction mixture was stirred at room temperature for 12 h and then was quenched with 20 mL of water. The aqueous phase was extracted with 3 × 25 mL of AcOEt, and the combined organic layers were dried over Na_2SO_4. Removal of the solvent under reduced pressure gave the amidopyridinate ligand as a crude dark white solid. The ligand was purified by crystallization from hot MeOH, by cooling the resulting solution to −20 °C overnight to afford white crystals in 89% yield (0.79 g). ^{1}H NMR (400 MHz, CD_2Cl_2, 293 K): δ 1.07 (d, 12H, $^3J_{HH}$ = 6.8 Hz, $CH(CH_3)$, $H^{23,24,25,26}$), 1.49 (s, 6H, $C(CH_3)_2$, $H^{13,14}$), 2.12 (s, 6H, $C(CH_3)$, $H^{27,28}$), 3.23 (sept, $^3J_{HH}$ = 6.8 Hz, 2H, $CH(CH_3)$, $H^{21,22}$), 4.14 (bs, 1H, N*H*), 7,08 (bs, 3H, C*H* Ar, $H^{17,18,19}$), 7.14−7.17 (m, 4H, C*H* Ar, $H^{2,8,9,10}$), 7.57 (dd, 1H, $^3J_{HH}$ = 7.9 Hz, $^3J_{HH}$ = 0.9 Hz, C*H* Ar, H^4), 7.80 (t, 1H, $^3J_{HH}$ = 7.9 Hz, C*H* Ar, H^3). ^{13}C{^{1}H} NMR (100 MHz, C_6D_6, 293 K): δ 20.1 ($C(CH_3)_2$, $C^{13,14}$), 23.7 ($CH(CH_3)_2$, $C^{23,24,25,26}$), 28.1 ($CH(CH_3)_2$, $C^{21,22}$), 29.1 ($C(CH_3)$, $C^{27,28}$), 58.9 ($C(CH_3)_2$; C^{12}), 116.9 (C^2), 122.1 (C^4), 122.9 ($C^{17,19}$), 124.2 (C^{18}), 127.4 ($C^{8,10}$), 127.6 (C^9), 135.9 (C^6), 136.5 ($C^{16,20}$), 140.8 (C^3), 141.0 (C^{15}), 146.3 ($C^{7,11}$), 158.3 (C^5), 168.5 (C^1). Mp: 109.6 °C. Anal. Calcd for $C_{28}H_{36}N_2$ (400.6): C, 83.95; H, 9.06; N, 6.99. Found: C, 83.7; H, 8.97; N, 7.02.

Synthesis of $N_2^{Ph}Y(CH_2SiMe_3)(THF)_2$ (5). A solution of $N_2^{Ph}H$ (**3**; 0.182 g, 0.49 mmol) in *n*-hexane (15 mL) was added to a solution of $(Me_3SiCH_2)_3Y(THF)_2$ (0.242 g, 0.49 mmol) in *n*-hexane (10 mL) at 0 °C. The reaction mixture was stirred at 0 °C for 1 h. The solution was concentrated under vacuum and was kept overnight at −20 °C. Complex **5** was isolated as a yellow microcrystalline solid in 87% yield (0.294 g). ^{1}H NMR (400 MHz, C_6D_6, 293 K): δ −0.54 (d, $^2J_{YH}$ = 3.0 Hz, 2H, YCH_2), 0.22 (s, 9H, $Si(CH_3)$), 1.07 (m, 8H, β-CH_2 THF), 1.21 (d, $^3J_{HH}$ = 6.8 Hz, 6H, $CH(CH_3)$; $H^{23,24,25,26}$), 1.31 (d, $^3J_{HH}$ = 6.8 Hz, 6H, $CH(CH_3)$, $H^{23,24,25,26}$), 1.44 (s, 6H, $C(CH_3)_2$, $H^{13,14}$), 3.55 (m, 8H, α-CH_2 THF), 3.80 (sept, $^3J_{HH}$ = 6.8 Hz, 2H, $CH(CH_3)$, $H^{21,22}$), 6.76 (d, $^3J_{HH}$ = 7.9 Hz, 1H, C*H* Ar, H^2), 7.19 (m, together 2H, C*H* Ar, $H^{3,18}$), 7.27 (m, together 3H, C*H* Ar, $H^{10,17,19}$), 7.39 (t, $^3J_{HH}$ = 7.3 Hz, 1H, C*H* Ar, H^9), 7.45 (d, $^3J_{HH}$ = 7.5 Hz, 1H, C*H* Ar, H^4), 7.79 (d, $^3J_{HH}$ = 8.0 Hz, 1H, C*H* Ar, H^{11}), 8.15 (d, $^3J_{HH}$ = 6.8 Hz, 1H, C*H* Ar, H^8). ^{13}C{^{1}H} NMR (100 MHz, C_6D_6, 293 K): δ 4.6 (s, $Si(CH_3)_3$), 23.8 (s, $CH(CH_3)_2$, $C^{23,24,25,26}$), 24.7 (s, β-CH_2, THF), 27.5 (s, $CH(CH_3)_2$, $C^{3,24,25,26}$), 27.6 (s, $CH(CH_3)_2$, $C^{21,22}$), 30.3 (d, $^1J_{YC}$ = 39.5 Hz, YCH_2), 32.1 (s, $C(CH_3)_2$, $C^{13,14}$), 68.5 (s, $C(CH_3)_2$; C^{12}), 69.6 (s, α-CH_2 THF), 115.2 (s, C^4), 117.7 (s, C^2), 122.9 (s, C^{11}), 123.6 (s, $C^{17,19}$), 123.7 (s, C^{18}), 125.3 (s, C^{10}), 127.9 (s, C^9), 138.0 (s, C^8), 138.6 (s, C^3), 145.3 (s, C^6), 147.6 (s, C^{15}), 150.2 (s, $C^{16,20}$), 164.6 (s, C^5), 175.8 (s, C^1), 190.6 (d, $^1J_{YC}$ = 41.2 Hz, Y*C*, C^7). Anal. Calcd for $C_{38}H_{57}N_2O_2SiY$ (690.86): C, 66.06; H, 8.32; N, 4.05; Y, 12.87. Found: C, 66.38; H, 8.52; N, 4.09; Y, 12.64.

(22) (a) Scott, N. M.; Schareina, T.; Tock, O.; Kempe, R. *Eur. J. Inorg. Chem.* **2004**, 3297–3304. (b) Labonne, A.; Kribber, T.; Hintermann, L. *Org. Lett.* **2006**, *8*, 5853–5856.

Synthesis of $N_2^{Xyl}Y(CH_2SiMe_3)(THF)$ (6). A solution of $N_2^{Xy}H$ (**4**; 0.215 g, 0.54 mmol) in *n*-hexane (15 mL) was added to a solution of $(Me_3SiCH_2)_3Y(THF)_2$ (0.266 g, 0.54 mmol) in *n*-hexane (10 mL) at 0 °C. The reaction mixture was stirred at 0 °C for 1 h. The solution was concentrated under vacuum and kept overnight at −20 °C. Complex **6** was isolated as an orange crystalline solid in 79% yield (0.274 g). ^{1}H NMR (400 MHz, C_6D_6, 293 K): δ −0.92 (dd, $^2J_{HH}$ = 10.8 Hz, $^2J_{YH}$ = 3.0 Hz, 1H, YCH_2SiMe$_3$), −0.76 (dd, $^2J_{HH}$ = 10.8 Hz, $^2J_{YH}$ = 3.0 Hz, 1H, YCH_2SiMe$_3$), 0.23 (s, 9H, Si(CH_3)$_3$), 0.96 (d, $^3J_{HH}$ = 6.3 Hz, 3H, CH(CH_3), H^{23,24,25,26}), 1.02 (br m, β-CH_2 THF), 1.15 (m, together 6H, CH(CH_3)$_2$ and C(CH_3)$_2$, H^{13,14,23,24,25,26}), 1.38 (d, $^3J_{HH}$ = 6.8 Hz, 3H, CH(CH_3)$_2$, H^{23,24,25,26}), 1.39 (d, $^3J_{HH}$ = 6.8 Hz, 3H, CH(CH_3)$_2$, H^{23,24,25,26}), 1.81 (dd, d, $^2J_{HH}$ = 5.5 Hz, $^2J_{YH}$ = 2.0 Hz, 1H, ArCH_2Y, H^{28}), 1.89 (s, 3H, ArCH_3, C^{27}), 2.00 (dd, d, $^2J_{HH}$ = 5.5 Hz, $^2J_{YH}$ = 2.0 Hz, 1H, ArCH_2Y, H^{28}), 2.20 (s, 3H, C(CH_3)$_2$, C^{13,14}), 3.00 (br m, 2H, α-CH_2, THF), 3.11 (br m, 2H, α-CH_2 THF), 3.18 (sept, $^3J_{HH}$ = 6.8 Hz, 1H, CH(CH$_3$), H^{21,22}), 4.50 (sept, $^3J_{HH}$ = 6.3 Hz, 1H, CH(CH$_3$), H^{21,22}), 6.74 (d, $^3J_{HH}$ = 8.0 Hz, 1H, CH Ar, H^2), 6.80 (m, 2H, CH Ar, H^{4,8}), 6.98 (d, $^3J_{HH}$ = 7.8 Hz, 1H, CH Ar, H^{10}), 7.05−7.22 (m, 5H, CH, H^{3,9,17,18,19}). ^{13}C{^{1}H} NMR (100 MHz, C_6D_6, 293 K): δ 4.7 (s, Si(CH_3)$_3$), 21.5 (s, C(CH_3)$_2$, C^{13,14}), 24.1 (s, CH(CH_3)$_2$, C^{23,24,25,26}), 24.8 (s, β-CH_2 THF), 24.9 (s, C(CH_3)$_2$, C^{13,14}), 25.6 (s, CH(CH_3)$_2$, C^{23,24,25,26}), 26.7 (s, CH(CH_3)$_2$, C^{23,24,25,26}), 27.2 (s, CH(CH$_3$)$_2$, C^{23,24,25,26}), 27.3 (d, $^1J_{YC}$ = 41.4 Hz, YCH_2Si), 27.4 (s, CH(CH$_3$)$_2$, C^{21,22}), 28.1 (s, CH(CH$_3$)$_2$, C^{21,22}), 40.8 (s, ArCH_3, C^{27}), 49.2 (d, $^1J_{YC}$ = 23.1 Hz, YCH_2, C^{28}), 65.4 (s, C(CH$_3$)$_2$, C^{12}), 69.5 (s, α-CH_2 THF), 115.5 (s, Ar, C^4), 119.8 (s, Ar, C^2), 122.8 (s, Ar, C^{10}), 123.5 (s, Ar, C^{17,19}), 123.6 (s, Ar, C^{17,19}), 123.7 (s, Ar, C^{18}), 124.0 (s, Ar, C^8), 130.5 (s, Ar, C^9), 136.5 (s, Ar, C^{11}), 139.0 (s, Ar, C^3), 145.6 (s, Ar, C^6), 149.3 (s, Ar, C^{15}), 150.0 (s, Ar, C^{16,20}), 150.2 (s, Ar, C^{16,20}) 150.6 (s, Ar, C^7), 158.3 (s, Ar, C^5), 176.0 (s, Ar, C^1). Anal. Calcd for $C_{36}H_{53}N_2OSiY$ (646.30): C, 66.85; H, 8.26; N, 4.33; Y, 13.76. Found: C, 66.63; H, 8.03; N, 4.29; Y, 13.64.

Synthesis of $[N_2^{Ph}Y(\mu\text{-}H)(THF)]_2$ (7). $PhSiH_3$ (0.035 g, 0.318 mmol) was added to a solution of **5** (0.220 g, 0.318 mmol) in *n*-hexane (25 mL) at 0 °C. The reaction mixture was stirred at 0 °C for 1 h and kept overnight at room temperature. The solution was concentrated under vacuum and was kept overnight at −20 °C. Complex **7** was isolated as a yellow microcrystalline solid in 69% yield (0.117 g). ^{1}H NMR (400 MHz, C_6D_6, 293 K): δ 1.03 (br s, 8H, β-CH_2 THF), 1.18 (br m, 12H, CH(CH_3); H^{23,24,25,26}), 1.35 (br m, 12H, CH(CH_3), H^{23,24,25,26}), 1.55 (s, 12H, C(CH_3)$_2$, H^{13,14}), 3.21 (br m, together 12H, α-CH_2 THF and CH(CH$_3$), H^{21,22}), 6.84 (d, $^3J_{HH}$ = 7.6 Hz, 2H, CH Ar, H^2), 6.95 (d, $^3J_{HH}$ = 7.5 Hz, 2H, CH Ar, H^{18}), 7.04 (d, $^3J_{HH}$ = 7.5 Hz, 4H, CH Ar, C^{17,19}), 7.23 (m, together 4H, CH Ar, H^{3,10}), 7.36 (t, $^3J_{HH}$ = 7.0 Hz, 2H, CH Ar, H^9), 7.47 (d, $^3J_{HH}$ = 8.0 Hz, 2H, CH Ar, H^4), 7.76 (t, $^1J_{YH}$ = 27.7 Hz, 2H, Y(μ-H)), 7.85 (d, $^3J_{HH}$ = 7.8 Hz, 2H, CH Ar, H^{11}), 8.07 (d, $^3J_{HH}$ = 6.5 Hz, 2H, CH Ar, H^8). ^{13}C{^{1}H} NMR (100 MHz, C_6D_6, 293 K): δ 24.8 (s, β-CH_2 THF), 25.6 (s, CH(CH_3)$_2$, C^{23,24,25,26}), 27.5 (s, CH(CH_3)$_2$, C^{23,24,25,26}), 28.3 (s, CH(CH$_3$)$_2$, C^{21,22}), 29.2 (s, C(CH_3)$_2$, C^{13,14}), 66.2 (s, C(CH$_3$)$_2$, C^{12}), 70.0 (s, α-CH_2 THF), 115.2 (s, C^2), 115.5 (s, C^4), 122.2 (s, C^{18}), 122.8 (s, C^{17,19}), 123.1 (s, C^{11}), 125.1 (s, C^{10}), 126.9 (s, C^9), 138.0 (s, C^8), 138.6 (s, C^3), 147.8 (s, C^6), 148.1 (s, C^{15}), 148.9 (s, C^{16,20}), 164.0 (s, C^5), 176.0 (s, C^1), 193.1 (d, $^1J_{YC}$ = 46.2 Hz, YC). Anal. Calcd for $C_{60}H_{78}N_4O_2Y_2$ (1065.10): C, 67.66; H, 7.38; N, 5.26; Y, 16.69. Found: C, 67.23; H, 7.42; N, 5.15; Y, 16.43.

Synthesis of $[N_2^{Xyl}Y(\mu\text{-}H)(THF)]_2$ (8). $PhSiH_3$ (0.048 g, 0.444 mmol) was added to a solution of **6** (0.287 g, 0.444 mmol) in *n*-hexane (25 mL) at 0 °C. The reaction mixture was stirred at 0 °C for 1 h and kept overnight at room temperature. The solution was concentrated under vacuum and was kept overnight at −20 °C. Complex **8** was isolated as an orange microcrystalline solid in 63% yield (0.157 g). ^{1}H NMR (400 MHz, C_6D_6, 293 K): δ 1.03 (d, $^3J_{HH}$ = 6.3 Hz, 6H, CH(CH_3), H^{23,24,25,26}), 1.08 (d, $^3J_{HH}$ = 6.3 Hz, 6H, CH(CH_3), H^{23,24,25,26}), 1.13 (m, together 12H, CH(CH_3)$_2$ and C(CH_3)$_2$, H^{13,14,23,24,25,26}), 1.27 (br m, together 14H, CH(CH_3)$_2$ and β-CH_2 THF, H^{23,24,25,26}), 1.76 (d, $^2J_{HH}$ = 5.5 Hz, 2H, ArCH_2Y, H^8), 1.87 (d, $^2J_{HH}$ = 5.5 Hz, 2H, ArCH_2Y, H^{28}), 2.15 (s, 6H, C(CH_3)$_2$, C^{13,14}), 2.18 (s, 6H, ArCH_3, H^{27}) 2.83 (sept, $^3J_{HH}$ = 6.5 Hz, 2H, CH(CH$_3$), H^{21,22}), 2.92 (br m, 4H, α-CH_2 THF), 3.17 (br m, 4H, α-CH_2 THF), 4.33 (sept, $^3J_{HH}$ = 6.5 Hz, 2H, CH(CH$_3$), H^{21,22}), 6.32 (d, $^3J_{HH}$ = 6.5 Hz, 2H, CH Ar, H^2), 6.76 (d, $^3J_{HH}$ = 8.5 Hz, 2H, CH Ar, H^4), 6.81 (m, 4H, CH Ar, H^{9,10}), 6.88 (d, $^3J_{HH}$ = 7.8 Hz, 2H, CH Ar, H^8), 7.06 (m, 4H, CH Ar, H^{17,19}), 7.15 (m, 4H, CH Ar, H^{3,18}), 7.37 (t, $^1J_{YH}$ = 26.5 Hz, 2 H, YH). ^{13}C{^{1}H} NMR (100 MHz, C_6D_6, 293 K): δ 21.3 (s, C(CH_3)$_2$, C^{13,14}), 24.6 (s, CH(CH_3)$_2$, C^{23,24,25,26}), 24.5 (s, CH(CH$_3$)$_2$, C^{23,24,25,26}), 25.2 (s, C(CH_3)$_2$, C^{13,14}), 25.4 (s, CH(CH_3)$_2$, C^{23,24,25,26}), 25.5 (s, β-CH_2 THF), 26.3 (s, CH(CH_3)$_2$, C^{23,24,25,26}), 26.9 (s, CH(CH$_3$)$_2$, C^{21,22}), 27.7 (s, CH(CH$_3$)$_2$, C^{21,22}), 43.3 (s, ArCH_3, C^{27}), 51.3 (d,$^1J_{YC}$ = 24.9 Hz, YCH_2), 63.6 (s, C(CH$_3$)$_2$, C^{12}), 69.3 (s, α-CH_2 THF), 113.1 (s, C^4), 118.0 (s, C^2), 122.0 (s, C^{10}), 122.9 (s, C^{17,19}), 123.0 (s, C^{17,19}), 123.2 (s, C^{18}), 123.7 (s, C^8), 128.7 (s, C^9), 134.5 (s, C^3), 137.8 (s, C^{11}), 146.7 (s, C^6) 147.8 (s, C^{15}), 148.5 (s, C^{16,20}), 148.7 (s, C^{16,20}), 150.8 (s, C^7), 159.0 (s, C^5), 176.0 (s, C^1). Anal. Calcd for $C_{64}H_{86}N_4O_2Y_2$ (1121.20): C, 68.56; H, 7.73; N, 5.00; Y, 15.86. Found: C, 68.41; H, 7.33; N, 4.92; Y, 15.76.

Acknowledgment. This work has been supported by the Russian Foundation for Basic Research (Grant Nos. 08-03-00391-a, 06-03-32728). Thanks are also due to the European Commission (NoE IDECAT, NMP3-CT-2005-011730) and the Ministero dell'Istruzione, dell'Università e della Ricerca of Italy (NANOPACK - FIRB project no. RBNE03R78E) for support.

Supporting Information Available: Tables and CIF files giving crystallographic data for the compounds $N_2^{Xyl}Y(CH_2SiMe_3)(THF)$ (**6**) and $[N_2^{Ph}Y(\mu\text{-}H)(THF)]_2$ (**7**). This material is available free of charge via the Internet at http://pubs.acs.org.

OM801044H

DOI: 10.1002/ejic.200900934

Yttrium-Amidopyridinate Complexes: Synthesis and Characterization of Yttrium-Alkyl and Yttrium-Hydrido Derivatives

Lapo Luconi,[a] Dmitrii M. Lyubov,[b] Claudio Bianchini,[a] Andrea Rossin,[a] Cristina Faggi,[c] Georgii K. Fukin,[b] Anton V. Cherkasov,[b] Andrei S. Shavyrin,[b] Alexander A. Trifonov,*[b] and Giuliano Giambastiani*[a]

Keywords: Amidopyridinate / Yttrium / Hydrides / Metathesis / Ethylene / Polymerization

Aryl- or heteroaryl-substituted aminopyridine ligands (N_2H^{Ar}) react with an equimolar amount of $[Y(CH_2SiMe_3)_3(thf)_2]$ to give yttrium(III)-monoalkyl complexes. The process involves the deprotonation of N_2H^{Ar} by a yttrium alkyl followed by a rapid and quantitative intramolecular sp^2-CH bond activation of the aryl or heteroaryl pyridine substituents. As a result, new Y complexes distinguished by rare examples of CH bond activations have been isolated and completely characterized. Selective σ-bond metathesis reactions take place on the residual Y–alkyl bonds upon treatment with $PhSiH_3$. Unusual binuclear metallacyclic yttrium(III)-hydrido complexes have been obtained and characterized by NMR spectroscopy and X-ray diffraction analysis.

Introduction

Cyclopentadienyl-free rare-earth-metal alkyls or hydrides are target compounds in organometallic chemistry due to their unique properties and intriguing reactivity in polymerization catalysis.[1] To date, rare-earth-metal complexes have been dominated by cyclopentadienyl moieties, including mono-, bis- and ansa-systems.[2] Only recently, systems such as bidentate amidinate,[3] guanidinate,[4] β-diketiminate[5] and salicylaldiminates[6] have emerged as valuable ancillary ligands for lanthanide ions by virtue of their ability to form strong metal–ligand bonds and to allow for an easy tuning of the steric and electronic properties of the ligand. Nevertheless, lanthanide-alkyl or -hydrido complexes stabilized by these type of ligands are still fairly rare species, largely because of their troublesome preparation. Indeed, the rare-earth-metal centres in these complexes are generally both electronically and sterically less saturated than those in metallocene or half-sandwich-type derivatives. As a result, unusual reactivity paths are often observed for cyclopentadienyl-free lanthanide complexes, including dimerizations, intra- and intermolecular C–H bond activations or ligand redistributions.[1g]

[a] Istituto di Chimica dei Composti Organometallici (ICCOM–CNR),
via Madonna del Piano 10, 50019 Sesto Fiorentino (Firenze), Italy
Fax: +39-055-5225203
E-mail: giuliano.giambastiani@iccom.cnr.it
[b] G. A. Razuvaev Institute of Organometallic Chemistry of Russian Academy of Sciences,
Tropinina 49, GSP-445, 603950 Nizhny Novgorod, Russia
E-mail: trif@iomc.ras.ru
[c] Dipartimento di Chimica Organica "U. Schiff", Università degli Studi di Firenze,
via della Lastruccia 13, 50019 Sesto Fiorentino (Firenze), Italy

A variety of bidentate or polydentate nitrogen-containing ligands (amide, imine) have been successfully employed for the synthesis of discrete organo-rare-earth-metal complexes, although the number of reported active catalysts remain still quite limited.[1f,7]

We have recently communicated on the synthesis of new yttrium(III)-monoalkyl and yttrium(III)-hydrido complexes stabilized by amidopyridinate ligands.[8] Interesting results have been obtained from the reaction of the pyridylamine ligands N_2H^{Ph} and N_2H^{Xyl} with $[Y(CH_2SiMe_3)_3(thf)_2]$. The reactions have been found to proceed rapidly at 0 °C and independently from the dilution conditions, with the elimination of 2 equiv. of tetramethylsilane, instead of the 1 equiv. expected and the concomitant formation of the monoalkyl sp^2 or sp^3 *ortho*-metalated complexes of the type shown in Scheme 1.

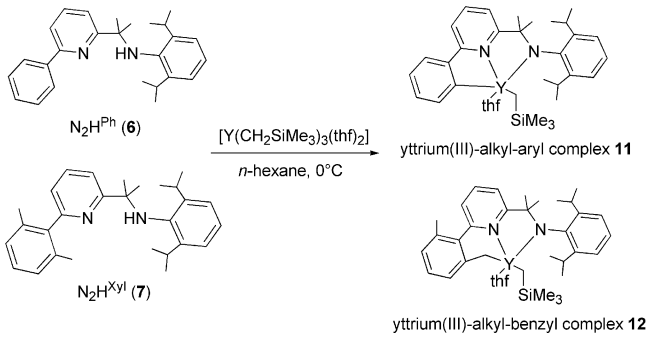

Scheme 1. Synthesis of yttrium(III)-alkyl-aryl and -alkyl-benzyl complexes.

Notably, both yttrium complexes undergo selective σ-bond metathesis on the residual CH_2SiMe_3 bond upon treatment with $PhSiH_3$. As a result, binuclear aryl-hydrido and benzyl-hydrido complexes of the type shown in Scheme 2 have been isolated and characterized.

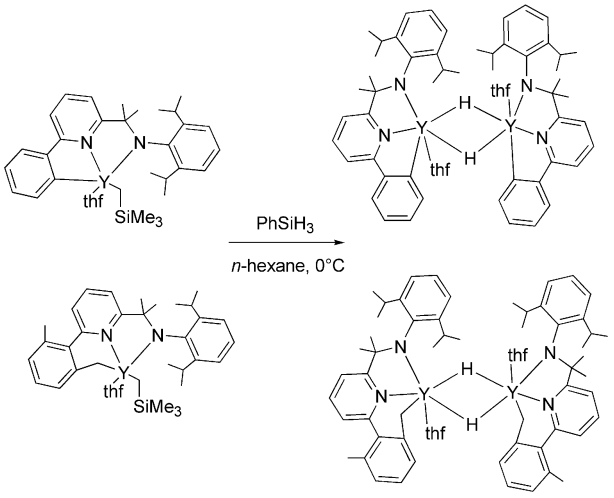

Scheme 2. Synthesis of binuclear yttrium(III)-hydrido complexes by selective σ-bond metathesis on the residual CH_2SiMe_3 group.

Much of the interest in group 4 and lanthanide-alkyl or -hydrido complexes stabilized with amidopyridinate ligands comes from their ability to undergo intramolecular C–H bond activation, thus providing metal complexes with unconventional structures. A new family of strictly related pyridylamido Hf^{IV} catalysts have been recently developed by the group of Busico and researchers at Dow as effective catalysts for the isotactic polymerization of propene in high-temperature solution processes.[9]

One of the most notable features of these group 4 precatalysts is the *ortho*-metalation of the aryl substituent on the pyridine ring, which results in the tridentate ligation of the pyridylamido moiety and a distorted trigonal-bipyramidal metal coordination (Figure 1a). The incorporation of sp^3-C donors into the imidopyridinate ligand framework has been successfully achieved by Coates and co-workers through an intramolecular migratory insertion of a cationic Hf^{IV} species onto a facing vinyl moiety (Figure 1b).[10]

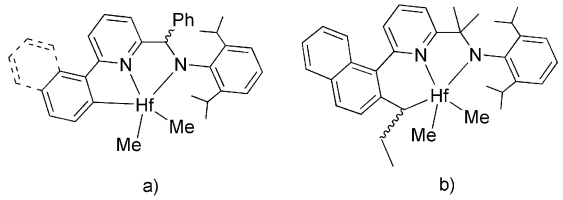

Figure 1. Group 4 metal complexes distinguished by amidopyridinate ligands showing a) sp^2 or b) sp^3 C–H bond activation.

Although inter- and intramolecular metalations of sp^2- and sp^3-hybridized C–H bonds have been previously documented for cyclopentadienyl[3b,11] and cyclopentadienyl-free[4b,12] lanthanide-alkyl and -hydride complexes, they still attract considerable interest due to the intrinsic difficulty for organometallic fragments to activate inert chemical bonds. In this paper we provide a full account on the synthesis, characterization and catalytic activity of a family of novel yttrium(III)-alkyl and -hydrido complexes distinguished by stable Y–C(aryl) or Y–C(heteroaryl) bonds.

Results and Discussion

Synthesis and Characterization of the Aminopyridinate Ligands 6–10

The 6-aryl-substituted ligands **6**–**10** were straightforwardly prepared, in fairly good yields (70–93% of isolated product) by reductive alkylation of the related iminopyridines (**1**–**5**) with a slight excess amount of trimethylaluminium in dry toluene at room temperature, followed by hydrolysis (Scheme 3).

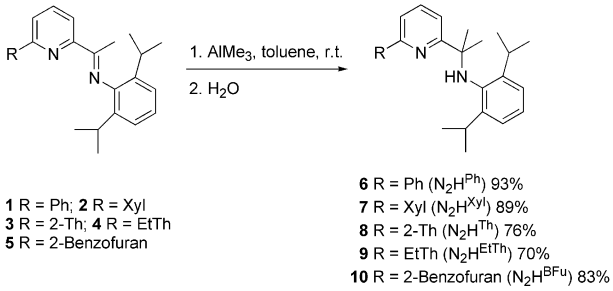

Scheme 3. Reductive alkylation of iminopyridines **1**–**5**.

The imino precursors **1**–**5** were obtained on a multigram scale according to procedures reported in the literature,[8,13] in some cases with little modification.[14] All aminopyridinate ligands appear as off-white/pale-yellow solids after extractive workup and solvent evaporation. Recrystallization from hot MeOH gave the pure compounds as white/pale yellow crystals with melting points ranging from 97 to 134 °C (see the Experimental Section).

The ^1H NMR spectra of aminopyridines **6**–**10** confirmed the formation of saturated –$C(Me)_2NH(2,6\text{-}iPr_2C_6H_3)$ moieties with the NH proton resonance appearing as a broad singlet between 4.1 and 4.6 ppm and the related $^{13}C\{^1H\}$ NMR spectra showing the expected number of independent carbon atom signals.

Suitable crystals for X-ray diffraction studies of compounds **6**–**10** were isolated by successive recrystallizations from hot MeOH (Table 4). A perspective view of all ligand structures is given in Figure 2, whereas selected bond lengths and angles are listed in Table 1. All structures consist of a central pyridine unit substituted at its 6-position by an aryl (Figure 2, ligands **6** and **7**) or a heteroaryl (Figure 2, ligands **8**–**10**) group and at its 2-position by the same amine-containing $C(Me)_2NH(2,6\text{-}iPr_2C_6H_3)$ fragment. The aryl or heteroaryl moieties are almost coplanar with respect

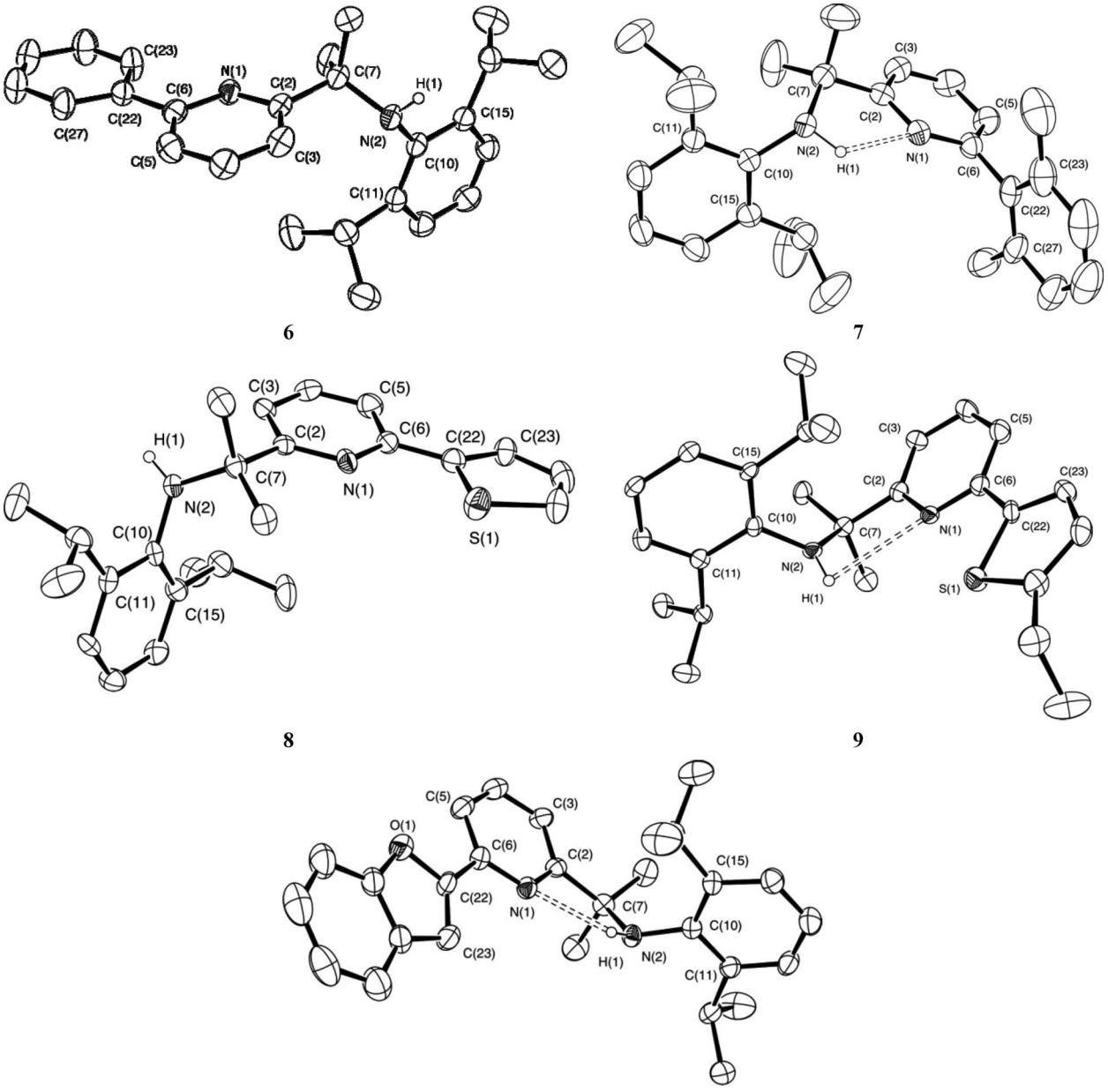

Figure 2. Crystal structures of ligands N_2H^{Ph} (**6**), N_2H^{Xyl} (**7**), N_2H^{Th} (**8**), N_2H^{EtTh} (**9**) and N_2H^{BFu} (**10**). Thermal ellipsoids are drawn at the 30% probability level. Hydrogen atoms, apart from those of the N–H moiety, are omitted for clarity.

to the pyridine unit [torsion angle (θ) N(1)–C(6)–C(22)–C(23): **6**, 7.32(2)°; **8**, 177.29(2)°; **9**, 177.41(5)°; **10**, –10.8(6)°] except for ligand **7**, in which the more sterically demanding xylyl group is nearly orthogonal to the pyridine plane, as expected [N(1)–C(6)–C(22)–C(23): –72.3(4)°]. The $C(2)_{Py}$–$C(7)_{alk}$ bond lengths are in the typical (sp^2)–(sp^3) range of values.[15] The C(7)–N(2) vector is rotated closer to the pyridine plane for all ligand structures, whereas the N(1)–C(2)–C(7)–N(2) torsion angle brings the N(2)H hydrogen atom

Table 1. Selected bond lengths [Å] and angles [°] for ligands **6**–**10**.

	6	7	8	9	10
N(2)–C(7)	1.492(4)	1.480(4)	1.497(9)	1.495(4)	1.493(4)
N(1)–H(1)	–	2.11(3)	–	2.61(4)	2.22(4)
N(2)–C(7)–C(2)	110.5(3)	110.0(3)	109.8(6)	108.1(3)	109.9(3)
N(1)–C(2)–C(7)	116.3(3)	115.9(3)	117.1(6)	113.9(4)	115.3(3)
N(1)–C(6)–C(22)–C(23)	7.32(2)	–72.3(4)	177.29(2)	177.41(5)	–10.8(6)

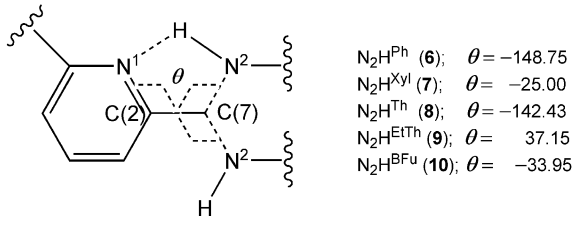

Figure 3. N(1)–C(2)–C(7)–N(2) torsion angles on ligands **6**–**10**.

into a position in which it is able to form a hydrogen bond to the neighbouring pyridine nitrogen atom only for ligands **7**, **9** and **10** (Figure 3) [calculated N(1)···HN(2) distances [Å]: **7**, 2.11(3); **9**, 2.61(4); **10**, 2.22(4)].

Synthesis and Characterization of the Yttrium-Alkyl-Aryl and -Alkyl-Benzyl Complexes

The reaction of the neutral aminopyridines **6** and **7** with $[Y(CH_2SiMe_3)_3(thf)_2]$ (1 equiv.) in hexane at 0 °C have been already discussed in our previous work[8] and are mentioned here only for completeness. In both cases, the reaction is almost instantaneous and gives the mono(alkyl) complexes **11** and **12**, respectively (Scheme 1).

By following similar procedures as those reported for the preparation of **11** and **12**, the ligands containing either 2-thienyl (**8** and **9**) or 2-benzofuryl (**10**) pendant groups have been employed to study their coordination behaviour at the metal centre.

Several cyclopentadienyl-based rare-earth-metal complexes have previously been reported to yield *ortho*-metalation products in the presence of aromatic heterocycles such as furan and thiophene (Th).[11b,16] To date, a few examples of cyclopentadienyl-free lanthanide complexes bearing potentially coordinating sulfur or oxygen atoms have been investigated,[17] whereas those containing thienyl or furanyl groups remain much less explored.[18]

Unexpectedly, the reaction of the thienyl-containing ligands **8** and **9** with $[Y(CH_2SiMe_3)_3(thf)_2]$ (1 equiv.) in hexane at 0 °C resulted in the unique formation of **13** and **14** by means of alkane elimination and C–H bond activation *at the β position of the thienyl moiety* (Scheme 4).

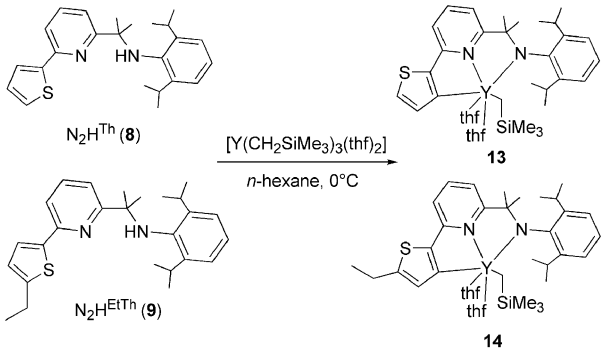

Scheme 4. Synthesis of yttrium(III)-alkyl-aryl complexes **13** and **14** by means of an alkyl elimination reaction.

Attempts to isolate yttrium-bis(alkyl) species by means of monoalkane elimination always resulted in the quantitative generation of the six-coordinate alkyl-heteroaryl complexes, as a result of a deprotonation of the N–H moiety followed by a rapid intramolecular sp^2-CH bond activation at the β position of the heteroaryl fragment (Scheme 4). Further experiments conducted using different dilution conditions never allowed the isolation of dialkyl species. Finally, the reaction monitoring through ^1H NMR spectroscopic experiments has revealed that the cyclometalation step occurs immediately upon mixing of the ligands and metal precursor with no evidence for the formation of transient dialkyl intermediates.

Apparently, the presence of a coordinating thien-2-yl sulfur atom on the ligand backbone does not compete with the intramolecular sp^2 C–H bond activation for the coordination to the metal centre, which occurs rapidly, even under diluted reaction conditions, on the less acidic 3-position of the heteroaryl group.[18] ^1H NMR spectra for **13** and **14** are consistent with six-coordinate yttrium complexes, each of which contains a tridentate dianionic (L^{2-}) amidopyridinate ligand, a residual trimethylsilylmethylene fragment and two thf molecules. Both complexes contain Y–C(alkyl) and Y–C(aryl) bonds; clear doublets could be seen in the ^1H NMR spectrum centred at –0.77 ppm ($^2J_{Y,H}$ = 3.0 Hz) and –0.69 ppm ($^2J_{Y,H}$ = 3.0 Hz), respectively, and are attributed to the hydrogen atoms of each residual methylene group attached to yttrium. The latter appears in the $^{13}C\{^1H\}$ NMR spectra as a doublet centred at 30.0 ppm ($^1J_{Y,C}$ = 39.6 Hz) and 30.1 ppm ($^1J_{Y,C}$ = 39.6 Hz), for complexes **13** and **14**, respectively, whereas further low-field doublets [**13**: 195.2 ppm ($^1J_{Y,C}$ = 38.9 Hz); **14**: 198.6 ppm ($^1J_{Y,C}$ = 38.9 Hz)] unambiguously indicate that the aryl rings are σ-bonded to the metal centre.[18,19] Crystals of **14** suitable for X-ray analysis were grown by cooling at –20 °C a concentrated solution in *n*-hexane (Table 5). The molecular structure of **14** is shown in Figure 4.

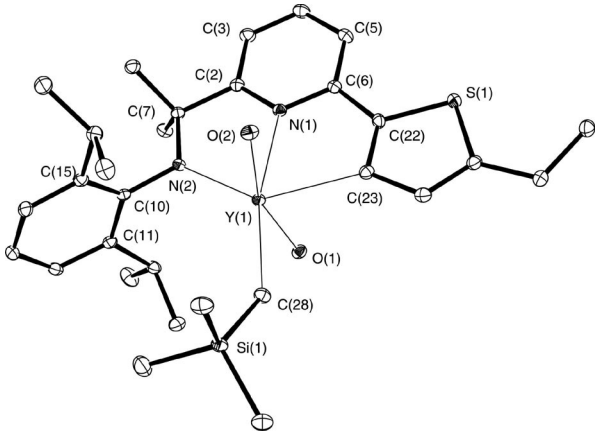

Figure 4. Crystal structure of $[N_2^{EtTh}Y(CH_2SiMe_3)(thf)_2]$ (**14**). Thermal ellipsoids are drawn at the 30% probability level. Hydrogen atoms and methylene groups of the thf molecules are omitted for clarity.

The X-ray diffraction study has shown the monomeric nature of **14**. The coordination environment at the yttrium centre is set up by two nitrogen atoms and one carbon atom from the dianionic tridentate amidopyridinate ligand, one carbon atom from the residual alkyl group and two oxygen atoms from the two thf molecules. Overall, the coordination can be considered to be a strongly distorted octahedron. The yttrium coordination number in **14** is 6. The Y–amidopyridinate fragment is planar (average deviation from the plane is 0.0156 Å) and the Y–C(alkyl) bond length [2.455(2) Å] is comparable to the values reported for related six-coordinate yttrium-monoalkyl compounds.[18,20] The Y–

Table 2. Selected bond lengths [Å] and angles [°] for complexes **12**, **14**, and **16**–**18**.

	12[a]	**14**	**16**[a]	**17**	**18**
Y–H	–	–	2.15	2.44	2.09(2)
Y(1)–N(1)	2.42(14)	2.4616(17)	2.4252(17)	2.472(7)	2.450(2)
Y(1)–N(2)	2.2015(14)	2.2543(17)	2.2205(18)	2.198(7)	2.206(2)
Y(1)–O(1)	2.3422(13)	2.4035(14)	2.3609(15)	2.346(6)	–
Y(1)–O(2)	–	2.3816(14)	–	–	2.355(2)
Y(1)–C(23)	2.9421(17)	2.482(2)	2.469(2)	–	2.514(3)
Y(1)–C(28)	–	2.455(2)	–	–	–
Y(1)–C(29)	2.4520(18)	–	–	2.462(9)	–
Y(1)–C(30)	2.4139(17)	–	–	–	–
Y(1)–Y(1)′	–		3.5780(4)	3.6917(14)	3.53(11)
C(28)–Y(1)–C(23)	–	98.04(7)	–	–	–
C(29)–Y(1)–C(23)	29.47(5)	–	–	–	–
C(30)–Y(1)–C(29)	117.20(6)	–	–	–	–
N(1)–Y(1)–N(2)	70.00(5)	67.44(6)	68.24(6)	69.1(3)	66.39(8)
N(1)–Y(1)–C(29)	–	–	–	72.1(3)	–
N(1)–Y(1)–C(23)	–	–	68.43(7)	–	69.55(9)
N(2)–Y(1)–C(23)	–	–	130.34(7)	–	131.49(9)
N(2)–Y(1)–C(29)	–	–	–	111.8(3)	–
N(1)–C(6)–C(22)–C(23)	–52.57(6)	–4.13(2)	–7.52(3)	50.5(15)	8.5(4)

[a] Selected data from the literature[20] listed here for completeness.

C(thien-2-yl) bond [2.482(2) Å] is slightly longer than that observed for related yttrium-monoalkyl thien-2-yl species featured by analogue intramolecular C–H bond activation at the β position of the thienyl moiety [2.423(3) Å].[18] Related yttrium complexes that contain an amidopyridinate ligand with a shorter ligand backbone[21] have shown a dramatic perturbation of the ligand coordination mode once an intramolecular C–H bond activation occurs {the Y–N covalent bond [2.431(8) Å] becomes longer than the coordinative one [2.338(7) Å]}. In contrast to this, the presence of an additional CMe_2 group between the two nitrogen atoms always results in a "classic" bonding mode (Y–N covalent bonds shorter than coordinative ones; Table 2).

In spite of the well-known oxophilic character of lanthanide ions, the reaction of the 2-benzofuryl-substituted ligand **10** with $[Y(CH_2SiMe_3)_3(thf)_2]$ in hexane at 0 °C yields the monoalkyl complex **15** (Scheme 5).

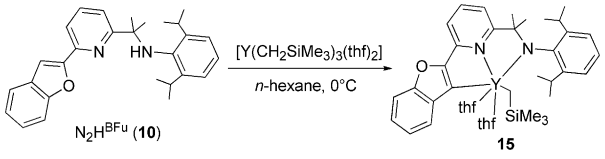

Scheme 5. Synthesis of the ytrrium(III)-alkyl-aryl complex **15**.

As observed for the thienyl-containing systems, the 2-benzofuryl group appended to the amidopyridinate ligand **10** rapidly undergoes metalation on the 3-position irrespective of the dilution conditions used, thus affording the first example of stable cyclopentadienyl-free yttrium(III)-benzofuryl-amidopyridinate complex. Complex **15** could not be obtained in the form of single crystals. The identification as a six-coordinate yttrium complex with a tridentate dianionic (L^{2-}) aminopyridinate ligand, a residual trimethylsilylmethylene fragment and two thf molecules is based on several spectroscopic features (see the Experimental Section). All the aforementioned monoalkyl complexes were highly soluble in hydrocarbon solvents and a comparison of their ^1H and $^{13}C\{^1H\}$ NMR spectra showed many similarities. The ^1H NMR spectrum of **15**, which contains both Y–C(alkyl) and Y–C(aryl) bonds, shows one clear doublet centred at –0.69 ppm ($^2J_{Y,H}$ = 3.0 Hz) attributed to the hydrogen atoms of the residual methylene group bound to yttrium. The $^{13}C\{^1H\}$ NMR spectrum contains a doublet for the sp^3-carbon atom centred at 30.1 ppm ($^1J_{Y,C}$ = 37.6 Hz), whereas a further doublet at 158.6 ppm ($^1J_{Y,C}$ = 38.9 Hz) is assigned to the sp^2 carbon of the benzofuryl moiety σ-bonded to the metal centre.

Recently Okuda and co-workers[16a,16d] have shown that the introduction of a furan-2-yl group on the cyclopentadienyl ring of a half-sandwich lanthanide complex results in a rapid intramolecular C_β–H bond activation, thereby triggering the formation of a thermally more stable yne-enolate yttrium product by means of furanyl ring opening[22] (Scheme 6).

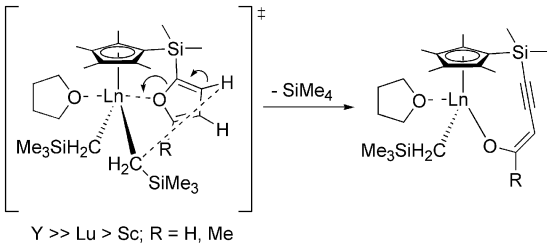

Scheme 6. Furanyl ring opening in lanthanide-cyclopentadienyl complexes.

In addition, in monitoring the intramolecular C_β–H bond activation and the subsequent yne-enolate formation by ^1H NMR spectroscopy, the same authors have found first-order kinetics with respect to the complex concentration as well as an increase of the reaction rate with increasing metal size.[16d] In our case, there is no evidence for the formation of a dialkyl intermediate with the furanyl oxygen

occupying a coordinative position at the metal centre, whereas a rapid metalation at the β position of the heteroaryl substituent takes place to give **15**. This complex is very stable, with no appreciable decomposition even in noncoordinating solvents for days. The close proximity of the Y–alkyl and the C_β–H bond in **15**, due to the free rotation of the pendant donor, is expected to affect the C–H bond-activation rate strongly and make it predominant over oxygen coordination.[16d]

Synthesis and Characterization of the Yttrium-Aryl-Hydrido and -Benzyl-Hydrido Derivatives

The most common synthetic procedures for the preparation of rare-earth hydrido complexes from their M–alkyl counterparts make use of either dihydrogen[2b,23] or phenylsilane[8,24] as reagents. We have already reported on the treatment of **11** and **12** with an equimolecular amount of $PhSiH_3$. In both cases the reaction proceeds rapidly in *n*-hexane at 0 °C, thus resulting in the formation of binuclear yttrium-aryl-hydrido and -benzyl-hydrido complexes **16** and **17** (Scheme 2). Although the crystallographic characterization of **16** has already been reported previously,[8] orange crystals of **17** suitable for X-ray diffraction have now been prepared by the slow cooling of a benzene/*n*-hexane mixture (1:3) down to 10 °C.

Complex **17** crystallizes as a solvate with one hexane molecule per molecule of binuclear species. Its molecular structure is illustrated in Figure 5.

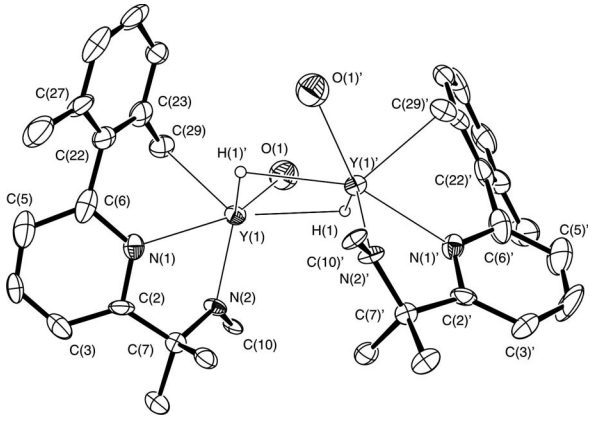

Figure 5. Crystal structure of $[\{N_2^{Xyl}Y(\mu\text{-}H)(thf)\}_2]$ (**17**). Thermal ellipsoids are drawn at the 30% probability level. Hydrogen atoms (apart from yttrium hydrides), 2,6-diisopropylphenyl fragments and methylene groups of the thf molecules and one molecule of hexane (crystallization solvent) are omitted for clarity.

By following the same chemistry, the treatment of **15** with an equimolecular amount of $PhSiH_3$ resulted in the formation of the binuclear heteroaryl-hydrido complex **18**. Yellow-brown crystals of complex **18** were obtained by the slow cooling of a benzene/*n*-hexane mixture (1:3) down to 10 °C. The molecular structure of the benzene solvate complex **18** is illustrated in Figure 6.

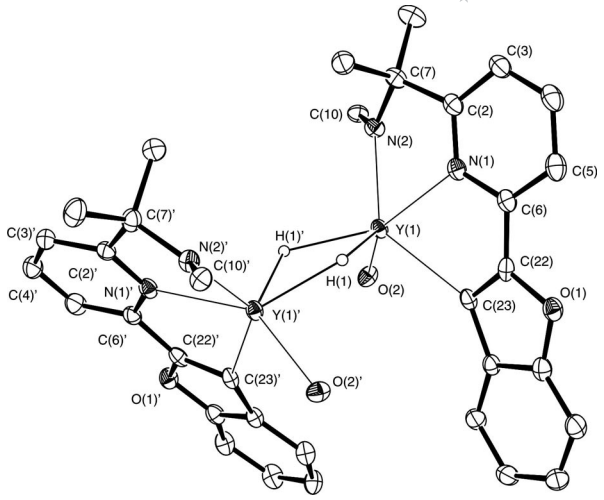

Figure 6. Crystal structure of $[\{N_2^{BFu}Y(\mu\text{-}H)(thf)\}_2]$ (**18**). Thermal ellipsoids are drawn at the 30% probability level. Hydrogen atoms (apart from yttrium hydrides), 2,6-diisopropylphenyl fragments, methylene groups of the thf molecules and two molecules of benzene (crystallization solvent) are omitted for clarity.

Unfortunately, all attempts to synthesize the hydrido complexes supported by thiophenyl-substituted amidopyridinate ligands by treating the monoalkyl complexes **13** and **14** with $PhSiH_3$ failed and intractable materials were invariably isolated.

The complexes adopt binuclear structures with two six-coordinate yttrium atoms. The metal coordination spheres are determined by the two nitrogen and one carbon atoms from the tridentate amidopyridinate ligand, two bridging hydrido ligands and one oxygen atom from a residual thf molecule. Unlike the majority of binuclear hydrido species, the tetranuclear Y_2H_2 cores are not planar. For complexes **16** and **18**, the dihedral angles between the Y(1)H(1)H(1′) and Y(1′)H(1)H(1′) planes have close values (20.1 and 21.0°), whereas for **17** this angle is much smaller (12.4°). A similar trend is finally observed for the Y–H bonds. In complexes **16** and **18**, the Y–H bonds are significantly shorter [2.15 and 2.09(2) Å, respectively] than that measured for **17** (2.44 Å). It should be noted that the coordinated N and C atoms from the tridentate amidopyridinate ligands in **16**–**18** lie in the same plane, although the chelating ligand is not wholly planar. The Y–C bond lengths in **16** [2.469(2) Å], **17** [2.462(9) Å] and **18** [2.514(4) Å] match well the values previously reported for similar six-coordinate yttrium-aryl species,[25] whereas the Y–Y distances [**16**: 3.5780(4) Å; **17**: 3.6917(14) Å; **18**: 3.53(11) Å] are noticeably shorter than those measured in related binuclear yttrium hydrides.[1i,6,26]

Notably, the Y–C(aryl) and Y–C(Bn) (Bn = benzyl) bonds do not react with $PhSiH_3$ even in the presence of a twofold excess amount of the reagent for prolonged reaction times. Indeed, all of the binuclear hydrido complexes can been recovered after stirring of the reagents for 24 h at room temperature in the presence of an excess amount of $PhSiH_3$, with no appreciable decomposition. Unlike $PhSiH_3$, the reaction of **11**, **12** and **15** with H_2 (1 bar) in

Table 3. Ethylene polymerization with yttrium(III)-alkyl and -hydride precursors.[a]

Run	Precatalyst[a]	Cocatalyst (number of equiv.)	T [°C]	Polymer yield [g]	TOF [kg of PE ({mol of Y} bar h)$^{-1}$]	TOF [mol of C_2H_4 conv. ({mol of Y} bar h)$^{-1}$]
1	11	MAO (300)	22	0.144	2.4	85.7
2	11	MAO (300)	50	0.096	1.6	57.1
3	12	MAO (300)	22	0.018	0.3	10.7
4	13	MAO (300)	22	0.132	2.2	78.6
5	14	MAO (300)	22	0.186	3.1	110.7
6	14	MAO (300)	50	0.162	2.7	96.4
7	11	$[Me_2PhNH][B(C_6F_5)_4]$/Al*i*Bu$_3$ (1.2)/(200)	65	0.048	0.8	28.6
8	14	$[Me_2PhNH][B(C_6F_5)_4]$/Al*i*Bu$_3$ (1.2)/(200)	65	0.024	0.4	14.3
9	16	MAO (300)	22	traces	–	–
10	16	$[Me_2PhNH][B(C_6F_5)_4]$/Al*i*Bu$_3$ (1.2)/(200)	65	traces	–	–
11	17	MAO (300)	22	traces	–	–
12	18	$[Me_2PhNH][B(C_6F_5)_4]$/Al*i*Bu$_3$ (1.2)/(200)	65	traces	–	–

[a] Reaction conditions: toluene (final volume 50 mL), precatalyst 12 μmol, 30 min.

toluene at room temperature led to their complete decomposition within a few minutes, followed by the precipitation of insoluble off-white solid materials. This result proves the effectiveness of $PhSiH_3$ as a reagent for the synthesis of the binuclear hydrido complexes **16**–**18** through a selective σ-bond metathesis of the residual Y–CH_2SiMe_3 bond.

Ethylene Polymerization Tests

The catalytic performances of the mononuclear yttrium(III)-monoalkyl complexes and of their binuclear hydride counterparts have been systematically scrutinized for ethylene polymerization under different reaction conditions. Although all these complexes turned out to be completely inert in the absence of a proper activator, some of them have shown a moderate activity upon treatment with methylaluminoxane (MAO; see the Experimental Section and Table 3). Particularly, complexes **11** and **14** have shown activities at room temperature up to 2.4 and 3.1 kg of PE [(mol of Y) bar h]$^{-1}$, respectively. When the sp^2-coordinative carbon atom from the aryl or heteroaryl substituent of the pyridine ring is replaced by an sp^3 donor, as for complex **12**, a significant decrease in the catalytic activity is observed {0.3 kg of PE [(mol of Y) bar h]$^{-1}$}. Finally, no polymerization activity has been observed with the more sterically crowded Y–H dimers **16**–**18** under similar experimental conditions. High-temperature polymerization tests (from 80 to 90 °C) have resulted in the rapid deactivation of the catalyst with the formation of traces of insoluble polyolefinic materials.

Cationic active species are also generated from catalyst precursors **11** and **14** upon treatment with $[Me_2PhNH][B(C_6F_5)_4]$ in combination with Al*i*Bu$_3$ in toluene at 65 °C (see the Experimental Section and Table 3) and were screened in the polymerization of ethylene.[27] Very modest activity was observed with either catalyst precursor {0.8 and 0.4 kg of PE [(mol of Y) bar h]$^{-1}$, respectively}, which we attribute to a rapid catalyst deactivation as indicated by the drop in ethylene consumption in the first two minutes of the reaction. The melting points (138–139 °C) of the PEs produced with catalyst precursors **11** and **14** are in the typical range of values for linear high-density polyethylene (HDPE), and the absence of any type of branches has been unambiguously confirmed by $^{13}C\{^1H\}$ NMR spectroscopy. Finally, the thermogravimetric analysis (TGA) of all polyolefin materials showed comparable thermal stability within all the samples.

Conclusion

We have shown in this paper that aminopyridinate ligands bearing aryl or heteroaryl substituents at the 6-position of the pyridine ring undergo fast intramolecular sp^2 C–H bond activation upon treatment with an equimolecular amount of $[Y(CH_2SiMe_3)_3(thf)_2]$, thereby leading to a novel class of yttrium complexes with unusual Y–C bonds.

Aminopyridinate systems that contain 2-thiophene or 2-benzofuryl moieties have been used to generate stable cyclopentadienyl-free yttrium(III) complexes in which the intramolecular C–H bond activation takes place at the less acidic 3-position of the heteroaryl groups. The reaction of the benzofuryl-containing ligand with the yttrium–tris(alkyl) complex gives the first example of a stable yttrium(III)-alkyl-aryl complex in which the C–H bond activation takes place at the β position of the benzofuryl group with no apparent decomposition of the heteroaromatic moiety (furan ring opening), even upon standing in solution for days.

All monoalkyl complexes undergo selective σ-bond metathesis at the residual Y–$CH_2Si(CH_3)_3$ bond upon treatment with phenylsilane. As a result, binuclear yttrium-heteroaryl-hydrido and -benzyl-hydrido complexes have been synthesized and characterized by spectroscopic and XRD methods. Selected complexes have been also scrutinized as catalyst precursors for ethylene polymerization and show moderate HDPE production.

Experimental Section

General: All air- and/or water-sensitive reactions were performed under either nitrogen or argon in flame-dried flasks using standard Schlenk-type techniques. thf was purified by distillation from sodium/benzophenone ketyl after drying with KOH. Et_2O, benzene,

n-hexane and toluene were purified by distillation from sodium/triglyme benzophenone ketyl or were obtained by means of a MBraun Solvent Purification Systems, whereas MeOH was distilled from Mg prior to use. C_6D_6 was dried with sodium/benzophenone ketyl and condensed in vacuo prior to use, whereas CD_2Cl_2 or $CDCl_3$ were dried with activated 4 Å molecular sieves. Literature methods were used to synthesize both the iminopyridine ligands N_2^{Ph}, N_2^{Th}, N_2^{EtTh},[13] N_2^{BFu},[14] N_2^{Xyl}[8] and the aminopyridine systems N_2H^{Ph} and N_2H^{Xyl}.[8] $[Y(CH_2SiMe_3)_3(thf)_2]$[2b,23,28] $[N_2^{Ph}Y(CH_2SiMe_3)(thf)_2]$ (**11**),[8] $[N_2^{Xyl}Y(CH_2SiMe_3)(thf)]$ (**12**),[8] $[\{N_2^{Ph}Y(\mu\text{-}H)(thf)\}_2]$ (**16**)[8] and $[\{N_2^{Xyl}Y(\mu\text{-}H)(thf)\}_2]$ (**17**)[8] were prepared according to previously reported procedures. All the other reagents and solvents were used as purchased from commercial suppliers. ^1H and $^{13}C\{^1H\}$ NMR spectra were obtained with either a Bruker ACP 200 (200.13 and 50.32 MHz, respectively) or a Bruker Avance DRX-400 (400.13 and 100.62 MHz, respectively). Chemical shifts are reported in ppm (δ) relative to TMS, referenced to the chemical shifts of residual solvent resonances (^1H and ^{13}C). IR spectra were recorded as Nujol mulls or KBr plates with FSM 1201 and Bruker-Vertex 70 instruments. Lanthanide analyses were carried out by complexometric titration. The C, H, N elemental analyses were made in the microanalytical laboratory of IOMC or at ICCOM–CNR with a Carlo Erba Model 1106 elemental analyzer with an accepted tolerance of ±0.4 units on carbon (C), hydrogen (H) and nitrogen (N). Melting points were ensured with a Stuart Scientific Melting Point apparatus SMP3. Catalytic reactions were performed with a 250 mL stainless steel reactor constructed at ICCOM–CNR (Firenze, Italy) and equipped with a mechanical stirrer, a Parr 4842 temperature and pressure controller, a mass-flow meter equipped with a digital control for the connection to the PC and an external jacket for the temperature control. The reactor was connected to an ethylene reservoir to maintain a constant pressure throughout the catalytic runs. Ethylene was purified before use by passing it through two columns filled with activated molecular sieves (4 Å) and BASF R3-11G catalysts, respectively. The MAO solution was filtered through a D4 funnel and the solvents evaporated to dryness at 50 °C under vacuum. The resulting white residue was heated further to 50 °C under vacuum overnight. A stock solution of MAO was prepared by dissolving solid MAO in toluene (100 mg mL^{-1}). The solution was used within three weeks to avoid self-condensation effects of the MAO. Other activators/cocatalysts were used as received from the providers. Melting temperatures of the polymer materials were determined by differential scanning calorimetry (DSC) with a Perkin–Elmer DSC-7 instrument equipped with CCA-7 cooling device and calibrated with the melting transition of indium and *n*-heptane as references (156.1 and –90.61 °C, respectively). The polymer sample mass was 10 mg and aluminium pans were used. Any thermal history in the polymers was eliminated by first heating the specimen at a heating rate of 20 °C min^{-1} to 200 °C, cooling at 20 °C min^{-1} to –100 °C, and then recording the second scan from –100 to 200 °C. Thermogravimetric analysis (TGA) was obtained under nitrogen (60 mL min^{-1}) with a TGA Mettler Toledo instrument at a heating rate of 10 °C min^{-1} from 50 to 700 °C.

General Procedure for the Synthesis of Aminopyridinate Ligands 6–10: A solution of the appropriate iminopyridine ligand (**1**–**5**; 2 mmol) in toluene (20 mL) was cooled to 0 °C in an ice bath and treated dropwise with a 2.0 M solution of trimethylaluminium (TMA) in toluene (1.5 mL, 3 mmol). The reaction mixture was allowed to stir at room temperature for 12 h and then was quenched with water (15 mL). The aqueous phase was extracted with AcOEt (3 × 20 mL) and the combined organic layers were dried with Na_2SO_4. Removal of the solvent under reduced pressure gave the amidopyridinate ligands (**6**–**10**) as crude off-white solids. The ligands were purified by crystallization from hot MeOH by cooling the resulting solution at either 4 °C (**6**, **8**, **10**) or –20 °C (**7**, **9**) overnight to afford crystals. Suitable crystals for X-ray diffraction were collected after successive recrystallization from hot MeOH. N_2H^{Ph} (**6**): 93% yield, white crystals;[8] N_2H^{Xyl} (**7**): 89% yield, white crystals;[8] N_2H^{Th} (**8**): 76% yield, pale yellow microcrystals; N_2H^{EtTh} (**9**): 70% yield, white needles; N_2H^{BFu} (**10**): 83% yield, white crystals.

N_2H^{Th} (8): ^1H NMR (300 MHz, CD_2Cl_2, 293 K): δ = 1.10 [d, $^3J_{H,H}$ = 6.8 Hz, 12 H, CH(CH_3), H^{17,18,19,20}], 1.48 [s, 6 H, C(CH_3)$_2$, H^{7,8}], 3.39 [sept, $^3J_{H,H}$ = 6.8 Hz, 2 H, CH(CH$_3$), H^{15,16}], 4.52 (br. s, 1 H, NH), 7.09 (m, 3 H, CH Ar, H^{11,12,13}), 7.16 (dd, ^3J = 3.7 Hz, 1 H, CH Th, H^{23}), 7.43 (dd, ^3J = 7.7 Hz, 1 H, CH Ar, H^2), 7.44 (dd, ^3J = 3.7 Hz, 1 H, CCH Th, H^{22}), 7.60 (dd, ^3J = 7.7 Hz, 1 H, CH Ar, H^4), 7.67 (dd, ^3J = 3.7 Hz, 1 H, CCH Th, H^{24}), 7.73 (t, ^3J = 7.8 Hz, 1 H, CH Ar, H^3) ppm. $^{13}C\{^1H\}$ NMR (100 MHz, CD_2Cl_2, 293 K): δ = 23.8 [CH(*C*H$_3$)$_2$, C^{17,18,19,20}], 28.1 [*C*H(CH$_3$)$_2$, C^{15,16}], 28.7 [C(*C*H$_3$)$_2$, C^{7,8}], 59.2 [*C*(CH$_3$)$_2$, C^6], 116.1 (C^4), 117.4 (C^2), 122.9 (C^{11,13}), 124.2 (C^{24}), 124.4 (C^{12}), 127.3 (C^{22}), 127.8 (C^{23}), 137.1 (C^3), 140.3 (C^{21}), 145.5 (C^9), 146.9 (C^{14,10}), 150.9 (C^5), 167.8 (C^1) ppm. M.p. 99.3 °C. $C_{24}H_{30}N_2S$ (378.56 g mol^{-1}): calcd. C 76.14, H 7.99, N 7.40, S 8.47; found C 76.71, H 7.85, N 7.24, S 8.20.

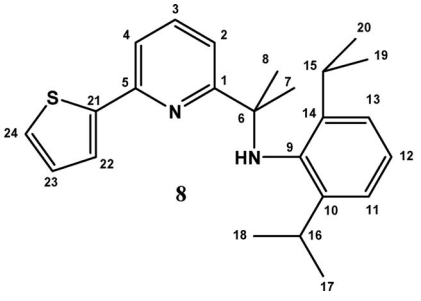

8

N_2H^{EtTh} (9): ^1H NMR (300 MHz, CD_2Cl_2, 293 K): δ = 1.12 [d, $^3J_{H,H}$ = 6.8 Hz, 12 H, CH(CH_3), H^{17,18,19,20}], 1.37 (t, $^3J_{H,H}$ = 7.5 Hz, 3 H, CH$_2$CH_3, H^{26}), 1.47 [s, 6 H, C(CH_3)$_2$, H^{7,8}], 2.91 (q, $^3J_{H,H}$ = 7.5 Hz, 2 H, CH_2CH$_3$, H^{25}), 3.42 [sept, $^3J_{H,H}$ = 6.8 Hz, 2 H, CH(CH$_3$), H^{15,16}], 4.52 (br. s, 1 H, NH), 6.85–6.87 (m, 1 H, CCH Th, H^{23}), 7.10 (m, 3 H, CH Ar, H^{11,12,13}), 7.37 (dd, ^3J = 7.8, ^4J = 0.87 Hz, 1 H, CH Ar, H^2), 7.49 (d, ^3J = 3.6 Hz, 1 H, CCH Th, H^{22}), 7.53 (dd, ^3J = 7.8, ^4J = 0.87 Hz, 1 H, CH Ar, H^4), 7.70 (t, ^3J = 7.8 Hz, 1 H, CH Ar, H^3) ppm. $^{13}C\{^1H\}$ NMR (100 MHz, CD_2Cl_2, 293 K): δ = 15.6 (CH$_2$*C*H$_3$, C^{26}), 23.8 (*C*H$_2$CH$_3$, C^{25}), 23.8 [CH(*C*H$_3$)$_2$, C^{17,18,19,20}], 28.1 [*C*H(CH$_3$)$_2$, C^{15,16}], 28.7 [C(*C*H$_3$)$_2$, C^{7,8}], 59.2 [*C*(CH$_3$)$_2$, C^6], 115.6 (C^2), 116.8 (C^4), 122.9 (C^{11,13}), 124.1 (C^{22}), 124.3 (C^{23}), 124.4 (C^{12}), 137.0 (C^3), 140.3 (C^{24}), 142.5 (C^{21}), 146.9 (C^{10,14}), 150.1 (C^9), 151.2 (C^5), 167.6 (C^1) ppm. M.p. 97.6 °C. $C_{26}H_{34}N_2S$ (406.63 g mol^{-1}): calcd. C 76.80, H 8.43, N 6.89, S 7.89; found C 76.91, H 8.40, N 6.75, S 7.94.

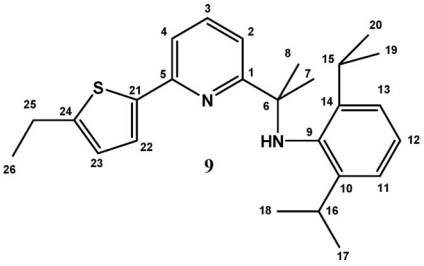

9

N_2H^{BFu} (10): ^1H NMR (300 MHz, CD_2Cl_2, 293 K): δ = 1.12 [d, $^3J_{H,H}$ = 6.8 Hz, 12 H, CH(CH_3), H^{17,18,19,20}], 1.52 [s, 6 H,

C(CH_3)$_2$, H^{7,8}], 3.36 [sept, $^3J_{H,H}$ = 6.8 Hz, 2 H, CH(CH$_3$), H^{15,16}], 4.58 (br. s, 1 H, NH), 7.10 (m, 3 H, CH Ar, H^{11,12,13}), 7.30 (m, 1 H, CH BFu, H^{25}), 7.38 (m, 1 H, CH BFu, H^{26}), 7.55–7.58 (2 H, CCH Th, H^{2,22}), 7.61 (1 H, CH BFu, H^{27}), 7.69 (m, 1 H, CH BFu, H^{24}), 7.84–7.85 (2 H, CH Ar, H^{3,4}) ppm. ^{13}C{^{1}H} NMR (100 MHz, CD_2Cl_2, 293 K): δ = 23.7 [CH(CH_3)$_2$, C^{17,18,19,20}], 28.2 [CH-(CH$_3$)$_2$, C^{15,16}], 28.9 [C(CH_3)$_2$, C^{7,8}], 59.2 [C(CH$_3$)$_2$, C^6], 104.4 (C^{22}), 111.2 (C^{27}), 117.0 (C^2), 118.9 (C^4), 121.5 (C^{24}), 122.9 (C^{11,13}), 123.1 (C^{25}), 124.5 (C^{12}), 125.0 (C^{26}), 128.9 (C^{24,27}), 137.2 (C^3), 140.5 (C^9), 146.7 (C^{23}), 147.4 (C^{21}), 155.2 (C^{28}), 155.8 (C^5), 168.3 (C^1) ppm. M.p. 133.7 °C. $C_{27}H_{29}N_2O$ (397.53 g mol^{-1}): calcd. C 81.58, H 7.35, N 7.05, O 4.02; found C 76.71, H 7.85, N 7.24, O 8.20.

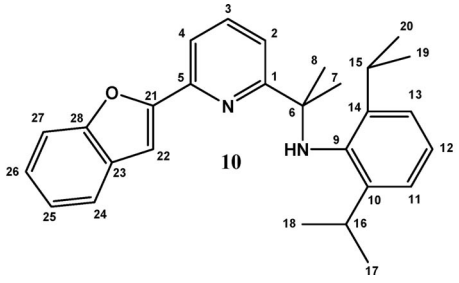

Synthesis of [N$_2^{Th}$Y(CH$_2$SiMe$_3$)(thf)$_2$] (13): A solution of N$_2^{Th}$H (**8**) (0.152 g, 0.401 mmol) in *n*-hexane (15 mL) was added to a solution of [Y(CH$_2$SiMe$_3$)$_3$(thf)$_2$] (0.401 mmol, 0.198 g) in *n*-hexane (10 mL) at 0 °C. The solution immediately became dark yellow. The reaction mixture was stirred at the same temperature for 1 h. After 15 min, the precipitation of a yellow-brown microcrystalline solid started. The solution was concentrated in vacuo to approximately one third of its initial volume and was kept overnight at –20 °C. Complex **13** was isolated as a dark yellow microcrystalline solid in 69% yield (0.193 g). ^{1}H NMR (400 MHz, C_6D_6, 293 K): δ = –0.77 (d, $^2J_{Y,H}$ = 3.0 Hz, 2 H, YCH_2), 0.22 [s, 9 H, Si(CH_3)], 1.06 (m, 8 H, β-CH_2 thf), 1.26 [d, $^3J_{H,H}$ = 6.8 Hz, 6 H, CH(CH_3)$_2$; H^{17,18,19,20}], 1.32 [compl. m., together 12 H, CH(CH_3)$_2$ and C(CH_3)$_2$, H^{7,8,17,18,19,20}], 3.60 (m, 8 H, α-CH_2 thf), 3.80 [sept, $^3J_{H,H}$ = 6.8 Hz, 2 H, CH(CH$_3$)$_2$, H^{15,16}], 6.59 (d, $^3J_{H,H}$ = 7.8 Hz, 1 H, CH Ar, H^2), 7.00 (t, $^3J_{H,H}$ = 7.8 Hz, 1 H, CH Ar, H^3), 7.13–7.23 (compl. m, together 3 H, CH Ar, H^{4,12,23}), 7.29 (m, together 2 H, CH Ar, H^{11,13}), 7.47 (d, $^3J_{H,H}$ = 4.2 Hz, 1 H, H^{24}) ppm. ^{13}C{H} NMR (100 MHz, C_6D_6, 293 K): δ = 4.4 [s, Si(CH_3)$_3$], 23.9 [s, CH(CH_3)$_2$, C^{17,18,19,20}], 24.6 (s, β-CH_2, thf), 27.6 [s, CH(CH$_3$)$_2$, C^{15,16}], 27.8 [s, CH(CH_3)$_2$, C^{17,18,19,20}], 30.0 (d, $^1J_{Y,C}$ = 39.6 Hz, YCH_2), 31.5 [s, C(CH_3)$_2$, C^{7,8}], 68.5 [d, $J_{Y,C}$ = 2.0 Hz, C(CH$_3$)$_2$, C^6], 69.8 (s, α-CH_2 thf), 115.0 (s, C^4), 116.3 (s, C^2), 123.7 (s, C^{11,13}), 123.8 (s, C^{12}), 125.6 (s, C^{24}) 137.6 (s, C^{23}), 139.1 (s, C^3), 144.7 (s, C^{21}), 147.1 (d, $^2J_{Y,C}$ = 2.2 Hz, C^9), 149.8 (s, C^{10,14}), 158.4 (d, $^2J_{Y,C}$ = 1.7 Hz, C^5), 174.6 (d, $J_{Y,C}$ = 1.5 Hz, C^1), 195.2 (d, $^1J_{Y,C}$ = 38.9 Hz, YC, C^{22}) ppm. IR (Nujol, KBr): $\tilde{\nu}$ = 3045 (m), 1590 (s), 1570 (s), 1415 (s), 1300 (m), 1260 (m), 1245 (m), 1235 (m), 1220 (s), 1175 (s), 1130 (s), 1130 (s), 1105 (m), 1085 (s), 1070 (m), 1045 (w), 1035 (m), 1025 (s), 1000 (w), 970 (w), 915 (w), 890 (m), 865 (m), 840 (s), 805 (s), 800 (s), 780 (m), 745 (m), 705 (m), 670 (m), 630 (w) cm^{-1}. $C_{36}H_{55}N_2O_2SSiY$ (696.89 g mol^{-1}): calcd. C 62.04, H 7.95, N 4.02, Y 12.76; found C 62.33, H 8.15, N 4.09, Y 12.54.

Synthesis of [N$_2^{EtTh}$Y(CH$_2$SiMe$_3$)(thf)$_2$] (14): A solution of N$_2^{EtTh}$H (**9**) (0.231 g, 0.57 mmol) in *n*-hexane (15 mL) was added to a solution of [Y(CH$_2$SiMe$_3$)$_3$(thf)$_2$] (0.281 g, 0.57 mmol) in *n*-hexane (10 mL) at 0 °C. The reaction mixture was stirred at the same temperature for 1 h. After 15 min, the precipitation of a pale yellow microcrystalline solid started. The solution was concentrated in vacuo to approximately one third of its initial volume and was kept overnight at –20 °C. Complex **14** was isolated as a yellow microcrystalline solid in 84% yield (0.346 g). Crystals suitable for X-ray analysis were obtained by slow evaporation of a solution of complex **14** in toluene at room temperature. ^{1}H NMR (400 MHz, C_6D_6, 293 K): δ = –0.69 (d, $^2J_{Y,H}$ = 3.0 Hz, 2 H, YCH_2), 0.25 [s, 9 H, Si(CH_3)], 1.11 (m, 8 H, β-CH_2 thf), 1.27 [d, $^3J_{H,H}$ = 6.8 Hz, 6 H, CH(CH_3)$_2$, H^{17,18,19,20}], 1.33 (t, $^3J_{H,H}$ = 7.5 Hz, 3 H, CH$_2$CH_3, H^{26}), 1.34 [d, $^3J_{H,H}$ = 6.8 Hz, 6 H, CH(CH_3)$_2$, H^{17,18,19,20}], 1.36 [s, 6 H, C(CH_3)$_2$, H^{7,8}], 2.91 [qd, $^3J_{H^{25},H^{26}}$ = 7.5, $^4J_{H^{25},H^{23}}$ = 0.7 Hz (interaction between CH$_2$ protons of ethyl group with aromatic proton of the thiophene ring) 2 H, CH_2CH$_3$, H^{25}], 3.63 (m, 8 H, α-CH_2 thf), 3.83 [sept, $^3J_{H,H}$ = 6.8 Hz, 2 H, CH(CH$_3$)$_2$, H^{15,16}], 6.57 (d, $^3J_{H,H}$ = 7.8 Hz, 1 H, CH Ar, H^2), 7.08 (t, $^3J_{H,H}$ = 7.8 Hz, 1 H, CH Ar, H^3), 7.18–7.24 (compl. m, together 3 H, CH Ar, H^{4,12,23}), 7.31 (m, together 2 H, CH Ar, H^{11,13}) ppm. ^{13}C{H} NMR (100 MHz, C_6D_6, 293 K): δ = 4.5 [s, Si(CH_3)$_3$], 17.0 (s, CH$_2$$CH_3$, C^{26}), 23.6 (s, CH_2CH$_3$, C^{25}), 24.0 [s, CH(CH_3)$_2$, C^{17,18,19,20}], 24.7 (s, β-CH_2, thf), 27.6 [s, CH(CH$_3$)$_2$, C^{15,16}], 27.8 [s, CH(CH_3)$_2$, C^{17,18,19,20}], 30.1 (d, $^1J_{Y,C}$ = 39.6 Hz, YCH_2), 31.7 [s, C(CH_3)$_2$, C^{7,8}], 68.6 [d, $J_{Y,C}$ = 2.2 Hz, C(CH$_3$)$_2$, C^6], 70.0 (s, α-CH_2 thf), 114.7 (s, C^4), 115.8 (s, C^2), 123.8 (s, C^{11,13}), 123.7 (s, C^{12}), 135.0 (d, $^2J_{Y,C}$ = 2.9 Hz, C^{23}), 139.2 (s, C^3), 144.9 (s, C^{24}), 145.2 (d, $^2J_{Y,C}$ = 2.2 Hz, C^{21}), 149.3 (d, $^2J_{Y,C}$ = 2.2 Hz, C^9), 150.0 (s, C^{10,14}), 158.8 (d, $^2J_{Y,C}$ = 1.7 Hz, C^5), 174.8 (d, $J_{Y,C}$ = 1.5 Hz, C^1), 198.6 (d, $^1J_{Y,C}$ = 38.9 Hz, YC, C^{22}) ppm. IR (Nujol, KBr): $\tilde{\nu}$ = 3040 (m), 1590 (s), 1570 (s), 1420 (m), 1395 (m), 1260 (m), 1250 (m), 1230 (s), 1220 (m), 1180 (s), 1125 (m), 1105 (w), 1085 (s), 1030 (s), 1005 (s), 970 (w), 920 (w), 890 (m), 865 (s), 840 (s), 800 (s), 780 (m), 745 (m), 705 (m), 670 (m), 630 (w) cm^{-1}. $C_{38}H_{59}N_2O_2SSiY$ (724.9 g mol^{-1}): calcd. C 62.96, H 8.20, N 3.86, Y 12.26; found C 63.08, H 8.35, N 3.74, Y 12.17.

Synthesis of [N$_2^{BFu}$Y(CH$_2$SiMe$_3$)(thf)$_2$] (15): A solution of N$_2^{BFu}$H (**10**) (0.190 g, 0.46 mmol) in *n*-hexane (15 mL) was added to a solution of [Y(Me$_3$SiCH$_2$)$_3$(thf)$_2$] (0.228 g, 0.46 mmol) in *n*-hexane (10 mL) at 0 °C. The reaction mixture was stirred at 0 °C for 1 h. The solution was concentrated in vacuo to approximately one third of its initial volume and was kept overnight at –20 °C. Complex **15** was isolated as a yellow-orange microcrystalline solid in 69% yield (0.232 g). ^{1}H NMR (400 MHz, C_6D_6, 293 K): δ = –0.69 (d, $^2J_{Y,H}$ = 3.0 Hz, 2 H, YCH_2), 0.20 [s, 9 H, Si(CH_3)], 0.95 (m, 8 H, β-CH_2 thf), 1.27 [s, 6 H, C(CH_3)$_2$, H^{7,8}], 1.30 [d, $^3J_{H,H}$ = 6.9 Hz, 6 H, CH(CH_3)$_2$; H^{17,18,19,20}], 1.34 [d, $^3J_{H,H}$ = 6.9 Hz, 6 H, CH(CH_3)$_2$, H^{17,18,19,20}], 3.65 (m, 8 H, α-CH_2 thf), 3.79 [sept, $^3J_{H,H}$ = 6.8 Hz, 2 H, CH(CH$_3$)$_2$, H^{15,16}], 6.63 (d, $^3J_{H,H}$ = 8.0 Hz, 1 H, CH Ar, H^2), 7.17–7.26 (compl. m, together 4 H, CH Ar, H^{3,12,25,26}), 7.32 (m, 2 H, CH Ar, H^{11,13}), 7.57 (d, $^3J_{H,H}$ = 8.0 Hz, 1 H, CH Ar, H^4), 7.62 (dd, $^3J_{H,H}$ = 6.8, $^4J_{H,H}$ = 2.0 Hz, 1 H, CH Ar, H^{27}), 8.12 (dd, $^3J_{H,H}$ = 6.8, $^4J_{H,H}$ = 2.0 Hz, 1 H, CH Ar, H^{24}) ppm. ^{13}C{H} NMR (100 MHz, C_6D_6, 293 K): δ = 4.5 [s, Si(CH_3)$_3$], 23.8 [s, CH(CH_3)$_2$, C^{17,18,19,20}], 24.7 (s, β-CH_2, thf), 27.7 [s, CH(CH$_3$)$_2$, C^{15,16}], 27.7 [s, CH(CH$_3$)$_2$, C^{17,18,19,20}], 30.1 (d, $^1J_{Y,C}$ = 37.6 Hz, YCH_2), 31.1 [s, C(CH_3)$_2$, C^{7,8}], 68.6 [d, $J_{Y,C}$ = 2.6 Hz, C(CH$_3$)$_2$, C^6], 70.2 (s, α-CH_2 thf), 110.5 (s, C^{27}) 113.5 (s, C^4), 117.8 (s, C^2), 122.1 (s, C^{26}) 123.8 (s, C^{11,13}), 124.1 (s, C^{12}), 124.5 (s, C^{25}), 126.7 (s, C^{24}), 139.0 (s, C^3), 140.0 (d, $^2J_{Y,C}$ = 2.8 Hz, C^{23}), 144.1 (s, C^9), 149.7 (s, C^{10,14}), 153.4 (br. s, C^5), 156.6 (s, C^{28}), 158.6 (d, $^1J_{Y,C}$ = 38.9 Hz, YC, C^{22}), 160.8 (br. s, C^{21}), 175.0 (br. s, C^1) ppm. IR (Nujol, KBr): $\tilde{\nu}$ = 3075 (w), 3045 (m), 1600 (s), 1585 (w), 1570 (s), 1500 (s), 1415 (s), 1350 (m), 1335 (w), 1325 (m), 1300 (m), 1255 (s), 1235 (m), 1220 (s), 1200 (w), 1175 (s), 1145 (s), 1120 (m), 1005 (m), 1080 (s), 1045 (w), 1025 (s), 1010 (m), 970 (w), 925 (s), 895 (w), 885 (m), 865 (s), 850 (s), 820 (m), 810 (s), 795 (m), 770 (m), 715 (m), 705 (m), 675 (s), 635

(w), 620 (m) cm^{-1}. $C_{40}H_{57}N_2O_3SiY$ (730.88 $g\,mol^{-1}$): calcd. C 65.73, H 7.68, N 3.83, Y 12.16; found C 65.32, H 7.93, N 3.71, Y 12.04.

Synthesis of [{N_2^{BFu}Y(μ-H)(thf)}$_2$] (18): $PhSiH_3$ (0.047 g, 0.431 mmol) was added to a solution of **12** (0.315 g, 0.431 mmol) in *n*-hexane (25 mL) at 0 °C. The reaction mixture was stirred at 0 °C for 1 h and kept overnight at room temperature. The solution was concentrated in vacuo and maintained overnight at –20 °C. Complex **18** was isolated as a yellow-brown crystalline solid in 72% yield (0.201 g). ^{1}H NMR (400 MHz, C_6D_6, 293 K): δ = 0.72 [br. s, 6 H, CH(CH_3)$_2$; H^{17,18,19,20}], 0.79 [s, 6 H, C(CH_3)$_2$, H^{7,8}], 1.01 [m, 12 H, CH(CH_3)$_2$; H^{17,18,19,20}], 1.24 (m, 8 H, β-CH_2 thf), 1.33 [s, 6 H, CH(CH_3)$_2$; H^{17,18,19,20}], 2.17 (s, 6 H, H^{7,8}), 2.72 [m, 2 H, CH(CH$_3$)$_2$, H^{15,16}], 3.19 (m, 4 H, α-CH_2 thf), 3.42 (m, 4 H, α-CH_2 thf), 4.54 [m, 2 H, CH(CH$_3$)$_2$, H^{15,16}], 6.75 (d, $^3J_{H,H}$ = 8.0 Hz, 1 H, CH Ar, H^2), 6.92–7.18 (compl. m, together 8 H, CH Ar, H^{3,11,12,13}), 7.23 (t, $^3J_{H,H}$ = 7.2 Hz, 2 H, CH Ar, H^{26}), 7.33 (t, $^3J_{H,H}$ = 7.8 Hz, 2 H, CH Ar, H^{25}), 7.61 (d, $^3J_{H,H}$ = 7.5 Hz, 2 H, CH Ar, H^4), 7.64 (d, $^3J_{H,H}$ = 7.5 Hz, 2 H, CH Ar, H^{27}), 7.71 (t, $^1J_{Y,H}$ = 27.0 Hz, 2 H, YH) 7.99 (d, $^3J_{H,H}$ = 7.5 Hz, 2 H, CH Ar, H^{24}) ppm. ^{13}C{H} NMR (100 MHz, C_6D_6, 293 K): δ = 23.0 [s, CH(CH_3)$_2$, C^{17,18,19,20}], 23.9 (s, β-CH_2, thf), 24.2 [s, CH(CH_3)$_2$, C^{17,18,19,20}], 25.9 [s, CH(CH_3)$_2$, C^{17,18,19,20}], 26.7 [s, CH(CH_3)$_2$, C^{17,18,19,20}], 26.8 [s, CH(CH$_3$)$_2$, C^{15,16}], 28.3 [s, C(CH_3)$_2$, C^{7,8}], 29.1 [s, CH(CH$_3$)$_2$, C^{15,16}], 42.9 [s, C(CH_3)$_2$, C^{7,8}], 66.2 [d, $J_{Y,C}$ = 2.6 Hz, C(CH$_3$)$_2$, C^6], 70.3 (s, α-CH_2 thf), 110.6 (s, C^{27}), 114.3 (s, C^4), 115.2 (s, C^2), 121.2 (s, C^{26}), 122.8 (s, C^{11,13}), 123.2 (s, C^{11,13}), 124.0 (s, C^{12}), 127.0 (s, C^{25}), 128.0 (s, C^{24}), 138.9 (s, C^3), 140.4 (d, $^2J_{Y,C}$ = 2.8 Hz, C^{23}), 147.1 (s, C^9), 148.6 (s, C^{10,14}), 150.2 (s, C^{10,14}), 153.2 (br. s, C^5), 156.6 (s, C^{28}), 160.1 (d, $^1J_{Y,C}$ = 43.3 Hz, YC, C^{22}), 162.6 (br. s, C^{21}), 175.8 (br. s, C^1) ppm. IR (Nujol, KBr): $\tilde{\nu}$ = 3080 (w), 3050 (m), 1605 (s), 1580 (w), 1560 (s), 1505 (s), 1425 (s), 1340 (m), 1330 (w), 1320 (m), 1295 (m), 1230 (m), 1220 (s), 1200 (w), 1170 (s), 1140 (s), 1120 (m), 1010 (m), 1085 (s), 1040 (w), 1025 (s), 1015 (m), 975 (w), 935 (s), 895 (w), 880 (m), 820 (m), 810 (s), 790 (m), 770 (m), 710 (m), 675 (s), 635 (w), 615 (m) cm^{-1}. $C_{64}H_{76}N_4O_2Y_2$ (1145.14 $g\,mol^{-1}$): calcd. C 67.13, H 6.87, N 4.89, Y 15.53; found C 66.98, H 7.11, N 4.91, Y 15.44.

General Procedure for Ethylene Polymerization: A 200 mL stainless steel reactor was heated to 60 °C under vacuum overnight and then cooled to room temperature under a nitrogen atmosphere.

Activation with MAO: The solid precatalyst (12 μmol) was charged into the reactor, which was sealed and placed under vacuum. A solution of MAO in toluene (3600 μmol, 300 equiv.), prepared by diluting a standard solution of MAO (2.4 mL, 10 wt% in toluene) in toluene (47.6 mL), was then introduced by suction into the reactor previously evacuated by a vacuum pump. The system was heated to the desired temperature, pressurized with ethylene to the final pressure (10 bar), and stirred at 1500 rpm for 30 min.

Activation with [Me_2PhNH][$B(C_6F_5)_4$]/Al*i*Bu_3: The reactor was charged with a suspension of the cocatalyst [Me_2PhNH][$B(C_6F_5)_4$] (14.4 μmol) in toluene (35 mL) followed by the rapid addition of a 25 wt% solution of Al*i*Bu_3 in toluene (2.4 mL, 2.4 mmol, 200 equiv.). After sealing the reactor, the system was pressurized with ethylene at 2 bar and heated at 65 °C for 10 min so as to dissolve the activator. The ethylene pressure was then released slowly and a precatalyst solution (2.5 mL), prepared by dissolving the solid precatalyst (12 μmol) in toluene (2.5 mL), was added into the reactor with a syringe. The autoclave was then pressurized with ethylene to the final pressure (10 bar) and stirred at 1500 rpm for 30 min. Irrespective of the procedure used, catalysts and cocatalyst (activator) solutions were handled in the glove box and ethylene

Table 4. Crystal data and structure refinement for ligands **6**–**10**.[a]

	6	**7**	**8**	**9**	**10**
Empirical formula	$C_{26}H_{32}N_2$	$C_{28}H_{36}N_2$	$C_{24}H_{30}N_2S$	$C_{52}H_{68}N_4S_2$	$C_{28}H_{32}N_2O$
M_r	372.54	400.59	378.56	813.22	412.56
T [K]	293(2)	293(2)	293(2)	150(2)	293(2)
λ [Å]	1.54180	0.71069	0.71073	0.71069	0.71069
Crystal system	monoclinic	monoclinic	orthorhombic	orthorhombic	monoclinic
Space group	*P*21/*n*	*P*21/*n*	*Pc*21*n*	*Pna*21	*P*21*c*
a [Å]	8.9657(10)	12.087(1)	8.8099(14)	14.551(1)	15.321(17)
b [Å]	22.814(4)	13.064(1)	10.711(4)	9.164(1)	13.032(16)
c [Å]	10.8298(10)	15.807(1)	22.911(10)	35.733(2)	12.129(12)
α [°]	90	90	90	90(5)	90(5)
β [°]	95.554(10)	97.095(4)	90	90(4)	102.738(11)
γ [°]	90	90	90	90(4)	90(5)
V [Å^3]	2204.7(5)	2476.9(3)	2162.0(10)	4764.8(7)	2362(5)
$D_{calcd.}$ [g m^{-3}]	1.122	1.074	1.163	1.134	1.160
Absorption coefficient [mm^{-1}]	0.491	0.062	0.160	0.150	0.070
F(000)	808	872	816	1760	888
Crystal size [mm]	0.52 × 0.28 × 0.15	0.1 × 0.1 × 0.2	0.33 × 0.30 × 0.20	0.25 × 0.3 × 0.3	0.01 × 0.01 × 0.01
θ range for data collection [°]	3.88–60.06	3.71–25.70	2.48–24.96	3.75–28.90	3.75–24.36
Limiting indices	$-10 \le h \le 10$, $-5 \le k \le 25$, $0 \le l \le 12$	$-14 \le h \le 12$, $-15 \le k \le 15$, $-19 \le l \le 19$	$0 \le h \le 10$, $0 \le k \le 12$, $0 \le l \le 27$	$-19 \le h \le 18$, $-7 \le k \le 12$, $-39 \le l \le 47$	$-17 \le h \le 12$, $-14 \le k \le 14$, $-13 \le l \le 13$
Reflections collected/unique	3467/3275	13804/4654	2013/2013	15778/8366	6754/2914
GOF on F^2	1.028	0.914	1.042	0.776	0.815
Data/restraints/parameters	3275/1/252	4654/0/275	2013/1/252	8366/1/539	2914/0/283
Final R indices [$I > 2\sigma(I)$]	$R1$ = 0.0830, $wR2$ = 0.2039	$R1$ = 0.0717, $wR2$ = 0.1748	$R1$ = 0.0699, $wR2$ = 0.1318	$R1$ = 0.0456, $wR2$ = 0.0804	$R1$ = 0.0507, $wR2$ = 0.0749
R indices (all data)	$R1$ = 0.1075, $wR2$ = 0.2264	$R1$ = 0.1809, $wR2$ = 0.2169	$R1$ = 0.1579, $wR2$ = 0.1623	$R1$ = 0.1354, $wR2$ = 0.0987	$R1$ = 0.1557, $wR2$ = 0.0918
Largest diff. peak and hole [e Å^{-3}]	0.2063 and –0.241	0.255 and –0.192	0.250 and –0.245	0.330 and –0.303	0.151 and –0.156

[a] For all compounds, Z = 4.

Table 5. Crystal data and structure refinement for complexes **12**, **14**, and **16**–**18**.[a]

	12[b]	**14**	**16**[a]	**17**	**18**
Empirical formula	$C_{36}H_{53}N_2OSiY$	$C_{38}H_{59}N_2O_2SiY$	$C_{60}H_{78}N_4O_2Y_2$	$C_{70}H_{10}N_4O_2Y_2$	$C_{76}H_{90}N_4O_4Y_2$
M_r	646.80	724.93	1065.08	1207.36	1301.34
T [K]	100(2)	100(2)	100(2)	100(2)	100(2)
λ [Å]	0.71073	0.71073	0.71073	0.71069	0.71069
Crystal system	monoclinic	monoclinic	tetragonal	tetragonal	orthorhombic
Space group	$P2_1/c$	$P2_1/c$	$P4_12_12$	$\bar{P}4n2$	$Pbcn$
a [Å]	10.0924(5)	17.5740(7)	12.9842(3)	23.7470(6)	17.666(5)
b [Å]	18.8418(9)	12.4289(5)	12.9842(3)	23.7470(6)	17.642(9)
c [Å]	18.4703(9)	18.4721(7)	33.0971(1)	12.3501(4)	21.625(7)
α [°]	90	90	90	90	90(5)
β [°]	99.8130(10)	110.97(10)	90	90	90(5)
γ [°]	90	90	90	90	90(5)
V [Å^3]	3460.9(3)	3767.5(3)	5579.8(3)	6964.5(3)	6740(4)
$D_{calcd.}$ [g m^{-3}]	1.241	1.278	1.268	1.151	1.283
Absorption coefficient [mm^{-1}]	1.749	1.669	2.113	1.701	1.765
F(000)	1376	1544	2240	2568	2736
Crystal size [mm]	$0.30\times0.20\times0.15$	$0.35\times0.26\times0.13$	$0.15\times0.12\times0.06$	$0.2\times0.1\times0.1$	$0.05\times0.01\times0.1$
θ range for data collection [°]	2.43–26.00	2.75–26.00	2.42–26.00	3.82–26.45	3.83–27.51
Limiting indices	$-12 \le h \le 12$, $-23 \le k \le 23$, $22 \le l \le 22$	$-21 \le h \le 21$, $-15 \le k \le 15$, $-22 \le l \le 22$	$-16 \le h \le 15$, $-16 \le k \le 16$, $-40 \le l \le 40$	$-28 \le h \le 14$, $-12 \le k \le 28$, $-15 \le l \le 8$	$-21 \le h \le 21$, $-15 \le k \le 20$, $-27 \le l \le 14$
Reflections collected/unique	29249/6787	31546/7391	48076/5466	13954/5555	18112/6035
GOF on F^2	1.032	1.037	1.079	0.972	0.903
Data/restraints/parameters	6787/3/380	7391/4/419	5466/0/316	5555/22/361	6035/0/391
Final R indices [$I>2\sigma(I)$]	$R1$ = 0.0349, $wR2$ = 0.0761	$R1$ = 0.0326, $wR2$ = 0.0747	$R1$ = 0.0257, $wR2$ = 0.0608	$R1$ = 0.0630, $wR2$ = 0.1591	$R1$ = 0.0363, $wR2$ = 0.08
R indices (all data)	$R1$ = 0.0523, $wR2$ = 0.0806	$R1$ = 0.0489, $wR2$ = 0.0792	$R1$ = 0.0301, $wR2$ = 0.0619	$R1$ = 0.1205, $wR2$ = 0.1731	$R1$ = 0.0838, $wR2$ = 0.0877
Largest diff. peak and hole [e Å^{-3}]	0.439 and –0.289	0.996 and –0.367	–0.190 and 0.389	0.941 and –0.349	0.470 and –0.471

[a] For all compounds, Z = 4. [b] Selected data in the literature[20] listed here for completeness.

was continuously fed to maintain the reactor pressure at the desired value throughout the catalytic run. After 30 min, the reaction was terminated by cooling the reactor to 0 °C, venting off the volatiles, and introducing acidic MeOH (1 mL, 5% HCl v/v). The solid products were filtered off, washed with cold toluene and MeOH, and dried in a vacuum oven at 50 °C. The filtrates were analyzed by GC and GC–MS for detecting the presence of short oligomers.

X-ray Diffraction Data: Crystallographic data of ligands **6**–**10** and complexes **12**, **14**, **16**–**18** are reported in Tables 4 and 5, respectively. X-ray diffraction intensity data were collected with either a SMART APEX or Oxford Diffraction CCD diffractometer with graphite monochromated Mo-K_α radiation (λ = 0.71073 Å) using ω scans. Cell refinement, data reduction and empirical absorption correction were carried out with the Oxford diffraction software and SADABS.[29] All structure determination calculations were performed with the WINGX package[30] with SIR-97,[31] SHELXL-97[32] and ORTEP-3 programs.[33] Final refinements based on F^2 were carried out with anisotropic thermal parameters for all non-hydrogen atoms, which were included using a riding model with isotropic U values depending on the U_{eq} of the adjacent carbon atoms. In **9**, a nonmerohedral twin is present; the twin component was found to be 0.7(1). Two molecules are present in the asymmetric unit, thus generating a "pseudochiral" helical lattice packing [for this reason the space group found ($Pna2_1$) is noncentrosymmetric]. The hydride ligand positions in complexes **16** and **17** were determined from the residual density map during the refinement and subsequently fixed at 2.15 and 2.44 Å from the Y atom, respectively. The accessible voids of 273 Å^3 found in the lattice of **17** are probably occupied by disordered thf crystallization molecules that could not be located precisely. The coordinated thf molecules are disordered as well, even at 100 K; this disorder was not explicitly treated since the final $R1$/$wR2$ values do not change significantly when it is included in the refinement. CCDC-740105 (**6**), -740107 (**7**), -740106 (**8**), -740104 (**9**), -740103 (**10**), -740102 (**14**), -740100 (**17**) and -740101 (**18**) contain the supplementary crystallographic data for this paper. These data can be obtained free of charge from The Cambridge Crystallographic Data Centre via www.ccdc.cam.ac.uk/data_request/cif.

Acknowledgments

The authors thank the Ministero dell'Istruzione, dell'Università e della Ricerca of Italy (NANOPACK - FIRB project no. RBNE03R78E), the Russian Foundation for Basic Research (grant no. 08-03-00391-a, 06-03-32728), FIRENZE HYDROLAB project by Ente Cassa di Risparmio di Firenze (http://www.iccom.cnr.it/hydrolab/) and the GDRE network "*Homogeneous Catalysis for Sustainable Development*" for financial support of this work. G. G. also thanks Dr. Andrea Meli and Dr. Andrea Ienco for fruitful discussions.

[1] a) S. Bambirra, D. van Leusen, A. Meetsma, B. Hessen, J. H. Teuben, *Chem. Commun.* **2001**, 637–638; b) S. Bambirra, M. W. Bouwkamp, A. Meetsma, B. Hessen, *J. Am. Chem. Soc.* **2004**, *126*, 9182–9183; c) S. Bambirra, S. T. Boot, D. van Leusen, A. Meetsma, B. Hessen, *Organometallics* **2004**, *23*, 1891–1898; d) S. Bambirra, D. van Leusen, A. Meetsma, B. Hessen, J. H. Teuben, *Chem. Commun.* **2003**, 522–523; e) P. G. Hayes, W. E. Piers, R. McDonald, *J. Am. Chem. Soc.* **2002**, *124*, 2132–2133; f) W. P. Kretschmer, A. Meetsma, B. Hessen, T. Schmalz, S.

Qayyum, R. Kempe, *Chem. Eur. J.* **2006**, *12*, 8969–8978; g) W. E. Piers, D. J. H. Emslie, *Coord. Chem. Rev.* **2002**, *233–234*, 131–155; h) S. Bambirra, D. van Leusen, C. G. J. Tazelaar, A. Meetsma, B. Hessen, *Organometallics* **2007**, *26*, 1014–1023; i) A. A. Trifonov, *Russ. Chem. Rev.* **2007**, *76*, 1051–1072.

[2] a) S. Arndt, J. Okuda, *Chem. Rev.* **2002**, *102*, 1953–1976; b) G. Jeske, L. E. Schock, P. N. Swepston, H. Schumann, T. J. Marks, *J. Am. Chem. Soc.* **1985**, *107*, 8103–8110; c) W. Roll, H.-H. Brintzinger, B. Rieger, R. Zolk, *Angew. Chem. Int. Ed. Engl.* **1990**, *29*, 279–280; d) H. Schumann, J. A. Meese-Marktscheffel, L. Esser, *Chem. Rev.* **1995**, *95*, 865–986; e) O. Tardif, M. Nishiura, Z. Hou, *Tetrahedron* **2003**, *59*, 10525–10539.

[3] a) K. B. Aubrecht, K. Chang, M. A. Hillmyer, W. B. Tolman, *J. Polym. Sci., Part A* **2001**, *39*, 284–293; b) R. Duchateau, C. T. van Wee, J. H. Teuben, *Organometallics* **1996**, *15*, 2291–2302; c) Y. Luo, X. Wang, J. Chen, C. Luo, Y. Zhang, Y. Yao, *J. Organomet. Chem.* **2009**, *694*, 1289–1296.

[4] a) P. J. Bailey, S. Pace, *Coord. Chem. Rev.* **2001**, *214*, 91–141; b) R. Duchateau, C. T. van Wee, A. Meetsma, J. H. Teuben, *J. Am. Chem. Soc.* **1993**, *115*, 4931–4932; c) G. R. Giesbrecht, G. D. Whitener, J. Arnold, *J. Chem. Soc., Dalton Trans.* **2001**, *6*, 923–927; d) Z. Lu, G. P. A. Yap, D. S. Richeson, *Organometallics* **2001**, *20*, 706–712; e) N. Ajellal, D. M. Lyubov, M. A. Sinenkov, G. K. Fukin, A. V. Cherkasov, C. M. Thomas, J. F. Carpentier, A. A. Trifonov, *Chem. Eur. J.* **2008**, *14*, 5440–5448.

[5] a) P. G. Hayes, W. E. Piers, L. W. M. Lee, L. K. Knight, M. Parvez, M. R. J. Elsegood, W. Clegg, *Organometallics* **2001**, *20*, 2533–2544; b) L. Bourget-Merle, M. F. Lappert, J. R. Severn, *Chem. Rev.* **2002**, *102*, 3031–3065 and references cited therein; c) L. F. Sanchez-Barba, D. L. Hughes, S. M. Humphrey, M. Bochmann, *Organometallics* **2006**, *25*, 1012–1020.

[6] D. J. H. Emslie, W. E. Piers, R. McDonald, *J. Chem. Soc., Dalton Trans.* **2002**, 293–294.

[7] a) J. Gromada, J. F. Carpentier, A. Mortreux, *Coord. Chem. Rev.* **2002**, *231*, 1–22; b) M. Zimmermann, L. W. Tornroos, R. M. Waymouth, R. Anwander, *Organometallics* **2008**, *27*, 4310–4317 and references cited therein; c) C. Döring, R. Kempe, *Eur. J. Inorg. Chem.* **2009**, 412–418; d) A. M. Dietel, C. Döring, G. Glatz, M. V. Butovskii, O. Tok, F. M. Schappacher, R. Pöttgen, R. Kempe, *Eur. J. Inorg. Chem.* **2009**, 1051–1059; e) C. Döring, W. P. Kretschmer, T. Bauer, R. Kempe, *Eur. J. Inorg. Chem.* **2009**, 4255–4264.

[8] D. M. Lyubov, G. K. Fukin, A. V. Cherkasov, A. S. Shavyrin, A. A. Trifonov, L. Luconi, C. Bianchini, A. Meli, G. Giambastiani, *Organometallics* **2009**, *28*, 1227–1232.

[9] a) R. T. Boussie, G. M. Diamond, C. Goh, K. A. Hall, A. M. LaPointe, M. K. Leclerc, V. Murphy, J. A. W. Shoemaker, H. Turner, R. K. Rosen, J. C. Stevens, F. Alfano, V. Busico, R. Cipullo, G. Talarico, *Angew. Chem. Int. Ed.* **2006**, *45*, 3278–3283 and references cited therein; b) C. Zuccaccia, A. Macchioni, V. Busico, R. Cipullo, G. Talarico, F. Alfano, H. W. Boone, K. A. Frazier, P. D. Hustad, J. C. Stevens, P. C. Vosejpka, K. A. Abboud, *J. Am. Chem. Soc.* **2008**, *130*, 10354–10368 and references cited therein.

[10] G. J. Domski, J. B. Edson, I. Keresztes, E. B. Lobkovsky, G. W. Coates, *Chem. Commun.* **2008**, 6137–6139.

[11] a) M. Booij, N. H. Kiers, A. Meetsma, J. H. Teuben, W. J. J. Smeets, A. L. Spek, *Organometallics* **1986**, *8*, 2454–2461; b) K. H. den Haan, Y. Wiestra, J. H. Teuben, *Organometallics* **1987**, *6*, 2053–2060; c) W. J. Evans, M. T. Champagne, J. W. Ziller, *J. Am. Chem. Soc.* **2006**, *128*, 14270–14271; d) W. J. Evans, J. M. Perotti, J. W. Ziller, *J. Am. Chem. Soc.* **2005**, *127*, 1068–1069; e) Y. Mu, W. E. Piers, D. C. MacQuarrie, M. J. Zaworotko, V. G. Young, *Organometallics* **1996**, *15*, 2720–2726; f) J. Okuda, *Dalton Trans.* **2003**, 2367–2378; g) M. E. Thompson, S. M. Baxter, A. R. Bulls, B. J. Burger, M. C. Nolan, B. D. Santarsiero, W. P. Schaefer, J. E. Bercaw, *J. Am. Chem. Soc.* **1987**, *109*, 203–219; h) P. L. Watson, *J. Chem. Soc., Chem. Commun.* **1983**, 276–277; i) P. L. Watson, *J. Am. Chem. Soc.* **1983**, *105*, 6491–6493; j) P. L. Watson, G. B. Parshall, *Acc. Chem. Res.* **1985**, *18*, 51–55.

[12] a) R. Duchateau, T. Tuinstra, E. A. C. Brussee, A. Meetsma, P. T. van Duijnen, J. H. Teuben, *Organometallics* **1997**, *16*, 3511–3522; b) D. J. H. Emslie, W. E. Piers, M. Parvez, *Dalton Trans.* **2003**, 2615–2620; c) D. J. H. Emslie, W. E. Piers, M. Parvez, R. McDonald, *Organometallics* **2002**, *21*, 4226–4240; d) M. D. Fryzuk, T. S. Haddad, S. J. Retting, *Organometallics* **1991**, *10*, 2026–2036; e) H. Sigiyama, S. Gambarotta, G. P. A. Yap, D. R. Wilson, S. K.-H. Thiele, *Organometallics* **2004**, *23*, 5054–5061.

[13] a) C. Bianchini, G. Giambastiani, I. Guerrero Rios, A. Meli, A. M. Segarra, A. Toti, F. Vizza, *J. Mol. Catal. A* **2007**, *277*, 40–46; b) C. Bianchini, G. Giambastiani, G. Mantovani, A. Meli, D. Mimeau, *J. Organomet. Chem.* **2004**, *689*, 1356–1361; c) C. Bianchini, G. Mantovani, A. Meli, F. Migliacci, *Organometallics* **2003**, *22*, 2545–2547; d) C. Bianchini, A. Sommazzi, G. Mantovani, R. Santi, F. Masi, 6,916,931 B2, July 12, **2005**; e) C. Bianchini, D. Gatteschi, G. Giambastiani, I. Guerrero Rios, A. Ienco, F. Laschi, C. Mealli, A. Meli, L. Sorace, A. Toti, F. Vizza, *Organometallics* **2007**, *26*, 726–739.

[14] The iminopyridine ligand containing the benzofuryl moiety (N_2^{BFu}) was obtained in 88% yield according to the procedure reported in the literature for the furanyl-containing analogue (see refs.[13b,13c]), using benzofuran-2-yltrimethylstannane instead of furan-2-yltrimethylstannane.

[15] F. H. Allen, O. Kennard, D. G. Watson, *J. Chem. Soc., Perkin Trans. 2* **1987**, S1.

[16] a) S. Arndt, T. P. Spaniol, J. Okuda, *Organometallics* **2003**, *22*, 775–781; b) B.-J. Deelman, M. Booij, A. Meetsma, J. H. Teuben, H. Kooijman, A. L. Spek, *Organometallics* **1995**, *14*, 2306–2317; c) W. J. Evans, T. A. Ulibarri, J. W. Ziller, *Organometallics* **1991**, *10*, 134–142; d) J. Hitzbleck, J. Okuda, *Organometallics* **2007**, *26*, 3227–3235; e) N. S. Radu, S. L. Buchwald, B. Scott, C. J. Burns, *Organometallics* **1996**, *15*, 3913–3915; f) S. N. Ringelberg, A. Meetsma, B. Hessen, J. H. Teuben, *J. Am. Chem. Soc.* **1999**, *121*, 6082–6083; g) S. N. Ringelberg, A. Meetsma, S. I. Troyanov, B. Hessen, J. H. Teuben, *Organometallics* **2002**, *21*, 1759–1765.

[17] a) S. Banerjee, T. J. Emge, J. G. Brennan, *Inorg. Chem.* **2004**, *43*, 6307–6312; b) H. C. Aspinall, S. A. Cunningham, P. Maestro, P. Macaudiere, *Inorg. Chem.* **1998**, *37*, 5396–5398; c) J. Lee, D. Freedman, J. H. Melman, M. Brewer, L. Sun, T. J. Emge, F. H. Long, J. G. Brennan, *Inorg. Chem.* **1998**, *37*, 2512–2519; d) M. Niemeyer, *Eur. J. Inorg. Chem.* **2001**, 1969–1981.

[18] D. Wang, D. Cui, M. Miao, B. Huang, *Dalton Trans.* **2007**, 4576–4581.

[19] B. Liu, D. Cui, J. Ma, X. Chen, X. Jing, *Chem. Eur. J.* **2007**, *13*, 834–845.

[20] X. Liu, X. Shang, T. Tang, N. Hu, F. Pei, D. Cui, X. Chen, X. Jing, *Organometallics* **2007**, *26*, 2747–2757.

[21] G. G. Skvortsov, G. K. Fukin, A. A. Trifonov, A. Noor, C. Döring, R. Kempe, *Organometallics* **2007**, *26*, 5770–5773.

[22] For previous works on the ring-opening reaction of furan with lanthanide-cyclopentadienyl complexes see also ref.[16g].

[23] G. Jeske, H. Lauke, H. Mauermann, P. N. Swepston, H. Schumann, T. J. Marks, *J. Am. Chem. Soc.* **1985**, *107*, 8091–8103.

[24] A. Z. Voskoboinikov, I. N. Parshina, A. K. Shestakova, K. P. Butim, I. P. Beletskaya, L. G. Kuz'mina, J. A. K. Howard, *Organometallics* **1997**, *16*, 4041–4055.

[25] a) M. D. Fryzuk, L. Jafarpour, F. M. Kerton, J. B. Love, B. O. Patrick, S. J. Rettig, *Organometallics* **2001**, *20*, 1387–1396; b) G. W. Rabe, C. D. Bérubé, G. P. A. Yap, K.-C. Lam, T. E. Concolino, A. L. Rheingold, *Inorg. Chem.* **2002**, *41*, 1446–1453; c) G. W. Rabe, M. Zhang-Presse, F. A. Riederer, G. P. A. Yap, *Inorg. Chem.* **2003**, *42*, 3527–3533.

[26] a) S. Harder, *Organometallics* **2005**, *24*, 373–379; b) D. M. Lyubov, A. M. Bubnov, G. K. Fukin, F. M. Dolgushin, M. Antipin, O. Pelcé, M. Schappacher, S. M. Guillaume, A. A. Trifonov, *Eur. J. Inorg. Chem.* **2008**, 2090–2098.

[27] a) D. Wang, S. Li, X. Liu, W. Gao, D. Cui, *Organometallics* **2008**, *27*, 6531–6538; b) E. Y.-X. Chen, T. J. Marks, *Chem. Rev.* **2000**, *100*, 1391–1434.

[28] a) R. Anwander in *Homogeneous Catalysis with Organometallic Compounds* (Eds.: B. Cornils, W. A. Hermann), Wiley-VCH, Weinheim, **2002**; b) G. Desurmont, Y. Li, H. Yasuda, T. Maruo, N. Kanehisa, Y. Kai, *Organometallics* **2000**, *19*, 1811–1813; c) G. Desurmont, T. Tokomitsu, H. Yasuda, *Macromolecules* **2000**, *33*, 7679–7681; d) F. T. Edelmann, *Top. Curr. Chem.* **1996**, *179*, 247–276; e) M. A. Giardello, V. P. Conticello, L. Brard, M. R. Gagne, T. J. Marks, *J. Am. Chem. Soc.* **1995**, *117*, 7157–7168; f) S. Arndt, P. Voth, T. P. Spaniol, J. Okuda, *Organometallics* **2000**, *19*, 4690–4700; g) F. Estler, G. Eickerling, E. Herdtweck, R. Anwander, *Organometallics* **2003**, *22*, 1212–1222.

[29] G. M. Sheldrick, *SADABS*, Program for Empirical Absorption Corrections, University of Göttingen, Göttingen, Germany, **1986**.

[30] L. Farrugia, *J. Appl. Crystallogr.* **1999**, *32*, 837–838.

[31] A. Altomare, M. C. Burla, M. Cavalli, G. L. Cascarano, C. Giacovazzo, A. Gagliardi, G. G. Moliterni, G. Polidori, R. Spagna, *J. Appl. Crystallogr.* **1999**, *32*, 115–119.

[32] G. M. Sheldrick, *SHELX-97*, University of Göttingen, Göttingen, Germany, **1997**.

[33] M. N. Burnett, C. K. Johnson, *ORTEP-3*, Report ORNL-6895, Oak Ridge National Laboratory, Oak Ridge, TN, USA, **1996**.

Received: September 18, 2009
Published Online: December 15, 2009

ORGANOMETALLICS

Article

pubs.acs.org/Organometallics

Yttrium Complexes Featuring Different Y−C Bonds. Comparative Reactivity Studies: Toward Terminal Imido Complexes

Alexander A. Karpov,[†] Anton V. Cherkasov,[†] Georgy K. Fukin,[†] Andrei S. Shavyrin,[†] Lapo Luconi,[‡] Giuliano Giambastiani,[‡] and Alexander A. Trifonov*[,†]

[†]G. A. Razuvaev Institute of Organometallic Chemistry of the Russian Academy of Sciences, Tropinina 49, GSP-445, 603950 Nizhny Novgorod, Russia

[‡]Institute of Chemistry of OrganoMetallic Compounds, ICCOM-CNR, Via Madonna del Piano, 10, 50019 Sesto Fiorentino (Florence), Italy

Supporting Information

ABSTRACT: The reactions of 2,6-diisopropylaniline with equimolar amounts of alkyl−heteroaryl yttrium complexes containing Y−C(sp^3, alkyl) along with Y−C(sp^2, heteroaryl) bonds resulting from intramolecular C−H bond activation of the amido−pyridinate ligands [NNO^{BzFur}]YCH$_2$SiMe$_3$(THF)$_2$, [NNS^{BzTh}]YCH$_2$SiMe$_3$(THF)$_2$, and [NNS^{EtTh}]YCH$_2$SiMe$_3$(THF)$_2$ have been scrutinized with the aim of synthesizing yttrium terminal imido species. These reactions occur at ambient temperature with the protonolysis of the Y−C(sp^3, alkyl) bond, thus affording anilido−heteroaryl species and maintaining the residual Y−C(sp^2, heteroaryl) bond untouched. However, the subsequent transformation of the as-synthesized anilido−heteroaryl complexes depends on the nature of the substituent on the 6-position of the pyridyl ring. In the case of the benzofuryl yttrium derivative [NNO^{BzFur}]YNH-2,6-^{i}Pr$_2$C$_6$H$_3$(THF)$_2$ (**4**), heating to 50 °C results in benzofuran ring opening with the formation of an anilido species supported by a dianionic amido−yne−phenolate ligand framework, [NNC≡CO]YNH-2,6-^{i}Pr$_2$C$_6$H$_3$(THF) (**6**). In contrast, a complex containing a benzothiophenyl moiety, [NNS^{BzTh}]YNH-2,6-^{i}Pr$_2$C$_6$H$_3$(THF)$_2$ (**7**), slowly undergoes protonation of the Y−C(sp^2, heteroaryl) bond and a ligand redistribution reaction takes place, affording an yttrium bis(anilido) species supported by a monoanionic amido−pyridinate ligand featuring intramolecular Y−S heteroaryl coordination, [NNS^{BzTh}]Y[NH-2,6-^{i}Pr$_2$C$_6$H$_3$]$_2$ (**9**). It is worth noting that an yttrium complex containing α-thiophenyl fragment, [NNS^{EtTh}]YNH-2,6-^{i}Pr$_2$C$_6$H$_3$(THF)$_2$ (**10**), turned out to be extraordinarily robust and no transformation was ever detected even upon heating the complex at 100 °C for prolonged times.

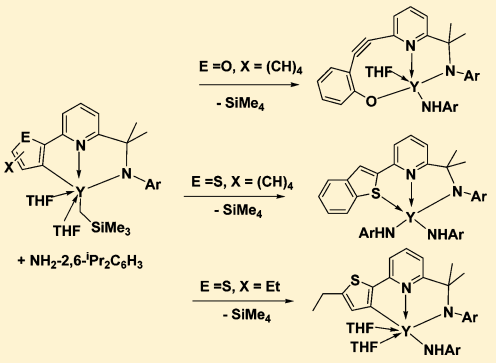

INTRODUCTION

Rare-earth complexes containing M−C σ bonds still deserve particular interest as highly active species that exhibit unique reactivity[1] and ability to promote activation and derivatization of unsaturated[2] and saturated[3] substrates. Recently we have reported how the reaction of an equimolar amount of [Y(CH$_2$SiMe$_3$)$_3$(thf)$_2$] with aminopyridine ligands bearing aryl or heteroaryl substituents at the 6-position of the pyridine ring results in quantitative intramolecular sp^2 or sp^3 C−H bond activations. These reactions proved to be a useful synthetic approach, allowing for the convenient synthesis of novel yttrium complexes featuring the simultaneous presence of two different Y−C bonds (Y−benzyl, Y−aryl, or Y−heteroaryl together with Y−alkyl).[4] Notably, the Y−C bonds in the isolated complexes showed different reactivities: i.e., upon complex treatment with an excess of PhSiH$_3$, a σ-bond metathesis reaction took place selectively on the residual Y−alkyl bonds, leading to the formation of unique yttrium aryl−-hydrido, benzyl−hydrido, and heteroaryl−hydrido species.

Chen et al. reported in 2010 on the synthesis and characterization of the first (and still the only) example of a rare-earth complex with a terminal imido ligand.[5] Complexes containing a double nitrogen−metal bond have important synthetic potentialities due to the ability of the M═N functional group to undergo several reactions/transformations (metathesis of imines and carbodiimides, metallacycle formation with alkynes and alkenes, and C−H bond activation).[6] It is worth noting that, unlike the well-established imido chemistry based on transition metals,[7] that of rare-earth metals is still in its infancy.[8] Synthetic difficulties are basically related to the pronounced tendency of these large metal ions to assemble in the form of more stable bi- or polymetallic complexes with μ_2-imido ligands.[8,9] Several examples of C−H bond activation resulting from the transformation of terminal imido rare-earth complexes have been also documented.[8d,f] Bulky polydentate ligands able to provide kinetic stability to the final imido species may be employed in order to overcome these synthetic limitations. Accordingly, the aforementioned alkyl−heteroaryl yttrium complexes[4] coordinated by amidopyr-

Received: February 4, 2013
Published: April 5, 2013

   dx.doi.org/10.1021/om400099z | *Organometallics* 2013, 32, 2379−2388

Chart 1. Yttrium Alkyl−Heteroaryl Complexes Containing Potentially Coordinative S and O Donor Sites

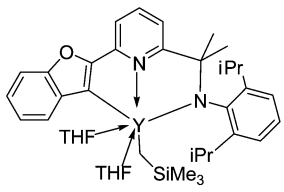

$[NNO^{BzFur}]YCH_2SiMe_3(THF)_2$

(1)

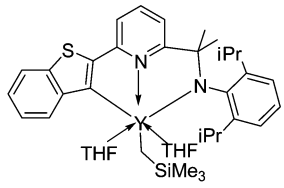

$[NNS^{BzTh}]YCH_2SiMe_3(THF)_2$

(2)

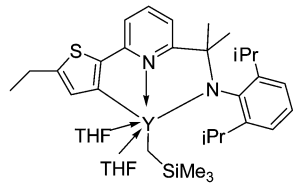

$[NNS^{EtTh}]YCH_2SiMe_3(THF)_2$

(3)

idinate ligands represent good candidates for the synthesis of related derivatives bearing terminal imido fragments via reaction with sterically demanding anilines. Indeed, the stabilization of the terminal imido species would potentially be assisted from an intramolecular coordination of either S (soft) or O (hard) donors belonging to the tridentate amidopyridinate system (N,N,O or N,N,S) itself; the Y−C(heteroaryl) bond protonolysis carried out by the aniline reagent would render accessible those ligand donor sites not available in the former species. In this regard, inspired by the challenging synthesis of rare-earth terminal imido complexes, we have explored the reactions of yttrium alkyl−heteroaryl complexes with 2,6-diisopropylaniline.

RESULTS AND DISCUSSION

In order to prepare terminal imido yttrium species, we attempted the reactions of equimolar amounts of alkyl−heteroaryl complexes **1**−**3** (Chart 1) with 2,6-diisopropylaniline. As the crucial role of a Lewis base coordination to the metal center is emphasized as a prerequisite for the formation of terminal imido complexes,[5] we fix upon the use of tridentate ligands combining both hard/hard (N,O) and hard/soft (N,S) basic centers (Chart 1).

The NMR-tube reaction of **1** with 2,6-diisopropylaniline was carried in C_6D_6 at ambient temperature. The disappearance of the doublet at −0.69 ppm (attributed to the hydrogen atoms of the residual methylene group bound to the yttrium center) and the concomitant release of $SiMe_4$ were indicative of Y−C(alkyl) bond protonolysis. Furthermore, the persistence (in the $^{13}C\{^1H\}$ NMR spectrum) of a doublet centered at 157.3 ppm ($^1J_{YC}$ = 40.0 Hz) assigned to the sp^2 carbon of the benzofuryl moiety σ-bonded to the metal center, together with the appearance (in the ^1H NMR spectrum) of a doublet at 5.10 ppm ($^2J_{YH}$ = 2.2 Hz), characteristic for an NH anilido proton,[17] supported the formation of the benzofuryl−anilido species **4** (Scheme 1).

Complex **4** was isolated and completely characterized by ^1H and $^{13}C\{^1H\}$ NMR spectroscopy and microanalysis. Following the behavior of **4** in C_6D_6 solution at room temperature by ^1H NMR spectroscopy revealed that neither decomposition nor further transformation took place even after several days. In contrast, when the complex solution temperature was raised to 50 °C, a relatively rapid conversion of **4** into a new species was observed (50% of conversion within 15 h).

The preparative-scale reaction of **1** with 2,6-diisopropylaniline was carried out in a toluene/hexane mixture (toluene/hexane 1/4) at room temperature, and the mixture was then heated at 50 °C for 30 h. The reaction mixture turned from yellow to deep red, and yellowish orange crystals suitable for X-ray analysis were isolated in 54% yield after cooling the mixture to −20 °C.

Scheme 1. Synthesis of the Anilido Complex 4 and Its Subsequent Thermal Rearrangement (Furyl Ring Opening) to Complex 6 Stabilized by a Dianionic Amido−Yne−Phenolate Ligand

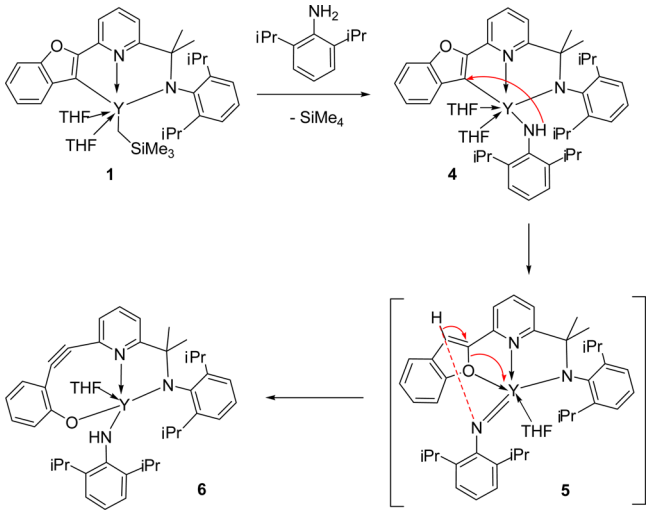

An X-ray diffraction study showed that the anilido complex **6** contains a dianionic amido−yne−phenolate ligand (Figure 1). Complex **6** crystallizes as a solvate species (**6**·C_7H_8). Due to the furyl fragment ring opening an 11-membered chelating amido−yne−phenolate group metallacycle was formed. This metallocycle is not planar, the maximum deviation of the atoms from its plane being 0.690(1) Å. The yttrium atom in **6** is covalently bonded with one oxygen and one nitrogen atom from the amido−yne−phenolate framework (Y(1)−O(1) = 2.1808(9) Å, Y(1)−N(1) = 2.244(1) Å), while the nitrogen of the pyridine fragment forms with yttrium a coordinative bond (Y(1)−N(2) = 2.409(1) Å). Due to covalent bonding with the anilido fragment (Y(1)−N(3) = 2.203(1) Å) and coordination of one THF molecule, the coordination number at the yttrium is 5. The complex adopts a distorted-square-pyramidal coordination geometry, whose base is set up by the N and O atoms from the amido−yne−phenolate moiety and one O atom from a THF molecule. The covalent Y−N bonds in **6** are somewhat nonequivalent, but their values are comparable to those reported for related amides on five-coordinated yttrium[10] complexes. The Y−O bond length is also in a good agreement with the values reported for five-coordinated yttrium alkoxides.[10b,11] The angles around carbon atoms C(21) and C(22) (C(21)−C(22)−C(23) = 173.3(2)°, C(20)−C(21)−C(22) = 163.9(2)°) are consistent with a C_{sp} hybridization of the acetylenic moiety. The corresponding C(21)−C(22) bond distance of 1.200(2) Å is also in agreement with triple-bond character.[12] The C(23)−C(24) bond length (1.410(2) Å) is

dx.doi.org/10.1021/om400099z | Organometallics 2013, 32, 2379−2388

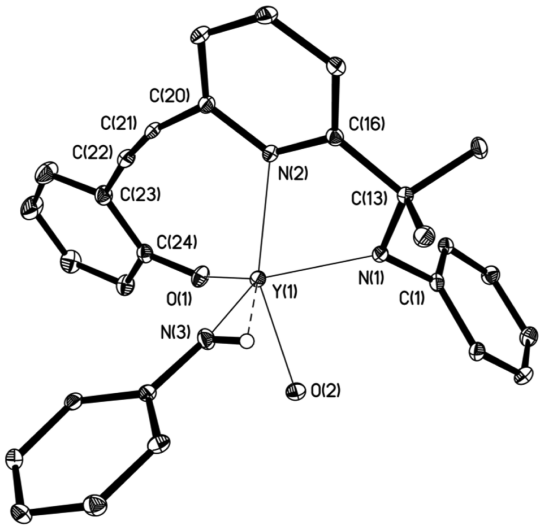

Figure 1. Molecular structure of complex **6** with 30% probability ellipsoids. The ^{i}Pr substituents of the aminopyridinate ligand, the methylene groups of THF molecules, and hydrogen atoms are omitted for clarity. Selected distances (Å) and angles (deg): Y(1)−O(1) = 2.1808(9), Y(1)−O(2) = 2.361(1), Y(1)−N(1) = 2.244(1), Y(1)−N(2) = 2.409(1), Y(1)−N(3) = 2.203(1), O(1)−C(24) = 1.321(2), C(20)−C(21) = 1.432(2), C(21)−C(22) = 1.200(2), C(22)−C(23) = 1.425(2), C(23)−C(24) = 1.410(2); C(20)−C(21)−C(22) = 163.9(2), C(21)−C(22)−C(23) = 173.3(2).

characteristic for aromatic C−C bonds.[12] The single bonds next to the triple bond (C(22)−C(23) = 1.425(2) Å) and C(20)−C(21) = 1.432(2) Å) show distances within the range for those in eneynes.[13]

Additionally, an intense band at 2250 cm^{-1} in the Raman spectrum of complex **6** gives further evidence of the presence of a triple bond.[29]

Furan ring-opening reactions, triggered by intramolecular C−H bond activation in alkyl and heteroaryl species, have been reported in a few cases.[14] Formation of complex **6** can be rationalized by a sequence of transformations of the benzofuryl−amido species **4**, a reliable representation of which is provided in Scheme 1. First, an intramolecular protonolysis of the Y−C(heteroaryl) bond promoted by the residual proton of the NH amido function takes place, leading to the formation of the terminal imido complex **5** (Scheme 1). Afterward, the transient terminal imido complex undergoes rapid intramolecular C−H bond activation, leading to the ring opening of the furyl cycle with the generation of **6**. It is worth noting that, when the reaction course of the thermal rearrangement of **4** is followed by NMR spectroscopy, no signals attributed to the transient terminal imido species **5** were ever detected, thus revealing an extremely short lifetime (on the NMR time scale) of the imido intermediate itself.

Aiming at stabilizing the terminal imido species as well as evaluating the general character of this heterocycle ring-opening reaction, we have investigated the reaction of 2,6-diisopropylaniline with the analogous thio analogue **2** (Scheme 2). The coordination of a soft Lewis base along with a lower energy of the covalent Y−S bond (in comparison to that of Y−O)[15] was thought to be beneficial to the final stabilization of the expected terminal imido yttrium species. It is worth noting that we found a dramatic impact on the reaction outcome by the replacement of the benzofuryl fragment with the benzothiophenyl fragment. Indeed, the reaction of **2** with 2,6-diisopropylaniline in both

Scheme 2. Synthesis of the Anilido Complexes 7 and 8

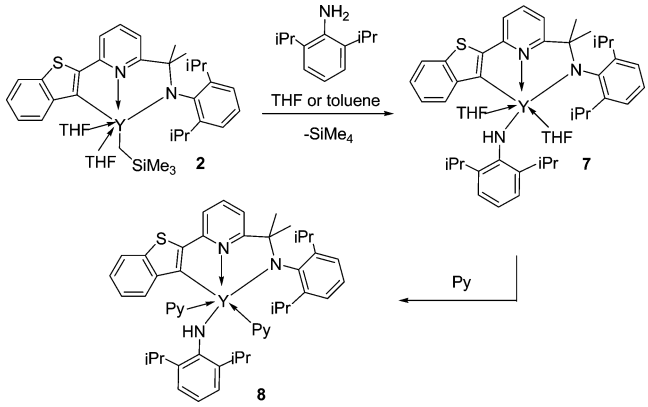

toluene and THF afforded the benzothiophenyl−amido complex **7**, which was isolated as a yellow crystalline solid in 78% yield (Scheme 2). Complex **7** was characterized by ^{1}H and ^{13}C{^{1}H} NMR spectroscopy and microanalysis. Unfortunately, all our attempts to obtain single crystals of **7** suitable for X-ray diffraction studies failed. Nevertheless, the treatment of **7** with pyridine and its subsequent recrystallization from benzene allowed for the isolation of the bis(pyridine) adduct **8**, which was characterized by an X-ray diffraction study (Figure 2). The

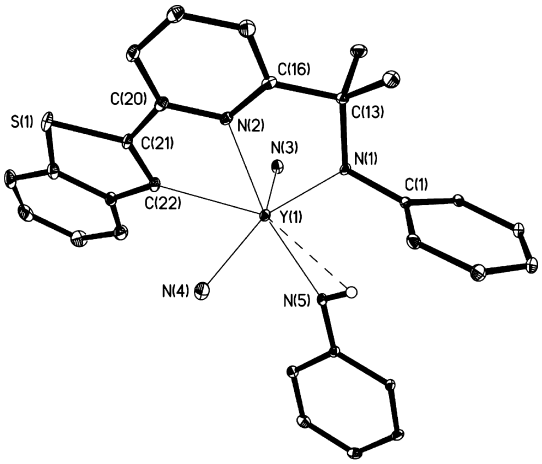

Figure 2. Molecular structure of complex **8** with 30% probability ellipsoids. The ^{i}Pr substituents in the aminopyridinate and aniline ligands, the CH groups of the Py molecules, and hydrogen atoms are omitted for clarity. Selected distances (Å) and angles (deg): Y(1)−N(1) = 2.253(2), Y(1)−N(2) = 2.475(2), Y(1)−N(3) = 2.481(2), Y(1)−N(4) = 2.506(3), Y(1)−N(5) = 2.293(2), Y(1)−C(22) = 2.551(3); N(1)−Y(1)−N(2) = 67.64(8), N(1)−Y(1)−N(5) = 94.81(9), N(1)−Y(1)−N(3) = 102.73(8), N(1)−Y(1)−N(4) = 107.18(9), N(2)−Y(1)−N(3) = 98.81(8), N(2)−Y(1)−N(4) = 90.03(9), N(2)−Y(1)−N(5) = 160.90(8), N(3)−Y(1)−N(5) = 92.22(9), N(4)−Y(1)−N(5) = 88.10(9).

proton of the NH group in **7** was clearly evidenced by a singlet at 4.46 ppm, while the presence of a doublet at 194.7 ppm in the ^{13}C{^{1}H} NMR spectrum ($^{1}J_{YC}$ = 40.3 Hz) was consistent with the sp^{2}-carbon atom of the benzothiophene ring still covalently bound to the yttrium center.

The X-ray diffraction study of **8** revealed that it crystallizes as a solvate (**8**·C_6H_6). The yttrium atom in **8** is covalently bound by the amido nitrogen of the amidopyridinate ligand, the sp^{2} carbon of the thiophenyl ring, and a nitrogen atom of the

dx.doi.org/10.1021/om400099z | Organometallics 2013, 32, 2379−2388

anilido fragment (Figure 2). Moreover, yttrium is coordinated by one nitrogen from the pyridyl central unit and two nitrogens from the ancillary pyridine molecules. The coordination number of yttrium in **8** is 6, with a distorted-square-bipyramidal coordination geometry. The Y−C bond length in **8** (2.551(3) Å) is slightly longer in comparison to that measured in related heteroaryl−hydrido complexes (2.514(3) Å).[4b] The distances between yttrium and nitrogen atoms of the amidopyridinate ligand (Y(1)−N(1) = 2.253(2) Å, Y(1)−N(2) = 2.475(2) Å) are close to those previously reported for related six-coordinated yttrium complexes[4a,b] (2.202(1)−2.254(1) and 2.420(1)−2.462(2) Å, respectively). The amidopyridinate ligand is not planar, showing a maximum deviation of atoms from the eight-membered metallacycle of 0.343(2) Å (C(13)). The angle between the planes containing the pyridine central unit and the benzothiophenyl fragments is 13.6°. The measured covalent Y−N(5) bond distance is 2.293(2) Å.

When a yellow solution of **7** in toluene was kept at room temperature for 1 week, the precipitation of orange crystals took place. Notably, an X-ray diffraction study of the isolated crystals revealed the formation of a bis(anilido) yttrium compound **9** supported by the tridentate amidopyridinate ligand (Scheme 3). Isolation of **9** was continued after the

Scheme 3. Synthesis of the Bis-Anilido Complex 9

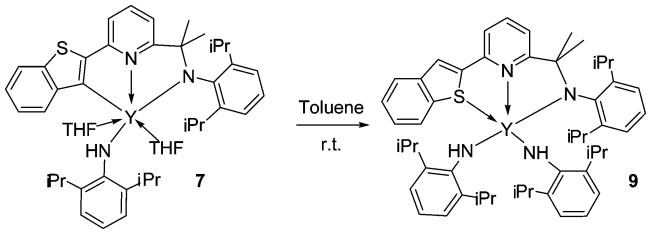

separation of the first batch of crystals ,and an overall 30% yield of **9** were collected from the mother liquor after maintaining the solution for 2 weeks at room temperature.

Complex **9** crystallizes as a solvate with one molecule of toluene per unit. In **9** the yttrium atom is coordinated by a monoanionic tridentate amidopyridinate ligand, the latter resulting from the intramolecular protonolysis of the Y−C(heteroaryl) bond on precursor **7** (Scheme 3 and Figure 3).

The Y−C(heteroaryl) bond protonolysis allows the sulfur atom to coordinate the yttrium center. As Figure 3 shows, the coordination number of yttrium is 5. Unlike the case in complex **7**, the amidopyridinate ligand in **9** is bound to the yttrium center via one covalent Y−N bond, while both sulfur and nitrogen atoms form coordinative bonds with the metal center. The length of the covalent Y−N(1) bond (2.177(3) Å) in **9** is slightly shorter than that measured in related six-coordinated yttrium complexes stabilized by dianionic amidopyridinate ligands (2.206(2)−2.254(2) Å),[4] but it falls into the range of values reported for five-coordinate yttrium amides.[10] The length of the coordination bond between yttrium and the nitrogen atom of the amidopyridinate ligand (Y(1)−N(2) = 2.475(2) Å) is close to those previously reported for related six-coordinated yttrium complexes (2.420(1)−2.462(2) Å).[4a,b] Finally, the Y−S bond distance in **9** (3.0755(9) Å) is much longer in comparison to the distances measured in five-coordinated yttrium complexes with either chelating bis(thiophosphinic amide) (2.7910(6) Å)[16a] or bis(thiophosphinic amidate) (2.718(1) and 2.741(1) Å) ligands.[16b] The Y−S

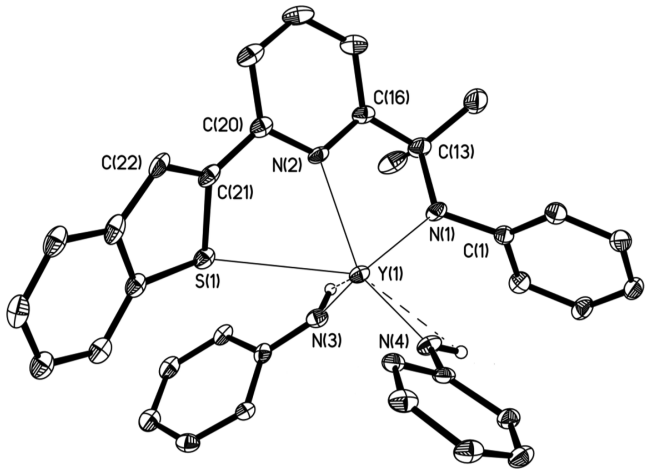

Figure 3. Molecular structure of complex **9** with 30% probability ellipsoids. The ^{i}Pr substituents of the aminopyridinate ligand, the aniline ligands, and hydrogen atoms are omitted for clarity. Selected distances (Å) and angles (deg): Y(1)−N(1) = 2.177(3), Y(1)−N(2) = 2.475(2), Y(1)−N(3) = 2.236(3), Y(1)−N(4) = 2.231(2), Y(1)−S(1) = 3.0755(9); N(1)−Y(1)−N(2) = 70.70(9), N(1)−Y(1)−S(1) = 132.79(7), N(2)−Y(1)−S(1) = 65.26(6), N(3)−Y(1)−N(4) = 116.36(9).

distance in **9** significantly exceeds the sum of the covalent radii of these atoms (2.82 Å); nevertheless, it still lies below the sum of van der Waals radii (4.25 Å) (Y, R_{coval} = 1.68, R_{VdW} = 2.4; S, R_{coval} = 1.14, R_{VdW} = 1.85).[22] It is worth noting that complexes containing Y−S coordination bonds are still rather rare. The bond lengths between yttrium and anilido nitrogens (Y−N(3,4) = 2.231(2) and 2.236(3) Å, respectively) slightly exceed those measured in **6** (2.203(1) Å) but are somewhat longer than those found in **8** (2.293(2) Å). The dihedral angle between the pyridinate and benzothiophenyl fragments (29.8°) is significantly larger in comparison to that measured in **8** (13.6°) as well as those found in other related yttrium complexes.[4b]

The generation of a bis(anilido) species, in pursuit of the synthesis of rare-earth terminal imido complexes, has been already documented.[17] Complex **9** may result from a hydrogen abstraction by a transient terminal imido complex followed by a ligand redistribution reaction. Unfortunately, all our attempts to isolate the imido intermediate still failed. The source for hydrogen abstraction also remains unclear, but THF seems to be a plausible candidate for that role. The intermolecular protonolysis and ligand redistribution reactions can be also evoked as possible routes of formation of **9**.

All these data taken together make reasonable the assumption of the crucial role played by the nature of the heterocyclic group at the amidopyridinate ligand in controlling/driving the evolution path of the intermediate terminal imido complexes. While in the case of a benzofuryl-containing system a concerted intramolecular C−H bond activation and ring-opening reaction occur, when a benzothiophene-containing analogue (having similar steric and electronic properties) is employed, the reaction pathway changes dramatically: no heterocycle ring opening is observed, while protonolysis and ligand redistribution reactions take place. Such a different behavior could originate in the contribution of either different Lewis base softness/hardness of the oxygen and the sulfur atoms or by a substantial difference of in terms of energies of Y−O and Y−S covalent bonds (Y−O, 692.5−719.0 kJ/mol; Y−

dx.doi.org/10.1021/om400099z | Organometallics 2013, 32, 2379−2388

S, 528.4 ± 10.5 kJ/mol).[15] In our opinion, the formation of a strong covalent Y−O bond is largely responsible for the ring-opening reaction occurring at the benzofuryl moiety and leading to complex **6**.

As an additional proof of the relevant contribution played by the ligand's heteroaromatic group on the transformation/rearrangement path of the rare-earth terminal imido intermediates, we finally investigated the reaction of 2,6-diisopropylaniline with complex **3** (containing an α-ethylthiophene substituent at the 6-position of the pyridine ring; see Chart 1). The NMR-tube reaction of **3** with an equimolar amount of 2,6-diisopropylaniline in C_6D_6 at room temperature showed the occurrence of a selective protonolysis of the Y−C(alkyl) bond exclusively while the Y−C(thien-2-yl) bond remained untouched (as confirmed by a clear doublet at 202.1 ppm (d, $^1J_{YC}$ = 36.2 Hz) in the $^{13}C\{^1H\}$ NMR spectrum). The reaction takes place with the simultaneous release of $SiMe_4$ and formation of the anilido species **10**. A similar reactivity between 2,6-diisopropylaniline and yttrium complexes containing both Y−C(alkyl) and Y−C(aryl) bonds has been recently documented by Chen et al.[5] Complex **10** was characterized by spectroscopic analysis and microanalysis. Unfortunately, all attempts to obtain suitable crystals of **10** for X-ray analysis failed. However, the treatment of **10** with an excess of pyridine and the subsequent recrystallization from toluene allowed us to obtain high-quality crystals of the pyridine adduct **11** (Scheme 4).

Scheme 4. Synthesis of the Anilido Complexes 10 and 11

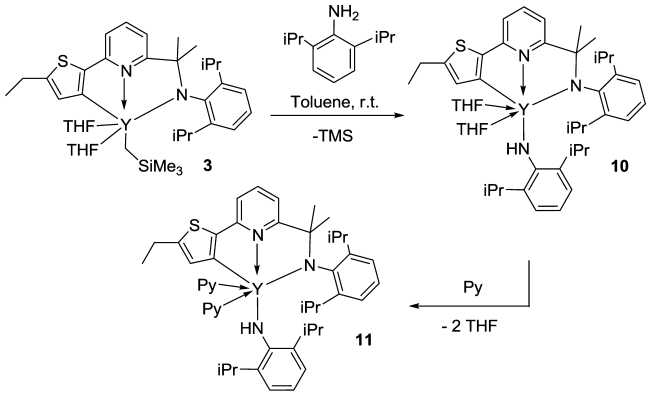

An X-ray diffraction study of **11** (Figure 4) revealed that the coordination environment at the yttrium center was set up by two nitrogen atoms and one carbon atom from the dianionic tridentate amidopyridinate ligand, one nitrogen atom from the monoanionic anilido group, and two nitrogen atoms from the two pyridine molecules. The coordination number of yttrium in **11** is 6. The coordination environment around the yttrium ion can be considered as a distorted octahedron where the amidopyridinate and anilido ligands are located in the equatorial plane, while two pyridine molecules occupy the apical positions. Complex **11** crystallizes as a solvate with one toluene molecule and contains two crystallographically independent molecules in the asymmetric unit. Both molecules have similar parameters, and therefore only one of them will be discussed.

The coordination mode of the amidopyridinate ligand in **11** is similar to that observed in the parent alkyl species.[4b] The Y−amidopyridinate fragment is planar (the maximum deviation from the plane is 0.047(1) Å). The Y−C(22) bond (2.506(2)

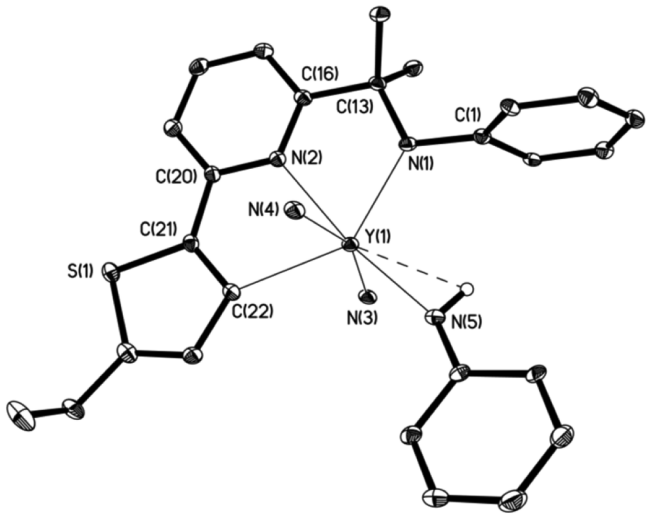

Figure 4. Molecular structure of complex **11** with 30% probability ellipsoids; the ^{i}Pr substituents in amidopyridinate and aniline ligands, the CH groups of the Py molecules, and hydrogen atoms are omitted for clarity. Selected distances (Å) and angles (deg): Y(1)−N(1) = 2.247(2), Y(1)−N(5) = 2.289(2), Y(1)−N(2) = 2.452(2), Y(1)−N(3) = 2.496(2), Y(1)−N(4) = 2.495(2), Y(1)−C(22) = 2.506(2); N(1)−Y(1)−N(2) = 68.17(7), N(1)−Y(1)−C(2) = 137.13(8), N(3)−Y(1)−N(4) = 161.97(7).

Å) in **11** is slightly longer than those measured in both the alkyl precursor **3** (2.482(2) Å)[4b] and in the related yttrium monoalkyl thien-2-yl species, the latter featuring an analogue intramolecular C−H bond activation at the β position of the thienyl moiety (2.423(3) Å).[19] The distance between the Y center and the anilido nitrogen atom (2.289(2) Å) is slightly longer than that measured for the amido Y−N bond, the latter being similar to those observed in related structures.[17a,20] The dihedral angle between the pyridinate and thiophenyl fragments is 1.7°, and it is significantly lower than that observed in **8**.

For all compounds (**6**, **8**, **9**, and **11**) featuring anilido fragments, the observed bond distances between the Y atom and the centers of N−H bonds (2.27−2.37 Å) together with the measured Y−N−H angles (85.4−101.2°) suggest the presence of agostic Y−NH bond interactions.[23]

It is worth noting that complex **10** is distinguished by its extraordinary stability. Unlike complexes **4** and **7**, neither intramolecular protonolysis of Y−C(thien-2-yl) bond by the anilido NH group nor a ligand redistribution reaction takes place both at room temperature (for prolonged times—up to 1 month) and upon heating at 80 °C for several hours. No decomposition/rearrangement takes place even after heating at 100 °C for 3 h. Such a result demonstrates, once more, how small modifications on the ligand framework can change the reactivity at the metal center remarkably, driving the reaction course toward different (and differently stable) organolanthanide species.

CONCLUSION

In this paper we have described the reactions of alkyl−heteroaryl complexes **1**−**3**, containing Y−C(sp^3, alkyl) and Y−C(sp^2, heteroaryl) bonds, with an equimolar amount of 2,6-diisopropylaniline. For all scrutinized systems the protonolysis of the Y−C(alkyl) bond takes place selectively at room temperature, leading to the formation of the corresponding anilido−heteroaryl species which keep the Y−C(sp^2, hetero-

dx.doi.org/10.1021/om400099z | Organometallics 2013, 32, 2379−2388

aryl) bonds untouched. Notably, both the stability of the anilido−heteroaryl derivatives and their potential transformation/rearrangement paths remarkably differentiate one from the other upon heating the complexes at elevated temperatures. In this regard, we have demonstrated how the nature of the heteroaryl framework attached to the 6-position of the pyridine ring can strongly influence both the reaction course and the complex stability. Thus, in the case of the anilido complex **4** a furyl ring opening takes place, leading to the unprecedented amido−yne−phenolate derivative **6**. Supposedly, complex **6** results from an intramolecular protonolysis of the Y−C(heteroaryl) bond (promoted by the residual proton of the NH anilido group), formation of the terminal imido complex, and its subsequent and rapid intramolecular hydrogen abstraction at the β-position of the heteroaromatic moiety. For the analogous complex **7**, containing a benzothiopheyl fragment with stereoelectronic properties similar to those of **4**, no heteroaryl ring opening takes place. It seems reasonable to invoke the formation of a strong covalent Y−O bond as the main driving force toward the generation of **6**. Unlike **4**, a solution of complex **7** undergoes slow Y−C(heteroaryl) bond protonolysis, leading to the formation of a complex stabilized by a monoanionic amidopyridinate ligand featuring a coordinative intramolecular Y−S interaction. Finally, the anilido−heteroaryl complex **10** featuring an α-ethylthiophenyl group turns out to be extraordinarily inert, since no reaction/rearrangement takes place even after prolonged heating at high temperatures (up to 100 °C). Further studies are currently ongoing in our laboratories with the aim at exploring the role of both the multidentate ancillary ligands and the rare-earth metal ion sizes on the formation and stability of terminal imido species.

EXPERIMENTAL SECTION

All experiments were performed in evacuated tubes by using standard Schlenk techniques, with rigorous exclusion of traces of moisture and air. After being dried over KOH, THF was purified by distillation from sodium/benzophenone ketyl; hexane and toluene were dried by distillation from sodium/triglyme and benzophenone ketyl prior to use. C_6D_6 was dried with sodium and condensed under vacuum into NMR tubes prior to use. 2,6-Diisopropylaniline was purchased from Acros and was dried over CaH_2 and molecular sieves. Anhydrous $(Me_3SiCH_2)_3Y(THF)_2$[24] and compounds **1** and **3**[4] were prepared according to literature procedures. The imino precursor (N^{2BTh}) to the benzothiophene-containing aminopyridinate ligand (N^2H^{BTh}) was prepared according to similar procedures reported in the literature.[25] All other commercially available chemicals were used after the appropriate purifications. NMR spectra were recorded with either a Bruker DPX 200 or a Bruker Avance DRX-400 spectrometer in $CDCl_3$ or C_6D_6 at 25 °C, unless otherwise stated. Chemical shifts for ^1H and $^{13}C\{^1H\}$ NMR spectra were referenced internally to the residual solvent resonances and are reported in ppm relative to TMS. IR spectra were recorded as Nujol mulls with a Bruker Vertex 70 instrument. Raman spectra were recorded with the RAM II accessory module coupled to the Bruker Vertex 70, equipped with a InGaAs detector and an Nd:YAG laser source (1064 nm) for sample excitation at a power of ∼450 mW and resolution of 4 cm^{-1}. All of the Raman spectra were recorded in the wavenumber range 50−3500 cm^{-1}. Lanthanide metal analyses were carried out by complexometric titrations. The C, H, N elemental analyses were performed in the microanalytical laboratory of the G. A. Razuvaev Institute of Organometallic Chemistry.

Synthesis of the Benzothiophene-Containing Aminopyridinate Ligand (N_2H^{BzTh}). A solution of the iminopyridine ligand N_2^{BTh} (1.00 g, 2.49 mmol) in dry and degassed toluene (20 mL) was cooled to 0 °C in an ice bath and treated dropwise with a 2.0 M toluene solution of trimethylaluminum (TMA; 1.86 mL, 3.73 mmol). The reaction mixture was stirred at room temperature for 12 h and then was quenched with 20 mL of water. The aqueous phase was extracted with 3 × 15 mL of AcOEt, and the combined organic layers were dried over Na_2SO_4. Removal of the solvent under reduced pressure gave the amidopyridinate ligand as a crude pale yellow solid. The ligand was purified by crystallization from hot MeOH, by cooling the resulting solution to −20 °C overnight to afford white crystals in 89% yield (0.95 g). ^1H NMR (200 MHz, CD_2Cl_2, 293 K): 1.12 (12H, d, $^3J_{HH}$ = 6.8 Hz, $CH(CH_3)$); 1.52 (6H, s, $C(CH_3)_2$); 3.38 (2H, sept, $^3J_{HH}$ = 6.8 Hz, $CH(CH_3)$); 4.40 (1H, bs, NH); 7.10 (3H, m, Ar); 7.40−7.35 (2H, m, Ar); 7.51 (1H, m, Ar); 7.92−7.75 (5H, Ar). $^{13}C\{^1H\}$ NMR (50 MHz, CD_2Cl_2, 293 K): 23.9 ($CH(CH_3)_2$); 28.3 ($CH(CH_3)_2$); 28.9 ($C(CH_3)_2$); 59.3 ($C(CH_3)_2$); 117.0 (Ar); 118.4 (Ar); 120.7 (Ar); 122.4 (Ar); 123.0 (Ar); 124.0 (Ar); 124.0 (Ar); 124.4 (Ar); 124.5 (Ar); 124.9 (Ar); 137.1 (Ar); 140.3 (Ar); 140.7 (Ar); 145.7 (Ar); 146.8 (Ar); 150.8 (Ar); 168.1 (Ar). IR (KBr): 573 (m); 645 (s); 713 (s); 742 (s); 750 (s); 781 (m); 805 (s); 829 (s); 838 (m); 860 (m); 897 (w); 931 (m); 938 (m); 995 (s); 1089 (s); 1124 (s); 1154 (s); 1180 (m); 1203 (s); 1248 (s); 1256 (s); 1330 (m); 1359 (s); 1240 (s); 1440 (s); 1528 (m); 1570 (s); 1583 (s); 1645 (w); 3054 (w); 3343 (s) cm^{-1}. Anal. Calcd for $C_{28}H_{32}N_2S$: C, 78.46; H, 7.52; N, 6.54; S, 7.48. Found: C, 79.01; H, 7.58; N, 6.50; S, 6.91.

Synthesis of $[NNS^{BzTh}]YCH_2SiMe_3(THF)_2$ (2). To a solution of $Y(CH_2SiMe_3)_3(THF)_2$ (0.4284 g, 0.87 mmol) in hexane (25 mL) was added a solution of N_2H^{BTh} (0.3526 g, 0.82 mmol) in hexane (15 mL) at 0 °C, and the reaction mixture was stirred for 0.5 h. The product crystallized from the reaction mixture as a pale yellow microcrystalline solid and was isolated in a yield of 91% (0.5475 g). ^1H NMR (400 MHz, C_6D_6, 293 K): −0.62 (2H, d, $^2J_{YH}$ = 2.6 Hz, YCH_2); 0.18 (9H, s, $SiMe_3$); 0.94 (8H, m, THF); 1.28 (6H, s, $C(CH_3)_2$); 1.31 (6H, d, $^3J_{HH}$ = 6.8 Hz, CH_3(i-Pr)); 1.35 (6H, d, $^3J_{HH}$ = 6.8 Hz, CH_3(i-Pr)); 3.62 (8H, m, THF); 3.80 (2H, sept, $^3J_{HH}$ = 6.8 Hz, $CH(CH_3)_2$); 6.62 (1H, d, $^3J_{HH}$ = 7.9 Hz, m-Py); 7.07−7.15 (3H, m, p-Py, p-NPh, BTh); 7.30 (1H, d, $^3J_{HH}$ = 7.6 Hz, m-Py); 7.31 (1H, d, $^3J_{HH}$ = 6.0 Hz, BTh); 7.34−7.37 (2H, m, m-NPh); 7.95 (1H, d, $^3J_{HH}$ = 7.9 Hz, BTh); 8.60 (1H, d, $^3J_{HH}$ = 7.8 Hz, BTh). $^{13}C\{^1H\}$ NMR (100 MHz, C_6D_6, 293 K): 4.3 ($SiMe_3$); 23.7 (CH_3(i-Pr)); 24.4 (THF); 27.8 (CH(i-Pr)); 28.3-(CH_3(i-Pr)); 31.2 ($C(CH_3)_2$); 31.6 (YCH_2); 69.2 (d, $^2J_{YC}$ = 2.3 Hz, $C(CH_3)_2$); 70.0 (THF); 116.0 (m-Py); 117.6 (m-Py); 122.1 (Ar); 123.9 (Ar); 124.0 (Ar); 124.1 (Ar); 124.6 (Ar); 129.7 (Ar); 139.1 (p-Py); 143.7 (d, $^3J_{YC}$ = 1.8 Hz, YCCCS); 143.8 (d, $^2J_{YC}$ = 3.1 Hz, YCC); 144.2 (Ar); 149.7 (Ar); 152.0 (d, $^2J_{YC}$ = 2.4 Hz, Ar); 158.5 (Ar); 174.8 (Ar); 195.9 (d, $^1J_{YC}$ = 37.2 Hz, Y−C). IR (KBr): 479 (w); 574 (w); 669 (w); 724 (s); 740 (s); 805 (s); 838 (m); 862 (s); 934 (w); 970 (w); 1026 (m); 1073 (w); 1090 (m); 1125 (m); 1159 (w); 1178 (m); 1226 (w); 1234 (w); 1247 (w); 1307 (m); 1530 (w); 1570 (s); 1590 (m) cm^{-1}. Anal. Calcd for $C_{40}H_{57}N_2O_2SSiY$: C, 64.32; H, 7.69; N, 3.75; Y, 11.90. Found: C, 64.51; H, 7.64; N, 3.54; Y, 11.92.

Synthesis of $[NNO^{BzFur}]YNH\text{-}2,6\text{-}^iPr_2C_6H_3(THF)_2$ (4). A solution of 2,6-diisopropylaniline (0.0517 g, 0.29 mmol) in hexane (10 mL) was added to a solution of **1** (0.2132 g, 0.29 mmol) in a hexane/toluene mixture (20 mL, 4/1) at room temperature, and the reaction mixture was stirred for 0.5 h. The reaction mixture changed from yellow to red. The reaction mixture was kept at −18 °C overnight. Complex **4** was isolated as a yellow-orange microcrystalline solid in 76% yield (0.182 g). ^1H NMR (400 MHz, C_6D_6, 293 K): 1.16−1.18 (14H, m, CH_3(i-Pr), THF); 1.33 (6H, d, $^3J_{HH}$ = 6.7 Hz, CH_3(i-Pr)); 1.38 (12H, d, $^3J_{HH}$ = 6.5 Hz, CH_3(i-Pr)); 1.23 (6H, s, $C(CH_3)_2$); 2.71−2.84 (2H, compl m, CH(i-Pr)); 3.56 (8H, m, THF); 3.76 (2H, sept, $^3J_{HH}$ = 6.5 Hz, CH(i-Pr)); 4.13 (1H, s, NH anilido); 6.63 (1H, m, m-Py); 6.98−7.18 (6H, m, o-,p-NPh, o-,p-anilido); 7.19−7.22 (1H, m-,p-Py); 7.25 (1H, m, Ph); 7.32 (1H, m, Ph); 7.68 (1H, m, Ph); 8.27 (1H, m, Ph); 7.66 (1H, m, m-Py). $^{13}C\{^1H\}$ NMR (100 MHz, C_6D_6, 293K): 24.1 (CH_3(i-Pr)); 24.9 (CH_3(i-Pr)); 26.3 (THF); 27.4 (CH_3(i-Pr)); 27.9 (CH(i-Pr)); 31.1 ($C(CH_3)_2$); 68.3 ($C(CH_3)_2$); 68.6 (THF); 113.9 (Ar); 114.4 (m-Py); 117.5 (m-Py); 121.5 (Ar); 122.5 (Ar, anilido); 122.8 (Ar, anilido); 124.6 (Ar, anilido); 124.2 (Ar); 127.1 (Ar); 132.8 (Ar, anilido); 133.4 (Ar, anilido); 139.0 (p-Py); 140.4 (Ar); 148.4 (Ar, anilido); 149.0 (Ar, anilido); 151.8 (Ar);

dx.doi.org/10.1021/om400099z | Organometallics 2013, 32, 2379−2388

156.6 (Ap); 157.2 (d, $^1J_{YC}$ = 40.9 Hz, Y−C); 161.0 (Ar); 175.1 (Ar). IR (KBr): 467 (w); 484 (w); 514 (w); 552 (w); 570 (w); 617 (w); 635 (w); 649 (w); 678 (w); 695 (w); 743 (s); 775 (w); 799 (m); 810 (m); 840 (m); 852 (m); 880 (m); 894(m); 926 (w); 936 (m); 960 (w); 967 (w); 990 (w); 1007 (w); 1026 (m); 1046 (m); 1084 (m); 1095 (w); 1107 (w); 1122 (m); 1170 (m); 1178 (m); 1197 (w); 1229 (w); 1254 (s); 1303 (w); 1318 (w); 1341 (w); 1363 (w); 1424 (s); 1462 (s); 1506 (w); 1573 (m); 1588 (w); 1601 (w); 3405 (w); 3482 (w) cm^{-1}. Anal. Calcd for $C_{48}H_{64}N_3O_3Y$: C, 70.31; H, 7.87; N, 5.12; Y, 10.84. Found: C, 70.42; H, N, 4.75; 7.98; Y, 10.77.

Synthesis of [NNC≡CO]YNH-2,6-^{i}Pr$_2$C$_6$H$_3$(THF) (6). A solution of 2,6-diisopropylaniline (0.0869 g, 0.49 mmol) in hexane (10 mL) was added to a solution of **1** (0.3582 g, 0.49 mmol) in a hexane/toluene mixture (30 mL, 4/1) at room temperature, and the reaction mixture was stirred for 0.5 h and then was heated to 50 °C for 30 h. The reaction mixture turned from yellow to deep red. The solution was kept at −18 °C overnight. Complex **6** was isolated as yellow-orange crystals in 54% yield (0.1981 g). ^{1}H NMR (400 MHz, C_6D_6, 293 K): 1.06−1.18 (10H, m, CH_3(i-Pr), THF); 1.27 (12H, d, $^3J_{HH}$ = 6.7 Hz, CH_3(i-Pr)); 1.37−1.50 (6H, broad m, CH_3(i-Pr)); 1.98 (6H, s, $C(CH_3)_2$); 2.95−3.63 (7H, compl m, CH(i-Pr), THF); 4.42 (1H, broad m, CH(i-Pr)); 5.31 (1H, s, NH); 6.50−6.58 (2H, m, m-Py, p-Ph); 6.60 (2H, t, $^3J_{HH}$ = 8.3 Hz, m-Ph); 6.74−6.83 (2H, m, p-Py, p-Ph); 7.08−7.15 (6H, m, o-NPh, o-anilido, p-NPh, p-anilido); 7.42 (1H, dd, $^3J_{HH}$ = 7.4 Hz, $^3J_{HH}$ = 1.4 Hz, m-Py). ^{13}C{^{1}H} NMR (100 MHz, C_6D_6, 293 K): 22.6−24.6 (broad s, Ar, anilido); 24.9 (THF); 25.3−27.0 (broad s, Ar, anilido); 27.0−28.9 (broad s, Ar, anilido); 29.8 (broad s, Ar, anilido); 64.7 (d, $^3J_{YC}$ = 2.6 Hz, Ar); 69.6 (broad s, THF); 93.4 (Ph-*C*C); 101.2 (Ph−*C*C); 115.5 (Ar); 115.8 (Ar); 118.2 (m-Py); 118.7 (Ar); 119.9 (Ar); 122.7 (Ar, anilido); 123.3 (Ar, anilido); 123.4 (Ar, anilido); 127.9 (Ar); 129.3 (m-Py); 132.3 (Ar, anilido); 133.0 (Ar, anilido); 137.5 (Ar, anilido); 138.8 (p-Py); 140.5 (Ar); 148.0 (Ar); 151.4 (d, $^2J_{YC}$ = 4.5 Hz, Ar anilido); 171.6 (d, $^2J_{YC}$ = 3.5 Hz, Ar); 177.3 (Y−O−C). IR (KBr): 569 (w); 605 (w); 743 (s); 806 (s); 850 (m); 935 (m); 1027 (s); 1044 (s); 1096 (s); 1147 (w); 1170 (w); 1193 (w); 1260 (s); 1308 (s); 1323 (m); 1364 (m); 1439 (s); 1564 (m); 1573 (s); 1589 (m); 1618 (m); 2196 (m); 3342 (w); 3404 (w); 3482 (w) cm^{-1}. Anal. Calcd for $C_{44}H_{56}N_3O_2Y$: C, 70.67; H, 7.55; N, 5.62; Y, 11.89. Found: C, 70.32; H, 7.61; N, 5.20; Y, 11.79.

Synthesis of [NNS^{BzTh}]YNH-2,6-^{i}Pr$_2$C$_6$H$_3$(THF)$_2$ (7). A solution of 2,6-diisopropylaniline (0.0803 g, 0.45 mmol) in hexane (10 mL) was added to a solution of **2** (0.3384 g, 0.45 mmol) in a toluene/hexane mixture (30 mL) at room temperature, and the reaction mixture was stirred for 0.5 h. The volatiles were removed under vacuum, and the solid residue was recrystallized from toluene to give 0.2952 g (78% yield) of **7** as a yellow microcrystalline solid. ^{1}H NMR (400 MHz, C_6D_6, 293 K): 1.10 (8H, m, THF); 1.17 (6H, d, $^3J_{HH}$ = 6.5 Hz, CH_3(i-Pr)); 1.25 (12H, d, $^3J_{HH}$ = 6.6 Hz, CH_3(i-Pr) anilido); 1.29 (6H, d, $^3J_{HH}$ = 6.8 Hz, CH_3(i-Pr)); 1.36 (6H, s, $C(CH_3)_2$); 2.96 (2H, sept, $^3J_{HH}$ = 6.8 Hz, CH(i-Pr) anilido); 3.55 (8H, m, THF); 3.73 (2H, sept, $^3J_{HH}$ = 6.82 Hz, CH(i-Pr)); 4.52 (1H, s, NH anilido); 6.63 (1H, d, $^3J_{HH}$ = 7.9 Hz, m-Py); 6.81 (1H, t, $^3J_{HH}$ = 7.5 Hz, p-anilido); 7.07−7.12 (2H, m, p-Py, m-Ph); 7.16−7.19 (3H, m, p-NPh, m-anilido); 7.21−7.25 (2H, m, m-NPh); 7.33 (2H, d, $^3J_{HH}$ = 7.9 Hz, o-Ph, m-Py); 7.96 (1H, d, $^3J_{HH}$ = 7.5 Hz, o-Ph); 8.22 (1H, d, $^3J_{HH}$ = 7.8 Hz, p-Ph). ^{13}C{^{1}H} NMR (100 MHz, C_6D_6, 292 K): 24.0 (*C*H$_3$(i-Pr) anilido); 24.4 (*C*H$_3$(i-Pr)); 24.9 (THF); 27.0 (*C*H$_3$(i-Pr)); 27.8 (*C*H(i-Pr)); 29.1 (*C*H(i-Pr) anilido); 31.8 (*C*(CH$_3$)$_2$); 67.5 (*C*(CH$_3$)$_2$); 69.4 (THF); 114.7 (anilido); 116.3 (m-Py); 116.6 (m-Py); 122.2, (Ar); 122.5 (Ar); 122.6 (Ar); 123.3 (Ar); 123.6 (Ar); 123.9 (Ar); 129.6 (Ar); 133.1 (Ar); 139.6 (p-Py); 143.5 (Ar); 145.6 (Ar); 147.5 (Ar); 149.1 (Ar); 152.1 (Ar); 152.4 (Ar); 158.4 (Ar); 175.5 (Ar); 194.6 ppm (d, $^1J_{YC}$ = 40.4 Hz, Y−C). IR (KBr): 479 (w); 519 (w); 555 (w); 644 (w); 727 (m); 743 (s); 805 (s); 839 (m); 846 (w); 883 (m); 913 (w); 931 (w); 962 (w); 944 (w); 1027 (w); 1042 (w); 1074 (w); 1096 (w); 1124 (w); 1156 (w); 1181(m); 1200 (w); 1246 (s); 1257 (s); 1302 (w); 1321 (w); 1363 (m); 1425 (s); 1445 (s); 1528 (w); 1571 (s); 1588 (s); 1621 (w); 3342 (w); 3354 (w); 3473 (w) cm^{-1}. Anal. Calcd for $C_{48}H_{64}N_3O_2SY$: C, 68.96; H, N, 5.02; 7.72; Y, 10.63. Found: C, 69.01; H, 7.75; N, 4.69; Y, 10.72.

Synthesis of [NNS^{BzTh}]YNH-2,6-^{i}Pr$_2$C$_6$H$_3$(py)$_2$ (8). A 0.2516 g amount (0.30 mmol) of **7** was dissolved in pyridine (4 mL). The solution was kept at room temperature for 0.5 h, and the volatiles were removed under vacuum. The orange-yellow solid residue was dissolved in a minimum volume of toluene, and the solution was slowly concentrated at ambient temperature. Complex **8** was isolated as orange-yellow crystals in 77% yield (0.1968 g). ^{1}H NMR (400 MHz, C_6D_6, 293 K): 0.83 (6H, d, $^3J_{HH}$ = 6.8 Hz, CH_3(i-Pr)); 1.22 (6H, d, $^3J_{HH}$ = 7.1 Hz, CH_3(i-Pr)); 1.23 (12H, d, $^3J_{HH}$ = 6.7 Hz, CH_3(i-Pr)); 1.29 (6H, s, $C(CH_3)_2$); 2.87 (2H, sept, $^3J_{HH}$ = 6.5 Hz, CH(i-Pr)); 3.71 (2H, sept, $^3J_{HH}$ = 6.6 Hz, CH(i-Pr)); 4.73 (1H, s, NH anilido); 6.30 (4H, t, $^3J_{HH}$ = 6.3 Hz, Py); 6.60 (2H, t, $^3J_{HH}$ = 7.6 Hz, Py); 6.72 (1H, d, $^3J_{HH}$ = 7.9 Hz, m-Py); 6.87 (1H, t, $^3J_{HH}$ = 7.3 Hz, p-anilido); 6.99 (1H, dd, $^3J_{HH}$ = 7.8 Hz, $^3J_{HH}$ = 7.9 Hz, m-Ph); 7.09 (1H, dd, $^3J_{HH}$ = 7.9 Hz, $^3J_{HH}$ = 7.8 Hz, m-Ph); 7.12 (1H, m, p-NPh); 7.18−7.22 (3H, compl. m, m-NPh, p-Py); 7.25 (2H, d, $^3J_{HH}$ = 6.8 Hz, m-Ph); 7.44 (1H, d, $^3J_{HH}$ = 7.7 Hz, m-Py); 7.80 (1H, d, $^3J_{HH}$ = 7.8 Hz, o-Ph); 7.96 (1H, d, $^3J_{HH}$ = 7.9 Hz, p-Ph); 8.62 (4H, s, Py). ^{13}C{^{1}H} NMR (100 MHz, C_6D_6, 293 K): 24.9 (*C*H$_3$(i-Pr)); 25.0 (*C*H$_3$(i-Pr)); 26.6 (*C*H$_3$(i-Pr)); 27.8 (*C*H(i-Pr)); 28.4 (*C*H(i-Pr)); 32.1 (*C*(CH$_3$)$_2$); 67.7 (d, $^2J_{YC}$ = 2.0 Hz, *C*(CH$_3$)$_2$); 114.6 (Ar); 115.0 (m-Py); 116.5 (m-Py); 121.8 (Ar); 122.6 (Ar); 122.8 (Ar); 123.3 (Ar)); 123.6 (Py); 124.1 (Ar); 124.4 (Ar); 129.8 (Ar); 133.7 (Ar)); 137.2 (Py); 139.9 (p-Py); 143.4 (d, $^3J_{YC}$ = 1.5 Hz, YCCCS); 143.9 (d, $^2J_{YC}$ = 2.2 Hz, YCCS); 148.5 (Ar); 149.9 (Py); 149.9 (Ar); 151.9 (d, $^2J_{YC}$ = 2.0 Hz, YCCCS); 152.5 (d, $^2J_{YC}$ = 3.9 Hz, ipso-Ar); 159.2 (Py Ar); 176.1 (Py); 199.9 ppm (d, $^1J_{YC}$ = 34.4 Hz, Y−C). IR (KBr): 556 (w); 626 (m); 675 (m); 683 (m); 703 (s); 728 (w); 748 (s); 798 (m); 807 (m); 842 (m); 884 (w); 952 (w); 1006 (m); 1017 (w); 1038 (s); 1069 (m); 1092 (w); 1109 (w); 1125 (w); 1152 (m); 1179 (m); 1216 (m); 1225 (m); 1259 (s); 1308 (w); 1319 (w); 1324 (s); 1343 (s); 1568 (s); 1590 (s); 1599 (s); 1622 (w); 3455 (w); 3467 (w) cm^{-1}. Anal. Calcd for $C_{50}H_{58}N_5SY$: C, 70.65; H, 6.88; N, 8.24; Y, 10.46. Found: C, 70.78; H, 7.14; N, 7.89; Y, 10.51.

Synthesis of [NNS^{BzThH}]Y(NH-2,6-^{i}Pr$_2$C$_6$H$_3$)$_2$ (9). A solution of **7** (0.2785 g, 0.33 mmol) in a toluene/hexane mixture (5 mL, 3/2) was kept at room temperature for 2 weeks. Complex **9** slowly formed as fine bright-orange crystals and was isolated in 30% yield (0.0864 g). ^{1}H NMR (400 MHz, C_6D_6, 293 K): 1.06 (24H, d, $^3J_{HH}$ = 6.7 Hz, CH_3(i-Pr)); 1.28 (6H, d, $^3J_{HH}$ = 6.9 Hz, CH_3(i-Pr)); 1.48 (6H, d, $^3J_{HH}$ = 6.9 Hz, CH_3(i-Pr)); 1.56 (6H, s, $C(CH_3)_2$); 2.66 (4H, sept, $^3J_{HH}$ = 6.4 Hz, CH(i-Pr)); 3.72 (2H, sept, $^3J_{HH}$ = 6.8 Hz, CH(i-Pr)); 5.01 (2H, s, NH anilido); 6.79 (3H, t, $^3J_{HH}$ = 7.6 Hz, p-Ph, m-Py); 6.84 (1H, dd, $^3J_{HH}$ = 7.30 Hz, $^3J_{HH}$ = 7.10 Hz, Ar); 6.91 (1H, dd, $^3J_{HH}$ = 7.7 Hz, $^3J_{HH}$ = 7.6 Hz, m-Py); 6.98 (3H, compl m, p-Py); 7.07(4H, d, $^3J_{HH}$ = 7.6 Hz, m-Ph); 7.09−7.14 (2H, compl m, p-NPh); 7.21 (2H, d, $^3J_{HH}$ = 7.5 Hz, m-NPh); 7.37 (1H, d, $^3J_{HH}$ = 8.0 Hz, Ar). ^{13}C{^{1}H} NMR (100 MHz, C_6D_6, 293 K): 23.1 (*C*H$_3$(i-Pr)); 24.3 (*C*H$_3$(i-Pr)); 26.4 (*C*H$_3$(i-Pr)); 28.5 (*C*H(i-Pr)); 30.3 (*C*H(i-Pr)); 32.6 (*C*(CH$_3$)$_2$); 63.9 (d, $^2J_{YC}$ = 2.1 Hz, *C*(CH$_3$)$_2$); 1154.0 (Ar); 118.6 (m-Py); 119.7 (m-Py); 122.5 (Ar); 123.2 (Ar); 123.8 (Ar); 124.6 (Ar); 126.9 (Ar); 127.0 (Ar); 132.8 (Ar); 137.0 (Ar); 139.3 (Ar);139.7 (Ar); 140.4 (Ar); 141.2 (Ar); 147.6 (Ar); 150.1 (Ar); 152.0 (d, $^2J_{YC}$ = 4.1 Hz, ipso-anilido); 178.6 (Ar). IR (KBr): 464 (m); 515 (w); 537 (w); 557 (w); 695 (s); 728 (s); 747 (s); 794 (m); 809 (m); 841 (m); 866 (w); 881 (w); 891 (w); 960 (w); 1007 (w); 1036 (m); 1079 (w); 1096 (m); 1122 (w); 1148 (w); 1181 (m); 1217 (w); 1230 (w); 1247 (w); 1263 (s); 1304 (w); 1340 (w); 1423 (s); 1461 (s); 1495 (w); 1563 (w); 1571 (m); 1588 (s); 3356 (w) cm^{-1}. Anal. Calcd for $C_{52}H_{67}N_4SY$: C, 71.86; H, 7.77; N, 6.44; Y, 10.23. Found: C, 71.84; H, 7.80; N, 6.75; Y, 10.31.

Synthesis of [NNS^{EtTh}]YNH-2,6-^{i}Pr$_2$C$_6$H$_3$(py)$_2$ (11). A solution of 2,6-diisopropylaniline (0.0812 g, 0.46 mmol) in toluene (10 mL) was added to a solution of **3** (0.3320 g, 0.46 mmol) in toluene (30 mL) at room temperature, and the reaction mixture was stirred for 0.5 h. The volatiles were removed under vacuum, and the solid residue was treated with pyridine. The resulting orange oil was dried under vacuum for 0.5 h and was dissolved in toluene. Slow concentration of the resulting solution at ambient temperature afforded crystals of **11** in 64% yield (0.2427 g). ^{1}H NMR (400 MHz, C_6D_6, 293 K): 0.78 (12H, broad d, $^3J_{HH}$ = 6.2 Hz, CH_3(i-Pr)); 1.06 (3H, t, $^3J_{HH}$ = 7.4 Hz, Et-

dx.doi.org/10.1021/om400099z | *Organometallics* 2013, 32, 2379−2388

Table 1. Crystallographic Data and Structure Refinement Details for Complexes 6, 8, 9, and 11

	6	8	9	11
empirical formula	$C_{51}H_{64}N_3O_2Y$	$C_{56}H_{64}N_5SY$	$C_{55.50}H_{71}N_4SY$	$C_{55}H_{68}N_5SY$
formula wt	839.96	928.09	915.13	920.11
cryst syst	triclinic	orthorhombic	monoclinic	monoclinic
space group	$P\bar{1}$	*Pbca*	$P2_1/c$	$P2_1/c$
a, Å	10.0359(6)	10.51965(15)	21.976(2)	16.9665(3)
b, Å	11.6546(8)	19.8913(4)	13.4831(13)	19.4635(3)
c, Å	20.5907(13)	47.7557(7)	17.1832(17)	30.0634(4)
α, deg	95.8550(10)	90	90	90
β, deg	90.2040(10)	90	104.695(2)	90.1406(13)
γ, deg	112.8730(10)	90	90	90
V, Å^3	2205.0(2)	9992.9(3)	4924.9(8)	9927.7(3)
Z	2	8	4	8
P_{calcd} (g/cm^3)	1.265	1.234	1.234	1.231
abs coeff (mm^{-1})	1.365	1.250	1.266	1.257
F(000)	892	3920	1948	3904
cryst size, mm	0.55 × 0.22 × 0.12	0.40 × 0.30 × 0.10	0.28 × 0.18 × 0.12	0.40 × 0.40 × 0.40
2θ, deg	52	60	52	60
index ranges	$-12 \le h \le 12$	$-14 \le h \le 14$	$-27 \le h \le 27$	$-23 \le h \le 23$
	$-12 \le k \le 14$	$-27 \le k \le 27$	$-16 \le k \le 16$	$-27 \le k \le 27$
	$-23 \le l \le 25$	$-67 \le l \le 67$	$-21 \le l \le 21$	$-42 \le l \le 42$
no. of rflns collected	10883	184929	41090	203301
no. of indep rflns (R_{int})	8215 (0.0226)	14479 (0.1038)	9646 (0.1332)	28866 (0.1638)
completeness to θ, %	94.6	99.3	99.6	99.7
max/min transmission	0.8533/0.5206	0.8852/0.6347	0.8629/0.7181	0.6332/0.6332
no. of data/restraints/params	8215/4/532	14479/0/582	9646/46/567	28866/4/1146
GOF on F^2	1.017	1.249	0.982	0.964
final *R* index ($I > 2\sigma(I)$)	0.0423	0.0748	0.0692	0.0677
R index (all data)	0.0978	0.1270	0.1613	0.1695
largest diff in peak/hole, e/Å^3	1.187/−0.924	0.718/−2.452	1.016/−0.544	1.503/−1.316

CH_3,); 1.17 (12H, broad d, $^3J_{HH}$ = 6.5 Hz, CH_3(i-Pr)); 1.36 (6H, s, $C(CH_3)_2$); 2.62 (2H, q, $^3J_{HH}$ = 7.4 Hz, Et-CH_2); 3.62 (4H, sept, $^3J_{HH}$ = 6.5 Hz, CH(i-Pr)); 4.62 (1H, s, NH); 6.25 (4H, m, Py); 6.59, (2H, m, Py); 6.76, (1H, d, $^3J_{HH}$ = 7.9 Hz, m-CH Py); 6.91 (1H, $^3J_{HH}$ = 7.4 Hz, p-Ph); 7.05 (1H, s, Ar); 7.19−7.30 (4H, compl m, p-Py, m- and p-NPh); 7.30 (2H, d, $^3J_{HH}$ = 7.4 Hz, m-Ph); 7.40 (1H, d, $^3J_{HH}$ = 7.8 Hz, m-Py); 8.59 (4H, m, Py). $^{13}C\{^1H\}$ NMR (100 MHz, C_6D_6, 293 K): 15.7 (CH_3(Et)); 23.2 (CH_2(Et)); 24.4, (CH_3(i-Pr)); 27.7 (CH_3(i-Pr)); 28.0 (CH(i-Pr)); 31.8 ($C(CH_3)_2$); 69.1 (d, $^2J_{YC}$ = 2.4 Hz, $C(CH_3)_2$); 114.4 (anilido); 1154.0 (Ar); 115.3, (Ar); 123.3 (Ar); 123.5 (Py); 123.6 (Ar); 124.2 (Ar); 133.4 (Ar); 134.9 (d, $^2J_{YC}$ = 2.0 Hz, SCCH); 137.5 (Py); 137.5 (Ar); 139.5 (Ar); 143.2 (d, $^2J_{YC}$ = 2.3 Hz, YCCS); 148.6 (Ar); 149.1 (Ar); 149.7 (Py); 152.6 (d, $^2J_{YC}$ = 3.9 Hz, ipso-anilido), 159.7 (Ar); 175.4 (Ar); 202.1 (d, $^1J_{YC}$ = 36.2 Hz, Y−C). IR (KBr): 464 (m); 523 (w); 565 (w); 601 (w); 625 (w); 677 (w); 696 (s); 702 (s); 729 (s); 744 (s); 800 (s); 843 (m); 888 (w); 931 (w); 965 (w); 977 (m); 1009 (m); 1030 (s); 1039 (s); 1069 (m); 1096 (m); 1126 (w); 1162 (m); 1180 (m); 1219 (w); 1261 (s); 1303 (w); 1322 (w); 1362 (m); 1425 (m); 1443 (s); 1479 (m); 1496 (m); 1571 (s); 1587 (s); 1600 (m); 1621 (w); 1800 (w); 1859 (w); 1939 (w); 3343 (w); 3406 (w); 3485 (w) cm^{-1}. Anal. Calcd for $C_{48}H_{60}N_5SY$: C, 69.63; H, 7.30; N, 8.46; Y, 10.74. Found: C, 69.70; H, 7.34; N, 8.95; Y, 10.78.

X-ray Crystallography. The X-ray data were collected on a Smart Apex diffractometer (for **6** and **9**, graphite-monochromated Mo Kα radiation, ω-scan technique, λ = 0.71073 Å, *T* = 100(2) K) and a Agilent Xcalibur E diffractometer (for **8** and **11**, graphite-monochromated Mo Kα radiation, ω-scan technique, λ = 0.71073 Å, *T* = 100(2) K). The structures were solved by direct methods and were refined on F^2 using SHELXTL[26] (**6** and **9**) and CrysAlis Pro[27] (**8** and **11**) package. All non-hydrogen atoms and H atoms in NH groups of anilido fragments were found from Fourier syntheses of electron density and were refined anisotropically and isotropically for hydrogens. All other hydrogen atoms were placed in calculated positions and were refined in the riding model. SADABS[28] (**6** and **9**) and ABSPACK (CrysAlis Pro)[27] (**8** and **11**) were used to perform area-detector scaling and absorption corrections. Details of crystallographic, collection, and refinement data are reported in Table 1. CCDC files 909588 (**6**), 909589 (**8**), 909590 (**9**), and 909592 (**11**) contain the supplementary crystallographic data for this paper. These data can be obtained free of charge from the Cambridge Crystallographic Data Centre via ccdc.cam.ac.uk/data_request/cif.

■ ASSOCIATED CONTENT

Supporting Information

Figures giving NMR spectra and CIF files giving crystallographic data. This material is available free of charge via the Internet at http://pubs.acs.org.

■ AUTHOR INFORMATION

Corresponding Author

*A.A.T.: fax, (+7)8314621497; e-mail, trif@iomc.ras.ru.

Notes

The authors declare no competing financial interest.

■ ACKNOWLEDGMENTS

The study was supported by the Ministry of education and science of Russian Federation, Project No. 8445, the Russian Foundation for Basic Research (grant 12-03-31865 mol_a), the Program of the Presidium of the Russian Academy of Science (RAS), and the RAS Chemistry and Material Science Division. We also thank the Groupe de Recherche International (GDRI) "Homogeneous Catalysis for Sustainable Development" for support.

REFERENCES

(1) (a) Cotton, S. A. *Coord. Chem. Rev.* **1997**, *160*, 93−127. (b) Marques, N.; Sella, A.; Takats. *J. Coord. Chem. Rev.* **2002**, *102*, 2137−2160. (c) Zimmermann, M.; Anwander, R. *Chem. Rev.* **2010**, *110*, 6194−6259. (d) Edelmann, F. T.; Freckmann, D. M. M.; Schumann, H. *Chem. Rev.* **2002**, *102*, 1851−1896. (e) Piers, W. E.; Emslie, D. J. H. *Coord. Chem. Rev.* **2002**, *233*−*234*, 131−155. (f) Trifonov, A. A. *Rus. Chem. Rev.* **2007**, *76*, 1051−1072.

(2) (a) Edelmann, F. T. *Top. Curr. Chem.* **1996**, *179*, 247−262. (b) Anwander, R. In *Applied Homogeneous Catalysis with Organometallic Compounds*; Cornils, B., Hermann, W. A., Eds.; Wiley-VCH: Weinheim, Germany, 2002; Vol. *2*, pp 974. (c) Molander, G. A.; Romero, J. A. C. *Chem. Rev.* **2002**, *102*, 2161−2185. (d) Hong, S.; Marks, T. J. *Acc. Chem. Res.* **2004**, *37*, 673−686. (e) Nakayama, Y.; Yasuda, H. *J. Organomet. Chem.* **2004**, *689*, 4489−4511. (f) Gromada, J.; Carpentier, J. F.; Mortreux, A. *Coord. Chem. Rev.* **2004**, *248*, 397−410.

(3) (a) Thompson, M. E.; Baxter, S. M.; Bulls, A. R.; Burger, B. J.; Nolan, M. C.; Santarsiero, B. D.; Schaefer, W. P.; Bercaw, J. E. *J. Am. Chem. Soc.* **1987**, *109*, 203−209. (b) Booij, M.; Deelman, B. J.; Duchateau, R.; Postma, D. S.; Mettsma, A.; Teuben, J. H. *Organometallics* **1993**, *12*, 3531−3540. (c) Den Haan, K. H.; Wielstra, Y.; Teuben, J. H. *Organometallics* **1987**, *6*, 2053−2060. (d) Fontaine, F. G.; Tilley, T. D. *Organometallics* **2005**, *24*, 4340−4342. (e) Sadow, A. D.; Don Tilley, T. *Angew. Chem., Int. Ed.* **2003**, *42*, 803−805. (f) Piers, W. E.; Shapiro, P.; Bunnek, E.; Bercaw, J. *Synlett* **1990**, 74−84.

(4) (a) Lyubov, D. M.; Fukin, G. K.; Cherkasov, A. V.; Shavyrin, A. S.; Trifonov, A. A.; Luconi, L.; Bianchini, C.; Meli, A.; Giambastiani, G. *Organometallics* **2009**, *28*, 1227−1232. (b) Luconi, L.; Lyubov, D. M.; Bianchini, C.; Rossin, A.; Faggi, C.; Fukin, G. K.; Cherkasov, A. V.; Shavyrin, A. S.; Trifonov, A. A.; Giambastiani, G. *Eur. J. Inorg. Chem.* **2010**, 608−620.

(5) (a) Li, E.; Chen, Y. *Chem. Commun.* **2010**, *46*, 4469−4471. (b) Chu, J.; Lu, E.; Liu, Zh.; Chen, Y.; Leng, X.; Song, H. *Angew. Chem., Int. Ed.* **2011**, *50*, 7677−7680. (c) Lu, E.; Chu, J.; Borzov, M. V.; Li, G. *Chem. Commun.* **2011**, 743−745.

(6) (a) Zuckerman, R. L.; Krska, S. W.; Bergman, R. G. *J. Am. Chem. Soc.* **2000**, *122*, 751−761. (b) Wang, W. D.; Espenson, J. H. *Organometallics* **1999**, *18*, 5170−5175. (c) Polse, J. L.; Andersen, R. A.; Bergman, R. G. *J. Am. Chem. Soc.* **1998**, *120*, 13405−13414. (d) Lee, S. Y.; Bergman, R. G. *Tetrahedron* **1995**, *51*, 4255−4276. (e) McGrane, P. L.; Jensen, M.; Livinghouse, T. *J. Am. Chem. Soc.* **1992**, *114*, 5459−5460. (f) Blake, R. E.; Antonelli, D. M.; Henling, L. M.; Schaefer, W. P.; Hardcastle, K. I.; Bercaw, J. E. *Organometallics* **1998**, *17*, 718−725. (g) Walsh, P. J.; Hollander, F. J.; Bergman, R. G. *J. Am. Chem. Soc.* **1988**, *110*, 8729−8731.

(7) (a) Nugent, W. A.; Mayer, J. M. *Metal-Ligand Multiple Bonds*; Wiley-Interscience: New York, 1988; p 334. (b) Wigley, D. E. *Prog. Inorg. Chem.* **1994**, *42*, 239−482. (c) Schrock, R. R. *Chem. Rev.* **2002**, *102*, 145−179. (d) Berry, J. F. *Comments Inorg. Chem.* **2009**, *30* (1−2), 28−66. (e) Winkler, J. R.; Gray, H. B. *Struct. Bonding (Berlin)* **2012**, *142*, 17−28.

(8) (a) Trifonov, A. A.; Bochkarev, M. N.; Schumann, H.; Loebel, J. *Angew. Chem., Int. Ed.* **1991**, *30*, 1149−1151. (b) Giesbrecht, G. R.; Gordon, J. C. *Dalton Trans.* **2004**, 2387−2393. (c) Panda, T. K.; Randoll, S.; Hrib, C. G.; Jones, P. G.; Bannenberg, T.; Tamm, M. *Chem. Commun.* **2007**, 5007−5009. (d) Scott, J.; Basuli, F.; Fout, A. R.; Huffmann, J. C.; Mindiola, D. J. *Angew. Chem.* **2008**, *47*, 8502−8505. (e) Chan, H. S.; Li, H. W.; Xie, Z. W. *Chem. Commun.* **2002**, 652−653. (f) Jian, Z.; Rong, W.; Pan, Y.; Xie, H.; Cui, D. *Chem. Commun.* **2012**, 7516−7518.

(9) (a) Xie, Z. W.; Wang, S. W.; Yang, Q. C.; Mak, T. C. W. *Organometallics* **1999**, *18*, 1578−1579. (b) Wang, S. W.; Yang, Q. C.; Mak, T. C. W.; Xie, Z. W. *Organometallics* **1999**, *18*, 5511−5517. (c) Gordon, J. C.; Giesbrecht, G. R.; Clark, D. L.; Hay, P. J.; Keogh, D. J.; Poli, R.; Scott, B. L.; Watkin, J. G. *Organometallics* **2002**, *21*, 4726−4734. (d) Beetstra, D. J.; Meetsma, A.; Hessen, B.; Teuben, J. H. *Organometallics* **2003**, *22*, 4372−4374. (e) Avent, A. G.; Hitchcock, P. B.; Khvostov, A. V.; Lappert, M. F.; Protchenko, A. V. *Dalton Trans.* **2004**, 2272−2280. (f) Pan, C. L.; Chen, W.; Song, S. Y.; Zhang, J. H.; Li, X. W. *Inorg. Chem.* **2009**, *48*, 6344−6346.

(10) (a) Lu, E.; Gan, W.; Chen, Y. *Dalton Trans.* **2011**, *40*, 2366−2374. (b) Evans, L. T. J.; Coles, M. P.; Cloke, F. G. N.; Hitchcock, P. B. *Inorg. Chim. Acta* **2010**, *363*, 1114−1125.

(11) (a) Emslie, D. J. H.; Piers, W. E.; Parvez, M.; McDonald, R. *Organometallics* **2002**, *21*, 4226−4240. (b) Aubrecht, K. B.; Chang, K.; Hillmyer, M. A.; Tolman, W. B. *J. Polym. Sci., Part A: Polym. Chem.* **2001**, *39*, 284−293. (c) Arnold, P. L.; Buffet, J. C.; Blaudeck, R.; Sujecki, S.; Wilson, C. *Chem. Eur. J.* **2009**, *15*, 8241−8250. (d) Emslie, D. J. H.; Piers, W. E.; MacDonald, R. *J. Chem. Soc., Dalton Trans.* **2002**, 293−294. (e) Westmoreland, I.; Arnold, J. *Dalton Trans.* **2006**, 4155−4163.

(12) Allen, F. H.; Kennard, O.; Watson, D. G.; Brammer, L.; Orpen, A. G.; Taylor, R. *J. Chem. Soc., Perkin Trans. 2* **1987**, S1−S19.

(13) Bent, H. A. *Chem. Rev.* **1961**, *61*, 275−311.

(14) (a) Hitzbleck, J.; Okuda, J. *Organometallics* **2007**, *26*, 3227−3235. (b) Arndt, S.; Spaniol, T. P.; Okuda, J. *Organometallics* **2003**, *22*, 775−781. (c) Deelman, B. J.; Booij, M.; Meetsma, A.; Teuben, J. H.; Kooijman, H.; Spek, A. A. *Organometallics* **1995**, *14*, 2306−2317. (d) Ringelberg, S. N.; Meetsma, A.; Troyanov, S. I.; Hessen, B.; Teuben, J. H. *Organometallics* **2002**, *21*, 1759−1765.

(15) Yu-Ran Luo, *Comprehensive Handbook of Chemical Bond Energies*; CRC Press: Boca Raton, FL, 2007.

(16) (a) Hodgson, L. M.; White, A. J. P.; Williams, C. K. *J. Polym. Sci., Part A: Polym. Chem.* **2006**, *44*, 6646−6651. (b) Kim, Y. K.; Livinghouse, T.; Horino, Y. *J. Am. Chem. Soc.* **2003**, *125*, 9560−9561.

(17) (a) Karpov, A. V.; Shavyrin, A. S.; Cherkasov, A. V.; Fukin, G. K.; Trifonov, A. A. *Organometallics* **2012**, *31*, 5349−5357. (b) Cameron, T. M.; Gordon, J. C.; Scott, B. L. *Organometallics* **2004**, *23*, 2995−3002. (c) Rad'kov, V. Yu.; Skvortsov, G. G.; Lyubov, D. M.; Cherkasov, A. V.; Fukin, G. K.; Shavyrin, A. S.; Cui, D.; Trifonov, A. A. *Eur. J. Inorg. Chem.* **2012**, 2289−2297. (d) Pawlikowski, A. V.; Ellern, A.; Sadow, A. D. *Inorg. Chem.* **2009**, *48*, 8020−8029. (e) Shang, X.; Liu, X.; Cui, D. *J. Polym. Sci.: Part A: Polym. Chem.* **2007**, *45*, 5662−5672. (f) Liu, B.; Cui, D.; Ma, J.; Chen, X.; Jing, X. *Chem. Eur. J.* **2007**, *13*, 834−845.

(18) Lu, E.; Can, W.; Chen, Y. *Dalton Trans.* **2011**, 2366−2374.

(19) Wang, D.; Cui, D.; Miao, M.; Huang, B. *Dalton Trans.* **2007**, 4576−4581.

(20) Yang, Y.; Li, S.; Cui, D.; Chen, X.; Jing, X. *Organometallics* **2007**, *26*, 671−678.

(21) (a) Knight, L. K.; Piers, W. E.; Fleurat-Lessard, P.; Parvez, M.; McDonald, R. *Organometallics* **2004**, *23*, 2087−2094. (b) Masuda, J. D.; Jantunen, K. C.; Scott, B.; Kiplinger, J. L. *Organometallics* **2008**, *27*, 1299−1304. (c) Cameron, T. M.; Gordon, J. C.; Scott, B. L.; Tumas, W. *Chem. Commun.* **2004**, 1398−1399.

(22) Batsanov, S. S. *Russ. J. Inorg. Chem.* **1991**, *36*, 1694−1705.

(23) (a) Brookhart, M.; Green, M. L. H.; Wong, L. L. *Prog. Inorg. Chem.* **1988**, *36*, 1−124. (b) Brookhart, M.; Green, M. L. H.; Parkin, G. *Proc. Natl. Acad. Sci. U.S.A.* **2007**, *104*, 6908−6914.

(24) (a) Lappert, M. F.; Pearce, M. J. *J. Chem. Soc., Chem. Commun.* **1973**, 126−127. (b) Schumann, H.; Freckmann, D. M. M.; Dechert, S. *Z. Anorg. Allg. Chem.* **2002**, *628*, 2422−2426.

(25) (a) Bianchini, C.; Giambastiani, G.; Guerrero Rios, I.; Meli, A.; Segarra, A. M.; Toti, A.; Vizza, F. *J. Mol. Catal. A* **2007**, *277*, 40−46. (b) Bianchini, C.; Giambastiani, G.; Mantovani, G.; Meli, A.; Mimeau, D. *J. Organomet. Chem.* **2004**, *689*, 1356−1361. (c) Bianchini, C.; Mantovani, G.; Meli, A.; Migliacci, F. *Organometallics* **2003**, *22*, 2545−2547. (d) Bianchini, C.; Sommazzi, A.; Mantovani, G.; Santi, R.; Masi, F. US Patent 6,916,931 B2, 2005. (e) Bianchini, C.; Gatteschi, D.; Giambastiani, G.; Guerrero Rios, I.; Ienco, A.; Laschi, F.; Mealli, C.; Meli, A.; Sorace, L.; Toti, A.; Vizza, F. *Organometallics* **2007**, *26*, 726−739.

(26) Sheldrick, G. M. *SHELXTL v.6.12, Structure Determination Software Suite*; Bruker AXS, Madison, WI, 2000.

(27) *CrysAlis Pro*; Agilent Technologies Ltd, Yarnton, England, 2011.

(28) Sheldrick, G. M. *SADABS v.2.01, Bruker/Siemens Area Detector Absorption Correction Program*; Bruker AXS, Madison, WI, 1998.
(29) Nakamoto, K. *Infrared and Raman Spectra of Inorganic and Coordination Compounds*; Wiley: Hoboken, NJ, 2009; Part B, p 408.

List of abbreviations

AcOEt	Ethyl acetate
Ar	Aryl group
Cat.	Catalyst
CGC	Constrained Geometry Catalyst
Cp	Cyclopentadienyl ligand
dba	*trans*, *trans*-dibenzylidene acetone
DFT	Differential Fourier Transform
DMF	N,N-dimethylformamide
DMSO	Methyl sulfoxide
Et	Ethyl
EtOH	Ethanol
Et_2O	Diethyl ether
FT	Fourier Transform
Fu	Furanyl
GC	Gas Chromatography
h	hour(s)
HDPE	High Density PolyEthylene
IR	Infrared
^{i}Pr	Isopropyl
L	generic ligand
LDPE	Low Density PolyEthylene
LLDPE	Linear Low Density PolyEthylene
M	Metal
MAO	Methylaluminoxane
Me	Methyl

MeOH	Methanol
min.	minutes
MMAO	Modified MAO
m.p.	Melting point
NMR	Nuclear Magnetic Resonance
ν	Stretching frequency
NEt_3	Triethylamine
PDI	Polydispersity Index (M_w/M_n)
PE	PolyEthylene
Ph	Phenyl
PP	PolyPropylene
Py	Pyridine
R	Generic group
r.t.	room temperature
T	Temperature
t	Time
T_g	Glass transition temperature
^{t}Bu	*tert*-buthyl
Th	Thyophenyl
THF	Tetrahydrofuran
TMS	Tetramethylsilyl
TS	Transition state
TOF	TurnOver Frequency
TON	TurnOver Number
ZN	Ziegler Natta

Acknowledgements

Desidero ringraziare tutti coloro che hanno collaborato e contribuito alla realizzazione di questo lavoro di Tesi.

Primo tra tutti voglio ringraziare il mio supervisor ***Dr. Giuliano Giambastiani*** *per la sua guida sapiente, gli insegnamenti, i continui stimoli, il suo supporto e, ultima ma non meno importante, la sua amicizia.*

Un ringraziamento sentito va alla mia amica e collega di laboratorio ***Giulia Tuci*** *per la compagnia, le risate, la collaborazione e l'incoraggiamento durante questo progetto.*

Ringrazio il ***Dr. Andrea Rossin*** *per il suo prezioso contributo in questo lavoro.*

Un pensiero va sicuramente a tutti i ragazzi dell'ICCOM per tutti i momenti passati insieme: ***Irene****,* ***Gabriele****,* ***Carmen****,* ***Noemi****,* ***Manuela****,* ***Andrea****,* ***Jonathan****,* ***Primiano****,* ***Francesca****,* ***Maria****,* ***Carlo****,* ***Francesco*** *e* ***Serena****. Grazie!*

Vorrei infine ringraziare le persone a me più ***care****: i miei amici, la mia fidanzata e compagna* ***Claudia*** *per il suo incondizionato* ***amore*** *e supporto morale, anche nei momenti più difficili, e infine i miei* ***genitori*** *ai quali questo lavoro è dedicato.*

Grazie di cuore a TUTTI!